



**HAL**  
open science

# Catalytic decarboxylation of palmitic acid to n-pentadecane

Anouchka Mapembé Kimené

► **To cite this version:**

Anouchka Mapembé Kimené. Catalytic decarboxylation of palmitic acid to n-pentadecane. Catalysis. Ecole Centrale de Lille, 2017. English. NNT : 2017ECLI0031 . tel-01785814

**HAL Id: tel-01785814**

**<https://theses.hal.science/tel-01785814>**

Submitted on 4 May 2018

**HAL** is a multi-disciplinary open access archive for the deposit and dissemination of scientific research documents, whether they are published or not. The documents may come from teaching and research institutions in France or abroad, or from public or private research centers.

L'archive ouverte pluridisciplinaire **HAL**, est destinée au dépôt et à la diffusion de documents scientifiques de niveau recherche, publiés ou non, émanant des établissements d'enseignement et de recherche français ou étrangers, des laboratoires publics ou privés.

N°d'ordre : 343

CENTRALE LILLE

## **THESE**

Présentée en vue

d'obtenir le grade de

## **DOCTEUR**

En

Spécialité : **Molécules et Matière Condensée**

Par

**Anouchka MAPEMBE KIMENE**

**DOCTORAT DELIVRE PAR CENTRALE LILLE**

**DECARBOXYLATION CATALYTIQUE DE L'ACIDE PALMITIQUE EN N-PENTADECANE**

Soutenue le 04 décembre 2017 devant le jury d'examen :

<b>Président</b>	Sébastien ROYER, Professeur (UCCS, Université Lille 1)
<b>Rapporteur</b>	Catherine ESPECEL, Maître de Conférences, HDR (IC2M, Université de Poitiers)
<b>Rapporteur</b>	Sophie HERMANS, Professeur (FNRS, Université catholique de Louvain, Belgique)
<b>Examineur</b>	Mohamed NAWFAL GHAZZAL, Maître de Conférences, (LCP, Université Paris Sud)
<b>Membre invité</b>	Claire DURLIN, Ingénieur de recherche (Weylchem)
<b>Membre invité</b>	Olivier SIMON, chef de développement de procédés de recherche (Weylchem)
<b>Encadrant</b>	Robert WOJCIESZAK, Chargé de recherches (UCCS, CNRS)
<b>Directeur</b>	Sébastien PAUL, Professeur (UCCS, Centrale Lille)

Thèse préparée dans le Laboratoire UCCS

Ecole Doctorale SMRE 104 (UCCS)



*A ma famille,*

---

## *Acknowledgments*

« La reconnaissance est la plus belle fleur qui jaillit de l'âme » disait Henry Ward Beecher. C'est pourquoi, avec une reconnaissance infiniment grande, je tiens particulièrement à remercier ici, toutes les personnes qui ont, de près ou de loin, contribué à l'aboutissement de ce projet de thèse et à la concrétisation de ma réussite.

Tout d'abord, je remercie la direction de l'UCCS, ainsi que tout le personnel de l'unité, pour leur accueil chaleureux. Je remercie également la direction de Centrale Lille ainsi que tout le personnel des ressources humaines pour la gestion de toute la partie administrative de ma thèse. Ensuite, j'adresse mes plus sincères remerciements à l'Entreprise Weylchem Lamotte SAS pour avoir accepté que je participe à ce projet de recherche et pour l'avoir soutenu financièrement. Au-delà de l'aspect financier, j'exprime particulièrement toute ma reconnaissance à Monsieur Olivier Simon, chef de développement de procédés de recherche chez Weylchem. Merci Olivier pour ton implication dans ce projet et pour le suivi de mes travaux. Merci également à Mme Claire Durlin pour sa disponibilité à répondre à mes questions. Merci spécial à Mr Fabrice Tanguy, Ingénieur en développement de Procédés chez Weylchem, pour son apport lors des réunions de suivi de mes travaux.

Mon cœur est profondément reconnaissant envers mon Directeur de thèse, le professeur Sébastien Paul, à qui je prie de trouver ici, l'expression de toute mon admiration, mon respect et ma profonde gratitude pour avoir été un directeur modèle, exemplaire et du temps qu'il a mis à ma disposition pour le suivi de ma thèse. Sébastien, j'ai beaucoup appris de toi, pour cela, je te remercie pour tes remarques, tes nombreuses questions, tes conseils avisés qui m'ont permis de prendre du recul, ainsi que ta rigueur scientifique et tes corrections méticuleuses qui m'ont permis d'évoluer rapidement. Merci également de m'avoir fait confiance et d'avoir été attentif à mes besoins professionnels sans lesquels je n'aurais pas réussi à me surpasser. Ta gentillesse, ta sympathie et ton si grand cœur font de toi une personne que je n'oublierai jamais.

Par la même occasion, je remercie le docteur Robert Wojcieszak pour m'avoir encadré pendant ma thèse avec beaucoup de sérieux et d'implication. Merci beaucoup Robert pour avoir partagé avec moi ton savoir et tes connaissances dans le domaine de la catalyse hétérogène. Merci également pour ta sympathie, ton humour, tes conseils et ton optimisme qui m'ont permis d'aller de l'avant.

J'adresse ma reconnaissance également à Mlle Karen Silva, stagiaire de Master 2 Catalyse et Procédés, qui a contribué à la partie optimisation de procédés de ma thèse. Merci Karen pour ton implication, ton dynamisme et au plaisir que tu m'as donné à travailler avec toi.

Je tiens également à exprimer ma profonde gratitude aux membres du jury de ma thèse pour l'intérêt qu'ils ont porté à lire et à évaluer ce manuscrit. Je remercie particulièrement le professeur Sophie Hermans et le Dr Cathérine Especel d'avoir rapporté avec bienveillance ce manuscrit et au Dr Mohamed Nawfal Ghazzal et professeur Sébastien Royer d'avoir examiné avec soin mon travail.

« La reconnaissance est la mémoire du cœur » [Hans Christian Andersen], c'est pourquoi, je remercie grandement toutes les personnes qui ont contribué à la partie technique de ce projet de thèse. Pour cela, je remercie tout d'abord, la plateforme REALCAT<sup>1</sup> dans laquelle ma thèse s'est déroulée ainsi que tous les ingénieurs de recherches pour leurs aides précieuses. Je pense tout particulièrement à Mme Svetlana Heyte pour m'avoir formé à l'utilisation des appareils sophistiqués de la plateforme. Merci également à Mme Joëlle Thuriot pour la partie caractérisation des catalyseurs, par ICP, XRD et XRF. Enfin, je remercie Mr Egon Heuson pour sa sympathie et son aide précieuse dans des choses du quotidien. Ensuite, je remercie Johann et Pascal pour les analyses BET, Monsieur Olivier Gardoll, pour sa contribution technique à la caractérisation par TPR, Mesdames Pardis Simon et Martine Trentesaux pour les analyses XPS de mes catalyseurs. Et enfin, merci à Mme Maya Marinova, ainsi qu'à Jin Sha et Alberto Mazzi pour la caractérisation de mes catalyseurs par TEM.

La bienveillance et l'atmosphère d'entraide que j'ai rencontrées au sein de ce labo m'ont permis d'effectuer ma thèse dans les meilleures conditions possibles. C'est pourquoi j'adresse un énorme merci à des personnes tout simplement géniales avec qui j'ai pris plaisir à travailler. Il s'agit particulièrement de mes chers collègues doctorants et posts docs, je pense particulièrement à Javier, Ana, Mehdi, Alxey, Samadhan, Alexandre, Xuemei, Haiting, Jin, Max, Feng, Lila, Yoichi (Magica), Alberto, Inès, Tong, Dimitri, Juliana, Thomas, Nicolas, et tous les autres doctorants de mécanique et du C3. Sans vous, ma thèse ne se serait assurément pas déroulée de la même façon. Vous êtes et vous resterez à jamais dans mon cœur.

Cette thèse de doctorat n'est que l'aboutissement d'un rêve nourrit depuis ma tendre enfance et des efforts que j'ai fournis pour arriver à mes fins. Ainsi, hormis les personnes citées précédemment, d'autres acteurs en amont ont contribué à la réalisation de mon rêve, dont le principal acteur est mon père, Mr. Albert Kiméné qui a été ma première source de motivation. Papa, cette thèse de doctorat je te la dédie particulièrement, car c'était l'un de tes plus grands souhaits.

---

<sup>1</sup> La plateforme REALCAT bénéficie d'une subvention gouvernementale administrée par l'Agence Nationale de la Recherche (ANR) dans le cadre du programme «Investissements d'avenir» (PIA), avec la référence contractuelle 'ANR-11-EQPX-0037'. L'Équipement d'Excellence REALCAT a été cofinancé par l'Union Européenne et Fondation Centrale Initiatives. Centrale Lille, le CNRS et l'Université Lille 1 ainsi que la Fondation Centrale Initiatives, sont remerciés pour leurs contributions financières à l'acquisition et à la mise en place de l'équipement de la plate-forme REALCAT.

J'ai toujours bossé dur afin que tu sois fière de moi. Merci beaucoup mon papa, tu as été et resteras à jamais ma principale source de motivation. Je t'aime fort.

Je remercie également ma mère, Mme Sergine Kiméné. Maman merci d'avoir été ma première institutrice et pour ton soutien financier durant mes longues études. Mes remerciements ne pourront jamais égaler ton grand cœur, ta générosité et tout l'amour que tu m'as apporté durant toutes ces années. Tu es et tu resteras ma maman au si bon cœur.

Merci également à toi tonton Isidore (feu), je sais que là où tu te trouves tu es fière de moi comme de ton vivant tu l'avais toujours été. Merci d'avoir été un bon tuteur pour moi. Je ne t'oublierai jamais.

Grand merci à ma tante, Mme Henriette Perbet, qui a été une mère pour moi, depuis mon arrivée en France. Maman Henriette, tu as été d'un très bon soutien moral. Tu m'as toujours comblée d'amour et tu as sans cesse veillé à mon bien-être et à ce que je ne manque de rien en France. Pour cela, je t'en suis amplement reconnaissante. Merci maman H d'amour.

La thèse de doctorat est gorgée de montagnes russes, tantôt elles montent et tantôt elles descendent. Seule la détermination est la force mentale permettant de déplacer ses montagnes quelques soient leurs tailles et d'aplanir son sentier afin d'avancer vers son but. C'est avec ces quelques phrases d'encouragements que je dédie ce manuscrit de thèse à tous mes neveux (Yann, Kent, Jordis, Elysée, Eli et Charyss) et à toutes mes nièces (Eva, Sem-triphène, Léona (feu), Carly, Chrismaelle, Sagesse, Tendresse, Néhémie et Rebecca) ainsi qu'à mes enfants à venir. Que chacun de vous, trouve ici la motivation dont il a besoin pour atteindre ses objectifs. Un conseil, n'arrêtez jamais d'essayer et de persévérer, car n'oubliez pas : « Tout est possible à celui qui croît ».

Je remercie aussi toutes mes grandes sœurs adorées (Anne, Carine, Vanessa, Mayeva) ainsi qu'à mes deux petites sœurs chéries (Lyvia et Flora). Merci les filles pour votre soutien moral, financier et pour tout l'amour que vous m'apportez. Je vous aime. Merci également à tous mes amis, notamment, Serge, Hamza, Saint-Clair, Nadège, Ednah, Winna, Michel, Dimitry, Daniel, Romain, Gérard, Candide, Marie, Joe et Aimée. Merci pour votre amitié et pour tous vos encouragements.

Je ne saurais terminer ces remerciements sans pourtant remercier la seule personne qui est la plus proche de moi. Mon très cher Mamoudou, je te remercie d'avoir cru en moi et de m'avoir encouragé pendant mes périodes de doute. Merci également de m'avoir donné ton épaule chaude où je pouvais reposer ma tête pour descendre la pression.

---

Résumé en français de la thèse intitulée :  
« Décarboxylation catalytique de l'acide palmitique en n-pentadécane »

## Introduction

Les alcanes-sulfonates de sodium (appelés en anglais Sodium Alkane Sulfonates (SAS)) sont des tensioactifs anioniques biodégradables largement utilisés dans les domaines de la détergence et des cosmétiques. Ils sont obtenus à partir de la sulfoxydation des alcanes linéaires (n-paraffines) de chaînes carbonées allant de C12 à C18 (appelé paraffines normales lourdes, en anglais Heavy Normal Paraffins (HNP)) [1]. Aujourd'hui les alcanes linéaires utilisés dans les procédés de fabrication de ces tensio-actifs anioniques sont tous issus du pétrole. Cependant, pour faire face aux préoccupations majeures que constituent l'épuisement des ressources fossiles et l'impact de leur utilisation massive sur l'environnement, la recherche permanente de procédés alternatifs utilisant des matières premières renouvelables telle que la biomasse est devenue une nécessité pour les industriels de la chimie. C'est dans ce contexte que la décarboxylation catalytique de l'acide palmitique (PA) en n-pentadécane (PD) a été étudiée en tant que réaction-modèle pour la production de HNP biosourcée. Ces derniers pourraient être utilisés pour la fabrication de détergents à la fois biodégradables et biosourcés.

Un des enjeux concerne la sélectivité obtenue car, dans les conditions de décarboxylation (DCX) de l'acide gras, d'autres types de réactions telles que la décarbonylation (DCN) ou l'hydrodéoxygénation (HDO) peuvent se dérouler dépendamment de l'atmosphère de réaction et du type de catalyseur utilisé. En effet, les réactions de DCX et DCN éliminent le groupe fonctionnel acide par clivage d'une liaison carbone-carbone, libérant respectivement du CO ou du CO<sub>2</sub>, ce qui conduit à la formation d'un hydrocarbure comportant un atome de carbone de moins que celui de l'acide gras d'origine. Ces deux réactions peuvent se dérouler sous atmosphère inerte et/ou en présence de faibles concentrations d'hydrogène [2-4], ce qui les rend particulièrement intéressantes en termes de rentabilité du procédé. Par contre, la réaction d'HDO nécessite la présence d'une concentration élevée d'hydrogène pour éliminer les espèces oxygénées présentes dans l'acide gras. Celle-ci conduit à la formation d'un hydrocarbure comportant le même nombre d'atomes de carbone que celui de l'acide gras d'origine [5]. Ainsi, la nécessité d'utiliser de fortes concentrations d'hydrogène pour le procédé d'HDO le rend moins intéressant d'un point de vue économique par rapport aux réactions DCN ou DCX. Outre les trois réactions précédentes, d'autres réactions indésirables telles que le craquage, la cétonisation et la déshydrogénation peuvent également se produire. Par ailleurs, en phase liquide, des réactions consécutives telles que l'isomérisation et l'oligomérisation, peuvent également se produire en fonction des conditions de réaction. En phase gaz, des réactions de méthanation et la réaction du gaz à l'eau (en anglais Water Gas Shift) peuvent se produire à partir de CO, CO<sub>2</sub>, H<sub>2</sub> et H<sub>2</sub>O qui sont des produits des réactions de DCX/DCN [6]. Par conséquent, comprendre les facteurs qui favorisent ces différentes voies de réactions est très important pour mieux contrôler la sélectivité et donc optimiser le rendement en alcane désiré.

Dans la littérature, des catalyseurs à base de métaux nobles ont montré d'excellents résultats pour la décarboxylation des acides gras en n-alcane [6-9]. Cependant, ces catalyseurs ont également montré une désactivation rapide après un seul test catalytique ce qui les rend

désavantageux en termes de recyclabilité [3]. De plus, le coût élevé et la faible abondance des métaux nobles sont des contraintes sérieuses à prendre en compte pour une application à grande échelle. Par conséquent, le développement de catalyseurs plus abordables présentant de bonnes performances catalytiques et une bonne stabilité présente un fort intérêt d'un point de vue industriel. Ainsi, le but de cette thèse a été de développer des catalyseurs hautement actifs, sélectifs et stables à base de métaux non-nobles pour la réaction de décarboxylation des acides gras en n-paraffines. De ce fait, un ensemble de catalyseurs mono- et bimétalliques supportés sur charbon actif a été synthétisé, caractérisé et testé avec pour objectif de sélectionner le meilleur système catalytique.

Le manuscrit de cette thèse a été organisé comme suit: tout d'abord, le chapitre 1 résume l'état de l'art sur la décarboxylation catalytique des acides gras en n-hydrocarbures, en mettant l'accent sur les recherches récentes impliquant l'utilisation de catalyseurs à base de métaux non nobles. Ensuite, le chapitre 2 décrit les outils et les procédures expérimentales utilisés. Il détaille notamment la préparation des catalyseurs, leurs méthodes de caractérisation, les protocoles d'évaluation de leurs performances catalytiques, ainsi que les méthodes analytiques. Les résultats de l'étude de caractérisation de ces catalyseurs sont présentés et discutés au chapitre 3. Le chapitre 4 présente les résultats de l'étude de réactivité des catalyseurs monométalliques pour la décarboxylation de l'acide palmitique, tandis que le chapitre 5 concerne celle effectuée pour les catalyseurs bimétalliques. Dans les deux cas, l'influence des conditions de réactions sur les performances catalytiques a été investiguée. Enfin, le manuscrit se termine par une conclusion générale et quelques perspectives à cette étude.

## **1. Procédure expérimentale**

### **1.1. Composés chimiques**

Les précurseurs utilisés pour la préparation des catalyseurs sont : le nitrate de nickel hexahydraté (97%); le nitrate de cuivre trihydraté (99-104%); le nitrate de fer nonahydraté ( $\geq 99,999\%$ ) et le nitrate d'argent ( $\geq 99,0\%$ ). Le support utilisé pour tous les catalyseurs synthétisés est le charbon actif Darco KB-g de volume poreux =  $1,1 \text{ cm}^3/\text{g}$  et de surface spécifique =  $1290 \text{ m}^2/\text{g}$ . L'hydrazine en solution aqueuse à 78-82% a été choisie comme agent réducteur. Tous les produits dans cette thèse ont été achetés chez Sigma-Aldrich et ont été utilisés tels que reçus.

### **1.2. Préparation des catalyseurs**

Une série de catalyseurs monométalliques (10% en masse de Ni, Cu, Fe et Ag) et bimétalliques (Ni-Me avec Me=Ag, Cu et Fe de ratio Ni/Me=1 et de composition totale Ni+Me=5, 10, 20 et 30% en masse) supportés sur charbon a été préparée en utilisant le robot Chemspeed CatImpreg HT disponible sur la plateforme REALCAT. De plus, deux catalyseurs (10%Ni/C et 10%Ni10%Cu/C) ont été préparés à la paillasse manuellement pour comparaison. Tous les catalyseurs ont été préparés par la méthode de dépôt précipitation (DP), excepté le catalyseur noté 10%Ni10%Cu/C-calc, qui a été préparé par la méthode d'imprégnation par voie humide et les catalyseurs commerciaux à base de métaux nobles 5%Pd/C et 5%Pt/C, qui ont été achetés chez Sigma-Aldrich. Au total 19 catalyseurs ont été testés.

### **1.3. Méthodes de caractérisation**

---

Parmi les catalyseurs synthétisés, certains ont été caractérisés afin de déterminer, d'une part, leurs propriétés physiques telles que la distribution de la taille des pores, le volume des pores, la surface spécifique, la taille des particules métalliques et, d'autre part, leurs propriétés de surface et de cœur telles que la composition, la taille des cristallites, la structure, etc.

### 1.3.1. Propriétés morphologiques et texturales

#### 1.3.1.1. Adsorption/désorption d'azote

La surface spécifique, le volume des pores et la distribution de la taille des pores des catalyseurs ont été déterminés par adsorption d'azote à 77,35 K en utilisant les appareils TriStar II Plus et 3Flex de Micromeritics. La surface spécifique (BET) a été évaluée en utilisant la méthode de BET (Brunauer, Emmet et Teller). Par ailleurs, la distribution de la taille des pores et le volume des pores ont été calculés selon la formule de Barrett-Joyner-Halenda (BJH) en tenant compte de la désorption.

#### 1.3.1.2. Microscopie électronique à transmission (MET)

La morphologie et la composition chimique de la surface du catalyseur ont été analysées par microscopie électronique à transmission en utilisant un microscope de marque FEI Tecnai G2 20, équipé d'une micro-analyse EDS (spectroscopie à rayons X à dispersion d'énergie), d'un filtre en énergie Gatan (EELS), de systèmes de précession et de tomographie électronique et d'une caméra CCD ORIUS. Ce microscope est également muni d'un filament LaB6 fonctionnant avec une tension d'accélération d'électron de 200 kV.

### 1.3.2. Propriétés de surface

#### 1.3.2.1. Spectroscopie photoélectronique par rayons X (XPS)

Cette technique a été utilisée pour collecter des informations sur l'état chimique de la surface du matériau étudié. Les spectres XPS ont été collectés sur un spectromètre hémisphérique à haute performance VG Escalab 220 XL «1996» et sur un spectromètre KRATOS, AXIS UltraDLD «2009» utilisant un rayonnement monochromatique Al K $\alpha$  ( $h\nu = 1486,6$  eV) comme source d'excitation. Pour l'interprétation des résultats, l'étalonnage des spectres XPS a été réalisé en utilisant la référence carbone C 1s de 284,8 eV.

### 1.3.3. Propriétés de cœur

#### 1.3.3.1. Spectrométrie à plasma à couplage inductif-spectrométrie optique (ICP-OES)

Les compositions quantitatives des catalyseurs ont été déterminées en utilisant un équipement ICP-OES-Agilent 720.

#### 1.3.3.2. Fluorescence des rayons X (XRF)

L'analyse par fluorescence à rayons X a été effectuée sur M4 Tornado de Bruker afin d'estimer le ratio Ni/Cu des échantillons testés.

#### 1.3.3.3. Diffraction des rayons X (DRX)

Des mesures de diffraction des rayons X ont été effectuées sur un diffractomètre à rayons X Discover D8 de Bruker en utilisant un tube à rayons X dans le rayonnement Cu (K $\alpha$ ) ( $\lambda = 1,538$  Å). L'angle de diffraction  $2\theta$  était dans la gamme de 10 à 70 ° avec des pas de 0,02 ° par seconde. L'interprétation du spectre DRX obtenu a été réalisée à partir du logiciel

Diffraction. Eva et l'identification des phases cristallines a été réalisée à partir des modèles standards de poudre de diffraction des rayons X (cartes PDF de référence).

#### 1.3.3.4. Réduction en température programmée (RTP)

La RTP a permis d'estimer la nature des espèces réductibles présentes dans le catalyseur et de révéler la température à laquelle se réduit chaque espèce. Le catalyseur a été purgé à température ambiante sous Ar pendant 1 h avant d'être chauffé de 25 jusqu'à 750 °C sous un mélange gazeux de 5% H<sub>2</sub>/Ar avec une rampe de 5 °C.min<sup>-1</sup> et maintenu à 750 °C pendant 1 heure. Le gaz effluent a été analysé par un détecteur de conductivité thermique (TCD).

## 2. Les tests catalytiques

Les substrats testés ont été l'acide palmitique, >> 99% et l'acide stéarique, ≥97,0%. L'hexadécane (ReagentPlus®, 99%) et le dodécane (anhydre, ≥99%) ont été utilisés comme solvants de la réaction. L'hexane (standard analytique, ≥ 99,7%) a été utilisé comme solvant pour diluer les produits de réaction et le pentadécane, ≥98,0% (GC) a été utilisé pour l'identification et l'étalonnage des produits en chromatographie en phase gazeuse (GC). Finalement, le toluène (chromatographie en phase gazeuse MS SupraSolv®, ≥ 99,8%) a été utilisé comme étalon interne pour l'analyse GC. Tous les produits présentés ici ont été achetés chez Sigma Aldrich et utilisés tels que reçus.

Les tests catalytiques ont été réalisés dans un système automatique de criblage sous pression et à haute température disponible sur la plateforme REALCAT. Il s'agit d'un Screening Pressure Reactor (SPR) de Freeslate équipé de 24 réacteurs discontinu en acier inoxydable de 6 mL chacun (Figure 1).

Avant les tests, les catalyseurs ont été activés dans cette même unité sous H<sub>2</sub> avec une rampe de 5 °C.min<sup>-1</sup> et maintenu à 350 °C pendant 3 h. Pour être chargé en réactifs, ces catalyseurs activés ont été transférés dans une boîte à gants pour éviter leur réoxydation au simple contact de l'air. Ensuite, les tests catalytiques ont été réalisés aux différentes conditions de températures, atmosphères et temps de réaction, concentrations du substrat, etc... sur l'unité SPR.

Après les tests catalytiques, les 24 réacteurs ont été chauffés à 80 °C sous ultrasons pour éviter la cristallisation de l'acide palmitique non converti restant dans le réacteur. Ensuite, les produits liquides de chaque réacteur ont été filtrés, puis 20 µL de chaque produit de réaction obtenu ont été introduits dans des flacons de 2 mL. Ces produits ont été dilués avec 980 µL d'hexane (solvant) et 100 µL de toluène (étalon interne). Les échantillons obtenus ont été placés dans le passeur d'échantillons chauffé à 40 °C du GC pour analyse.

Le chromatographe en phase gazeuse utilisé est un GC-MS-QP2010 de Shimadzu muni d'une colonne ZB\_5MS (30 m x 0,25 mm x 0,25 µm) et équipé de deux voies analytiques couplées à deux détecteurs : un détecteur à ionisation de flamme (FID) et un spectromètre de masse (simple quadripolaire QP2010 ULTRA) à mode d'ionisation à impact électronique. La



Figure 1 : les réacteurs SPR

quantification des composés a été effectuée en utilisant la méthode d'étalonnage interne en utilisant le toluène.

### 3. Résultats et discussion

Dans le chapitre 4, la décarboxylation catalytique de l'acide palmitique (AP) en n-pentadécane (n-PD) a été étudiée sur des catalyseurs monométalliques supportés sur charbon actif. Le but était de trouver un catalyseur contenant un métal non noble montrant des performances catalytiques identiques à celles obtenues avec les catalyseurs à base de métaux nobles. Pour ce faire, des catalyseurs commerciaux à base de métaux nobles (5%Pd/C et 5%Pt/C) ont été utilisés comme catalyseurs de référence. Ensuite, les catalyseurs monométalliques non nobles synthétisés ont été testés afin de trouver le meilleur candidat. Par ailleurs, l'influence des conditions de réaction telles que la température, le temps de réaction, la concentration en acide palmitique (AP) et la masse du catalyseur a également été étudiée. Enfin, l'effet de l'activation du catalyseur sous H<sub>2</sub> a aussi été mesurée.

Tout d'abord, un test à blanc a été réalisé. Pour ce faire, la réaction s'est déroulée en absence du catalyseur à 320 °C pendant 6h, pour 0.197 mmol d'AP. Les résultats obtenus ont montré 27% de conversion d'AP, 28% de sélectivité en n-PD et 8% de rendement en n-PD. Le bilan carbone obtenu était de 81%, indiquant la formation de produits indésirés de masses molaires relativement élevées.

Ensuite, les catalyseurs à base de métaux nobles 5%Pd/C et 5%Pt/C ont été étudiés en faisant varier les conditions de réactions telles que la température (de 300 à 320 °C), la concentration en réactif (de 0.05 à 0.15 mol/L), l'activation du catalyseur, ainsi que la masse du catalyseur (de 12,8 à 75 mg). Tout d'abord, dans les deux cas, l'étude de la température de réaction a montré que l'augmentation de la température entraîne une forte augmentation de la conversion en AP de 79 à 91 %. Par contre, en termes de sélectivité, seule une légère variation a été observée. Compte-tenu du rendement en n-pentadécane le plus élevé à 320°C, cette dernière température a été choisie comme optimale pour le reste de cette étude.

Concernant la concentration en acide gras, les performances des catalyseurs à base de métaux nobles ont montré des résultats presque similaires pour des concentrations de 0.1 et 0.15 mol/L. Ainsi, 0.1 mol/L a été choisie comme concentration optimale pour la suite de l'étude.

Lors de l'étude de la masse de catalyseur introduit dans le réacteur, les résultats obtenus ont montré une conversion totale pour le catalyseur à 5%Pd/C quelle que soit la masse de catalyseur utilisée dans la gamme étudiée. Par contre, une augmentation progressive de la sélectivité a été observée avec l'augmentation de la masse de catalyseur entre 12.8 et 75 mg. Les meilleurs résultats ont été obtenus à 91% de sélectivité en n-PD. Par contre, pour le catalyseur à 5%Pt/C, la conversion totale a été obtenue à partir de 52 mg de catalyseur. Quant à la sélectivité en n-PD, celle-ci a atteint son maximum à 75 mg. Mais, étant donné que la sélectivité augmente très peu entre 52 et 75 mg, la masse optimale de catalyseur choisie est de 52 mg.

En définitive, les conditions optimales pour la décarboxylation d'AP en n-PD sur les catalyseurs 5% Pd/C et 5% Pt/C ont été trouvées pour une concentration en réactif de 0,1 mol/L

---

à 320 °C, sous 10 vol.% de H<sub>2</sub> dans N<sub>2</sub>, à 20 bar de pression initiale, pendant 6 h de réaction. La masse optimale de catalyseur chargé a été de 52 mg. Dans ces conditions, les catalyseurs 5%Pd/C et 5%Pt/C ont conduit à des conversions totales de l'AP et à des sélectivités en n-PD de 84% et 89%, respectivement.

Une fois que ces conditions optimales obtenues, les catalyseurs monométalliques non nobles ont été étudiés pour la décarboxylation d'AP en n-PD dans les mêmes conditions, afin de trouver le meilleur candidat. Pour cela, les catalyseurs monométalliques 10%Ni/C, 10%Ag/C, 10%Fe/C et 10%Cu/C ont été étudiés. Les résultats obtenus ont montré la plus haute conversion pour le catalyseur 10%Ni/C et la plus haute sélectivité en n-PD pour le catalyseur 10%Cu/C. Par contre, le catalyseur 10%Ag/C a montré une très faible réactivité et 10%Fe/C n'a montré presque aucune réactivité. Parmi les catalyseurs étudiés, le plus prometteur était le catalyseur à base de nickel en termes de rendement. Pour cette raison, ce dernier a été étudié plus en détail. Comme observé avec les catalyseurs à base de métaux nobles, les performances peuvent être augmentées lorsque le catalyseur est activé sous H<sub>2</sub> avant le test. De plus, étant donné que les échantillons à base de métaux nobles ont montré les meilleures performances pour 52 mg de catalyseur, deux charges de quantités différentes de catalyseurs ont été étudiées pour le catalyseur à 10%Ni/C. Les résultats obtenus ont montré que l'augmentation de la quantité de catalyseur de 12,8 à 52 mg entraîne une augmentation de la conversion de 57 à 80% et de la sélectivité de 20 à 62%. Enfin, l'étude de la recyclabilité du catalyseur sur trois tests consécutifs a montré une désactivation progressive du catalyseur. Cette désactivation a été attribuée à l'adsorption éventuelle de sous-produits de réaction ou au dépôt de coke sur la surface du catalyseur. En effet, il a trouvé dans la littérature que les catalyseurs à base de nickel favoriseraient la réaction de décarbonylation en présence d'hydrogène, produisant ainsi du CO connu pour être un poison des catalyseurs. De plus, les catalyseurs à base de nickel ont également été trouvés sélectifs vis-à-vis des produits de craquage, conduisant à la formation de produits plus légers qui pourraient se déposer sur la surface des catalyseurs et donc être responsables de leur désactivation. Cependant, compte-tenu des résultats prometteurs observés avec ce catalyseur et pour éviter sa désactivation rapide, le catalyseur 10%Ni/C a été modifié en incorporant un second métal pour éviter le dépôt de coke. De ce fait, la réaction de décarboxylation catalytique de l'acide palmitique en n-PD a été étudié sur des catalyseurs bimétalliques de type Ni-Me (avec Me=Ag, Fe ou Cu).

Dans le chapitre 5, les catalyseurs bimétalliques Ni-Me (avec Me = Ag, Fe et Cu) supportés sur charbon actif ont été étudiés pour la décarboxylation de AP en n-PD. L'influence des conditions de réaction telles que la température, la durée de réaction, l'atmosphère de réaction, etc... sur leurs performances catalytiques a été discutée.

Tout d'abord, il a été observé que la combinaison du nickel avec un autre métal non noble, tel que Ag, Fe ou Cu, joue un rôle important dans l'amélioration de l'activité, de la sélectivité, du rendement ainsi que de la stabilité du catalyseur. Parmi les catalyseurs bimétalliques étudiés, les catalyseurs Ni-Cu/C ont montré les plus hautes performances catalytiques. Les études d'une série de trois catalyseurs bimétalliques de compositions différentes Ni-Cu/C (Ni/Cu=1) avec des charges métalliques totales de 5, 10, 20 et 30% ont

révélé que le catalyseur 10% Ni10% Cu/C est le plus actif pour effectuer la décarboxylation de PA en n-PD. Les différences de propriétés texturales et morphologiques des catalyseurs Ni-Cu (Tableau 1) pourraient expliquer les résultats catalytiques obtenus.

Tableau 1: propriétés des catalyseurs bimétalliques Ni-Cu

Catalyseur	S <sub>BET</sub> (m <sup>2</sup> /g)	Pore size (Å)	Pore volume (cm <sup>3</sup> /g)	Ni/Cu (XPS)	Ni/Cu (ICP)	Ni/Cu (XRF)	Ni/Cu (EDX)	Espèces détectées par XPS	Phases identifiées par DRX
5%Ni5%Cu/C	830	64	0,47	2,6	0,9	0,9		Cu(NO <sub>3</sub> ) <sub>2</sub> Ni(OH) <sub>2</sub>	Ni <sub>0.79</sub> Cu <sub>0.21</sub> O
10%Ni10%Cu/C	536	66	0,39	2	1,7	0,8	1,5	CuO, NiO, Ni(OH) <sub>2</sub>	CuO NiO
15%Ni15%Cu/C	645	64	0,39	3,3	0,6	0,6		Cu(NO <sub>3</sub> ) <sub>2</sub> Ni(OH) <sub>2</sub>	Ni <sub>0.79</sub> Cu <sub>0.21</sub> O

En effet, parmi les catalyseurs bimétalliques Ni-Cu synthétisés, le catalyseur le plus actif (10%Ni10%Cu/C) présente la plus faible surface spécifique et le plus petit volume poreux. En le comparant au catalyseur 5%Ni5%Cu/C, cette diminution des deux propriétés texturales a été attribuée au remplissage des pores dû à l'augmentation de la charge métallique. Cependant, comparés au catalyseur 15%Ni15%Cu/C, la faible surface spécifique et le faible volume des pores ont été attribués à la taille des particules de ce catalyseur, qui seraient plus grandes que celles du catalyseur le plus actif. En outre, les images TEM ont montré la présence de particules de nickel et de cuivre de forme sphérique allant de 2 à 6 nm de diamètre environ pour le catalyseur le plus actif, tandis que de grosses particules agglomérées ont été observées dans le 15%Ni15%Cu/C. Ces résultats confirment que la taille des particules du catalyseur le plus actif est plus petite que celle du catalyseur 15%Ni15%Cu/C.

De plus, les analyses ICP ont révélé qu'il y avait plus de cuivre que de nickel dans les catalyseurs bimétalliques 5%Ni5%Cu/C et 15%Ni15%Cu/C, alors que pour le catalyseur le plus actif (10%Ni10%Cu/C), le contraire a été observé. Ainsi, la majeure partie du catalyseur le plus actif est enrichi en nickel.

Malgré leurs différences dans la composition de cœur, l'analyse XPS a révélé que la surface de tous les catalyseurs bimétalliques est enrichie en Ni. Cependant, l'analyse XPS a également montré différentes espèces à la surface de chaque catalyseur. Le spectre XPS dans les régions Ni 2p et Cu 2p du catalyseur le plus actif a montré la présence des espèces NiO, Ni(OH)<sub>2</sub> et CuO sur la surface. En revanche, pour les catalyseurs 5%Ni5%Cu/C et 15%Ni15%Cu/C, la présence de Cu(NO<sub>3</sub>)<sub>2</sub> et de Ni(OH)<sub>2</sub> a été observée.

De plus, l'analyse DRX a révélé la présence de NiO et CuO dans le catalyseur le plus actif, tandis que dans les catalyseurs 5%Ni5%Cu/C et 15%Ni15%Cu/C Ni<sub>0.79</sub>Cu<sub>0.21</sub>O a été observé. Après la réduction des catalyseurs, les espèces métalliques Ni et Cu ont été détectés sur le catalyseur le plus actif, tandis que dans le cas des deux autres catalyseurs bimétalliques, des alliages de Ni et de Cu ont été observés. Le catalyseur 5%Ni5%Cu/C a révélé la présence

d'un mélange de deux alliages bimétalliques:  $\text{Ni}_{0.79}\text{Cu}_{0.21}$  et  $\text{Ni}_{0.5}\text{Cu}_{0.5}$ , tandis que le catalyseur 15%Ni15%Cu/C a montré un mélange d'espèces de  $\text{Ni}_{0.79}\text{Cu}_{0.21}$  et de cuivre métallique.

Le profil  $\text{H}_2$ -RTP des catalyseurs bimétalliques a également confirmé la présence de différentes espèces dans chaque catalyseur. Les catalyseurs bimétalliques 5%Ni5%Cu/C et 15%Ni15%Cu/C ont montré des pics de réduction de NiO et CuO en un alliage Ni-Cu et de  $\text{Cu}^{2+}$  en Cu. En revanche, le catalyseur le plus actif n'a montré que la réduction de CuO en  $\text{Cu}^0$ , NiO en  $\text{Ni}^0$  et  $\text{Cu}^{2+}$  en  $\text{Cu}^0$ .

Par conséquent, les différences observées dans la composition de cœur et de surface des systèmes bimétalliques étudiés ont été attribuées comme principales causes des performances catalytiques différentes observées sur chaque catalyseur. Le catalyseur le plus actif a été étudié en profondeur afin de trouver les meilleures conditions de réaction permettant d'atteindre leurs plus hautes performances.

L'étude des conditions de réaction a révélé que le catalyseur bimétallique le plus actif (10%Ni10% Cu/C) a atteint une conversion totale d'AP, lorsque la réaction de décarboxylation s'est déroulée à 320 °C, sous 10 vol.% de  $\text{H}_2$  dans  $\text{N}_2$  pour 6 h. En termes de sélectivité, le catalyseur a atteint 95% de n-PD. En revanche, sous atmosphère inerte, le même catalyseur présentait une conversion totale, mais la sélectivité vis-à-vis du n-PD diminuait significativement (seulement 59%). L'analyse GC-MS des produits obtenus pour différentes atmosphères a révélé la formation de différents sous-produits (Tableau 2).

Tableau 2 : Effet de l'atmosphère de réaction sur les performances catalytiques du 10%Ni10%Cu/C pour la décarboxylation de PA en n-PD. Conditions de réaction:  $T = 320$  °C, pression initiale = 20 bar,  $t = 6$  heures, vitesse de l'agitateur = 600 tr / min; charge de catalyseur = 52 mg; Charge PA = 0,197 mmol.

Atmosphère	$X_{\text{AP}}^a$ (%)	$S_{\text{n-C15}}^b$ (%)	$S_{\text{1-C15}}^c$ (%)	$S_{\Sigma\text{C15}}^d$ (%)	$S_{\text{n-C14}}^e$ (%)	$S_{\text{C16}}^f$ (%)	Carbon balance
10% $\text{H}_2/\text{N}_2$	100	95	-	95	-	<2	97
$\text{N}_2$	100	59	29	88	<4	-	93

a: conversion de l'acide palmitique, b: sélectivité en n-pentadécane, c: 1-pentadécène, d: sélectivité en totale en C15, e: sélectivité en n-tétradécane, f: sélectivité en n-hexadécane.

Des tests de recyclabilité du meilleur catalyseur (10%Ni10%Cu/C) ont également été effectués pour vérifier sa stabilité. Il a été constaté qu'après trois tests consécutifs, ce catalyseur a conservé l'intégralité de ses performances catalytiques sans nécessité de traitements régénératifs entre chaque test. Comparé au catalyseur 10%Ni/C, le catalyseur 10%Ni10%Cu/C a été trouvé très stable. Par conséquent, il a été conclu que l'addition du cuivre au catalyseur à base de nickel est très bénéfique. L'analyse XRD du catalyseur avant le test (catalyseur activé) et après les tests de recyclabilité (catalyseur recyclé) a montré les mêmes pics de diffraction (voir chapitre 3 de la thèse). Cependant, après le test de recyclabilité, la surface spécifique et le volume des pores du catalyseur ont diminué de façon drastique, tandis que la distribution des tailles de pores a augmenté significativement. La raison de ce phénomène a été attribuée au remplissage des pores du catalyseur par le solvant de réaction.

L'étude de l'effet du solvant utilisé (dodécane ou hexadécane) a montré qu'il n'y a aucun impact sur les performances catalytiques. De ce fait, l'utilisation de l'hydrocarbure désiré (le produit de la réaction de décarboxylation) en tant que solvant pourrait constituer un énorme avantage d'un point de vue industriel pour éviter des opérations complexes de séparation en aval après la réaction. Finalement, les tests catalytiques du catalyseur bimétallique 10%Ni10%Cu/C avec un autre substrat (acide stéarique (SA)) a montré une conversion totale de SA et une sélectivité en n-heptadécane de 90% à 320 °C pendant 3 h. Ces mêmes performances catalytiques ont été observées avec l'AP lorsque la réaction était effectuée dans les mêmes conditions. Cela est dû aux longueurs de chaîne carbonée proche des deux acides gras ainsi qu'à leurs acidités assez similaires.

## Conclusion

Le catalyseur bimétallique 10%Ni10%Cu/C permet de complètement convertir l'acide palmitique avec une sélectivité de 95% en n-pentadécane lorsque la réaction est réalisée à 320 °C, pendant 6h, sous une atmosphère contenant 10% en volume de H<sub>2</sub> dans N<sub>2</sub> à pression initiale de 20 bar. En outre, dans les mêmes conditions de réaction, ce catalyseur a présenté une excellente stabilité après trois tests de recyclage consécutifs. Par ailleurs, l'utilisation de ce catalyseur pour décarboxyler un autre acide gras plus lourd (l'acide stéarique) s'est avérée possible avec d'excellents résultats. En comparant les performances de ce catalyseur à celles du catalyseur monométallique 10%Ni/C, il est clair que la présence du cuivre favorise la dispersion des nanoparticules de métal sur le support, empêche la désactivation du catalyseur et améliore le rendement de la réaction. Il favorise surtout la formation de nanoparticules métalliques parfaitement réduites (état d'oxydation zéro). Ainsi, les catalyseurs Ni-Cu/C constituent une alternative très intéressante aux catalyseurs à base de métaux nobles pour conduire la réaction de décarboxylation des acides gras en alcanes linéaires.

## Références

- [1] P. Mul, H.C.W. Rommens, EP patent 2995669, March 16, 2016.
- [2] E. Santillan-Jimenez, T. Morgan, J. Lacny, S. Mohapatra, M. Crocker, *Fuel*. 103 (2013) 1010-1017.
- [3] E. Santillan-Jimenez, M. Crocker, *Journal of Chemical Technology & Biotechnology*. 87 (2012) 1041-1050.
- [4] I. Kubičková, M. Snåre, K. Eränen, P. Mäki-Arvela, D.Y. Murzin, *Catalysis Today*. 106 (2005) 197-200.
- [5] R.W. Gosselink, S.A. Hollak, S.W. Chang, J. van Haveren, K.P. de Jong, J.H. Bitter, D.S. van Es, *ChemSusChem*. 6 (2013) 1576-1594.
- [6] M. Snåre, I. Kubičková, P. Mäki-Arvela, K. Eränen, D.Y. Murzin, *Industrial & Engineering Chemistry Research*. 45 (2006) 5708-5715.
- [7] S. Lestari, P. Mäki-Arvela, I. Simakova, J. Beltramini, G.Q.M. Lu, D.Y. Murzin, *Catalysis Letters*. 130 (2009) 48-51.
- [8] J.G. Immer, M.J. Kelly, H.H. Lamb, *Applied Catalysis A: General*. 375 (2010) 134-139.
- [9] J.P. Ford, J.G. Immer, H.H. Lamb, *Topics in Catalysis*. 55 (2012) 175-184.

<b>GENERAL INTRODUCTION.....</b>	<b>20</b>
<b>REFERENCES.....</b>	<b>25</b>

### **Chapter 1: Bibliography synthesis**

<b>INTRODUCTION .....</b>	<b>28</b>
<b>I. DECARBOXYLATION OF FATTY ACIDS.....</b>	<b>29</b>
I.1. DEFINITION .....	29
I.2. DECARBOXYLATION/DECARBONYLATION PATHWAYS OF FATTY ACIDS.....	29
I.2.1. Influence of the nature of the catalyst .....	29
I.2.2. Influence of the reaction atmosphere .....	32
I.2.2.1. Under inert atmosphere .....	32
I.2.2.2. Under H <sub>2</sub> -containing atmosphere .....	33
<b>II. PD-BASED CATALYSTS FOR THE DECARBOXYLATION OF FATTY ACIDS .....</b>	<b>34</b>
II.1. PREPARATION OF THE PD-BASED CATALYSTS .....	34
II.2. INFLUENCE OF THE CATALYSTS PROPERTIES AND LOADING ON THE PERFORMANCES .....	34
II.2.1. Effect of the Pd metal particle size and dispersion .....	34
II.2.2. Effect of the Pd metal loading .....	35
II.2.3. Effect of the FFA/catalyst ratio .....	37
II.2.4. Deactivation of the Pd/C catalysts.....	37
<b>III. DECARBOXYLATION OF FATTY ACIDS OVER NON-NOBLE METAL-BASED CATALYSTS .....</b>	<b>39</b>
III.1. DECARBOXYLATION OF FATTY ACIDS OVER MONOMETALLIC CATALYSTS .....	39
III.2. INFLUENCE OF THE PREPARATION METHODS OF NI-BASED CATALYSTS.....	40
III.3. DECARBOXYLATION OF FATTY ACIDS OVER BIMETALLIC CATALYSTS.....	43
III.4. DECARBOXYLATION OF FATTY ACIDS OVER TRIMETALLIC CATALYSTS .....	43
<b>IV. CATALYTIC DECARBOXYLATION OF FATTY ACIDS: INFLUENCE OF THE REACTION CONDITIONS</b>	<b>44</b>
IV.1. INFLUENCE OF THE NATURE OF THE ATMOSPHERE .....	44
IV.2. INFLUENCE OF THE REACTION TEMPERATURE.....	47
IV.3. INFLUENCE OF THE REACTION PRESSURE .....	48
IV.4. INFLUENCE OF THE REACTION TIME .....	49
IV.5. INFLUENCE OF CHAIN LENGTH OF THE SATURATED FATTY ACID .....	49
IV.6. SUMMARY OF THE REPORTED PERFORMANCES ON NON-NOBLE METAL-BASED CATALYSTS .....	51
<b>CONCLUSION .....</b>	<b>53</b>
<b>REFERENCES.....</b>	<b>56</b>

### **Chapter 2: Experimental procedures**

<b>INTRODUCTION .....</b>	<b>60</b>
<b>I. SYNTHESIS AND CHARACTERIZATION OF THE CATALYSTS.....</b>	<b>60</b>
I.1. MATERIALS .....	60

I.2. PREPARATION OF MONO- AND BIMETALLIC CATALYSTS .....	60
I.2.1. Bench-scale manual preparation .....	60
I.2.2. High-throughput catalysts preparation .....	62
I.2.2.1. Preparation by deposition-precipitation method .....	62
I.2.2.2. Preparation by wet impregnation method .....	64
I.3. CHARACTERIZATION METHODS .....	65
I.3.1. Morphological and textural properties .....	65
I.3.1.1. Nitrogen adsorption/desorption .....	65
I.3.1.2. Transmission Electron Microscopy (TEM) .....	67
I.3.2. Surface properties .....	67
I.3.2.1. X-ray Photoelectron Spectroscopy (XPS).....	67
I.3.3. Bulk properties .....	69
I.3.3.1. X-ray fluorescence (XRF) .....	69
I.3.3.2. X-ray diffraction (XRD) .....	70
I.3.3.3. Inductively Coupled Plasma Optical Emission Spectroscopy (ICP-OES).....	71
I.3.3.4. Temperature-programmed reduction (TPR) .....	72
<b>II. CATALYTIC TESTS .....</b>	<b>74</b>
II.1. MATERIALS .....	74
II.2. EXPERIMENTAL SETUP.....	74
II.2.1. SPR system presentation .....	74
II.2.2. Description of the experimental protocol of catalyst reactivation .....	75
II.2.3. Description of the experimental protocol .....	76
<b>III. ANALYSIS OF THE PRODUCTS OF REACTION .....</b>	<b>76</b>
III.1. ANALYTICAL METHOD .....	76
III.1.1. GC analysis.....	76
III.1.2. Calibration of the GC .....	77
III.1.3. Sample preparation .....	77
III.2. DATA TREATMENT .....	78
<b>REFERENCES.....</b>	<b>79</b>

### Chapter 3: Characterization study

<b>INTRODUCTION .....</b>	<b>82</b>
<b>I. MORPHOLOGICAL AND TEXTURAL PROPERTIES .....</b>	<b>82</b>
I.1. NITROGEN ADSORPTION/DESORPTION .....	82
I.1.1. Textural properties of the bare carbon support and of the mono- and bimetallic catalysts	82
I.1.2. Textural properties of the bimetallic 10%Ni10%Cu/C .....	83
I.1.3. Impact of the preparation method of the catalyst on their textural proprieties .....	84
I.2. TEM AND EDX .....	85
<b>II. SURFACE PROPERTIES.....</b>	<b>89</b>
II.1. XPS .....	89
II.1.1. XPS Analysis of the 10%Ni10%Cu/C catalyst .....	90
II.1.2. Analysis of the Ni-Cu catalysts.....	93
<b>III. BULK PROPERTIES.....</b>	<b>98</b>

III.1. ICP-OES ANALYSIS .....	98
III.2. XRF .....	98
III.3. XRD .....	101
III.3.1. XRD analysis of the 10%Ni /C catalyst .....	101
III.3.2. XRD analysis of the 10%Ni10%Cu/C catalyst .....	102
III.3.3. XRD analysis of the 10%Ni10%Cu/C-calc catalyst.....	104
III.3.4. Determination of the crystallite size and of the d-spacings .....	105
III.3.5. XRD analysis of other monometallic and bimetallic catalysts .....	106
III.4. TPR.....	109
<b>CONCLUSION .....</b>	<b>112</b>
<b>REFERENCES.....</b>	<b>114</b>

#### **Chapter 4: Reactivity of monometallic catalysts in the decarboxylation of palmitic acid**

<b>INTRODUCTION .....</b>	<b>117</b>
<b>I.    DECARBOXYLATION OF PA OVER NOBLE METAL-BASED CATALYSTS.....</b>	<b>118</b>
I.1. BLANK TEST .....	118
I.2. EFFECT OF THE REACTION TEMPERATURE .....	119
I.3. EFFECT OF THE CONCENTRATION OF THE SUBSTRATE .....	120
I.4. EFFECT OF THE REDUCTION OF THE CATALYST WITH H <sub>2</sub> .....	121
I.5. EFFECT OF THE MASS OF CATALYST LOADED IN THE REACTOR .....	122
<b>II.    DECARBOXYLATION OF PA OVER NON-NOBLE METAL-BASED CATALYSTS.....</b>	<b>123</b>
II.1. EFFECT OF THE NATURE OF THE METAL.....	124
II.2. NICKEL-BASED CATALYSTS.....	125
II.2.1. Effect of the activation of the catalyst under H <sub>2</sub> .....	125
II.2.2. Effect of the nickel loading .....	126
II.2.3. Influence of the mass of catalyst loaded in the reactor .....	127
II.2.4. Recyclability of the catalyst .....	128
<b>DISCUSSION .....</b>	<b>130</b>
<b>CONCLUSION .....</b>	<b>132</b>
<b>REFERENCES.....</b>	<b>133</b>

#### **Chapter 5: Reactivity of bimetallic catalysts in the decarboxylation of palmitic acid**

<b>INTRODUCTION .....</b>	<b>136</b>
<b>I.    NI-ME BIMETALLIC CATALYSTS FOR THE DECARBOXYLATION OF PA TO N-PD .....</b>	<b>137</b>
I.1. NI-AG-BASED CATALYSTS .....	137
I.1.1. <i>Effect of Ag addition</i> .....	137
I.1.2. <i>Effect of the Ni-Ag loading</i> .....	138
I.2. NI-FE-BASED CATALYSTS .....	139
I.2.1. <i>Effect of the Fe addition</i> .....	139
I.2.2. <i>Effect of the Ni-Fe loading</i> .....	140

---

I.3. NI-CU-BASED CATALYSTS .....	141
<i>I.3.1. Effect of the Cu addition .....</i>	<i>141</i>
<i>I.3.2. Effect of the Ni-Cu loading.....</i>	<i>142</i>
I.4. OPTIMIZATION OF THE REACTION CONDITIONS OVER THE 10%Ni10%Cu/C CATALYST.....	143
<i>I.4.1. Effect of the amount of catalyst .....</i>	<i>143</i>
<i>I.4.2. Effect of the reaction temperature .....</i>	<i>145</i>
<i>I.4.3. Effect of the reaction time .....</i>	<i>146</i>
<i>I.4.4. Effect of the reaction atmosphere .....</i>	<i>147</i>
<i>I.4.5. Effect of the solvent .....</i>	<i>148</i>
<i>I.4.6. Manual and robotized preparations of the catalyst .....</i>	<i>149</i>
<i>I.4.7. Effect of the preparation method of the catalyst .....</i>	<i>150</i>
<b>II. RECYCLABILITY TESTS OF THE CATALYSTS .....</b>	<b>151</b>
<b>III. EFFECT OF THE FATTY ACID CARBON CHAIN LENGTH.....</b>	<b>152</b>
<b>DISCUSSION .....</b>	<b>154</b>
<b>CONCLUSION .....</b>	<b>160</b>
<b>REFERENCES.....</b>	<b>161</b>
<b>GENERAL CONCLUSION AND PERSEPECTIVES.....</b>	<b>162</b>
<b>ANNEXES.....</b>	<b>167</b>

---

## Glossary

Abbreviation	Notification
<b>AA</b>	Arachidic acid
<b>AC</b>	Activated carbon
<b>BA</b>	Behenic acid
<b>BET</b>	Brunauer, Emmett and Teller
<b>Co-I</b>	Co-impregnation
<b>DCX</b>	Decarboxylation
<b>DCN</b>	Decarbonylation
<b>DO</b>	Deoxygenation
<b>DP</b>	Deposition-precipitation
<b>FFA</b>	Free fatty acids
<b>FA</b>	Fatty acids
<b>HDO</b>	Hydrodeoxygenation
<b>IWI</b>	Incipient Wetness Impregnation
<b>LA</b>	Lauric acid
<b>MA</b>	Myristic acid
<b>NPs</b>	Nanoparticles
<b>PA</b>	Palmitic acid
<b>PD</b>	Pentadecane
<b>SA</b>	Stearic acid
<b>SAS</b>	Sodium Alkane Sulfonates
<b>TPR</b>	Temperature programmed reduction
<b>WI</b>	Wet impregnation
<b>XRD</b>	X-ray diffraction
<b>XPS</b>	X-ray photoelectron spectroscopy
<b>WGS</b>	Water-gas-shift

---

# General Introduction

Sodium alkanesulfonates (known as SAS) are important biodegradable anionic surfactants widely used in the fields of detergent and cosmetics. They are obtained from sulfoxidation of linear alkanes (n-paraffins), which are usually in the C12 to C18 range (the so-called Heavy Normal Paraffin HNP) [1]. The n-paraffins react with sulfur dioxide and oxygen in the presence of water, whilst irradiating with ultraviolet light, to form the sulfonic acid (1) and then put in contact with a base, generally sodium hydroxide, to form the desired SAS (2).



Nowadays, the linear paraffins used for the SAS manufacturing process are all issued from petroleum. However, to address the major concern of the forecasted depletion of fossil resources in the coming years (Figure 1), and the impact of their massive use on the environment because of greenhouse gases emissions, the chemical industry is actively looking for alternative processes using renewables as raw materials. In this context, biomass is generally considered as the best - if not single - option.

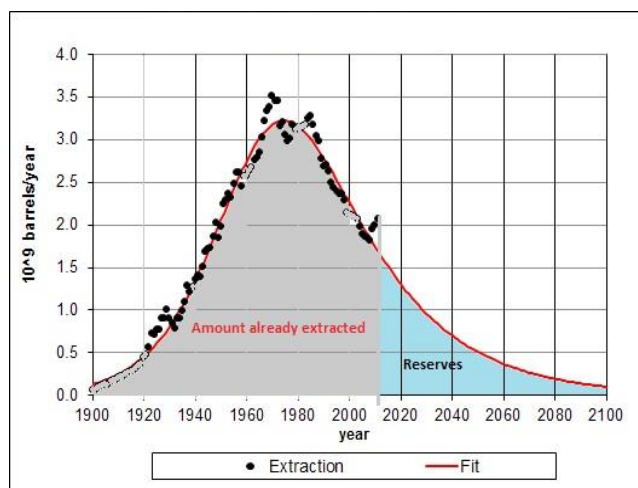


Figure 1: US Crude Oil Extraction Projection [2]

The biomass considered for being used as raw materials in the industry is most of the time plant-based materials. It can be classified in three principal categories: i) lignocellulosic biomass (wood, straw, green wastes, etc.); ii) starch biomass, which is rich in sugars (beet, sugar

cane, wheat, corn, etc.) and iii) oleaginous biomass, which is rich in triglycerides (rapeseed, soybean, palm, sunflower, etc.). Other sources of biomass can also be found, such as algae for instance. To obtain useful compounds from biomass, such as sugars or oils for example, various pre-treatments and transformation processes have been developed in the recent years [3, 4]. Biomass can be transformed into biofuels (gasoline, diesel and kerosene), into intermediates for the chemical industry or into many other products such as, for instance, bitumen and asphalt, polymers, fertilizers, pesticides, solvents, lubricants, pharmaceuticals, detergents, hygiene products and cosmetics, etc.

In this thesis, the use of fatty acids issued from oleaginous biomass has been considered to produce the n-paraffins needed to manufacture SAS. As a matter of fact, the oleaginous biomass is rich in lipids and is mainly composed of triglycerides, of esters of glycerol and of free fatty acids (FFA). FFA are carboxylic acids composed of a saturated or unsaturated aliphatic hydrocarbon tail and of a carboxylic group head (Figure 2). The FFA content in vegetable oils is usually high (Table 1).

**TABLE 1: FATTY ACID CONTENT (IN WT.%) OF COMMON NATURAL OILS AND FATS [5]**

Fatty acid (nn:x)	Palm	Soy bean	Rape	Sun flower	Cotton	Peanut	Maize	Olive	Palm kernel	Coconut
Butiric (4:0)	-	-	-	-	-	-	-	-	-	-
Caproic (6:0)	-	-	-	-	-	-	-	-	0.2	-
Caprylic (8:0)	-	-	-	-	-	0.1	-	-	4	7.1
Capric (10:0)	-	-	0.6	0.2	-	-	3.9	7.3	4.3	-
Lauric (12:0)	-	0.1	-	-	0.5	0.7	-	-	50.4	54.1
Myristic (14:0)	2.5	0.3	0.1	-	0.9	0.4	-	-	17.3	17.4
Palmitic (16:0)	40.8	10.9	5.1	6.5	20	13.7	11.2	11	7.9	6.1
Stearic (18:0)	3.6	3.2	2.1	4.5	3	2.3	1.8	2.2	2.3	1.6
Oleic (18:1)	45.2	24	57.9	21	25.9	-	25.4	77	11.9	5.1
Linoleic (18:2)	7.9	54.5	24.7	68	48.8	47.8	60.3	8.9	2.1	1.3
Linolenic (18:3)	-	6.8	7.9	-	0.3	29.2	1.1	0.6	-	-
Arachidic (20:0)	-	0.1	0.2	-	-	1.3	0	-	-	-
Gadoleic (20:1)	-	-	1	-	-	1.2	-	0.3	-	-
Behenic (22:0)	-	0.1	0.2	*	-	3	-	-	-	-
Erucic (22:1)	-	-	0.2	-	-	0.1	-	-	-	-
Saturated	46.9	14.7	8.3	11	25	21.7	13.2	13.2	86	93.6
Unsaturated	53.1	85.3	91.7	89	75	78.3	86.8	86.8	14	6.4

\*(nn:x) means a fatty acid with nn carbon atoms and x double bonds



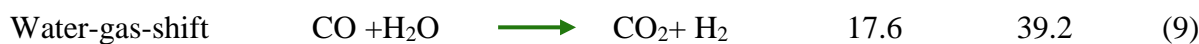
Figure 2: Examples of saturated and unsaturated free fatty acids

To convert a fatty acid into a hydrocarbon a deoxygenation (DO) reaction must be carried out. It is a widely used process for producing alternative fuels, the so-called biofuels, to the currently massively used petroleum-based fuels. Hence, many studies on the deoxygenation of fatty acids aiming to produce linear hydrocarbons following different routes of reaction can be found in the literature. The most commonly encountered pathways are: decarboxylation (DCX), (3), decarbonylation (DCN), (4), (5) and hydrodeoxygenation (HDO), (6). DCX and DCN remove the whole functional group by carbon–carbon bond cleavage, releasing respectively CO or CO<sub>2</sub>, hence producing a hydrocarbon with one carbon atom less than the original fatty acid. These two reactions can be carried out under inert atmosphere and with few amounts of hydrogen [6-8]. In contrast, HDO requires the presence of a high quantity of hydrogen to reduce the oxygenated species present in the FFA and leads to a hydrocarbon with the same number of carbon atoms as the original fatty acid [9]. The need of large amounts of hydrogen for HDO limits the process application from an economic standpoint compared to DCN or DCX reactions. Thus, DCX and DCN reactions are much more interesting compared to HDO in order to reduce hydrogen consumption and permit to design a more cost-effective process. In parallel to the deoxygenation, other undesirable reactions such as cracking, ketonisation and dehydrogenation can also occur. Other consecutive reactions can also occur depending on the reaction conditions. For instance CO, CO<sub>2</sub>, H<sub>2</sub> and H<sub>2</sub>O formed from DCX/DCN reactions can lead to Methanation (8) and water gas shift (9) reactions [10].

<b>Liquid-phase reactions</b>		$G^{\circ}_{573}$ (kJ.mol <sup>-1</sup> )	$\Delta H^{\circ}_{573}$ (kJ.mol <sup>-1</sup> )
Decarboxylation	$\text{RCOOH} \longrightarrow \text{RH} + \text{CO}_2$	-83.5	9.2 (3)
Decarbonylation	$\text{RCOOH} \longrightarrow \text{R}'\text{H} + \text{CO} + \text{H}_2\text{O}$	-17	179.1 (4)
Decarbonylation	$\text{RCOOH} + \text{H}_2 \longrightarrow \text{RH} + \text{CO} + \text{H}_2\text{O}$	-67.6	48.1 (5)
Hydrodeoxygenation	$\text{RCOOH} + 3\text{H}_2 \longrightarrow \text{RCH}_3 + 2\text{H}_2\text{O}$	-86.1	-115.0 (6)

R and R' are alkane and alkene respectively

---

**Gas-phase reactions**


For these reasons, a deep understanding of the factors favoring the different routes and the side reactions is highly important to better control the selectivity and hence optimize the yield in the desired alkane.

As it will be described in more details in the bibliography survey (Chapter 1), noble metals-based catalysts have shown excellent results for the decarboxylation of fatty acids to n-alkane [10]. However, they quickly deactivate, which is detrimental to the recyclability and economy of the process [6]. Additionally, the high cost and low abundance of noble metal are serious constraints for a large-scale application. Therefore, the development of more affordable catalysts showing good performances and stability is of great interest from an industrial point of view.

In consequence, the aim of this thesis is to develop highly active, selective and stable catalysts based non-noble metals for the decarboxylation of fatty acids to n-paraffins. In this context, a set of different mono and bimetallic nanoparticles-supported catalysts have been synthesized, characterized and tested using the high-throughput equipment of the REALCAT platform with the objective to select the best catalytic system before optimizing the operating conditions of the process. More particularly, the catalytic decarboxylation of palmitic acid (PA) into n-pentadecane (PD) was studied as a model reaction. Actually, the production of biosourced HNP would be of high interest for Weylchem, the company which funded this work, as it could be used for the manufacture of, not only biodegradable, but also biosourced detergents.

The present manuscript is organized as follows: Chapter 1 provides an overview of the literature on the decarboxylation of fatty acids into hydrocarbons with a special focus on the recent researches involving the use of non-noble metal catalysts. Chapter 2 concerns the description of the experimental set-ups and procedures. It describes in details the catalysts preparation, characterization, the method of evaluation of their catalytic performances, as well as the analytical methods. The results of the catalysts characterization are presented and

discussed in Chapter 3. Chapter 4 focusses on the reactivity of the monometallic catalysts in the decarboxylation of PA while Chapter 5 focusses on the reactivity of the bimetallic catalysts. In both cases, the influence of the operating parameters on the catalytic performance was studied. The manuscript ends by general conclusions and some perspectives to this study.

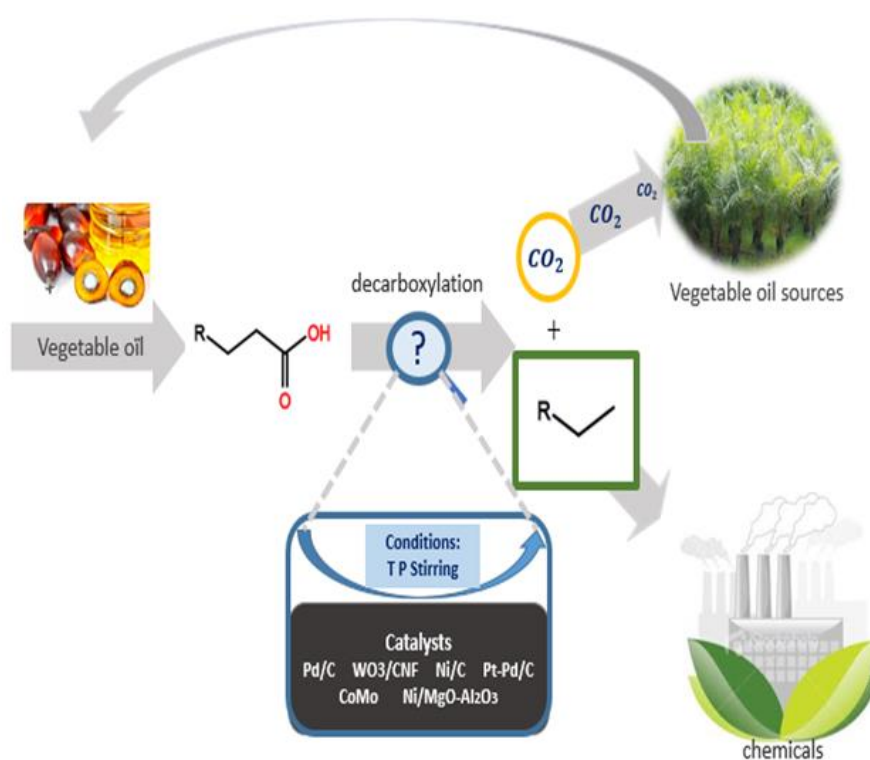
### References

- [1] P. Mul, H.C.W. Rommens, EP patent 2995669, March 16, 2016.
- [2] <http://www.roperId.com/science/minerals/FossilFuelsDepletion.htm>, accessed June 14, 2017.
- [3] V. Agbor, C. Carere, N. Cicek, R. Sparling, D. Levin, *Advances in Biorefineries*, Woodhead Publishing, 2014, pp. 234-258.
- [4] A.K. Kumar, S. Sharma, *Bioresources and Bioprocessing*. 4 (2017) 7.
- [5] [http://journeytoforever.org/biofuel\\_library/chemoils.html](http://journeytoforever.org/biofuel_library/chemoils.html), accessed, February 14, 2017.
- [6] E. Santillan-Jimenez, M. Crocker, *Journal of Chemical Technology & Biotechnology*. 87 (2012) 1041-1050.
- [7] E. Santillan-Jimenez, T. Morgan, J. Lacny, S. Mohapatra, M. Crocker, *Fuel*. 103 (2013) 1010-1017.
- [8] I. Kubičková, M. Snåre, K. Eränen, P. Mäki-Arvela, D.Y. Murzin, *Catalysis Today*. 106 (2005) 197-200.
- [9] R.W. Gosselink, S.A. Hollak, S.W. Chang, J. van Haveren, K.P. de Jong, J.H. Bitter, D.S. van Es, *ChemSusChem*. 6 (2013) 1576-1594.
- [10] M. Snåre, I. Kubičková, P. Mäki-Arvela, K. Eränen, D.Y. Murzin, *Industrial & Engineering Chemistry Research*. 45 (2006) 5708-5715.

---

# Chapter 1

## Bibliography Synthesis



## SUMMARY

<b>INTRODUCTION .....</b>	<b>28</b>
<b>I. DECARBOXYLATION OF FATTY ACIDS.....</b>	<b>29</b>
I.1. DEFINITION .....	29
I.2. DECARBOXYLATION/DECARBONYLATION PATHWAYS OF FATTY ACIDS.....	29
I.2.1. Influence of the nature of the catalyst .....	29
I.2.2. Influence of the reaction atmosphere.....	32
I.2.2.1. Under inert atmosphere .....	32
I.2.2.2. Under H <sub>2</sub> -containing atmosphere .....	33
<b>II. PD-BASED CATALYSTS FOR THE DECARBOXYLATION OF FATTY ACIDS .....</b>	<b>34</b>
II.1. PREPARATION OF THE PD-BASED CATALYSTS .....	34
II.2. INFLUENCE OF THE CATALYSTS PROPERTIES AND LOADING ON THE PERFORMANCES .....	34
II.2.1. Effect of the Pd metal particle size and dispersion .....	34
II.2.2. Effect of the Pd metal loading .....	35
II.2.3. Effect of the FFA/catalyst ratio .....	37
II.2.4. Deactivation of the Pd/C catalysts.....	37
<b>III. DECARBOXYLATION OF FATTY ACIDS OVER NON-NOBLE METAL-BASED CATALYSTS .....</b>	<b>39</b>
III.1. DECARBOXYLATION OF FATTY ACIDS OVER MONOMETALLIC CATALYSTS .....	39
III.2. INFLUENCE OF THE PREPARATION METHODS OF NI-BASED CATALYSTS.....	40
III.3. DECARBOXYLATION OF FATTY ACIDS OVER BIMETALLIC CATALYSTS.....	43
III.4. DECARBOXYLATION OF FATTY ACIDS OVER TRIMETALLIC CATALYSTS .....	43
<b>IV. CATALYTIC DECARBOXYLATION OF FATTY ACIDS: INFLUENCE OF THE REACTION CONDITIONS</b>	<b>44</b>
IV.1. INFLUENCE OF THE NATURE OF THE ATMOSPHERE .....	44
IV.2. INFLUENCE OF THE REACTION TEMPERATURE.....	47
IV.3. INFLUENCE OF THE REACTION PRESSURE .....	48
IV.4. INFLUENCE OF THE REACTION TIME .....	49
IV.5. INFLUENCE OF CHAIN LENGTH OF THE SATURATED FATTY ACID .....	49
IV.6. SUMMARY OF THE REPORTED PERFORMANCES ON NON-NOBLE METAL-BASED CATALYSTS .....	51
<b>CONCLUSION .....</b>	<b>53</b>
<b>REFERENCES.....</b>	<b>56</b>

## Introduction

The catalytic deoxygenation of FFA has been the subject of extensive researches for many years and is still under study with the aim to produce cost-effectively biosourced hydrocarbons and fuels. As said in the introduction the DO processes can follow three routes: decarboxylation (DCX), decarbonylation (DCN) and hydrodeoxygenation (HDO). The most economically attractive one is DCX because it uses very low amounts of hydrogen in contrast to HDO reaction. Moreover, in theory, this process only produces CO<sub>2</sub> and the desired hydrocarbons, which makes it very interesting. For these reasons, DCX reactions have been investigated intensively in the recent years. The reactions are generally performed in a semi-batch reactor, under an inert gas or hydrogen and preferentially at temperature and pressure ranges of 250-350°C and atmospheric pressure to 150 bar, respectively, taking into consideration the properties of the feedstock. The feedstocks studied are fatty acids in the C8 to C24 range.

In order to select the appropriate methodologies and to define the right strategy for this thesis work, it is highly important to sum up the “state of the art” on that topic. Thus, the factors influencing the catalytic decarboxylation of saturated fatty acids to alkanes over heterogeneous noble and non-noble metal catalysts will be discussed in detail in the following.

## I. Decarboxylation of fatty acids

### I.1. Definition

The decarboxylation reaction (DCX) removes the carboxyl group (-COOH) from the saturated fatty acid, hence releasing carbon dioxide (CO<sub>2</sub>) and yielding a paraffinic hydrocarbon. In the case of palmitic acid, a saturated fatty acid with 16 carbon atoms, the decarboxylation produces n-pentadecane according to the following reaction (10).



DCX was studied in the literature under different atmospheres (He, Ar, N<sub>2</sub> and 5-10 vol.%H<sub>2</sub> in N<sub>2</sub>) [1]. In parallel to DCX, other types of reaction can occur simultaneously, in particular decarbonylation (DCN), which releases CO and water and forms an olefin. However, when the reaction is carried out under hydrogen-rich atmosphere, two reactions compete: the hydrodeoxygenation reaction, which produces a n-alkane with the same number of carbon atoms than in the original fatty acid feedstock plus a molecule of water, and the decarbonylation reaction, which produces a n-paraffin with one carbon atom less than in the original fatty acid feedstock plus CO and water. Thus, to promote one route rather than another, it is necessary to better understand the possible catalytic deoxygenation pathways.

### I.2. Decarboxylation/decarbonylation pathways of fatty acids

Deoxygenation pathway of fatty acids mainly depends on the **nature of the catalyst used** [2] and the **reaction atmosphere** [3].

#### I.2.1. Influence of the nature of the catalyst

The **nature of the catalyst** is strongly related to the **nature of the metal and support** [4, 5]. To find the best catalyst for the decarboxylation reaction of fatty acids, a large variety of catalysts was developed and tested. Among all these catalysts, the most investigated are mono, bi and trimetallic catalysts supported on silica, alumina, zirconia or active carbon. Several metallic alloys have been studied as well.

Murzin and co-workers [6] have studied the deoxygenation of stearic acid (C18 saturated fatty acid) over metallic catalysts at 300 °C and under 6 bar of helium. The active phases studied were metals such as Pt, Pd, Mo, Ni, Ir, Ru, Rh, Os supported on oxides,

mesoporous materials or carbonaceous supports such as  $\text{Al}_2\text{O}_3$ ,  $\text{SiO}_2$ ,  $\text{Cr}_2\text{O}_3$ ,  $\text{MgO}$ ,  $\text{TiO}_2$  or active carbon (AC) [6]. The catalysts screening revealed that Pd and Pt supported on active carbon presented the best performances (Figure 3). For 5 wt.%Pd/AC full conversion and a selectivity as high as 95% to n-heptadecane could be obtained.

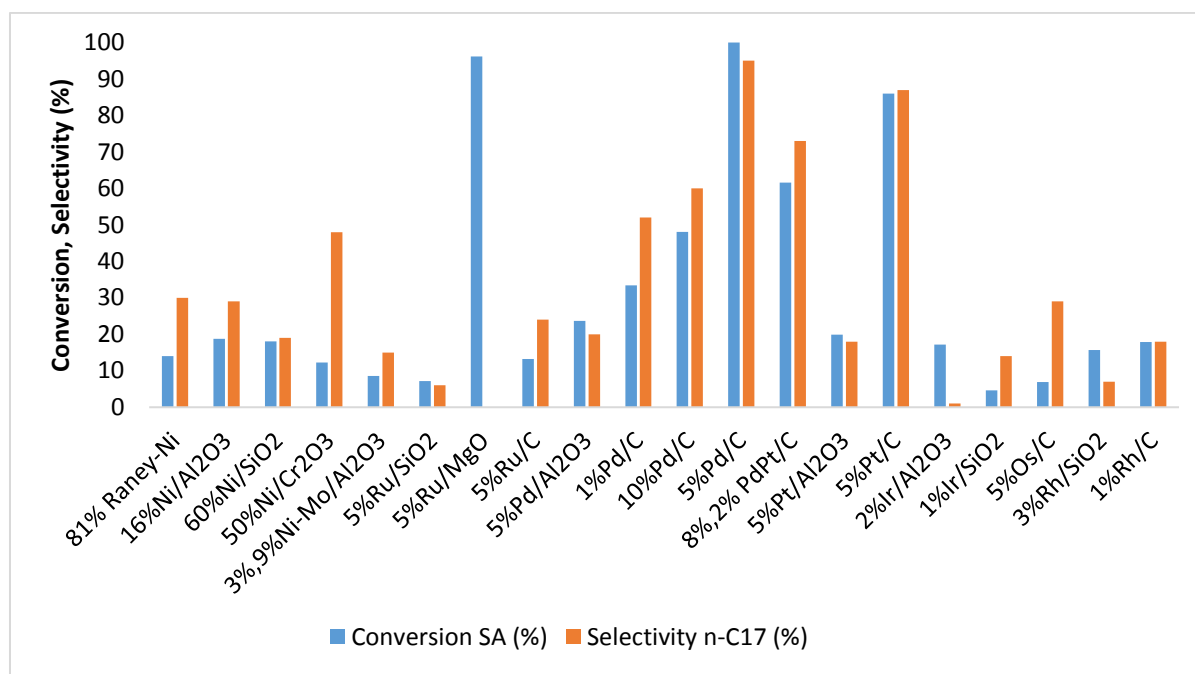
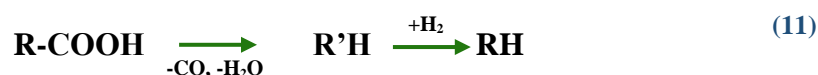


**Figure 3: Performances of a series of catalysts in the decarboxylation of stearic acid (SA) to n-heptadecane (C17). Reaction conditions:  $m_{\text{SA}} = 4.5$  g,  $m_{\text{dodecane}} = 86$  g,  $m_{\text{catalyst}} = 1$  g,  $T = 300$  °C,  $P = 6$  bar,  $F_{\text{carrier gas}} = 25$  mL/min (He). Adapted from [6]**

Immer *et al.* [5] compared the performances of catalysts containing 5 wt.% of palladium supported on  $\gamma$ -alumina ( $\text{Pd}/\gamma\text{-Al}_2\text{O}_3$ ), silica ( $\text{Pd}/\text{SiO}_2$ ) and carbon ( $\text{Pd}/\text{C}$ ) in the deoxygenation of stearic acid under an atmosphere composed of 5 vol.% of  $\text{H}_2$  in He. The results showed that the deoxygenation of SA over Pd/C proceeds *via* decarboxylation, whereas Pd/SiO<sub>2</sub> favoured decarbonylation but at a much slower rate. Pd/Al<sub>2</sub>O<sub>3</sub> exhibited a decarboxylation activity which started at lower temperatures than Pd/C. Unfortunately, this catalyst deactivated rapidly. Thus, these results imply that the decarboxylation rate of fatty acid can be greatly promoted using active carbon as support. This was attributed to the high surface area of the carbon support and to its amphoteric properties able to reduce the formation of coke inducing catalyst deactivation [6]. Moreover, it was observed that supports containing Brønsted acid sites favored isomerization reactions and Lewis acid sites lead to cracking and ketonisation [7, 8].

Berenblyum *et al.* [4] studied the influence of the nature of the metal and of the support on the DO of stearic acid to hydrocarbon under hydrogen. The catalysts based on Pd, Cu, Pt, and Ni supported on Al<sub>2</sub>O<sub>3</sub> and WO<sub>3</sub>/ZrO<sub>2</sub> were tested at 350°C. Table 2 showed the activity, selectivity and yield obtained for 5 wt.% of each metal supported on Al<sub>2</sub>O<sub>3</sub>. The results showed that the activity of the catalysts could be ranked as follows: Pd>Cu>Pt>Ni. The products distribution is also very depending on the nature of the metal employed. 5 wt.% Pd/Al<sub>2</sub>O<sub>3</sub> was reported to show an excellent selectivity to n-heptadecane, while 5 wt.% Cu/Al<sub>2</sub>O<sub>3</sub> showed a high selectivity to n-heptadecene. This is related to the fact that the activity for hydrogenation of a catalyst based on copper is very low compared to the one of a Pd-based catalyst which will favor the consecutive hydrogenation of the olefin formed by decarbonylation, as shown in reaction (11).



Where R and R' are saturated and unsaturated alkyl chains, respectively

**Table 2: Influence of the metal on the performances of the catalysts. Adapted from [4]**

Metal	Conversion, %	Selectivity, %		C <sub>17</sub> Yield, %
		Paraffins C <sub>17</sub>	Olefins C <sub>17</sub>	
Pd	100	90.1	–	90.1
Cu	95.5	20.6	60.7	77.6
Pt	92.4	48.3	0.4	45.0
Ni	60.5	49.0	10.5	36.0

Thus, the choice of the metal and of the support is highly important to determine the products distribution and the reaction rates.

### I.2.2. Influence of the reaction atmosphere

Generally, depending on the catalyst used, the DCX/DCN reactions will be favored when no H<sub>2</sub> or low concentrations of H<sub>2</sub> are used in the gas phase [6, 9, 10].

#### I.2.2.1. Under inert atmosphere

As illustrated by several studies in the literature, the catalytic deoxygenation pathway depends on the atmosphere of the reaction. Actually, it was observed that some routes are more dominant than others depending on the atmosphere of the reaction.

Murzin *et al.* [6] determined the reaction routes of stearic acid over several heterogeneous catalysts at 300 °C under inert atmosphere. Apart from the decarboxylation and decarbonylation reactions, ketonization and cracking and other consecutive reactions, such as isomerization, dehydrogenation, hydrogenation, cyclisation and dimerization occurred (Figure 4). The cracking produces shorter fatty acids and hydrocarbons, whereas the ketonization produces symmetrical ketones. Isomers of n-alkane and n-olefins can also be formed. Finally, cyclic and aromatic products can also be generated, but at very low amounts [6, 11].

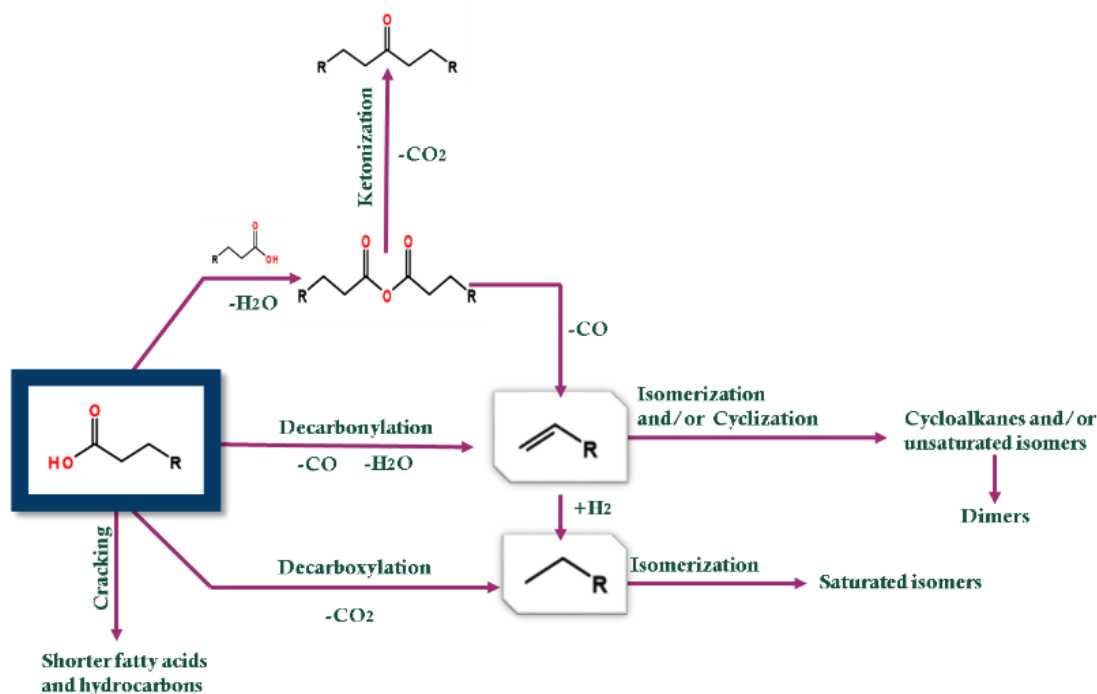
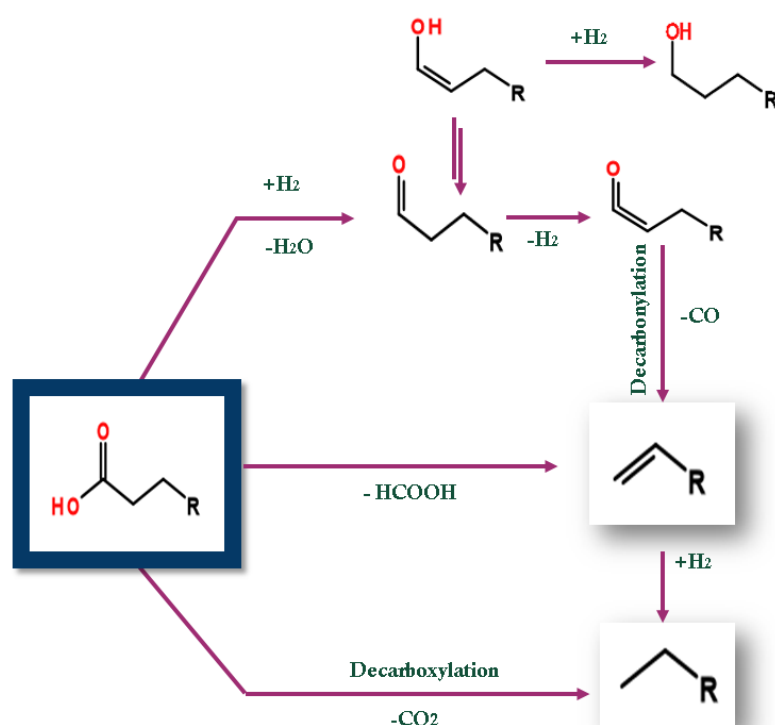


Figure 4: Deoxygenation through the decarboxylation/decarbonylation under an inert atmosphere. Adapted from [6, 11]

Under inert atmosphere, the DO of unsaturated fatty acid occurred firstly via the hydrogenation of the double bonds (C=C) to form the corresponding saturated fatty acid (for example, hydrogenation of oleic acid to stearic acid). Generally, the hydrogen needed to carry out this step originates either from residual H<sub>2</sub> present on the catalyst surface, which was adsorbed during the reductive pretreatment [11, 12] or was formed *in situ* via the simultaneous dehydrogenation reactions of the feed to unsaturated by-products such as diunsaturated acids, triunsaturated acids as well as aromatics [13]. Furthermore, compared to DO of saturated fatty acid, the DO of unsaturated fatty acid under inert gas leads to low conversion to hydrocarbons and to an increase of deactivation due to the presence of highly unsaturated compounds [11, 13, 14].

### I.2.2.2. Under H<sub>2</sub>-containing atmosphere

The reaction pathways of fatty acids deoxygenation over Pd/C catalyst under H<sub>2</sub> was investigated by Gosselink *et al.* [11] and the schematic representation is given on Figure 5. DCN of fatty acids under H<sub>2</sub> atmosphere occurs *via* an aldehyde and a subsequent ketene intermediate whereas DCX occurs *via* direct decarboxylation or *via* the release of formic acid and a subsequent hydrogenation of the olefin formed.



**Figure 5: Deoxygenation through the DCX/DCN under H<sub>2</sub> atmosphere. Adapted from [11, 15]**

The deoxygenation pathway of unsaturated fatty acids over Pd/C under H<sub>2</sub> occurs firstly *via* the hydrogenation of the double bonds to form a saturated fatty acid. This is due to the high hydrogenation activity of the Pd catalysts [4]. Then, through deoxygenation of the saturated acid, the final hydrocarbon is obtained [13, 16, 17]. Consequently, the deoxygenation pathway of unsaturated fatty acid is similar than those of a saturated fatty acid in its second step.

## II. Pd-based catalysts for the decarboxylation of fatty acids

Motivated by the high performances obtained in the first studies on catalytic deoxygenation of fatty acids over Pd/C catalyst, several studies were carried out to better understand the influence of the metal nanoparticles size, of their dispersion, of the support, of the metal loading and of the FFA/catalyst ratio. Various reaction conditions, in particular pressure, temperature, reaction time and nature of the carrier gas were also studied.

### II.1. Preparation of the Pd-based catalysts

Several techniques are described in the literature to prepare supported Pd-based catalysts as it strongly influences the physicochemical properties of the solid and, therefore, its catalytic performances. Among the various methods, the most commonly used are incipient wetness impregnation and wet impregnation [10]. But other techniques such as deposition of palladium hydroxide obtained by hydrolysis of PdCl<sub>2</sub> at different pH followed by adsorption on carbon were also used [12, 18, 19]. The variation of the pH of the palladium hydroxide solution was showed to lead to different metal particles dispersion [20]. It was observed that, to improve the total wetting of the carbon pores, the pre-treatment of its surface by HNO<sub>3</sub> during several hours is necessary [18]. However, it is also possible to use carbon directly for wet impregnation without prior treatment of the surface.

### II.2. Influence of the catalysts properties and loading on the performances

#### II.2.1. Effect of the Pd metal particle size and dispersion

Simakova *et al.* [20] studied the effect of the Pd particles size and of their dispersion on the catalytic properties in the decarboxylation of stearic acid using four different Pd/C (Sibunit) catalysts all containing 1 wt.% of Pd but with different dispersions obtained by changing the pH of the palladium hydroxide solution during the synthesis [21]. The reaction was carried out

at 300 °C under 17.5 bar of 5 vol.% of H<sub>2</sub> in Ar. The properties and performances of each catalyst are shown in Table 3. It was found that large particles (catalyst A) and highly dispersed Pd species (catalyst D) are not very active in the DO of the fatty acids. In fact, the authors found that it could be due to their small surface area and their strong interaction with the support, which lead to a modification of the metal structure of the Pd responsible for the cleavage of the C-C bonds and the effective decarboxylation of the fatty acid. Catalysts B and C showed the highest performance in stearic acid decarboxylation because of an optimal metal dispersion (with 47 and 65% respectively). The selectivity to n-heptadecane at fatty acids isoconversion shows clearly that the change in the metal dispersion affects much more the deoxygenation rate than the distribution of products.

**Table 3: Proprieties and kinetic data for deoxygenation of SA over 1wt. %Pd loading at different Pd dispersions. Adapted from [20]**

Catalyst	Metal dispersion (%)	d <sub>TEM(Pd)</sub> (nm) (b)	Initial rate (mmol/min/g <sub>cat</sub> )	TOF (s <sup>-1</sup> )	Conversion after 300 min (%)	Overall Selectivity to n-heptadecane at 50% conversion (%)	Overall Selectivity to n-heptadecane at 95% conversion (%)
A	18	6.1	0.03	30	68	49	(a)
B	47	3.1	0.2	79	100	52	47.5
C	65	2.3	0.4	109	99	54	47.5
D	72	2.8	0.05	12	96	51	48

Conditions: T = 300 °C, initial H<sub>2</sub>/N<sub>2</sub> pressure=17.5 bar, time = 5 h, catalyst loading = 1 g, stearic acid loading = 0.176 mmol. (a) 68% conversion achieved within 300 min. (b)-Pd particle size determined by TEM

### II.2.2. Effect of the Pd metal loading

Mohite *et al.* [22] studied the effect of the Pd loading on the decarboxylation of lauric acid (12:0 further noted LA) to undecane (C11). The reaction was carried out with 3 different Pd loadings, namely 1, 5 and 10 wt. % Pd/C. The results revealed that the highest activity (55%) and selectivity (67%) were reached for 10 wt. % Pd/C as presented in Figure 6.

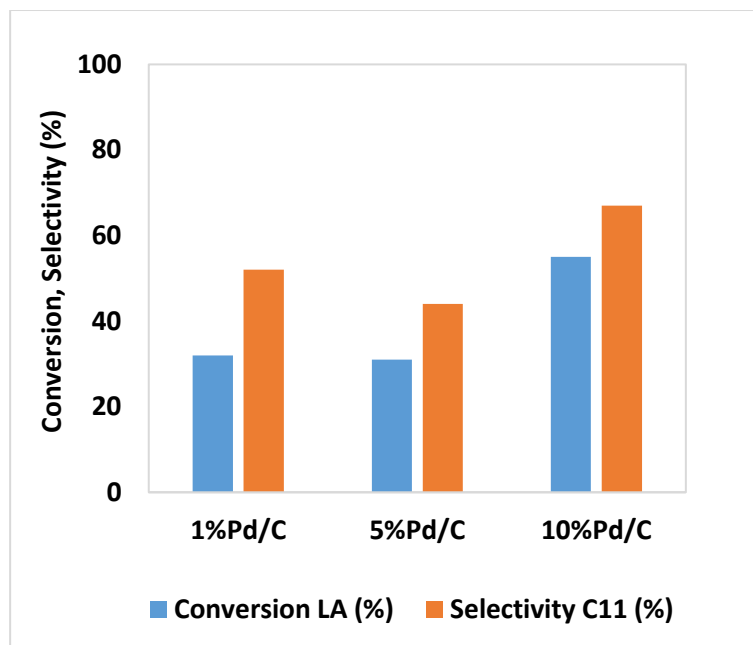


**Figure 6:** Effect of the Pd loading on the catalytic decarboxylation of lauric acid (LA). Conditions: 1.6 mmol of reactant, 100 mg of catalyst, 10 mL of solvent (dodecane+tetradecane), 300 °C, 6 h, 500 rpm, initial N<sub>2</sub> pressure 10 bar.

The effect of Pd loading was also investigated by Snåre *et al.* [6] in the same composition range as previously but this time stearic acid (SA) was used as a reactant. The results obtained (Figure 7) showed that 5%Pd/C permitted to reach the highest activity (100%) and selectivity to n-C17 (95%). On the contrary, 1%Pd/C and 10%Pd/C gave only 33.4% and 48.1% of conversion and 52% and 60% of selectivity to n-heptadecane, respectively. Indeed, it was observed that the initial reaction rates of SA is higher over 5%Pd/C than over 1%Pd/C and 10%Pd/C. The pH of the 1, 5 and 10%Pd/C catalysts slurry measured during preparation were 8.7, 10.2 and 4.9, respectively. The 5%Pd/C was therefore more alkaline compared to the two others catalysts. Thus, the authors suggested that the differences in activity observed over 5%Pd/C is due to its alkaline properties [6].

Although the Pd loading was the same in both studies of decarboxylation of LA and SA the catalytic activity of the samples was found very different. In fact, 5%Pd/C showed the best catalytic activity for the decarboxylation of stearic acid, whereas for lauric acid, 10%Pd/C was the best one. Thus, the catalytic decarboxylation of FFA depends not only on the metal loading but also, on one hand, on the catalyst properties (catalyst acidity, size and dispersion of the metal particles, textural properties, etc.) and, on the other hand, on the FFA chain length as it will also be discussed in section IV.5.

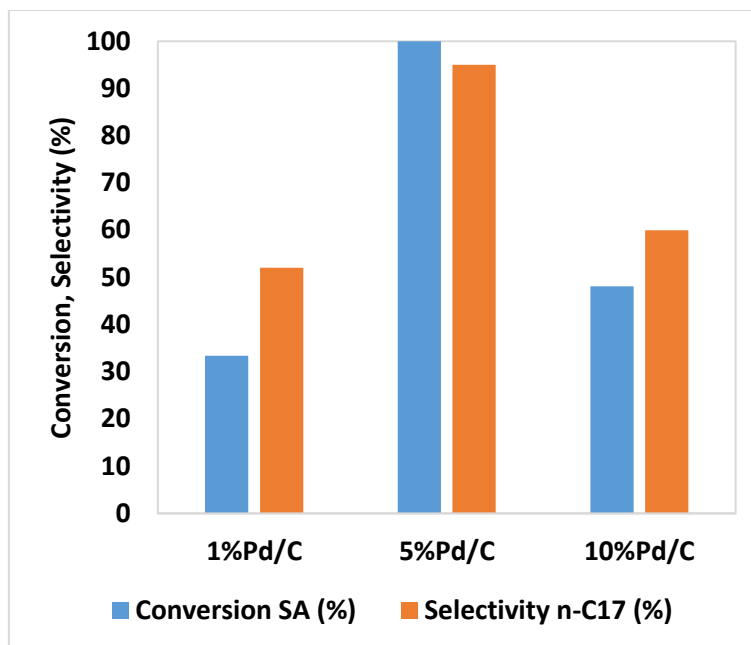


**Figure 7: Effect of the Pd loading on the catalytic decarboxylation of stearic acid (SA). Reaction Conditions:  $m_{\text{stearic acid}} = 4.5 \text{ g}$ ,  $m_{\text{dodecane}} = 86 \text{ g}$ ,  $m_{\text{catalyst}} = 1 \text{ g}$ ,  $T = 300 \text{ }^\circ\text{C}$ ,  $p = 6 \text{ Bar}$ ,  $F_{\text{carrier gas}} = 25 \text{ mL/min}$  (He)**

### II.2.3. Effect of the FFA/catalyst ratio

Maki-Arvela *et al.* [12] studied the effect of the FFA/catalyst ratio in the range 2.5-12.5 on the initial reaction rates during the SA decarboxylation over 5wt.% Pd/C catalyst at 300 °C under 6 bar of helium in dodecane. The initial reactant concentration was kept constant. As expected, it was found that the initial rate increased linearly with the FFA/catalyst ratio. Furthermore, the selectivity to n-alkane depended on the conversion. The increase of FFA/catalyst ratio decreases the reaction rate and therefore decreases the conversion and increases the selectivity to n-alkane. Finally, the higher the catalysts amount, the better the selectivity. In their study, the authors found that for the lower mass of catalyst, the formation of aromatic compounds occurred, due surely to diffusional limitations of the reactant molecules in the catalyst pores.

### II.2.4. Deactivation of the Pd/C catalysts

Ping *et al.* [23] studied the factors influencing the deactivation of Pd-based catalysts during the decarboxylation of fatty acids under hydrogen-free atmosphere. The decarboxylation of stearic acid was carried out in a batch reactor at 300 °C. The catalyst deactivated drastically after one cycle giving only 5% of conversion in the second cycle. The characterization results

of the catalyst before and after reaction revealed that deactivation was due to the coke deposition originated from the oligomerization of unsaturated hydrocarbons and heavy compounds [6]. In fact, the side reactions such as the aromatization, oligomerization, isomerization reactions and the adsorption of fatty acids and aromatic compounds on the metal sites (Pd), favor the poisoning of the catalyst which decreases its catalytic performances.

To avoid the rapid catalyst deactivation and then improve its activity and selectivity, it is also important to optimize the FFA/catalyst ratio [14]. Indeed, according to the literature, on the one hand, the increase of the mass of the catalyst during the catalytic test decreases its deactivation [12, 24]. Furthermore, in terms of selectivity, the use of a very small amount of the catalyst for DCX reactions leads to polymerization reaction, which increases the formation of undesirable aromatics and by-products [25]. On the other hand, selectivity in n-alkane over the Pd/C catalyst was found to be higher for low substrate concentrations (<0.2M).[19, 26]. Based on the literature, the best catalytic performances of the Pd/C catalyst were obtained for concentrations in 0.05-0.15 M range [6, 27, 28].

Apart from the high concentrations of FA and the small amounts of catalysts which can cause catalyst deactivation, other factors such as the reaction atmosphere, temperature and reaction time may lead to the formation of other byproducts. This will be discussed in detail in the next section.

### III. Decarboxylation of fatty acids over non-noble metal-based catalysts

Currently, many research programs concerning the decarboxylation of fatty acids are aiming to substitute noble metals by non-noble metals due to their much better availability and lower price. The main challenge is to obtain similar catalytic performances than those obtained previously with noble-metals. That is why, in the last decade, developments of non-noble metal catalyst, which would be highly active, selective and stable has been continuing to grow. In this section, the state of the art on non-noble mono-, bi- and tri-metallic catalysts used for fatty acids decarboxylation will be presented.

#### III.1. Decarboxylation of fatty acids over monometallic catalysts

Recently, Wu *et al.* [29] have screened under inert gas a set of three metallic (Ni, Co and Cu) catalysts supported on alumina, zirconia, silica and carbon for catalytic decarboxylation of SA into heptadecane. The metal loading of each metal was 20%, excepted for this supported on silica, which was loaded at 40%. As observed (Figure 8), the catalytic performances of the catalyst are influenced not only by the metal loading, but also by the choice of the support used. The results showed that, Cu is more active (36.3 %) and less selective (22.9%) when it is supported on zirconia than when the support is alumina. Indeed, the SA conversion was only 17%, whereas the selectivity to heptadecane reached 59% in the latter case. Similarly, the Ni/C showed 37.1% of conversion and 89.1% of selectivity, whilst the conversion increased slightly (37.4%) and the selectivity decreased (79.4%) on Ni/ZrO<sub>2</sub>. Concerning the catalytic performances of the 40%Ni/SiO<sub>2</sub> catalyst, the conversion and the selectivity to heptadecane were higher than 50%. However, the yield of heptadecane was lower (27.7%) than that obtained on Ni/C (33.1%).

The comparison of the catalytic performances for Cu, Co and Ni based-catalysts supported on zirconia showed that, Co is more active (74.8%) for the decarboxylation of SA, but weakly selective to heptadecane (8.9%). In contrast, Ni/ZrO<sub>2</sub> showed good activity (37.4%) and high selectivity to heptadecane (79.4). The conversion over Cu/ZrO<sub>2</sub> showed lower activity (36.3%) and selectivity (22.9%) than the Ni/ZrO<sub>2</sub> catalyst.

To conclude, Ni is the most interesting metal as it is simultaneously active and selective. When supported on carbon it can reach very high selectivity to heptadecane.

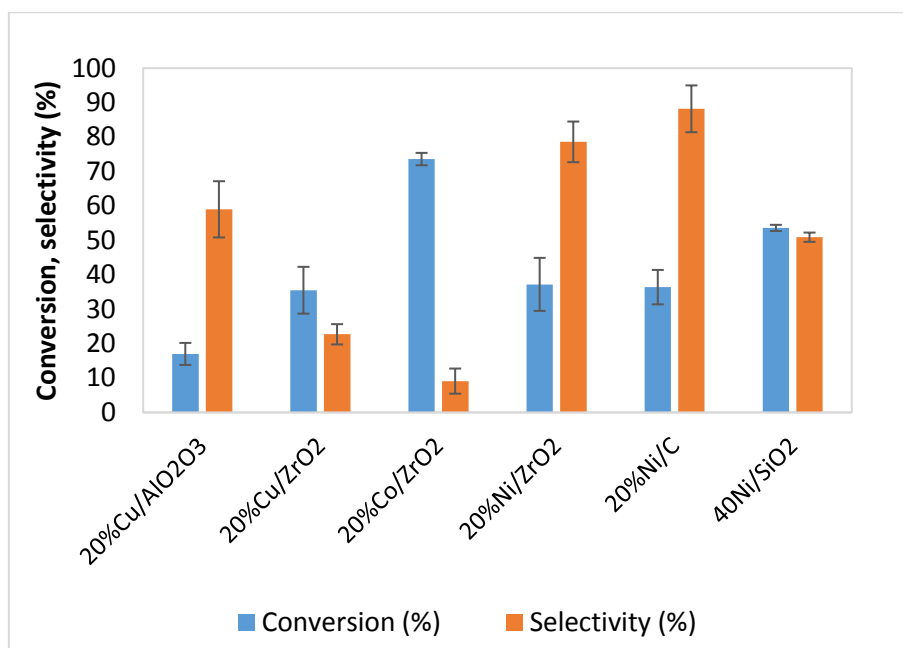


**Figure 8: Catalysts screening in the decarboxylation of SA. Reaction conditions: T = 330 °C, time = 5 h, catalyst loading = 30 mg, stearic acid loading = 0.176 mmol.**

Based on the previous encouraging results, Wu *et al.* [29] decided to study in more detail the decarboxylation of saturated fatty acids over the Ni/C catalyst under an inert atmosphere. The results showed that stearic acid can be completely converted at 370 °C in 5 h with about 80% of selectivity to heptadecane.

### III.2. Influence of the preparation methods of Ni-based catalysts

The performances of a supported metal catalysts are strongly influenced by the nature and physicochemical properties of the support and, of course, by the nature of the active metal selected but also and mainly by the method used for the preparation as it defines the properties of the active species (size of the metal particles, dispersion, etc.)

Many protocols exist to prepare supported metal catalysts. Among them the most common ones are impregnation, ion-exchange, deposition-precipitation and co-precipitation [30].

Impregnation is a technique in which a solution of the precursor of the active phase is contacted with the solid support. Among the methods of impregnation can be distinguished: incipient wetness impregnation (IWI), wet impregnation (WI), and co-impregnation (co-I). The

difference between IWI and WI is the volume of solution containing the precursor of active phase which is used. Indeed, WI is done using an excess of solution, while IWI required just enough solution of precursors to fill the pore volume of the support. Co-I is used when several active phase precursor solutions need to be simultaneously brought in contact with the support. After impregnation, the material obtained is dried to remove the solvent. However, depending on the metal loading, the size of the metal particles and the desired dispersion, the use of impregnation methods could be limited. For instance, in the case of the IWI method, the maximum of the active phase loading is limited by the solubility of the precursor in the solution and by the pore volume of the support. So, to obtain high loadings and high dispersion of the active phase material, successive impregnations need to be repeated. Furthermore, during the impregnation method, the active phase of the catalyst could be located outside of the particle, leading to the formation of large crystals. In general, with impregnation methods the interaction between the metal precursor and the support is very low. Thus, to obtain high active phase loadings with high dispersion on the support, another technique needs to be applied. The deposition-precipitation (DP) method is well known to be effective to obtain high loadings and homogeneous dispersion [31, 32]. This technique involves two main important steps. The first one is the precipitation of the metal ions from the bulk solutions, and the second step is the interaction with the support [33]. This technique is based on the use of a reducing agent which precipitates the precursor. Most of the reducing agents are effective under basic conditions that are above the point of zero charge (PZC) for most supports [31]. For instance,  $\text{NaBH}_4$ ,  $\text{NaOH}$ ,  $\text{CO}(\text{NH}_2)_2$  could be chosen as reducing agents. However, the choice of the reducing agent depend on the metal used (Table 4) [34].

The metal ions deposited after adding the reducing agent are in hydroxide form. When preparing supported catalysts, it is necessary to avoid the precipitation in the solution because this would lead to the deposition of the active metal outside of the pores of the support [31]. To avoid the latter, the suspension must be vigorously stirred and the pH must be adjusted slowly. A well-dispersed and homogeneous active phase is reached when the  $\text{OH}^-$  groups of the support interact directly with the ions present in the solution [33].

**Table 4: Reducing agents used for different metals. Adapted from [34]**

Reducing agent	Order of catalytic activity
HCHO at pH 12.5, 25°C	Cu > Co ~ Au > Ag > Pt > Pd > Ni
BH <sub>4</sub> <sup>-</sup> at pH 12.5, 25°C	Ni ~ Co ~ Pd > Pt > Ag ~ Au > Cu
DMAB at pH 7, 25°C	Ni > Co > Pd > Pt ~ Au > Ag > Cu
N <sub>2</sub> H <sub>4</sub> at pH 12, 25°C	Co > Ni > Pt ~ Pd > Cu > Ag > Au
H <sub>2</sub> PO <sub>2</sub> <sup>-</sup> at pH 9, 70°C	Au > Pd ~ Ni > Co > Pt > Cu > Ag

In the literature, 20 wt.%Ni/C catalyst was prepared by IWI using aqueous Ni(NO<sub>3</sub>)<sub>2</sub> as the precursor and activated carbon as the support. The impregnated material was aging at room temperature for 1 h and then dried in a rotary evaporator under vacuum at 80 °C. After drying, the material was calcined under flowing N<sub>2</sub> at 350 °C for 3 h to decompose the metal salt [35]. However, this catalyst was found to favor the strong adsorption of carbonaceous species on its surface and the formation of cracking reactions leading to a decrease of the conversion and of the selectivity to long chain hydrocarbons. The authors attributed that to the strong acidity of the catalyst in terms of strength and amounts of acid sites [10].

Wojcieszak *et al.* [36] demonstrated in their studies that nickel nanoparticles (Ni NPs) supported on activated carbon prepared by deposition-precipitation using hydrazine as reducing agent is more active than when the catalysts is prepared by classical impregnation methods. The authors attributed the increase of the performances of the catalyst to a combination of surface metal atom reactivity, metal–support interaction strength, and the increase of the specific surface area of the catalysts.[36].

Many researchers suggest that Ni-based catalysts favor the C–C cleavage. However, these catalysts are also known to favor the deposition of carbon, which is responsible for the rapid deactivation of the catalysts leading to a rapid decrease of their catalytic performances. Therefore, the bimetallic Ni-Cu catalysts were studied, in order to avoid deactivation by carbon formation. In fact, copper is known as a strong inhibitor of coke formation [37, 38]. Indeed, Galea *et al.* [39] suggest that the formation of carbon deposits on Ni particles occurs at step edges and that these are the sites preferentially occupied by Cu. That is the reason of the reduction of deactivation of the Ni-Cu catalyst [38, 39]. Furthermore, the catalytic

performances of the bimetallic Ni-Cu/AC was found to be significantly enhanced by the addition of an equal amount of Ni as compared to the monometallic counterpart [40].

Given that the metal loading content of the non-noble based catalysts is preferably in the range of 10%-30% [10, 24, 29], the deposition-precipitation method is the appropriate preparation method for this type of catalyst because, as said before, it allows to get a high dispersion of the active phase on the support at a high metal loading.

### III.3. Decarboxylation of fatty acids over bimetallic catalysts

In order to improve the catalytic performances of 20%Ni/Al<sub>2</sub>O<sub>3</sub>, Mark Crocker *et al.* [41] have studied the catalytic deoxygenation of stearic acid over alumina-supported bimetallic Ni-Cu and Ni-Sn catalysts. The reactions were performed at two different temperatures (260 and 300 °C), under 20 bar of H<sub>2</sub> and for 1.5 h. The results obtained are depicted in Table 5. The results show that Cu, contrary to Sn, is a very effective promoter of Ni for the DCX/DCN of stearic acid at both 260 and 300 °C. SA conversion increased from 92% over 20% Ni/Al<sub>2</sub>O<sub>3</sub> to 98% over 20% Ni-5%Cu/Al<sub>2</sub>O<sub>3</sub> at 300 °C. Also, the selectivity to C17 increased from 66 to 79 respectively at 300 °C. The reasons of this promoting effect of Ni by Cu is that Cu enhances the reducibility of Ni and suppresses both cracking reactions and coke-induced deactivation [41].

**Table 5: Deoxygenation of stearic acid over alumina-supported Ni-Cu-based catalysts (adapted from [41])**

Catalysts	T (°C)	Conversion (%)	Selectivity to C10-C17 (%)	Selectivity to C17 (%)
20% Ni/Al <sub>2</sub> O <sub>3</sub>	260	39	15	2
20% Ni-5% Cu/Al <sub>2</sub> O <sub>3</sub>	260	54	13	7
20% Ni-1% Sn/Al <sub>2</sub> O <sub>3</sub>	260	30	7	3
20% Ni/Al <sub>2</sub> O <sub>3</sub>	300	92	76	66
20% Ni-5% Cu/Al <sub>2</sub> O <sub>3</sub>	300	98	86	79
20% Ni-1% Sn/Al <sub>2</sub> O <sub>3</sub>	300	39	23	17

### III.4. Decarboxylation of fatty acids over trimetallic catalysts

In order to develop an economic catalyst for the deoxygenation reaction, Chiam *et al.* [42] decided to study the performances of the trimetallic NiSnK/SiO<sub>2</sub> catalyst for the DO of

palmitic acid. Firstly, they investigated palmitic acid DO at three different temperatures (250, 300 and 350 °C). They found that the highest conversion (about 90 %) of palmitic acid was achieved at higher temperature (350 °C) as expected. Secondly, they studied the effect of the WHSV (weight hourly space velocity) on the conversion. They found that the conversion of PA decreased with the increase of space velocity, as expected. Finally, they studied the influence of the time of reaction, varying the WHSV and they found that when the contact time increased, three isomers of n-pentadecane were formed as well as n-pentadecene and its isomers. Thus, NiSnK/SiO<sub>2</sub> was found to decarboxylate PA into n-pentadecane with some decarbonylation and isomerizations products. Unfortunately, the selectivities to C15 are not reported in the paper [42].

#### IV. Catalytic decarboxylation of fatty acids: influence of the reaction conditions

Previously, it was reported the nature of the catalyst used (depending on itself on the nature of the support, the metal used, the loading and dispersion of the active phase, etc.) has a strong effect on the deoxygenation process of fatty acids. However, apart from the type of heterogeneous catalyst used, the reaction conditions are known to impact significantly the deoxygenation process as well. For this reason, in the following section, the influence of carrier gas, temperature, pressure and of the length of the carbon chain of the FA will be presented, in order to discuss their impact on the activity and the selectivity to the desired hydrocarbon.

##### IV.1. Influence of the nature of the atmosphere

Crocker and co-workers reported deoxygenation through decarboxylation/decarbonylation of fatty acids over a 5 wt.%Pd/C catalyst as a function of the carrier gas employed for the reaction (N<sub>2</sub>, 10 vol.% H<sub>2</sub> in N<sub>2</sub> or H<sub>2</sub>) [9]. The results obtained are reported in Figure 9. Under 10% H<sub>2</sub>, very high activity (99%) and selectivity to heptadecane (97%) were obtained compared to under pure N<sub>2</sub> and H<sub>2</sub>. This was attributed to the presence of 10%.vol H<sub>2</sub> able to hydrogenate the unsaturated and aromatic hydrocarbons, which are responsible for coke formation and catalyst deactivation. Thus, the formation of undesirable byproducts was limited and the selectivity to the desired hydrocarbon was very high. In contrast, under inert atmosphere, the activity of the catalyst was only 58% and the selectivity to C17 was lower (87%). The reason was the lack of hydrogen in the atmosphere which increases the formation of unsaturated species that could be cracked and/or accumulate on the catalyst surface and

therefore decreases its catalytic performances [6]. Finally, under pure H<sub>2</sub>, the DCX reaction was slowed down because of the competitive adsorption between the fatty acid and H<sub>2</sub> [27, 43].

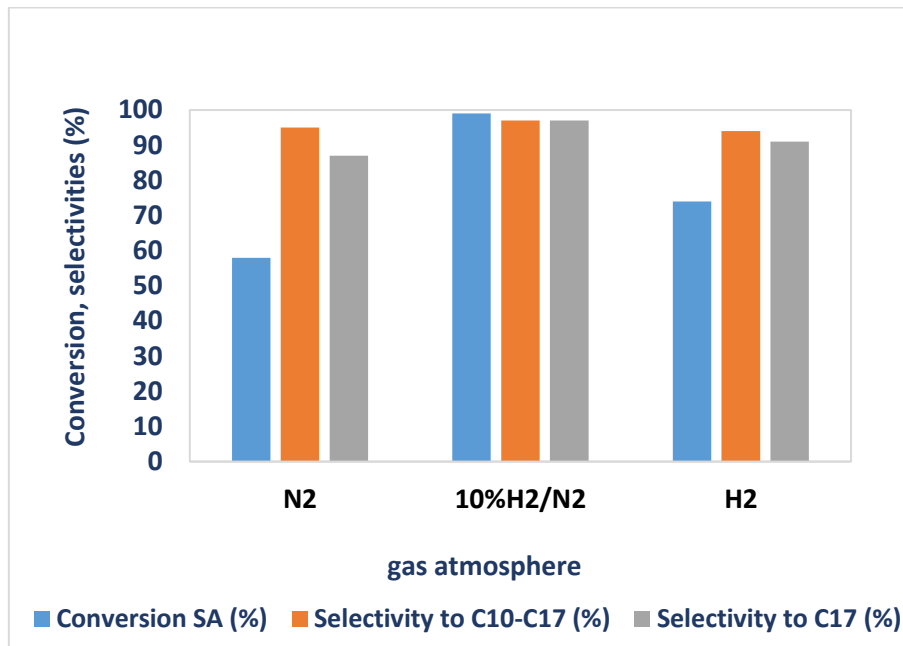
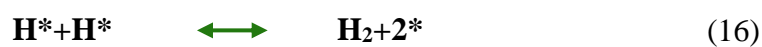
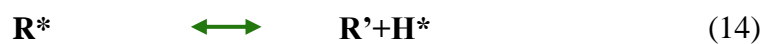


Figure 9: Effect of the gas atmosphere on the performances in SA decarboxylation of 5 wt.%Pd/C catalyst

As it was already stated before, under inert gas, the deoxygenation occurs *via* decarboxylation, whereas, under H<sub>2</sub>, decarbonylation prevails [6, 15]. Indeed, the increase of H<sub>2</sub> pressure strongly decreases the decarboxylation reaction rate. Therefore, H<sub>2</sub> is involved in the decarboxylation pathway [44].

Immer *et al.* [28] proposed the following sequence of elementary steps for decarboxylation of free fatty acids over a 5 wt.%Pd/C catalyst.



where \* is a catalytic site or ensemble, R is a paraffinic hydrocarbon and R' is an olefinic hydrocarbon.

In fact, the carboxylic group of the FA undergoes a dissociative chemisorption on the catalyst surface to form a surface carboxylate and an adsorbed H (equation (12)). Under high  $H_2$  pressure, this adsorption step is inhibited by the high concentration of H atoms on the catalyst surface, leading to the hydrogenation of the carboxylate. Under lower  $H_2$  pressures, this surface carboxylate is cleaved along the C-COOH bond, leaving an alkyl group bound to the catalyst (equation (13)). The resulting alkyl species can either undergo  $\beta$ -hydride elimination to yield an olefin and an excess H on the surface (equation (14)) or be hydrogenated by surface H to yield an n-alkane (equation (15)). Surface H species can also react to generate gaseous  $H_2$  (equation (16)) [44].

Furthermore, Immer *et al.* shown that the initial rate of decarboxylation of stearic acid under He is approximately 3-fold greater than under 10%  $H_2$ . However, rapid catalyst deactivation occurred under pure He [44]. In 10%  $H_2$ , catalyst lifetime was improved approximately 10 times. Thus, even if  $H_2$  is not consumed during the decarboxylation reaction, it improved significantly the lifetime of supported Pd catalysts. Moreover, the Immer group demonstrated that during the deoxygenation of fatty acids on 5 wt.%Pd/C catalyst under He a concomitant generation of  $CO_2$  and  $H_2$  occurred (Figure 10) [33].

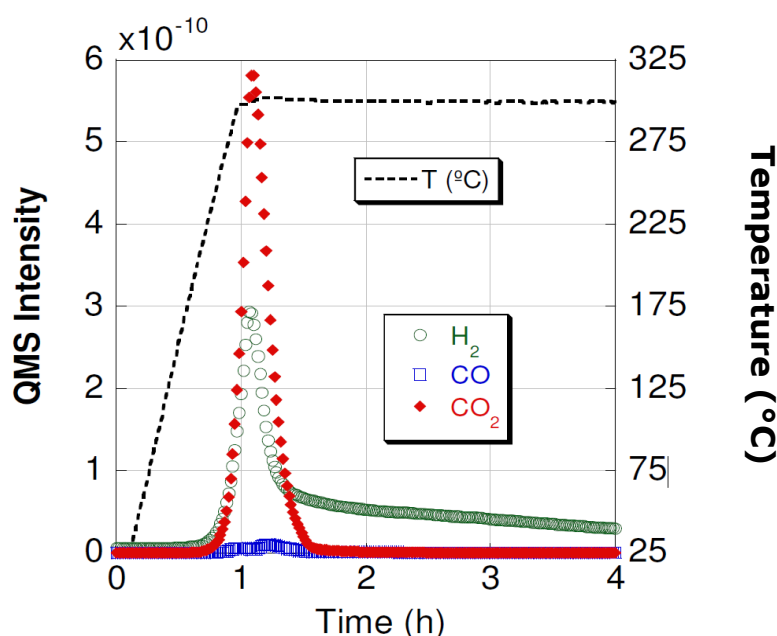


Figure 10: Stearic acid deoxygenation under He evidenced co-production of  $CO_2$  and  $H_2$ . Adapted from [33]

Crocker and co-workers carried out catalytic tests in a semi-batch reactor over 20 %Ni/C and 20%Ni/Al<sub>2</sub>O<sub>3</sub> catalysts. They studied the deoxygenation of stearic acid through a decarboxylation process. The tests were performed under three different atmospheres (N<sub>2</sub>, 10% vol. H<sub>2</sub> in N<sub>2</sub>, and H<sub>2</sub>) at 300 °C, for 1.5h. The results obtained are reported in Table 6.

**Table 6: Deoxygenation of stearic acid over carbon-supported nickel catalyst. Results adapted from [10]**

Catalyst	Feed	Gas	Conversion (%)	Selectivity to C10-C17 (%)	Selectivity to C17(%)
20%Ni/C	Stearic acid	N <sub>2</sub>	19	50	26
20%Ni/C	Stearic acid	10%H <sub>2</sub> /N <sub>2</sub>	64	77	51
20%Ni/C	Stearic acid	H <sub>2</sub>	80	88	81
20%Ni/Al <sub>2</sub> O <sub>3</sub>	Stearic acid	N <sub>2</sub>	9	48	38
20%Ni/Al <sub>2</sub> O <sub>3</sub>	Stearic acid	10%H <sub>2</sub> /N <sub>2</sub>	80	85	67
20%Ni/Al <sub>2</sub> O <sub>3</sub>	Stearic acid	H <sub>2</sub>	81	84	57

The results showed that the conversion of SA and the selectivity to heptadecane for 20%Ni/C catalyst are more effective when the reaction is run in the presence of pure hydrogen than under either N<sub>2</sub> or 10%H<sub>2</sub> in N<sub>2</sub>. The same observation was made for the 20%Ni/Al<sub>2</sub>O<sub>3</sub> catalyst. In all cases, the Ni-based catalysts showed the best performances when H<sub>2</sub> is used. Moreover, the selectivity to C17 obtained on 20%Ni/C catalyst was much higher than that obtained on 20%Ni/Al<sub>2</sub>O<sub>3</sub> catalyst.

## IV.2. Influence of the reaction temperature

The deoxygenation of fatty acids under inert atmosphere is endothermic. Thus, the DO reaction is preferable carried out at high temperature (250-380°C) [24]. Indeed, it was mentioned that the increase of the temperature enhanced the reaction rate of the DO of all of the fatty acids [45-47]. However, the selectivity depends on the reaction time and on the acid chain length. For long chain (C16), Simakova *et al.* [20] have obtained complete conversion of PA at 300 °C whereas, at 260 °C, only 50% was obtained. In fact, it was shown that an increase of temperature increases the initial reaction rate of the deoxygenation [18]. Thus, the conversion was increased by increasing the reaction temperature as expected. However, it was reported that at much higher temperature, the selectivity to the desired product could be affected by the formation of undesired products such as shorter fatty acids and hydrocarbons from cracking of high chain length species, symmetrical ketones from ketonization, dimers from aromatization

or oligomerization [6], or by the coke deposition at the surface of the catalyst [11, 14]. Wu *et al.* [29] also tested three different temperatures from 330 to 370 °C in the decarboxylation of SA over 20 wt.%Ni/C. It was observed that for the same reaction time, the conversion of fatty acid increased significantly when the temperature was increased and reached complete conversion after 5 h of reaction at 370 °C. In contrast, the selectivity is slightly higher at 330 °C compared to 370 °C for 5 h of reaction.

In contrary, for medium chain length (LA), Mohite *et al.* [22] found that the temperature increased not only the conversion but also accelerated the desired alkane formation by decarboxylation. Thus, the formation of the desired product was dominant over cracking of high chain length species to shorter fatty acids and hydrocarbons and other reactions susceptible to be formed at high temperature.

Similarly, the increase of the temperature for the deoxygenation of fatty acids under H<sub>2</sub> atmosphere promoted the increase of the conversion. According to that observation, temperature does not influence strongly the DO pathway. Therefore, the reaction pathway (DCX/DCN)/HDO depends essentially on the catalyst used [14].

Based on the foregoing results, to obtain the better catalytic performances in the DO reaction, it is important to optimize the temperature of the reaction to have a perfect equilibrium between the conversion and the selectivity to the desired product as a function of the fatty acid used and the time of reaction.

### IV.3. Influence of the reaction pressure

As previously mentioned, the DO reaction in liquid phase is preferably carried out at high temperature (250-380°C). Therefore, in order to maintain the reactants in the liquid phase at a given reaction temperature, it is preferable to use a reaction pressure higher than the vapor pressure of the reactants. Thus, the reaction pressure could be used from atmospheric pressure to 150 bar range, preferably between 1 and 50 bar, taking into account the properties of the reactants [14].

Mohite *et al.* [22] have studied the effect of the variation of the reaction pressure in (18-75 bar) range, using lauric acid (n-C12 noted LA) as the substrate. It was showed that an increase of pressure decreases the LA conversion from 55% to 40%, while, the selectivity to undecane (n-C11) increases from 67 to 90%. This phenomenon was found to keep the reaction yield constant. The authors attributed that to the ability of high pressure to suppress parallel

and/or consecutive side reactions, in particular those leading to an increased number of moles following Le Chatelier's principle [22].

#### IV.4. Influence of the reaction time

The residence time determines the distribution of the products. Indeed, Mohite *et al.* [22] reported that when the time of reaction increased, the conversion increased, while the selectivity to the desired product dropped down. This decreasing of the selectivity is due to the formation of undesired byproducts, which are produced by the secondary and competitive reactions of cracking, isomerization, dimerization, etc. [6]. Generally, the catalytic decarboxylation reaction is the major one after 5-6 h of reaction. Wu *et al.* [29] reported also that when the reaction was performed at 370 °C, the increase of the reaction time (1 h to 5 h) increases significantly the conversion but that the selectivity to the n-alkane decreased slightly. In their studies, Wu *et al.* [29] obtained the best performance after 5 h but obviously the optimal time of reaction depends on the reactivity of the catalyst used and on the other operating conditions.

#### IV.5. Influence of chain length of the saturated fatty acid

According to the sequence of elementary steps of decarboxylation of saturated FA over a 5 wt.%Pd/C catalyst proposed by Immer and coworkers, which is described in the section IV.1, the initial rates for decarboxylation of various saturated FA should be roughly the same over a given catalyst. Indeed, as it was observed, the hydrocarbon chain in fatty acid is inert towards the catalyst surface, whereas the carboxylic group is adsorbed on it [20]. This surface carboxylate is cleaved along the C-COOH bond, resulting in aliphatic straight chain hydrocarbons containing one carbon less than the corresponding carboxylic acids.

Simakova *et al.* [19] have determined the kinetic parameters for the decarboxylation of five different saturated fatty acids: C17:0 (margaric acid), C18:0 (stearic acid), C19:0 (nonadecanoic acid), C20:0 (arachidic acid) and C22:0 (behenic acid) over a 1wt.%Pd/C catalyst. A slight difference in the rate of the deoxygenation reaction was found. This difference was attributed to catalyst deactivation from feedstock impurities. Lestari *et al.* [27] observed also that the deoxygenation rates for C16 (palmitic acid C16:0) and C18 (stearic acid C18:0) over a 4wt.%Pd/C were independent of the fatty acid chain length. In contrast, Ford *et al.* [5] found that, for a series of C10-C18 fatty acids using a Pd/C catalyst, the initial decarboxylation

rates increased with the carbon number in the FA chain. In fact, the higher the carbon number of the acid, the stronger was its adsorption from diluted solution on the activated carbon. Ford *et al.* [5] attributed this trend to the decreasing of solubility of FA in the organic solvent and the increase of the molar heat of adsorption with increasing the chain length.

Recently, Mohite *et al.* [22] also reported on the decarboxylation of three different fatty acids (caprylic acid CA (C8:0), lauric acid LA (C12:0), and stearic acid SA (C18:0) under inert gas. They have studied the effect of the reactant chain length on the conversion and n-alkane selectivity using a 10 wt.%Pd/C catalyst. They reported that the conversion of fatty acids increased with the acid chain length. However, the selectivity toward the desired n-alkanes was the highest for LA (67%) and the lowest for SA (13%).

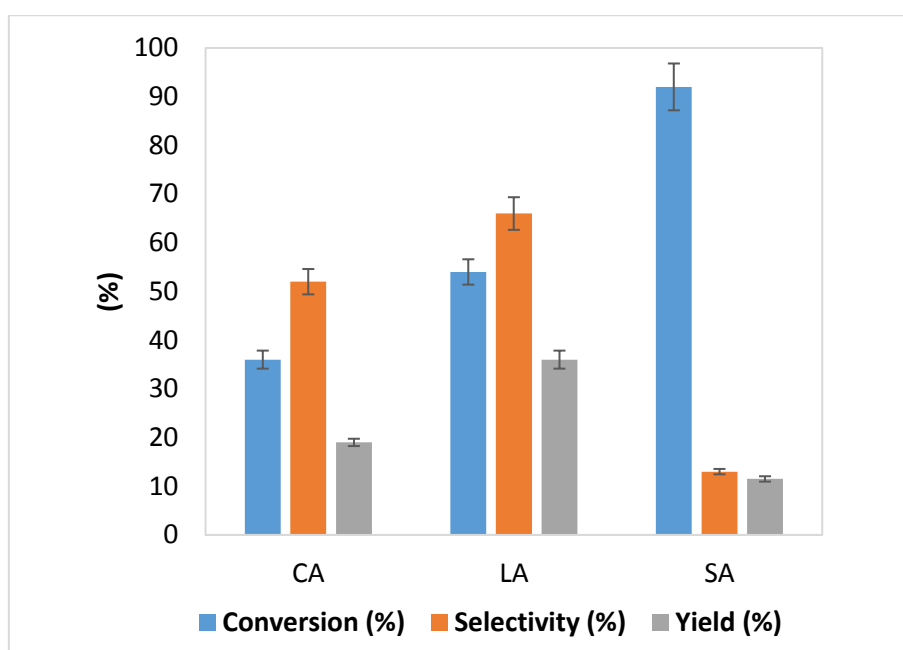


**Figure 11: Impact of the acid chain length of the reactant (caprylic-CA, lauric-LA and stearic-SA acids) on the decarboxylation reaction at T = 300 °C, P = 18 bar, t = 6 h, stirrer speed = 500 RPM, catalyst = 10%Pd/C [22].**

Concerning the non-noble metal-based catalysts, Wu *et al.* [29] investigated the decarboxylation of several fatty saturated acids (C12 to C22) over a 20 wt.%Ni/C catalyst. The reactions were performed under inert gas, in the same operating conditions. The results obtained showed the highest activities and selectivities for the FA from C12 to C14.

In general, it was reported that the conversions of fatty acids decreased when the carbon length chain increased. Similarly, the selectivity to the corresponding n-hydrocarbon decreased when the carbon length chain increased. This decrease of the selectivity was attributed to higher

ability of long-chain fatty acids to crack. Thus, for the 20 wt. %Ni/C, the shorter fatty acids chain promoted the decarboxylation while the longer FA favored the cracking.

In view of the above, for different fatty acids having close chain lengths, the catalytic performances should be quite similar over the same catalyst and under the same reaction conditions.

#### **IV.6. Summary of the reported performances on non-noble metal-based catalysts**

A rapid overview of the catalytic performances of the non-noble metal-based catalysts reported in the literature for the decarboxylation of free fatty-acids are shown in Table 7. It can be noted that the non-noble metal-based catalysts developed so far do not reach the same catalytic performances as those obtained with noble metals under the same conditions. However, the Ni-based catalysts already show very promising results and are worth to be developed further.

**Table 7: Overview of the catalytic performances of the non-noble metal catalysts in decarboxylation of free fatty-acids**

Feed	Catalyst	T(°C)	Time (h)	Conversion(%)	Selectivity(%) <sup>a</sup>	Yield(%) <sup>b</sup>	Gas atm	Reference
SA	20%Cu/Al <sub>2</sub> O <sub>3</sub>	330	5	17	59	10	Inert	[29]
SA	20%Cu/ZrO <sub>2</sub>	330	5	36	23	8	Inert	
SA	20%Co/ZrO <sub>2</sub>	330	5	75	9	7	Inert	
SA	20%Ni/ZrO <sub>2</sub>	330	5	37	79	30	Inert	
SA	20%Ni/C	330	5	37	89	33	Inert	
SA	40%Ni/SiO <sub>2</sub>	330	5	54	51	28	Inert	
SA	10%Ni/C	330	5	25	70	18	Inert	
SA	30%Ni/C	330	5	63	71	45	Inert	
SA	20%Ni/C	370	5	100	80	80	Inert	
LA	20%Ni/C	350	4	79	89	70	Inert	
MA	20%Ni/C	350	4	76	87	67	Inert	
PA	20%Ni/C	350	4	68	84	57	Inert	
SA	20%Ni/C	350	4	62	85	53	Inert	
AA	20%Ni/C	350	4	60	73	44	Inert	
BA	20%Ni/C	350	4	66	64	42	Inert	
SA	20%Ni/C	300	1.5	19	26	5	N <sub>2</sub>	[10]
SA	20%Ni/C	300	1.5	64	51	33	10%H <sub>2</sub> /N <sub>2</sub>	
SA	20%Ni/C	300	1.5	80	81	65	H <sub>2</sub>	
SA	20%Ni/Al <sub>2</sub> O <sub>3</sub>	300	1.5	9	38	3	N <sub>2</sub>	[48]
SA	20%Ni/Al <sub>2</sub> O <sub>3</sub>	300	1.5	80	67	54	10%H <sub>2</sub> /N <sub>2</sub>	
SA	20%Ni/Al <sub>2</sub> O <sub>3</sub>	300	1.5	81	57	46	H <sub>2</sub>	
SA	20%Ni/Al <sub>2</sub> O <sub>3</sub>	260	1.5	39	2	1	H <sub>2</sub>	[41]
SA	20%Ni-5%Cu/Al <sub>2</sub> O <sub>3</sub>	260	1.5	54	7	4	H <sub>2</sub>	
SA	20%Ni-1%Sn/Al <sub>2</sub> O <sub>3</sub>	260	1.5	30	3	1	H <sub>2</sub>	
SA	20%Ni/Al <sub>2</sub> O <sub>3</sub>	300	1.5	92	66	61	H <sub>2</sub>	
SA	20%Ni-5%Cu/Al <sub>2</sub> O <sub>3</sub>	300	1.5	98	79	77	H <sub>2</sub>	
SA	20%Ni-1%Sn/Al <sub>2</sub> O <sub>3</sub>	300	1.5	39	17	7	H <sub>2</sub>	
SA	5%Cu/Al <sub>2</sub> O <sub>3</sub>	350	6	96	21	20	H <sub>2</sub>	[4]
SA	5%Ni/Al <sub>2</sub> O <sub>3</sub>	350	6	61	49	30	H <sub>2</sub>	
SA	5%Cu/WO <sub>3</sub> /ZrO <sub>2</sub>	350	6	99	7	7	H <sub>2</sub>	
SA	5%Ni/WO <sub>3</sub> /ZrO <sub>2</sub>	350	6	100	11	11	H <sub>2</sub>	

a and b correspond to the selectivity and yield to the corresponding hydrocarbons with one carbon atom less than the original fatty acid, i.e., LA: lauric acid to undecane (C11); MA: myristic acid to tridecane (C13); PA: Palmitic acid to pentadecane (C15); SA: Stearic acid to heptadecane (C17); AA: arachidic acid to nonadecane (C19) and BA: behenic acid to heneicosane (C21).

## Conclusion

The literature concerning the decarboxylation of saturated fatty acids to alkanes over heterogeneous metal-based catalysts was studied in detail. The pathway followed for the FA deoxygenation depends, on one hand, on the catalyst properties (nature of the support, metal particles size and dispersion, metal loading) and, on the other hand, on the conditions of reaction (temperature, pressure, FFA/catalyst ratio, nature of the atmosphere, reaction time). For instance, for the same  $\text{Al}_2\text{O}_3$  support, Pd was reported to lead to an excellent selectivity to the product of DCX, while Cu favored the DCN route. In the same way, Pd/C was very selective for DCX, while Pt/C and Ni/C favored the DCN pathway. In addition, for the same metal, the comparison between an oxide support and active carbon showed that, carbon is much more selective for DCX reaction. This difference of selectivity as a function of the support was attributed to their differences in acidity and specific surface areas.

Concerning the operating conditions, the bibliographic study has shown that the liquid phase DCX reaction is preferentially carried out in a temperature range from 250 to 380 °C. The pressure is chosen in order to maintain the reactants and main products in the liquid phase. The most frequently used pressures are between 1 and 50 bar. The increase of pressure was found to slightly decrease the conversion and increase the selectivity, keeping the yield of alkane constant. In contrast, the increase of reaction temperature was found to increase in a certain extent both conversion and selectivity. However, at too high temperature (350 °C) the formation of undesired products resulting from cracking occurs and this leads to the decrease of selectivity in the desired product [42]. Similarly, the increase of the reaction time enhances the cracking and other consecutive reactions leading to a significant decrease in the selectivity in the desired product by the formation of isomers and/or oligomers. Therefore, the reaction is preferably carried out at a short reaction time (1 to 6 h for example). The gas atmosphere was also found to have a significant effect on the DO pathway but it strongly depends on the type of metal used and on the FFA/catalyst ratio. For instance, the DO of stearic acid over Pd/C under inert atmosphere or low hydrogen quantity (5% or 10%  $\text{H}_2/\text{N}_2$ ) occurred *via* DCX, whereas under higher concentration of hydrogen DCN is dominant [15]. It also appears that under low partial pressure of hydrogen (10 vol.%) better conversion and selectivity to alkane can be obtained [10]. Apart from the properties of the catalyst used and the reaction conditions, the fatty acids chain length also has an impact on the catalytic performances in DO [5, 29]. In fact, the conversion of the fatty acids increases with the acid chain length, whereas the

selectivity to hydrocarbon decreases [22], due to the ease of long-chain fatty acids to crack. Therefore, for fatty acid having similar chain lengths, the difference of catalytic performances should not be significant.

This bibliographic study has shown that noble metals such as Pd and Pt are effective in catalyzing the decarboxylation of fatty acids and their derivatives [6]. But the high cost of these noble metal catalysts are serious constraints for large scale applications. That is why, deoxygenation of fatty acids was studied over non-noble metal-based catalysts such as Cu [4, 29], Ni [6, 9, 10, 29] and Co [29]. Among them, the Ni-supported catalysts showed the most promising results. E. Santillan-Jimenez *et al.* [10] demonstrated that the deoxygenation of stearic acid over Ni/C can reached 80% of conversion of SA and 81% of selectivity to heptadecane at 350 °C, under pure hydrogen. However, in their study, the optimization of the reaction over this catalyst was not studied. Wu *et al.* [29] studied this point in more details for the decarboxylation of stearic acid over Ni/C, but under inert gas to reduce the cost of the process. The results obtained showed that the Ni/C catalysts led to complete conversion of SA and to 80% of heptadecane selectivity under inert gas at 370 °C [29]. Unfortunately, to reach these catalytic performances, the DCX reaction over Ni/C is performed at 70°C above the temperature used for Pd/C. Furthermore, the catalyst reached 80% of heptadecane selectivity compared to 99% reached over 5%Pd/C [24]. Although the Ni/C showed very promising results, this catalyst still required improvements to reach a high selectivity to n-alkanes at a temperature much lower than 370 °C.

The method used for the catalyst preparation was showed to strongly influence its physicochemical properties and hence the catalytic performances. Among the different heterogeneous catalysts preparation methods as it was discussed in this first chapter, the deposition-precipitation method seems to be the most suitable for the preparation of a catalyst with high metal loading and showing at the same time a very good dispersion. For that, we propose to prepare, in addition to the monometallic Ni-based catalysts, other non-noble metals catalysts by deposition-precipitation method using hydrazine as reducing agent. Among the catalysts synthesized, some of them will be monometallic and others bimetallic. The bimetallic catalysts will be studied to check the synergetic effect of two different metals on the performances of the catalysts. In view of the fact that catalysts based on activated carbon compared to the other supports showed the highest selectivity towards the decarboxylation reaction, all the catalysts synthesized will be supported on the same activated carbon. The

catalytic performances of these synthesized catalysts will be compared with the ones of commercial noble metal-based catalysts supported on carbon, used as benchmarks.

Finally, based on the literature, the reactions conditions applied in this study to carry out the palmitic acid decarboxylation to n-pentadecane will be as follows: temperature range [250-320 °C], initial pressure 20 bar, reaction time in the range 1-12 h, reaction atmospheres [ $\text{N}_2$ ; 10 vol.%  $\text{H}_2$  in  $\text{N}_2$ ], initial concentration in PA [0.05 - 0.15] mol/L and FFA/catalyst mass ratio [1-4].

## References

- [1] I. Kubičková, M. Snåre, K. Eränen, P. Mäki-Arvela, D.Y. Murzin, *Catalysis Today*. 106 (2005) 197-200.
- [2] B. Veriansyah, J.Y. Han, S.K. Kim, S.-A. Hong, Y.J. Kim, J.S. Lim, Y.-W. Shu, S.-G. Oh, J. Kim, *Fuel*. 94 (2012) 578-585.
- [3] J.G. Immer, H.H. Lamb, *Energy & Fuels*. 24 (2010) 5291-5299.
- [4] A.S. Berenblyum, R.S. Shamsiev, T.A. Podoplelova, V.Y. Danyushevsky, *Russian Journal of Physical Chemistry A*. 86 (2012) 1199-1203.
- [5] J.P. Ford, J.G. Immer, H.H. Lamb, *Topics in Catalysis*. 55 (2012) 175-184.
- [6] M. Snåre, I. Kubičková, P. Mäki-Arvela, K. Eränen, D.Y. Murzin, *Industrial & Engineering Chemistry Research*. 45 (2006) 5708-5715.
- [7] B. Peng, C. Zhao, S. Kasakov, S. Foraita, J.A. Lercher, *Chemistry – A European Journal*. 19 (2013) 4732-4741.
- [8] Y. Liu, L. Yao, H. Xin, G. Wang, D. Li, C. Hu, *Applied Catalysis B: Environmental*. 174 (2015) 504-514.
- [9] E. Santillan-Jimenez, M. Crocker, *Journal of Chemical Technology & Biotechnology*. 87 (2012) 1041-1050.
- [10] E. Santillan-Jimenez, T. Morgan, J. Lacny, S. Mohapatra, M. Crocker, *Fuel*. 103 (2013) 1010-1017.
- [11] R.W. Gosselink, S.A. Hollak, S.W. Chang, J. van Haveren, K.P. de Jong, J.H. Bitter, D.S. van Es, *ChemSusChem*. 6 (2013) 1576-1594.
- [12] P. Mäki-Arvela, I. Kubickova, M. Snåre, K. Eränen, D.Y. Murzin, *Energy & Fuels*. 21 (2007) 30-41.
- [13] M. Snåre, I. Kubičková, P. Mäki-Arvela, D. Chichova, K. Eränen, D.Y. Murzin, *Fuel*. 87 (2008) 933-945.
- [14] B.P. Pattanaik, R.D. Misra, *Renewable and Sustainable Energy Reviews*. 73 (2017) 545-557.
- [15] B. Rozmysłowicz, P. Mäki-Arvela, A. Tokarev, A.-R. Leino, K. Eränen, D.Y. Murzin, *Industrial & Engineering Chemistry Research*. 51 (2012) 8922-8927.
- [16] L. Yang, G.L. Ruess, M.A. Carreon, *Catalysis Science & Technology*. 5 (2015) 2777-2782.
- [17] M. Ahmadi, A. Nambo, J.B. Jasinski, P. Ratnasamy, M.A. Carreon, *Catalysis Science & Technology*. 5 (2015) 380-388.
- [18] S. Lestari, I. Simakova, A. Tokarev, P. Mäki-Arvela, K. Eränen, D.Y. Murzin, *Catalysis Letters*. 122 (2008) 247-251.
- [19] I. Simakova, O. Simakova, P. Mäki-Arvela, D.Y. Murzin, *Catalysis Today*. 150 (2010) 28-31.
- [20] I. Simakova, O. Simakova, P. Mäki-Arvela, A. Simakov, M. Estrada, D.Y. Murzin, *Applied Catalysis A: General*. 355 (2009) 100-108.
- [21] P.A. Simonov, A.V. Romanenko, V.A. Likholobov, *Solid Fuel Chemistry*. 48 (2014) 364-370.
- [22] S. Mohite, U. Armbruster, M. Richter, A. Martin, *Journal of Sustainable Bioenergy Systems*. 4 (2014) 183.
- [23] E.W. Ping, J. Pierson, R. Wallace, J.T. Miller, T.F. Fuller, C.W. Jones, *Applied Catalysis A: General*. 396 (2011) 85-90.
- [24] D.Y. Murzin, I. Kubickova, M. Snare, P. Maeki-Arvela, J. Myllyoja, Fortum Oyj, Espoo (FI), 2006.
- [25] K.C. Kwon, H. Mayfield, T. Marolla, B. Nichols, M. Mashburn, *Renewable Energy*. 36 (2011) 907-915.

- [26] P. Mäki-Arvela, B. Rozmysłowicz, S. Lestari, O. Simakova, K. Eränen, T. Salmi, D.Y. Murzin, *Energy & Fuels*. 25 (2011) 2815-2825.
- [27] S. Lestari, P. Mäki-Arvela, I. Simakova, J. Beltramini, G.Q.M. Lu, D.Y. Murzin, *Catalysis Letters*. 130 (2009) 48-51.
- [28] J.G. Immer, M.J. Kelly, H.H. Lamb, *Applied Catalysis A: General*. 375 (2010) 134-139.
- [29] J. Wu, J. Shi, J. Fu, J.A. Leidl, Z. Hou, X. Lu, *Scientific Reports*. 6 (2016) 27820.
- [30] F. Pinna, *Catalysis Today*. 41 (1998) 129-137.
- [31] G. Mul, J.A. Moulijn, *ChemInform*. 36 (2005) 1-32.
- [32] J.W. Geus, A.J. van Dillen, *Handbook of Heterogeneous Catalysis*, Wiley-VCH Verlag GmbH & Co. KGaA, 2008.
- [33] I. Simakova, Laboratory of Industrial Chemistry and Reaction Engineering, Process Chemistry Centre, Department of Chemical Engineering, Åbo Akademi University, 2010, p. 57, Åbo Akademi University, 2010, p. 57.
- [34] I. Ohno, *Materials Science and Engineering: A*. 146 (1991) 33-49.
- [35] T. Morgan, D. Grubb, E. Santillan-Jimenez, M. Crocker, *Topics in Catalysis*. 53 (2010) 820-829.
- [36] R. Wojcieszak, M. Zieliński, S. Monteverdi, M.M. Bettahar, *Journal of Colloid and Interface Science*. 299 (2006) 238-248.
- [37] A. Carrero, J.A. Calles, A.J. Vizcaíno, *Applied Catalysis A: General*. 327 (2007) 82-94.
- [38] S. De, J. Zhang, R. Luque, N. Yan, *Energy & Environmental Science*. 9 (2016) 3314-3347.
- [39] N.M. Galea, D. Knapp, T. Ziegler, *Journal of Catalysis*. 247 (2007) 20-33.
- [40] M. Kimi, M.M.H. Jaidie, S.C. Pang, *Journal of Physics and Chemistry of Solids*. 112 (2018) 50-53.
- [41] R. Loe, E. Santillan-Jimenez, T. Morgan, L. Sewell, Y. Ji, S. Jones, M.A. Isaacs, A.F. Lee, M. Crocker, *Applied Catalysis B: Environmental*. 191 (2016) 147-156.
- [42] L.T. Chiam, C.T. Tye., *Malaysian Journal of Analytical Sciences*. 17 (2013) 129-138.
- [43] A.S. Berenblyum, V.Y. Danyushevsky, E.A. Katsman, T.A. Podoplelova, V.R. Flid, *Petroleum Chemistry*. 50 (2010) 305-311.
- [44] J.G. Immer, Department of Chemical and Biomolecular Engineering, Raleigh, North Carolina, 2010, p. 201.
- [45] H. Bernas, K. Eränen, I. Simakova, A.-R. Leino, K. Kordás, J. Myllyoja, P. Mäki-Arvela, T. Salmi, D.Y. Murzin, *Fuel*. 89 (2010) 2033-2039.
- [46] P. Mäki-Arvela, M. Snåre, K. Eränen, J. Myllyoja, D.Y. Murzin, *Fuel*. 87 (2008) 3543-3549.
- [47] B. Rozmysłowicz, P. Mäki-Arvela, S. Lestari, O.A. Simakova, K. Eränen, I.L. Simakova, D.Y. Murzin, T.O. Salmi, *Topics in Catalysis*. 53 (2010) 1274-1277.
- [48] E. Santillan-Jimenez, T. Morgan, J. Shoup, A.E. Harman-Ware, M. Crocker, *Catalysis Today*. 237 (2014) 136-144.

---

## Chapter 2

# Experimental Procedures



## SUMMARY

<b>INTRODUCTION .....</b>	<b>60</b>
<b>I. SYNTHESIS AND CHARACTERIZATION OF THE CATALYSTS.....</b>	<b>60</b>
I.1. MATERIALS .....	60
I.2. PREPARATION OF MONO- AND BIMETALLIC CATALYSTS .....	60
I.2.1. Bench-scale manual preparation.....	60
I.2.2. High-throughput catalysts preparation .....	62
I.2.2.1. Preparation by deposition-precipitation method .....	62
I.2.2.2. Preparation by wet impregnation method .....	64
I.3. CHARACTERIZATION METHODS .....	65
I.3.1. Morphological and textural properties .....	65
I.3.1.1. Nitrogen adsorption/desorption.....	65
I.3.1.2. Transmission Electron Microscopy (TEM) .....	67
I.3.2. Surface properties .....	67
I.3.2.1. X-ray Photoelectron Spectroscopy (XPS).....	67
I.3.3. Bulk properties .....	69
I.3.3.1. X-ray fluorescence (XRF) .....	69
I.3.3.2. X-ray diffraction (XRD) .....	70
I.3.3.3. Inductively Coupled Plasma Optical Emission Spectroscopy (ICP-OES).....	71
I.3.3.4. Temperature-programmed reduction (TPR) .....	72
<b>II. CATALYTIC TESTS .....</b>	<b>74</b>
II.1. MATERIALS .....	74
II.2. EXPERIMENTAL SETUP.....	74
II.2.1. SPR system presentation .....	74
II.2.2. Description of the experimental protocol of catalyst reactivation .....	75
II.2.3. Description of the experimental protocol .....	76
<b>III. ANALYSIS OF THE PRODUCTS OF REACTION .....</b>	<b>76</b>
III.1. ANALYTICAL METHOD .....	76
III.1.1. GC analysis.....	76
III.1.2. Calibration of the GC .....	77
III.1.3. Sample preparation .....	77
III.2. DATA TREATMENT .....	78
<b>REFERENCES.....</b>	<b>79</b>

## Introduction

On the basis of the literature survey described in the previous Chapter a strategy of research has been defined. A library of mono- and bimetallic supported Ni-based catalysts has been prepared, characterized and tested. Of course, the detailed characterization of this series of catalysts requires the use of different techniques and instruments to determine their chemical and physical properties, their morphology and structure, and to identify the species which have a direct impact on the catalytic performances (activity, selectivity and stability).

This Chapter described in detail the experimental procedures used in this thesis and is divided in 3 parts. The first part describes the preparation, pre-activation by reduction and characterization of the library of heterogeneous catalysts used in this work. The second part focusses on the description of the set-up and protocol for the catalytic tests. Finally, the third part is dedicated to the analysis of the products of reaction, notably the sample preparation and the GC analysis procedure.

## I. Synthesis and characterization of the catalysts

### I.1. Materials

The precursors for the preparation of the catalysts used in this work, namely, nickel nitrate hexahydrate (97%); copper nitrate trihydrate (99-104%); iron nitrate nonahydrate ( $\geq 99.999\%$  trace metals basis) and silver nitrate (ACS reagent,  $\geq 99.0\%$ ), were all purchased from Sigma-Aldrich and used as such. The support used for all the catalysts is the Darco KB-g activated carbon (pore volume =  $1.1 \text{ cm}^3/\text{g}$ , specific surface area =  $1290 \text{ m}^2/\text{g}$ ). The reducing agent chosen was hydrazine (78-82 % water solution). The support and hydrazine were also purchased from Sigma-Aldrich and used as received.

### I.2. Preparation of mono- and bimetallic catalysts

#### I.2.1. Bench-scale manual preparation

As discussed in Chapter 1, the deposition-precipitation method (DP) was selected for the preparation of nickel-based catalysts supported on active carbon (AC). Prior to Ni deposition, the Ni precursor  $\text{Ni}(\text{NO}_3)_2 \cdot 6\text{H}_2\text{O}$  was solubilized in deionized water in a flask. Then, the active carbon was added and the flask was plunged in an oil bath to heat the stirred suspension at  $50^\circ\text{C}$  Figure 12. After 30 min, 6 mL of hydrazine solution was added slowly in

the flask to reduce the Ni (II) ions into metal. The pH of the solution was adjusted to pH 10-12 using hydrazine and the temperature was maintained at 50°C for 1 h. The reduction of Ni (II) ions with hydrazine are expected to proceed according to the following reaction:



The production of hydrogen was attributed to hydrazine decomposition by the metallic nickel formed. The activated carbon provoked also  $\text{NH}_3$  production by hydrazine decomposition according to the equation:



After the Ni reduction, the catalyst was filtered and washed 3 times with deionized water and 3 times with acetone to remove all the impurities.

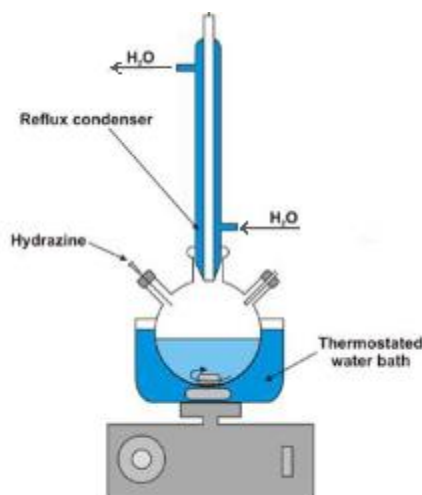


**Figure 12: Scheme of the experimental bench-scale set-up used for catalysts preparation**

In order to synthesize a wider range of Ni-based catalysts, a high-throughput device available on the REALCAT platform was used to prepare seven catalysts per run.

## I.2.2. High-throughput catalysts preparation

### I.2.2.1. Preparation by deposition-precipitation method

A library of mono- (Ni, Cu, Fe and Ag) and bimetallic (Ni-Ag, Ni-Cu and Ni-Fe) catalysts were prepared using the Chemspeed CatImpreg HT robot available on the REALCAT platform (Figure 13). The catalysts were prepared by the deposition-precipitation (DP) method. The automated protocol for the catalysts preparation was created on the Autosuite editor software piloting the Chemspeed workstation. This robot is equipped with systems of shaking, heating, reflux, filtration, vacuum, etc. It also includes online pH and density measurement and adjustment, as well as tools for volumetric and gravimetric dispensing of liquids and solids. 7 catalysts were prepared per run on this workstation. Each catalyst has been prepared in a



**Figure 13: The Chemspeed CatImpreg HT workstation**

20 mL vial where 1 g of support was previously weighted. The concentrations of the solutions of salts were as follows: 0.525 g/mL (10.5 g of  $\text{Ni}(\text{NO}_3)_2 \cdot 6\text{H}_2\text{O}$  in 20 mL  $\text{H}_2\text{O}$ ), 0.4 g/mL (8 g of  $\text{Cu}(\text{NO}_3)_2 \cdot 3\text{H}_2\text{O}$  in 20 mL  $\text{H}_2\text{O}$ ), 0.8 g/mL (16 g of  $\text{Fe}(\text{NO}_3)_3 \cdot 9\text{H}_2\text{O}$  in 20 mL  $\text{H}_2\text{O}$ ) and 0.25 g/mL (5 g of  $\text{Ag}(\text{NO}_3)$  in 20 mL  $\text{H}_2\text{O}$ ). The volumes used for each sample are presented in Table 8.

Firstly, 10 mL of deionized water were automatically dispensed by the robot in each reactor. Then, the appropriate amounts of the solution of Ni nitrate (Table 8) were distributed in each reactor to correspond to the desired metal loading. For the bimetallic catalysts, after the distribution of the solution of Ni precursor, the appropriate amounts of the solution of the other metals precursors (Table 8) were also distributed in each reactor. Then, the reactors were closed and the shaking was started and maintained constant at 400 rpm at 50 °C for 25 min. Then, the reactors were re-opened, and the solution of hydrazine (pH=10.7) was distributed until a pH of 10 in order to reduce the metal and deposit it on the support. If the solution did not reach pH=10 when a maximum of 2 mL of hydrazine solution was added then the dispense was stopped and the pH noted. After this step, the reactors were closed and the shaking was started again at 400 RPM for 55 min. After this time, the temperature was cooled down to 30 °C and the stirring

was stopped. Then, the filtration was done automatically by the robot on filters of porosity 4. 3 cycles of washing with deionized water were performed. At first, the reactors were opened and 10 mL of deionized water was distributed in each reactor. The reactors were then closed and the stirring was started at 400 rpm for 5 min. After that, the stirring was stopped and the filtration was started using a vacuum pump (200 mbar) during 10 min. At the end of the filtration process, the pump was stopped. Then, 3 cycles of washing with acetone were also performed using the same protocol as for the water washing. Finally, the catalyst was dried under inert gas under stirring at 400 rpm and at 101 °C. The vacuum pump was turned on at 600 mbar to dry the catalyst for 60 min. After this time, the vacuum pump was set at 400 mbar and the drying was continued for 30 min. At the end of the drying, the pump was stopped and the fresh catalysts were recovered.

**Table 8: Volumes of the salts precursors solutions distributed and pH of the suspension**

catalysts	V Ni(NO <sub>3</sub> ) <sub>2</sub> ,6H <sub>2</sub> O (mL)	V Cu(NO <sub>3</sub> ) <sub>2</sub> ,3H <sub>2</sub> O (mL)	pH
10%Ni	1.04	-	10
2.5%Ni2.5%Cu/C	0.25	0.25	9.6
5%Ni5%Cu/C	0.52	0.53	9.6
10%Cu/C	-	1.06	9.4
10%Ni10%Cu/C	1.17	1.19	9.6
15%Ni5%Cu/C	2.01	2.04	9.4
	V Ni(NO <sub>3</sub> ) <sub>2</sub> ,6H <sub>2</sub> O (mL)	V Fe(NO <sub>3</sub> ) <sub>3</sub> ,9H <sub>2</sub> O (mL)	
2.5%Ni2.5%Fe/C	0.25	0.24	9.8
5%Ni5%Fe/C	0.52	0.5	10.3
10%Fe/C	-	1	9.6
10%Ni10%Fe/C	1.17	1.13	10.6
15%Ni5%Fe/C	2.01	1.94	9.6
	V Ni(NO <sub>3</sub> ) <sub>2</sub> ,6H <sub>2</sub> O (mL)	V Ag(NO <sub>3</sub> ) (mL)	
2.5%Ni2.5%Ag/C	0.25	0.17	10
5%Ni5%Ag/C	0.52	0.35	9.9
10%Ag/C	-	0.7	9.3
10%Ni10%Ag/C	1.17	0.79	10
15%Ni5%Ag/C	2.01	1.35	9.4

### I.2.2.2. Preparation by wet impregnation method

In order to evaluate the impact of the method of preparation of the catalysts on their catalytic performances, the most active bimetallic catalyst (see Chapter 5) was prepared on the Chemspeed robot by a wet-impregnation method (WI). The protocol was almost the same than the one described above. The only difference was on the precipitation and calcination steps. Here, after the impregnation step, the stirring was started at 400 rpm and maintained during 55 min. After that, the catalyst was filtered and then, the catalyst was dried as previously. The catalyst recovered after drying was then calcined in an oven at 450 °C with 5 °C/min of temperature rate, under N<sub>2</sub>, for 3 h. The catalyst obtained after the calcination was noted: 10%Ni10%Cu/C-calc.

In total, the catalysts library comprises 19 samples, which are listed in Table 9.

**Table 9: Library of the catalysts used in this work with their theoretical compositions and preparation modes**

Preparation method	Monometallic catalysts		Preparation mode	
<b>Deposition-precipitation</b>	Ni/C	10%Ni/C	<b>Manual</b>	<b>High-throughput</b>
	Cu/C	10%Cu/C		
	Ag/C	10%Ag/C		
	Fe/C	10%Fe/C		
	<b>Bimetallic catalysts</b>		<b>Manual</b>	
	Ni-Cu	2.5%Ni2.5%Cu/C		
		5%Ni5%Cu/C		
		10%Ni10%Cu/C		
		15%Ni15%Cu/C		
	Ni-Fe	2.5%Ni2.5%Fe/C		
		5%Ni5%Fe/C		
		10%Ni10%Fe/C		
		15%Ni5%Fe/C		
	Ni-Ag	2.5%Ni2.5%Ag/C		
5%Ni5%Ag/C				
10%Ni10%Ag/C				
15%Ni5%Ag/C				
<b>Wet impregnation</b>	Ni-Cu	10%Ni10%Cu-calc		
<b>Commercial catalysts</b>	Pd/C	5%Pd/C		
	Pt/C	5%Pt/C		

### I.3. Characterization methods

The catalysts prepared were characterized in order to determine, on the one hand, their physical properties such as the pore size distribution, the pore volume, the specific surface area, the particles size and, on the other hand, their surface and bulk properties such as the composition, the crystallite size, the structure, etc.

In the present work, the techniques used to characterize the catalysts are divided in three groups corresponding to the determination of (i) morphological and textural properties by nitrogen adsorption and transmission electron microscopy (TEM); (ii) surface properties by X-ray photoelectron spectroscopy (XPS) and (iii) bulk properties by X-ray fluorescence (XRF), X-ray diffraction (XRD) and temperature programmed reduction of hydrogen (H<sub>2</sub>-TPR).

#### I.3.1. Morphological and textural properties

##### I.3.1.1. Nitrogen adsorption/desorption

In 1938, Brunauer, Emmett and Teller (BET) [1] proposed a theory of physical liquid nitrogen adsorption at constant temperature (-196 °C). Based on this theory, they determined the specific surface area corresponding to the sum of the inner surface of the pores and the outer surface of the grains. This technique gives information about surface porosity and pore size distribution and volume.

The determination of the S<sub>BET</sub> is based on the BET equation given by relation (17).

$$\frac{p}{v(p_0-p)} = \frac{1}{v_m} + \frac{c-1}{v_m c} \frac{p}{p_0} \quad (17)$$

Where

p and p<sub>0</sub> are the equilibrium and the saturation pressures of adsorbates at the temperature of adsorption, respectively,

v is the adsorbed gas quantity (for example, in volume units)

v<sub>m</sub> is the monolayer adsorbed gas quantity.

c is the BET constant, which is calculated by the following equation(18)

$$c = e^{\left(\frac{E_L - E_1}{RT}\right)} \quad (18)$$

E<sub>1</sub> is the heat of adsorption for the first layer, and E<sub>L</sub> is that for the second and higher layers and is equal to the heat of liquefaction.

The BET equation is generally applicable only for relative pressures  $p/p_0$  between 0.05 and 0.35. Indeed, the BET model does not take into account the heterogeneity of the surface of the solid that manifests for low-pressure values or the lateral interactions between adsorbed molecules that modify the isotherm when the pressure reaches a high value. Thus, in the range of  $0.05 < p/p_0 < 0.35$  the equation BET is represented by a straight line of equation  $y = \alpha \cdot x + \beta$ . From the resulting linear plot, the slope, which is equal to  $(c - 1)/v_m c$ , and the intercept, which is equal to  $1/v_m c$ , are evaluated by linear regression analysis. Thus, the constant  $c$  is calculated as (slope/intercept) + 1 which is expressed by equation (20), while  $v_m$  is calculated as  $1/(\text{slope} + \text{intercept})$  (19).

$$v_m = \frac{1}{\alpha + \beta} \quad (19) \qquad c = \frac{\alpha}{\beta} + 1 \quad (20)$$

The specific surface area is then calculated from the value of  $v_m$  by the equation given below (21).

$$S_{BET} = \sigma \times \frac{v_m * N_A}{V_M} = \frac{S_t}{m} \quad (21)$$

$N_A$ : Avogadro's constant (6.021023 mol<sup>-1</sup>)

$\sigma$ : adsorption cross section of the adsorbing species, 16.2 Å<sup>2</sup>

$V_M$ : Volume occupied by 1 mole of the adsorbate gas at STP (22414 cm<sup>3</sup>/mole).

$m$ : mass of the sample, in grams.

According to these numerical values,  $S_{BET}$  can be expressed by equation (22).

$$S_{BET} = 4.37 v_m \quad (22)$$

In this work, the surface areas, pore volumes and distributions of the pore sizes were determined by nitrogen adsorption/desorption at 77.35 K using a TriStar II Plus and a 3Flex apparatus from Micromeritics. Preliminary degassing of the samples was done at 150 °C for 45 min.

### **I.3.1.2. Transmission Electron Microscopy (TEM)**

Some catalysts were characterized by Transmission Electron Microscopy (TEM) to extract local information at the nanometric and atomic levels on the morphology, structure, chemical composition, size and distribution of the metallic nanoparticles and on their interface with the support.

In TEM a beam of electrons is transmitted through an ultra-thin sample, with which it interacts as it passes through. That generates an image of the internal structure of the thin sample which is focused by the objective lens to a point. The image is then magnified by a series of projector lenses to vary the size of the image on a fluorescent screen.

The principle of transmission is based on the same basic principles as the light microscope but the main difference is that light microscope uses a beam of light whereas TEM uses a beam of electrons [2]. Hence, a TEM uses electrons as “light source” to achieve much higher spatial resolution than in light microscopy. In fact, light microscopes are limited by the wavelength of light whereas, electrons and their much lower wavelength used as a “light source” make it possible to get a resolution 1000 times better than with a light microscope [2].

In this work, the transmission electron microscope use was a FEI Tecnai G2 20 (TEM) equipped with an EDX (Energy-dispersive X-ray spectroscopy) micro-analysis, a Gatan energy filter (EELS), precession and electron tomography systems and an ORIUS CCD camera. This microscope uses a voltage of 200 kV for the acceleration of electrons. Sample preparation was done by introducing one drop of catalyst dispersed in 10 mL of ethanol (for good dispersion, the catalyst in ethanol was homogenized by ultrasonic for about 10 minutes) on carbon coated copper grid and then the grid was dried at room temperature overnight. The day after, imaging was done.

## **I.3.2. Surface properties**

### **I.3.2.1. X-ray Photoelectron Spectroscopy (XPS)**

X-ray Photoelectron Spectroscopy (XPS) also known as Electron Spectroscopy for Chemical Analysis (ESCA) is a quantitative spectroscopic technique that measures the elemental composition, empirical formula, chemical state and electronic state of the elements that exist within a material. This technique is widely used to investigate the chemical state

information from the surface of the material being studied. XPS was developed in the mid-1960s by Kai Siegbahn and his research group [3].

The sample surface is irradiated with X-rays (commonly Al K $\alpha$  “1486.6eV” or Mg K $\alpha$  “1253.6eV”) in a ultra-high vacuum environment to prevent contamination of the surface and to aid an accurate analysis of the sample. When an X-ray photon hits and transfers its energy to a core-level electron, it is emitted from its initial state with a kinetic energy dependent on the incident X-ray and binding energy of the atomic orbital from which it originated [4].

Because the energy of an X-ray with particular wavelength is known, the electron binding energy of each of the emitted electrons can be determined by equation (23).

$$BE = h\nu - KE - \phi \quad (23)$$

where

BE is the binding energy (BE) of the electron,

$h\nu$  is the energy of the X-ray photons being used ( $h$  is the Planck constant which value is about:  $h \approx 6.63 \times 10^{-34}$  J.s and  $\nu$  the frequency (in Hertz) of the electromagnetic wave associated with the considered photon.

KE is the kinetic energy of the electron as measured by the instrument and  $\phi$  is the work function dependent on both the spectrometer and the material.

The energy and intensity of the emitted photoelectrons are analyzed to identify and determine the concentrations of the elements present. These photoelectrons originate from a depth of less than 10 nm, therefore, the information obtained is from within this depth. The identification of the XPS peaks is done starting from tables where KE and BE are already assigned to each element.

In our case, XPS spectra were collected on a high-performance hemispheric analyzer VG Escalab 220 XL spectrometer “1996” and on a XPS KRATOS, AXIS UltraDL D “2009” with monochromatic Al K $\alpha$  ( $h\nu = 1486.6$  eV) radiation as the excitation source. For interpretation of the results, the calibration of the XPS spectra was made using the carbon C 1s reference of 284.8 eV.

### I.3.3. Bulk properties

#### I.3.3.1. X-ray fluorescence (XRF)

X-ray fluorescence spectroscopy (XRF) is one of the most commonly used techniques for studying the elemental composition of different materials. The sample is irradiated with X-rays, which knock out electrons from atoms, leaving them in an excited state. During the relaxation of these atoms, the excess energy is released in the form of X-ray radiation. The energy and intensity of this radiation, however, depends directly on the composition of the material. Therefore, it is possible to study a material composition by detecting the X-rays that come out of the sample.

The generation of the X-ray fluorescence radiation is shown in Figure 14. One electron from the K shell is knocked. The resultant void is filled by either an electron from the L shell or an electron from the M shell. In the process, the  $K_{\alpha}$  and  $K_{\beta}$  radiation is generated, which is characteristic for a particular material.

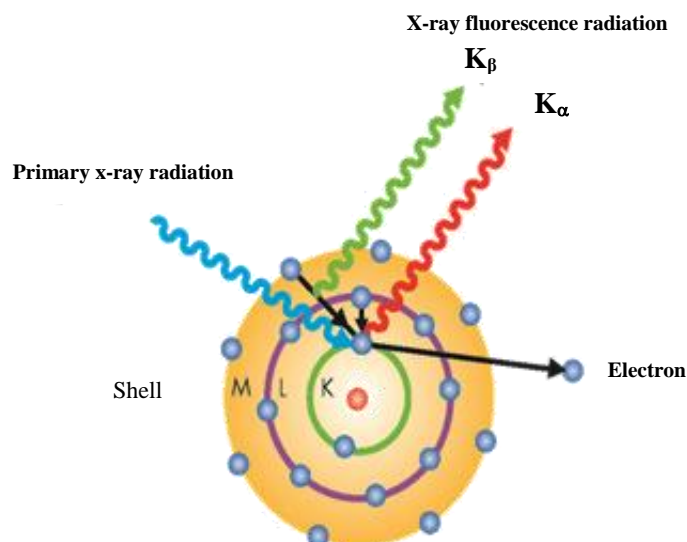


Figure 14: principle of XRF [5]

In the present work, a M4 Tornado from Bruker was used to estimate the elemental composition of the materials. To obtain accurate quantification of the metals present in the catalysts, each sample was irradiated 30 times in order to cover the whole catalyst surface. The mean value of the metal content was then determined.

### 1.3.3.2. X-ray diffraction (XRD)

X-Ray Diffraction (XRD) allows the determination of crystallographic density and hence crystal structure of unknown crystalline solids.

A crystal with planes oriented at an angle  $\theta$  to an incident X-ray beam of wavelength  $\lambda$  will diffract the rays according to Bragg's equation (24):

$$2d\sin\theta = n\lambda \quad (24)$$

Where

$n$  is an integer

$\lambda$  is the wavelength of the rays

$\theta$  is the angle between the incident rays and the surface of the crystal

$d$  is the spacing between layers of atoms

In this work, catalyst X-ray diffraction measurements were performed on a D8 Discover X-Ray Diffractometer from Bruker using a X-Ray tube in Cu ( $K\alpha$ ) radiation ( $\lambda=1.54060 \text{ \AA}$ ). The diffraction angle  $2\theta$  was in the  $10-70^\circ$  range with steps of  $0.02^\circ$  per second. The interpretation of the XRD spectrum obtained was done from Diffrac Eva software and the identification of the crystalline phase was done from reference standards. Finally, the average crystallite size of the metals particles in the catalyst was determined by the Scherrer formula (25).

$$D = \frac{K\lambda}{\beta \cos \Theta} \quad (25)$$

Where

$D$  is the average crystallite size ( $\text{\AA}$ )

$\lambda$  is the wavelength of the X-ray radiation (for  $\text{CuK}\alpha = 1.54060 \text{ \AA}$ ),

$K$  is Debye–Scherrer's constant =1,

$\beta$  is the peak widths at half-maximum intensity (FWHM) of the sample (radian) ,

$\Theta$  is the angle of diffraction.

The distance between two crystallographic planes (d-spacing) was determined from Bragg's law (equation (26))

$$d = \frac{n\lambda}{2 \sin \theta} \quad (26)$$

A X-ray diffractometer is composed of a X-ray tube, a sample holder and a X-ray detector (Figure 15). Firstly, the X-ray generated in a cathode ray tube by heating a filament to produce electrons are collimated and directed onto the sample. As the sample and detector are rotated, the intensity of the reflected X-rays is recorded. When the geometry of the incident X-rays impinging the sample satisfies the Bragg Equation, constructive interference occurs and a peak in intensity occurs. The detector records and processes this X-ray signal and converts the signal to a count rate which is output to a computer.

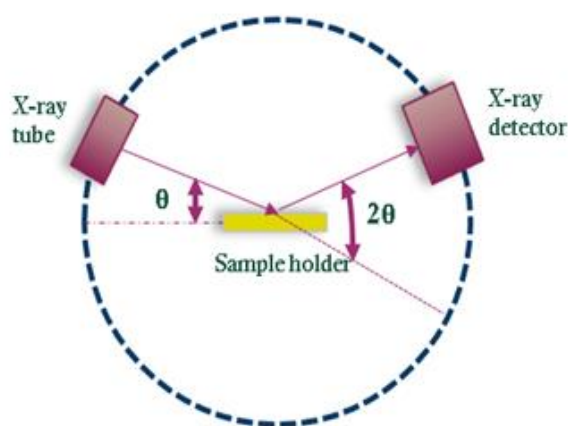


Figure 15: diffractometer

### I.3.3.3. Inductively Coupled Plasma Optical Emission Spectroscopy (ICP-OES)

ICP-OES (Inductively Coupled Plasma Optical Emission Spectrometry) is an analytical technique used for quantitative determination of trace metals in environmental samples. This technique consists in using an inductively coupled plasma to produce excited atoms and ions that emit electromagnetic radiation at wavelengths characteristic of a particular element [6]

In this present work, the quantitative catalysts compositions were determined using ICP-OES - Agilent 720.

Owing to their difficulty to be totally dissolved in *aqua regia*, the catalyst were calcined to burn all of the carbon prior to the analysis. Firstly, about 30 mg of catalysts were calcined at 350 °C (temperature rate of 5 °C/min) in a ceramic crucible under air, for 3 h. Once the

calcination achieved, the solid samples were dissolved or digested using a combination of acids (*aqua regia*). Then, the resulting samples solutions were heated at 50 °C to destroy any organic matter still present. The liquid sample was then converted in a nebulizer into fine droplets called aerosol, a small portion (typically less than 10%) of which went to the plasma.

The plasma is a highly energized ‘cloud’ of gaseous ions and their electrons. Considered to be the fourth state of matter, it is formed by isolated atoms in equilibrium between their neutral and their ionized states [7].

The resulting sample solution is then nebulized into the core of inductively coupled argon plasma, where a temperature of approximately 9000 K is attained. At such high temperatures, the nebulized solution is vaporized, and the analyte species are atomized, ionized and thermally excited. The analyte species can then be detected and quantified with an optical emission spectrometer (OES), which measures the intensity of radiation emitted at the element-specific, characteristic wavelength from thermally excited analyte atoms or ions. Intensity measurements are converted to elemental concentration by comparison with calibration standards.

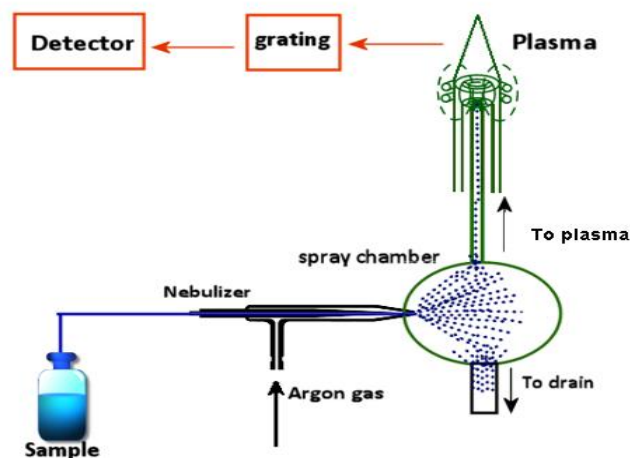


Figure 16: Sample introduction into the ICP-OES. Adapted from[8]

#### I.3.3.4. Temperature-programmed reduction (TPR)

Temperature-Programmed Reduction (TPR) is a technique of characterization of oxidized materials. TPR allows estimating the nature of reducible species present in the catalyst and revealing the temperature at which the reduction of each species occurs [9].

This technique consists in heating the oxidized material in a reducing gas mixture for instance  $H_2$  in He,  $N_2$  or Ar. The concentration of hydrogen in the reducing gas mixture is typically in the 3-17 vol.% range [9].

The TPR profile obtained (temperature of reduction, shape and peaks area, etc.) depend not only on the nature of the oxide, but also on the experimental conditions such as the pretreatment of the material, hydrogen concentration, flow rate of the reducing gas mixture, etc. Therefore, to have good interpretation or comparison of the results, the measurement should be performed in the same conditions. Indeed, for a same sample, the profiles could be significantly different if the measurement was done in different conditions.

In this work, all the catalysts were analyzed in the same conditions. The TPR analyses were performed on an automated AutoChem II 2920 Chemisorption Analyzer from Micromeritics. At first, 40 mg of catalyst were weighted and inserted into a glass reactor. Then, the sample was flushed with a mixture gas of 5 vol.%  $H_2$  in Ar at room temperature. While the gas was flowing, the temperature of the sample was increased linearly at a ramp rate of  $5^\circ C/min$  up to  $750^\circ C$  and then kept at this temperature for 1 h. Finally, the consumption of hydrogen by adsorption/reaction was monitored to get quantitative information on the reducibility of the species present in the catalyst.

## II. Catalytic tests

### II.1. Materials

The substrates tested were palmitic acid,  $>>99\%$  and stearic acid for synthesis,  $\geq 97.0\%$ . The solvents used for the reaction were: hexadecane (ReagentPlus®, 99%) and dodecane (anhydrous,  $\geq 99\%$ ). Hexane (analytical standard,  $\geq 99.7\%$ ) was used as solvent to dilute the reaction products and pentadecane,  $\geq 98.0\%$  (GC) was used for GC peaks identification and calibration. Finally, toluene (gas chromatography MS SupraSolv®,  $\geq 99.8\%$ ) was used as an internal standard for GC analysis. All the products presented here were purchased from Sigma Aldrich and used as such.

### II.2. Experimental setup

#### II.2.1. SPR system presentation

The screening of the catalysts was done in a Screening Pressure Reactor (SPR) system from Freeslate equipped with 24 parallel stainless steel batch reactors of 6 mL each (Figure 17). The SPR system has a wide process window. It operates automatically at temperatures up to  $400\text{ }^{\circ}\text{C}$  and pressures up to 50 bar. The stirring in the reactor vessels is assured by orbital shaking under controlled pressure and temperature conditions.

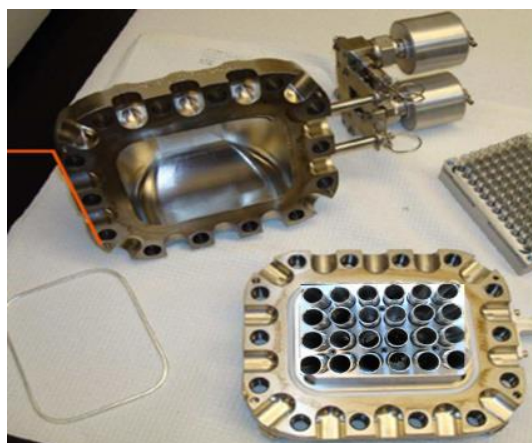


Figure 17: SPR reactors

The SPR is operated via a computer, equipped with softwares (Automation Studio and Library Studio) that provide an user interface, operational controls, process control and recording, and hardware to communicate with and control the SPR system. Automation Studio protocols were used to control the experiment, while, Library Studio was used to collect and store experimental parameters. The SPR system is primarily controlled by the system computer, however, there are also many user controllers located directly on the SPR panel (Figure 18 (a) and its gas control subsystem (Figure 18 (b)).

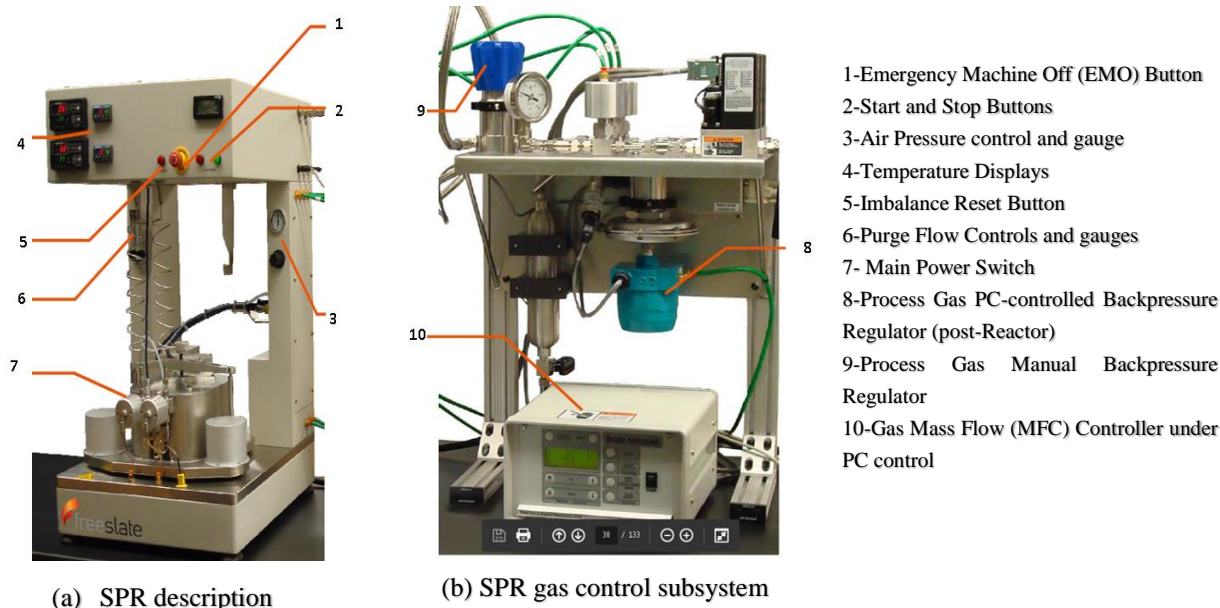


Figure 18: SPR description

### II.2.2. Description of the experimental protocol of catalyst reactivation

Due to their low resistance to spontaneous re-oxidation in contact with atmospheric air, the catalysts were systematically reactivated (i.e. reduced again) under pure hydrogen prior to the catalytic test. This pre-treatment was done directly in the SPR as follows. Firstly, the catalysts were weighted directly into each reactor. Then, the reactor vessel was hermetically sealed (Figure 19) and flushed by a gas flow according to the following protocol.



Figure 19: Sealing of the reactor vessel

At first, the reactors were flushed with  $N_2$  (250 mL/min) at room temperature to remove all the oxygen present. Then, a flow of pure hydrogen (30 mL/min) was flushed for 5 min, prior to gradually increase the temperature up to 350 °C with a temperature ramp rate of 5 °C/min. This temperature was kept constant 3 h always under hydrogen flow. After catalyst reactivation, the reactors were cooled to 30 °C and then flushed with pure  $N_2$  in order to remove the excess of hydrogen. Once the reactivation protocol was completed, the reactor vessel was hermetically sealed and then transferred to a glove box to be charged with the reagents and solvent without any contact with air to avoid the reoxidation of the metals. Finally, after loading the reactors,

the reactor vessel hermetically sealed was removed from the glove box and connected to the SPR unit (Figure 18 (a)) for the catalytic tests.

### II.2.3. Description of the experimental protocol

Connected to the SPR unit (Figure 20), inlet and outlet valves of the reactor vessel were opened. The reactors were flushed three times with N<sub>2</sub>. Then, reactant gas mixture (10% vol.% H<sub>2</sub> in N<sub>2</sub>) was introduced and the pressure was set up as the desired initial value. Then, the reactors were sealed and the heating was started (the temperature ramp rate was 5 °C/min). When the desired temperature was reached, stirring was turned on and the reaction started. At the end of the reaction, the temperature of the vessel was decreased. When the temperature reached 40°C, the valves of the reactor vessel were opened and the reactor was flushed with a N<sub>2</sub> gas flow to remove all the gases from the reactor.



Figure 20: SPR Freeslate Unit

## III. Analysis of the products of reaction

### III.1. Analytical method

#### III.1.1. GC analysis

In order to analyze the products obtained after the decarboxylation reaction, a Shimadzu GC-2010 Plus gas chromatograph equipped with a FID detector and a ZB-5MS column (30 m×0.25 mm×0.25 μm) was used. The choice of this column was determined on the basis of a bibliographic study and some preliminary tests carried out with palmitic acid. The details of the analytical method are presented in Table 10. To avoid the saturation of the column the products of reaction must be diluted using a solvent. Various organic solvents (methanol, ethanol, toluene and hexane) were tested. All of these solvents gave a good reproducibility of the hexadecane (solvent used for the reaction) and pentadecane analyses but only hexane also led to a good reproducibility for palmitic acid analysis. It was then chosen as the solvent for all the further sample preparations before GC analysis.

Table 10: Analytical method parameters

<b>injection</b>		
	Injection mode	Split ratio 100
	Temperature	320 °C
	Carrier gas	H <sub>2</sub>
	Pressure	89.2 kPa
	Total flow	246.6 mL/min
	Column flow	2.41 mL/min
<b>Column oven</b>		
	Initial temperature, T <sub>0</sub>	50 °C
	Rate-T <sub>1</sub>	10 °C/min -120 °C
	Rate-T <sub>2</sub>	50 °C/min-320 °C
	Plateau t <sub>2</sub>	4 min
	Equilibration time	0.5 min
	Total program time	14 min
	Final temperature	320 °C
<b>Detector</b>	FID	
	Temperature	320 °C
	H <sub>2</sub> flow	40 mL/min
	Air flow	400 mL/min
	Makeup gas	N <sub>2</sub>
	Makeup flow	30 mL/min

### III.1.2. Calibration of the GC

Analytically pure chemicals (pentadecane (PD)  $\geq 99\%$  (Aldrich), hexadecane (HD), ReagentPlus®,  $\geq 99\%$  (Sigma-Aldrich), palmitic acid (PA)  $\geq 99\%$  (Aldrich)) were used for calibration. Four samples were prepared from a stock solution S<sub>1</sub> containing a mixture of hexadecane, palmitic acid and pentadecane. The stock solution was diluted in hexane at 75, 50, 25 and 10 wt.% respectively.

### III.1.3. Sample preparation

After the catalytic test, the rack containing the 24 reactors were heated at 80 °C under ultrasonic to avoid the crystallization of unconverted palmitic acid remaining in the reactor at the end of the reaction. Then, the liquid products from each reactor were filtered with syringe filters (hydrophobic PTFE 0.2  $\mu\text{m}$ ) to remove any remaining small solid particles present. Thus, 20  $\mu\text{L}$  of the liquid products obtained were transferred to 2 mL vials and diluted with 980  $\mu\text{L}$  of hexane. Also, 100  $\mu\text{L}$  of toluene were added to the sample as an internal standard. To assure a good homogeneity of the solutions the samples were manually shaken and then placed into the sample holder for analysis.

### III.2. Data treatment

The conversion of PA, the selectivity and yield in PD were determined by equations (27), (28) (29) listed below, respectively. The carbon balance was also determined using (30).

$$\text{PA Conversion (\%)} = \frac{n_{\text{PA}}^0 - n_{\text{PA}}}{n_{\text{PA}}^0} * 100 \quad (27)$$

$$\text{PD Selectivity (\%)} = \frac{n_{\text{PD}}}{(n_{\text{PA}}^0 - n_{\text{PA}})} * 100 \quad (28)$$

$$\text{PD Yield (\%)} = \frac{n_{\text{PD}}}{n_{\text{PA}}^0} * 100 \quad (29)$$

$$\text{Carbon balance (\%)} = \frac{n_{\text{PD}} + n_{\text{PA}}}{n_{\text{PA}}^0} * 100 \quad (30)$$

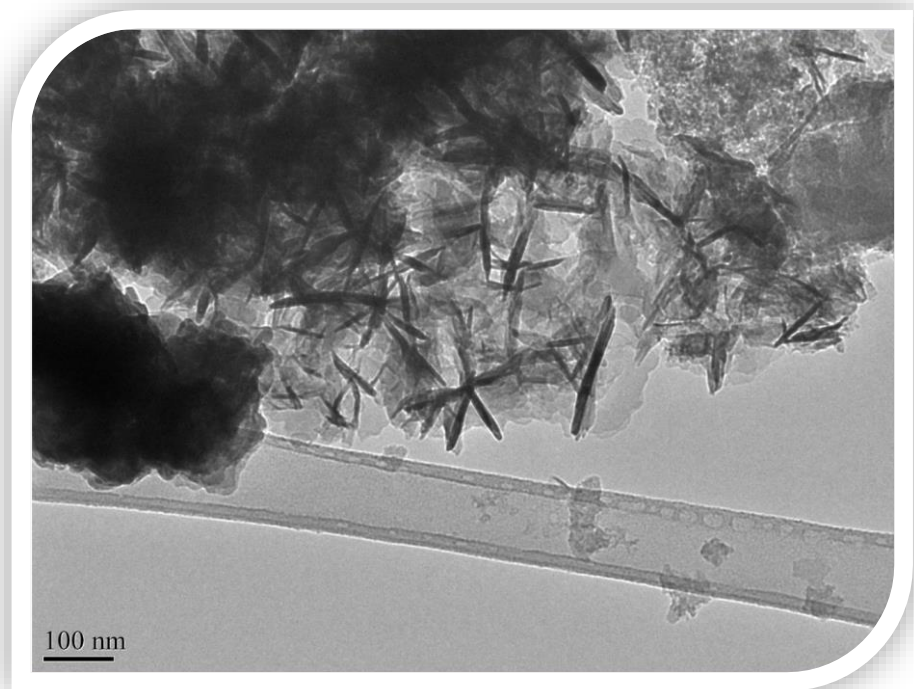
Where  $n_i^0$  and  $n_i$  correspond to the initial and final number of mole of the  $i$  chemical species, respectively.

**References**

- [1] S. Brunauer, P.H. Emmett, E. Teller, *Journal of the American Chemical Society*. 60 (1938) 309-319.
- [2] M. Winey, J.B. Meehl, E.T. O'Toole, T.H. Giddings, *Molecular Biology of the Cell*. 25 (2014) 319-323.
- [3] K.S. Kim, N. Winograd, *Surface Science*. 43 (1974) 625-643.
- [4] C. Battistoni, G. Mattogno, E. Paparazzo, *Surface and Interface Analysis*. 7 (1985) 117-121.
- [5] H. Fischer, <http://xrf-spectroscopy.com/>, accessed, February 23, 2017.
- [6] A. Stefánsson, I. Gunnarsson, N. Giroud, *Analytica Chimica Acta*. 582 (2007) 69-74.
- [7] J.K. Steehler, *Journal of Chemical Education*. 85 (2008) 373.
- [8] <http://www.chemiasoft.com/chemd/node/52>, accessed February 23, 2017.
- [9] J. Zhu, H. Li, L. Zhong, P. Xiao, X. Xu, X. Yang, Z. Zhao, J. Li, *ACS Catalysis*. 4 (2014) 2917-2940.

## Chapter 3

# Characterization study



**SUMMARY**

<b>INTRODUCTION.....</b>	<b>82</b>
<b>I. MORPHOLOGICAL AND TEXTURAL PROPERTIES.....</b>	<b>82</b>
I.1. NITROGEN ADSORPTION/DESORPTION .....	82
I.1.1. Textural properties of the bare carbon support and of the mono- and bimetallic catalysts ..	82
I.1.2. Textural properties of the bimetallic 10%Ni10%Cu/C .....	83
I.1.3. Impact of the preparation method of the catalyst on their textural proprieties .....	84
I.2. TEM AND EDX.....	85
<b>II. SURFACE PROPERTIES.....</b>	<b>89</b>
II.1. XPS .....	89
II.1.1. XPS Analysis of the 10%Ni10%Cu/C catalyst .....	90
II.1.2. Analysis of the Ni-Cu catalysts.....	93
<b>III. BULK PROPERTIES .....</b>	<b>98</b>
III.1. ICP-OES ANALYSIS .....	98
III.2. XRF .....	98
III.3. XRD.....	101
III.3.1. XRD analysis of the 10%Ni /C catalyst.....	101
III.3.2. XRD analysis of the 10%Ni10%Cu/C catalyst.....	102
III.3.3. XRD analysis of the 10%Ni10%Cu/C-calc catalyst .....	104
III.3.4. Determination of the crystallite size and of the d-spacings .....	105
III.3.5. XRD analysis of other monometallic and bimetallic catalysts .....	106
III.4. TPR.....	109
<b>CONCLUSION .....</b>	<b>112</b>
<b>REFERENCES.....</b>	<b>114</b>

## Introduction

The techniques of characterization described in Chapter 2 were used to study the catalysts synthesized by deposition-precipitation. Information on their elemental compositions, textural, structural and morphological properties were collected. Among all the catalysts synthesized in this work, the characterization study was more particularly focused on the carbon supported Ni-Cu bimetallic catalysts with different metals loadings and on two Ni- and Cu-based monometallic catalysts also supported on the same carbon. In this chapter, the results of this characterization study are presented and discussed.

## I. Morphological and textural properties

### I.1. Nitrogen adsorption/desorption

Specific surface areas, pore volumes and mean pore sizes were determined by nitrogen adsorption as described in Chapter 2 Section I.3.1.1.

#### I.1.1. Textural properties of the bare carbon support and of the mono- and bimetallic catalysts

Table 11 shows the textural properties of the bare carbon support and of a series of two monometallic (10%Ni/C and 10%Cu/C) and three bimetallic (5%Ni5%Cu/C, 10%Ni10%Cu/C, 15%Ni15%Cu/C) catalysts. All the catalysts are fresh, i.e. as prepared. The specific surface area of the bare commercial support is 1290 m<sup>2</sup>/g. Its mean pore size and pore volume are 67 Å and 0.68 cm<sup>3</sup>/g, respectively. For all the catalysts, the specific surface area and the pore volume are smaller in comparison with the bare support. That can be explained by the filling of the pores of the support by the metal particles leading to a decrease of the overall pore volume and of the accessible surface of the material. On the contrary, the mean pore size of the catalysts is generally close to the one of the support.

At equal metal loading (i.e; for the 10%Ni, 10%Cu/C and 5%Ni5%Cu/C catalysts), the surface area and pore volume of the monometallic Cu-based catalyst are 1073 m<sup>2</sup>/g and 0.60 cm<sup>3</sup>/g, respectively, whereas, when the metal is Ni, the surface specific and the pore volume decreases of about 200 m<sup>2</sup>/g and 0.09 cm<sup>3</sup>/g, respectively, compared to the values obtained with Cu. That means the mean particle size of Cu are bigger than those of Ni [1]. Nevertheless, the mean pore size is maintained at 67 Å. When the support is loaded with both Ni and Cu (5%Ni5%Cu/C), the surface area, the mean pore size and the pore volume are close but slightly

lower than those of the monometallic Ni-based catalyst. Regarding the bimetallic (5%Ni5%Cu/C, 10%Ni10%Cu/C and 15%Ni15%Cu/C) catalysts, the surface area and the pore volume do not decrease monotonously with the metal content. Surprisingly the 10%Ni10%Cu/C catalyst shows the lowest specific surface area, which could indicate that the particles size of this catalyst are smaller than that of the 15%Ni15%Cu/C sample.

**Table 11: Textural properties of the bare carbon support and of the mono- and bimetallic catalysts**

Catalyst	BET (m <sup>2</sup> /g)	Mean pore size (Å)	Total pore volume (cm <sup>3</sup> /g)
Bare carbon support	1290	67	0.68
10%Cu/C	1073	67	0.60
10%Ni/C	877	67	0.51
5%Ni5%Cu/C	830	64	0.47
10%Ni10%Cu/C	536	66	0.39
15%Ni15%Cu/C	645	64	0.39

### I.1.2. Textural properties of the bimetallic 10%Ni10%Cu/C

The 10%Ni10%Cu/C catalyst prepared by DP was analyzed after three different treatments: fresh (catalyst “as prepared”), activated (catalyst activated at 350 °C under H<sub>2</sub>) and recycled (catalyst obtained after the recyclability test). The results are shown in Table 12.

The specific surface area of the fresh catalyst was 536 m<sup>2</sup>/g. The pore size and pore volume were 66 Å and 0.39 cm<sup>3</sup>/g, respectively. After, the activation, the specific surface area and the pore volume decreased slightly from 536 m<sup>2</sup>/g to 479 m<sup>2</sup>/g and from 0.39 to 0.29 cm<sup>3</sup>/g, respectively. In contrast, the pore size remained almost constant. However, after test, the specific surface area and the pore volume of the catalyst decreased drastically, while, the pore size distribution increase significantly. The reason of this important change in the textural properties could be due to the plugging of the pores of the catalyst by the reaction solvent or by heavy products and coke deposition.

**Table 12: Textural properties of the bimetallic 10%Ni10%Cu/C catalyst at different states**

Catalyst	BET (m <sup>2</sup> /g)	Mean pore size (Å)	Total pore volume (cm <sup>3</sup> /g)
<b>10%Ni10%Cu fresh</b>	536	66	0.39
<b>10%Ni10%Cu activated</b>	479	67	0.29
<b>10%Ni10%Cu recycled</b>	59	89	0.11

### I.1.3. Impact of the preparation method of the catalyst on their textural properties

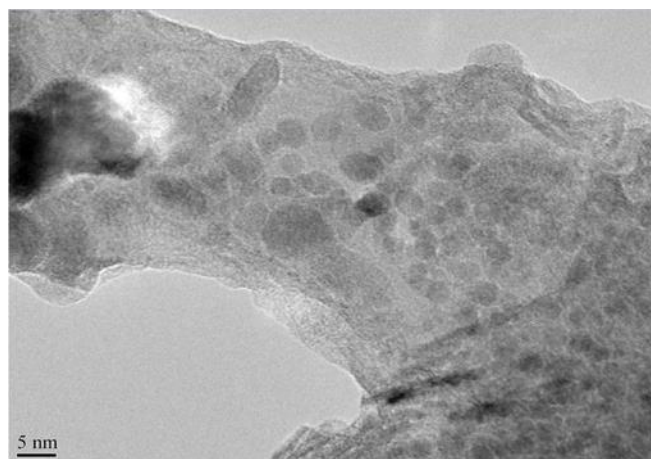
As mentioned in Chapter 2, the bimetallic 10%Ni10%Cu/C was prepared by two different methods (deposition-precipitation and wet impregnation) in order to see the impact on the textural properties. As observed in Table 13, the surface area and pore volume of the 10%Ni10%Cu/C prepared by DP is lower than those obtained with the 10%Ni10%Cu/C-calc prepared by WI. This indicates that, the filling of the pore of the support by the metal particles is more important for the catalyst prepared by DP than for the 10%Ni10%Cu/C-calc catalyst. However, to understand the difference observed with both catalysts, the fresh bare carbon support was also calcined in the same conditions than those of the 10%Ni10%Cu/C-calc. The results obtained showed that the specific surface area and the pore volume of the catalyst decreased from 1290 m<sup>2</sup>/g to 880 m<sup>2</sup>/g and from 0.68 to 0.48 cm<sup>3</sup>/g compared to the fresh bare carbon support. Thus, the decrease of the specific surface area could result from a partial obstruction of the pores during the calcination and/or significant gasification of carbon support [2]. Comparing the support calcined to the 10%Ni10%Cu/C-calc catalyst, the difference between both specific surface areas is only 35 m<sup>2</sup>/g. That means that, for the 10%Ni10%Cu/C-calc sample, the filling of the pores of the support by the active phase is not important. XRD analysis (III.3.3) showed that there are no crystalline phases of NiO and/or CuO in the catalyst calcined, only species in amorphous phases are present.

**Table 13: Textural properties of the bimetallic 10%Ni10%Cu/C and 10%Ni10%Cu-calc catalysts**

Catalyst	BET (m <sup>2</sup> /g)	Mean pore size (Å)	Total pore volume (cm <sup>3</sup> /g)
Bare carbon support	1290	67	0.68
Bare carbon support calcined (450 °C; 3 h; N <sub>2</sub> )	880	60	0.48
10%Ni10%Cu fresh	536	66	0.39
10%Ni10%Cu/C-calc	845	61	0.47

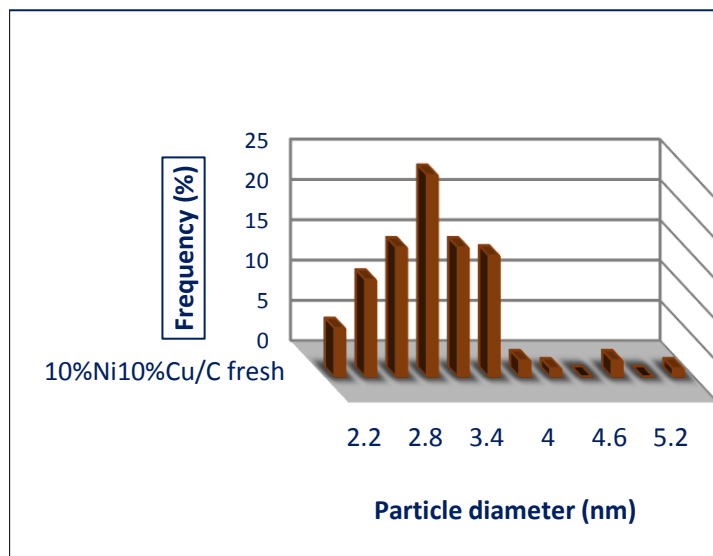
## I.2. TEM and EDX

As it will be shown in Chapter 5 the best catalyst in terms of performance is the 10%Ni10%Cu/C sample. So, it was selected for a detailed TEM study. The observations were performed for the fresh, activated and recycled (after three consecutive recyclability tests) samples. TEM image of the fresh catalyst showed (Figure 21) the presence of spherical shaped particles of nickel and copper ranging from ~2-6 nm and also the presence of agglomerated particles. The average particle size was determined taking into account more than 300 particles.



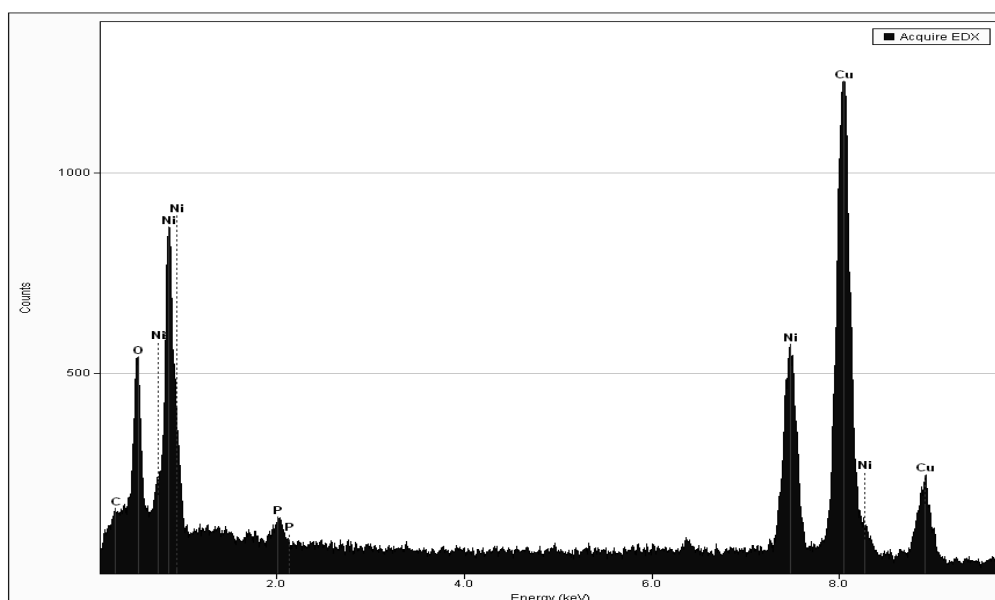
**Figure 21: TEM image of the fresh 10%Ni10%Cu/C catalyst**

Figure 22 shows the metal particle size distribution. As observed, there is a homogeneous distribution of the particles with the majority in the 3-3.3 nm range (3.01±0.6 nm of mean value). Unfortunately, it was difficult to distinguish from TEM images the two different metals, because of their quite similar molecular weights.



**Figure 22:** Particle size distribution for the fresh 10%Ni10%Cu/C catalyst

The composition of the fresh catalyst was determined by EDX. The energy dispersive spectrum is shown in Figure 23. It confirmed, as expected, the presence of copper, nickel, carbon and oxygen. The quantification of these elements are presented in Table 14. However, the energy dispersive spectrum showed also the presence of some traces of phosphorus on the surface of the catalyst. The XRF analysis of this catalyst confirmed also the presence of P, which is one of the impurities originating from the bare support (see description in section III.2).

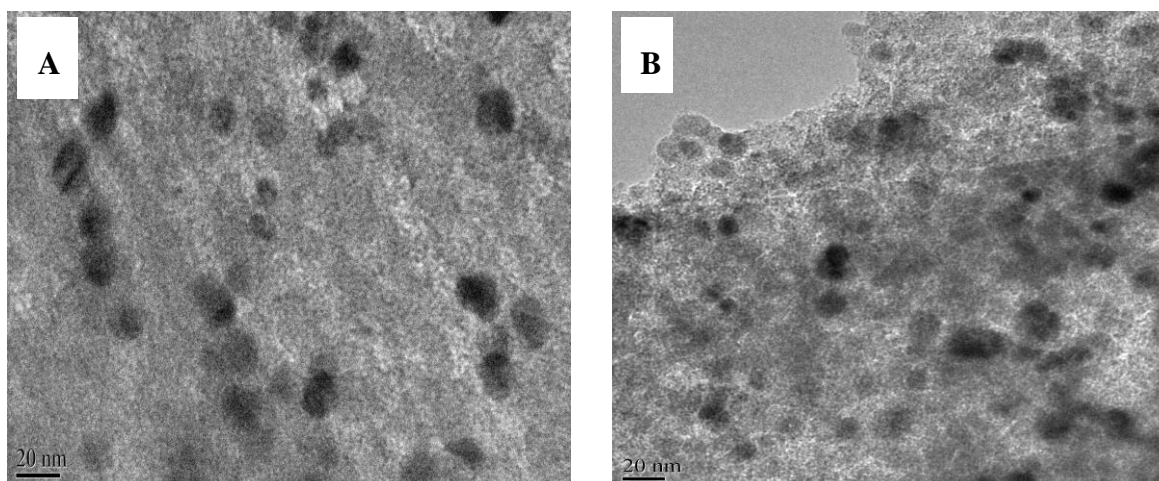


**Figure 23:** EDX analysis of the fresh 10%Ni10%Cu/C catalyst

**Table 14: Quantification of EDX spectra of the fresh 10%Ni10%Cu/C catalyst**

Element	Atomic, %	Ni/Cu ratio
C	37.45 +/- 0.43	
O	43.46 +/- 0.34	
Ni	11.58 +/- 0.27	1.54
Cu	7.49 +/- 0.24	

After reduction at 350 °C under hydrogen for 2 h, the particle size of the catalyst increased. Figure 24 (A) shows the typical image of material obtained after reduction. In this case, around 350 particles were considered to determine the average particle size. This image shows the presence of irregular spherical shapes of particles in the 20-25 nm range. The average particle size value is 17.05+/-3.7 nm.

**Figure 24 : TEM image of the activated (A) and recycled (B) 10%Ni10%Cu/C catalysts**

For the recycled catalyst, 312 particles were taken into account to determine the particles size distribution (Figure 24(B)), which is also in the 10-30 nm range. In this range, the mean value is 16.7+/- 3.4nm. Thus, after three recyclings, the particles size distribution did not change significantly as compared to the activated catalyst (i.e. before the first run) as shown on Figure 25.

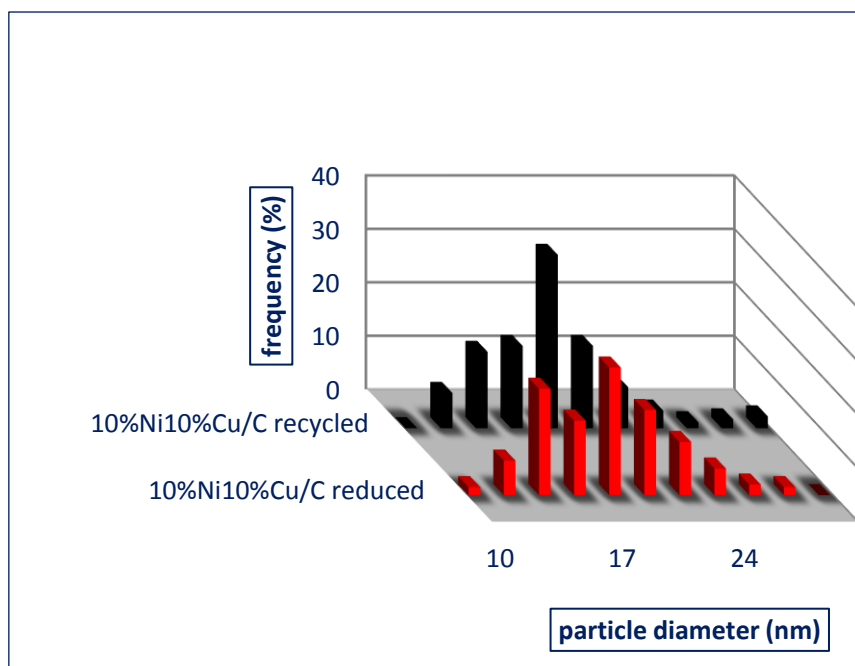


**Figure 25: Metal particle size distribution of 10%Ni-10%Cu/C before and after test**

TEM analysis of the fresh 15%Ni15%Cu/C catalyst was also performed in order to compare with the 10%Ni10%Cu/C sample. The difference is obvious as shown in Figure 26, which demonstrated the presence of two different regions. The first one (Zone 1) presents rod shape structures. A zoom on this zone shows inside of these rod shape, several lattice fringes with d-spacings of 6.3, 6.5 and 6.75 Å. These d-spacings correspond well to NiCuO, which is detected by XRD (see Section III.3.5). The EDX elementary analysis showed the presence of a high quantity of oxygen in this zone (Annex 1). That suggests that copper or/and nickel are present in their oxides forms. For the second zone (Zone 2), the presence of metallic nanoparticles agglomerates was confirmed. The EDX analysis of this zone gave very low quantity of oxygen (Annex 2), which revealed the metallic character of the particles in this zone. Thus, the increase of the metals amount modified the crystalline structure of the species and lead to particle agglomeration.

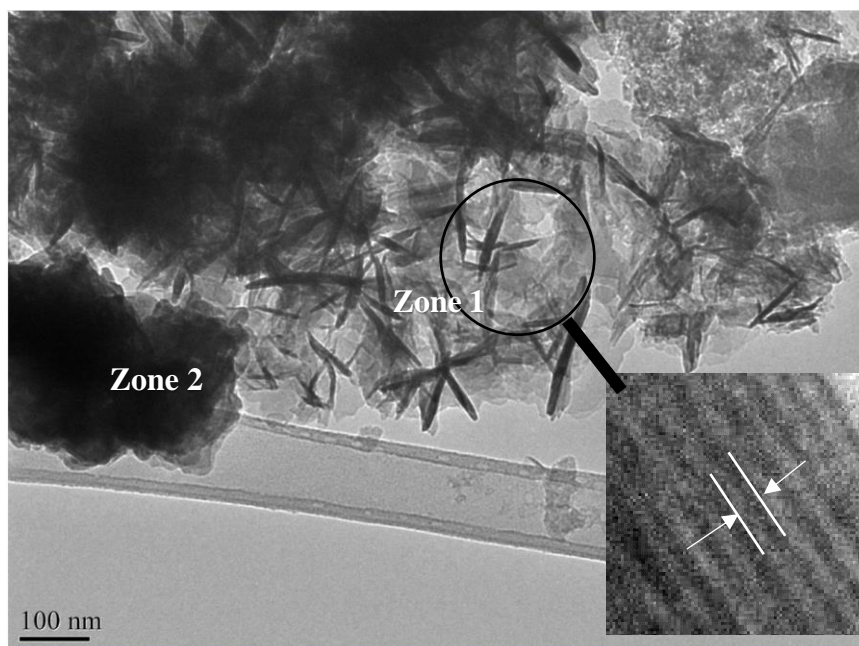


**Figure 26: TEM image of fresh 15%Ni15%Cu/C catalyst**

## II. Surface properties

### II.1. XPS

The bimetallic Ni-Cu catalysts supported on carbon with different loadings and the monometallic 10%Cu/C sample were characterized by X-ray photoelectron spectroscopy to get information about the chemical state of the surface species. All catalysts studied were analyzed before (fresh catalyst) and after activation (activated catalyst) under hydrogen. The 10%Ni10%Cu/C catalyst was analyzed in four different states: fresh; activated; activated-oxidized and recycled-oxidized. The description of these states are given in Table 15.

**Table 15: Description of the different states of the 10%Ni10%Cu/C catalyst**

Notation	Definition
Fresh	Catalyst as prepared
Activated	Catalyst obtained after activation at 350 °C, under hydrogen, for 2 h.
Activated-oxidized	Catalyst which has undergone activation under hydrogen, and which was oxidized on simple contact with the oxygen of the ambient air (room temperature).
Recycled	Catalyst recycled after three consecutive catalytic tests
Recycled-oxidized	Catalyst recycled and oxidized when exposed to air

### II.1.1. XPS Analysis of the 10%Ni10%Cu/C catalyst

Figure 27 shows the XPS spectra of Cu2p and Ni2p of the bimetallic 10%Ni10%Cu/C catalysts in the four different states.

Figure 27 (A1) shows the Cu 2p XPS spectrum of the fresh catalyst. A broad peak at 933.4 eV accompanied by a broad high-energy satellite peak between 938.4 and 945.6 eV correspond to copper oxide (II). The Auger peak observed at 917.5 eV [3] confirms the presence of CuO species on the surface of this sample. However, when the catalyst was activated under H<sub>2</sub>, (Figure 27(A4)), an intense peak was observed at 932.7 eV. This peak could be assigned to Cu or Cu<sub>2</sub>O but as the spectrum did not contain any satellite peak, it can be attributed to metallic copper. Furthermore, regarding the Auger kinetic energy, the peak of the Cu Auger is observed at 918.5 eV, which is characteristic of metallic copper [3]. Thus, the activation of the catalyst under hydrogen at 350 °C is sufficient to reduce all the copper oxide on the surface. Exposing the activated (Figure 27(A2)) and recycled (Figure 27(A3)) catalysts to atmospheric air, their XPS spectra showed a large intense peak, which could be deconvoluted into three peaks. The first one at 932.8 eV is characteristic of the metallic copper. Its presence is confirmed by the Auger peak observed at 918.8 eV. Then, the second peak at 933.8 eV can be attributed to the CuO species and finally the peak at 935.8 eV can be assigned to the presence of isolated-like ionic Cu<sup>2+</sup> species [4].

Similarly, the Ni 2p<sub>3/2</sub> spectra of the 10%Ni10%Cu/C catalyst was recorded for the four different states. Figure 27 (B1) shows the spectrum of the fresh catalyst. It shows two peaks at 853.5 and 855.6 eV, which, according to literature, could be assigned to NiO and Ni(OH)<sub>2</sub> respectively [5]. There is also the presence of a shake-up satellite at 860.6 eV, which confirmed the presence of NiO. After activation (Figure 27 (B4)), the XPS spectra of the catalyst showed the presence of one peak at 852.8 eV and the 2p<sub>3/2</sub> satellite peak at 858.6 eV, which are characteristic of the metallic nickel [5].

The Ni 2p<sub>3/2</sub> spectra of the activated-oxidized and recycled-oxidized 10%Ni10%Cu/C catalysts showed two Ni species in each sample.

For the activated-oxidized catalyst, the first Ni 2p<sub>3/2</sub> peak could be attributed to metallic nickel at 852.9 eV [6]. In fact the presence of oxygen slightly shifted the peak of pure metallic nickel from 852.6 to 852.9 eV. In contrast for the recycled-oxidized catalyst, the first peak identified at 852.7 eV is characteristic of pure metallic Ni. The second peak at 856.6 and at

856.2 eV for the activated-oxidized and recycled-oxidized catalysts, respectively, could be assigned to NiO or Ni(OH)<sub>2</sub>. However, these species have similar spectra and could be differentiated by their XPS O 1s spectra where a peak at 531.6 eV (Figure 28) was detected. This latter corresponds to the presence of Ni(OH)<sub>2</sub> [7]. Thus, the peaks at 856.6 and at 856.2 eV confirmed to the presence of Ni(OH)<sub>2</sub>.

However, these catalysts are very sensitive to oxidation in contact with air. Therefore, it is required to work in controlled atmosphere to avoid their reoxidation. Additionally, comparing the XPS spectra of the activated-oxidized and recycled-oxidized catalysts, it could be observed that the nickel species in both samples are the same but with different Ni/Ni(OH)<sub>2</sub> ratio. In fact, in the activated-oxidized catalyst, Ni/Ni(OH)<sub>2</sub> is 0.63, while, this of the recycled-oxidized catalyst is 1.06, which indicates that the activated catalyst is very sensitive to reoxidation by air. Two main reasons, could explain this behavior. The first one is that the recycled catalyst may contain either carbonaceous residues or solvent, which tend to physically cover the active surface and lead to pore blocking [8]. This could lead to a slow oxidation of metallic Ni with ambient air. The second reason could be the unequal duration of the contact of the two catalysts with ambient air, which leads to differentiate the oxidation level.

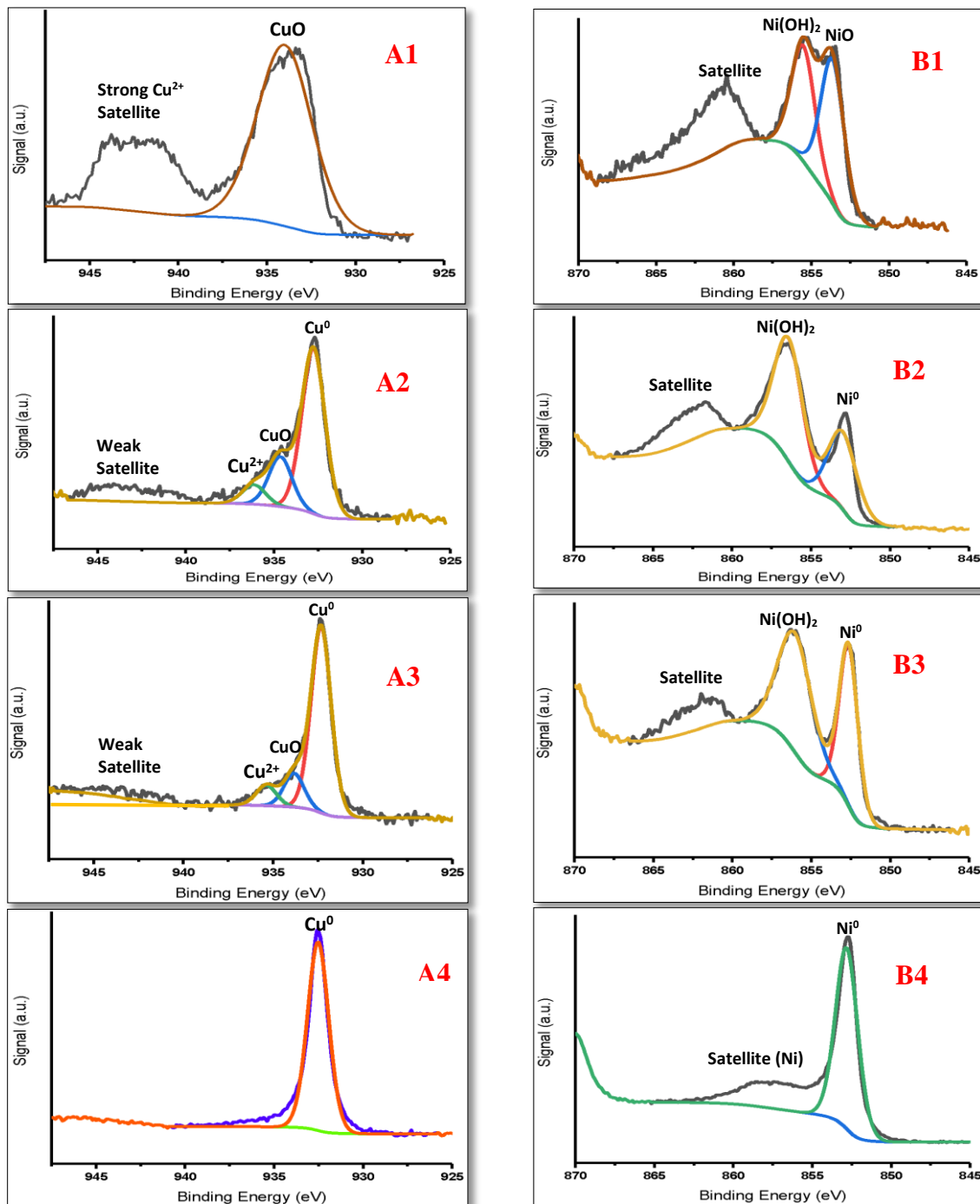


Figure 27: XPS spectra of Cu 2p<sub>3/2</sub> (A1-A4) and Ni 2p<sub>3/2</sub> (B1-B4) of the fresh (A1/B1), activated-oxidized (A2/B2), recycled-oxidized (A3/B3) and activated (A4/B4) 10%Ni10%Cu/C catalyst

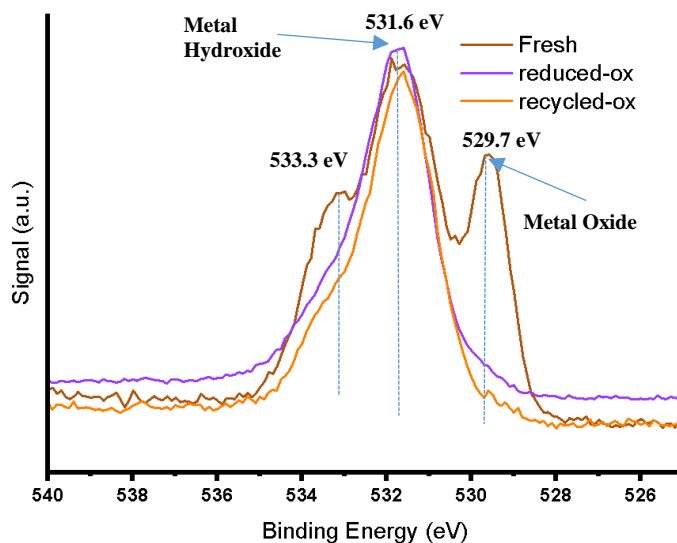


Figure 28: O 1s XPS spectrum of 10%Ni10%C at three different states

### II.1.2. Analysis of the Ni-Cu catalysts

The surface compositions of various Ni-Cu catalysts with different metal loadings were analyzed by XPS before and after activation under hydrogen at 350 °C for 2 h. Figure 29 and Figure 31 show the Cu 2p and Ni 2p XPS spectra of three bimetallic samples (5%Ni5%Cu/C; 10%Ni10%Cu/C; 15%Ni15%Cu/C) and one monometallic catalyst (10%Cu/C). The binding energies of Cu2p<sub>3/2</sub> and Ni2p<sub>3/2</sub> regions and Auger kinetic energies of CuLMM of the catalysts are summarized in Table 17.

Firstly, the XPS analysis revealed that, before activation (see Figure 29 (A) and Figure 31 (A) for Cu 2p and Ni 2p, respectively), all active phase species are in oxide state. For the 10%Cu/C catalyst (Figure 29 (A)), the XPS Cu p<sub>3/2</sub> spectra showed a broad signal which could be deconvoluted in two different species. The first peak located at 933.6 eV could be attributed to CuO according to the literature [9], while the second peak at 935.1 eV could be attributed to Cu(OH)<sub>2</sub> [10]. In addition, a satellite peak, characteristic of copper (II) species is located at 944 eV. Finally, the Auger peak at 916.2 eV confirmed the presence of Cu<sup>2+</sup> (most probably Cu(OH)<sub>2</sub>) [11]. Then, for the 5%Ni5%Cu/C and 15%Ni15%Cu/C catalysts (Figure 29), the XPS spectra of Cu 2p<sub>3/2</sub> showed the presence of Cu(NO<sub>3</sub>)<sub>2</sub> centered at 935.5 eV and a strong Cu<sup>2+</sup> satellite of Cu 2p<sub>3/2</sub> is observed at 944 eV, which confirms the presence of copper oxide (II). Regarding the Auger peak, it is located at 915.3 eV, which is characteristic of the presence of Cu(NO<sub>3</sub>)<sub>2</sub> [11]. The presence of copper nitrate obviously comes from the precursor salt used in the synthesis. This nitrate is of course unwanted in the final catalyst, because it promotes a

rapid deactivation [12]. In contrast, as mentioned above, the 10%Ni10%Cu (fresh) catalyst is composed of CuO and does not contain  $\text{Cu}(\text{NO}_3)_2$  species.

Regarding the Ni 2p (Figure 31 A), the XPS spectra of the 5%Ni5%Cu/C and 15%Ni15%Cu/C catalysts show the same profile. For both catalysts, the  $2p_{3/2}$  region shows two peaks at 856.5 and 861.5 corresponding to the  $\text{Ni}(\text{OH})_2$  species and Ni  $2p_{3/2}$  satellite of  $\text{Ni}(\text{OH})_2$ . In addition, the region  $2p_{1/2}$  shows two other peaks at 873.8 eV and 880 eV corresponding to  $\text{Ni}(\text{OH})_2$  and its satellite peak. Finally, for the fresh 10%Ni10%Cu catalyst, the Ni  $2p_{3/2}$  spectrum showed the presence of both NiO and  $\text{Ni}(\text{OH})_2$  species as previously mentioned.

After activation (Figure 29 B and Figure 31 B for Cu 2p and Ni 2p, respectively) the XPS analysis of the Cu  $2p_{3/2}$  spectrum revealed two clearly defined peaks at 932.7 and 952.7 eV which could be attributed to copper oxide (I) ( $\text{Cu}_2\text{O}$ ) or metallic copper (Cu). However, the Cu  $2p_{3/2}$  spectrum did not show any weak satellite peak and the Cu Auger kinetic energy shows the presence of the characteristic peak of the metallic copper located at 918.5 eV. Thus, undoubtedly, after activation, all copper species are in metallic state. Similarly, for the Ni 2p, after activation all nickel species are in the metallic phase. This is confirmed by the core level binding energy of metallic nickel identified at 852.8 and 870.1 eV respectively for  $2p_{3/2}$  and  $2p_{1/2}$  region.

To conclude, the XPS analysis revealed that the 5%Ni5%Cu/C and 15%Ni15%Cu/C catalysts contain the same species ( $\text{Ni}(\text{OH})_2$  and  $\text{Cu}(\text{NO}_3)_2$ ) before the activation while, the catalyst 10%Cu10%Ni/C only contains NiO,  $\text{Ni}(\text{OH})_2$ , and CuO. After activation, all of the bimetallic catalyst studied contain nickel and copper in the metallic state.

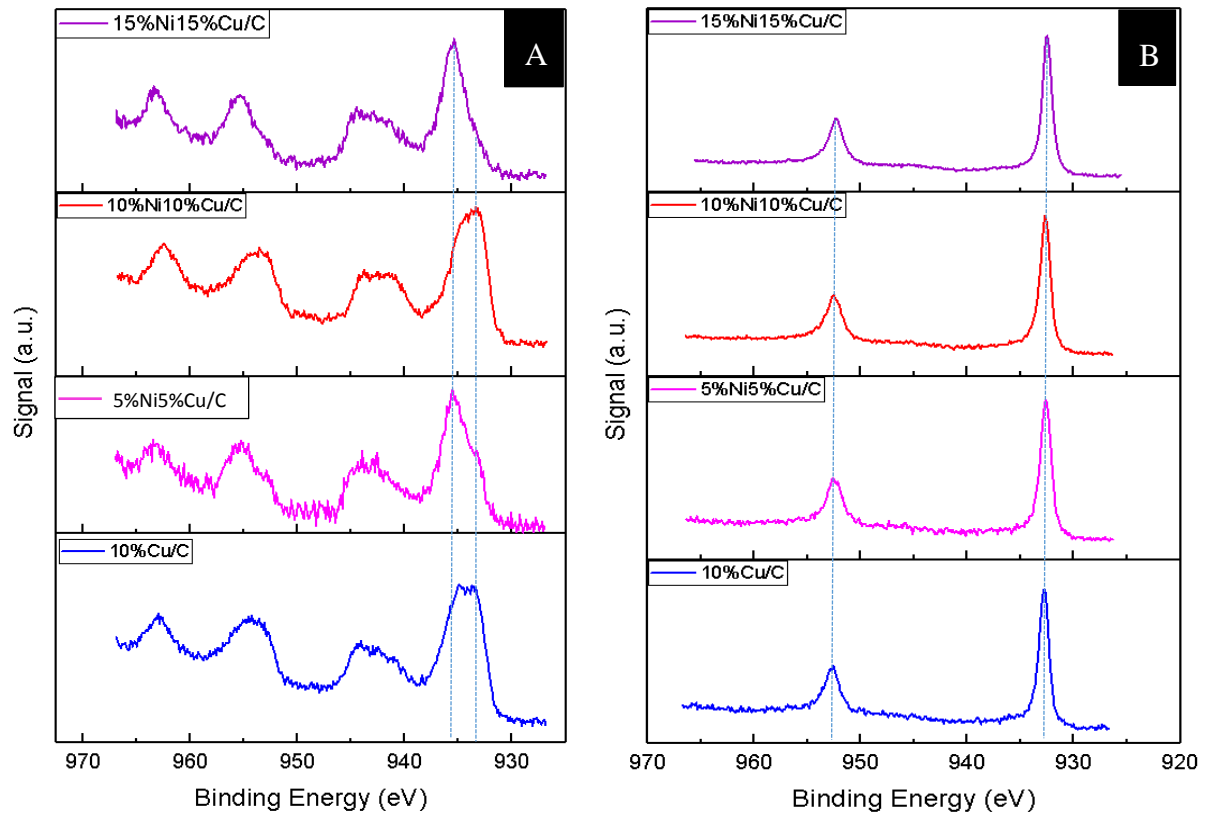


Figure 29: Cu 2p XPS spectra of the bimetallic and the monometallic catalysts before (A) and after (B) activation

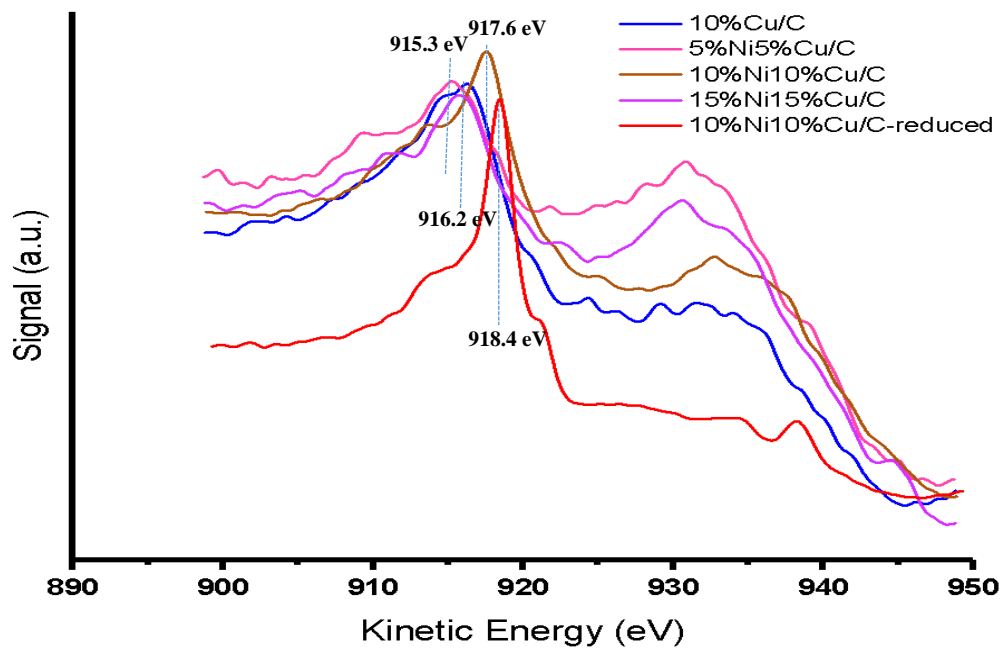
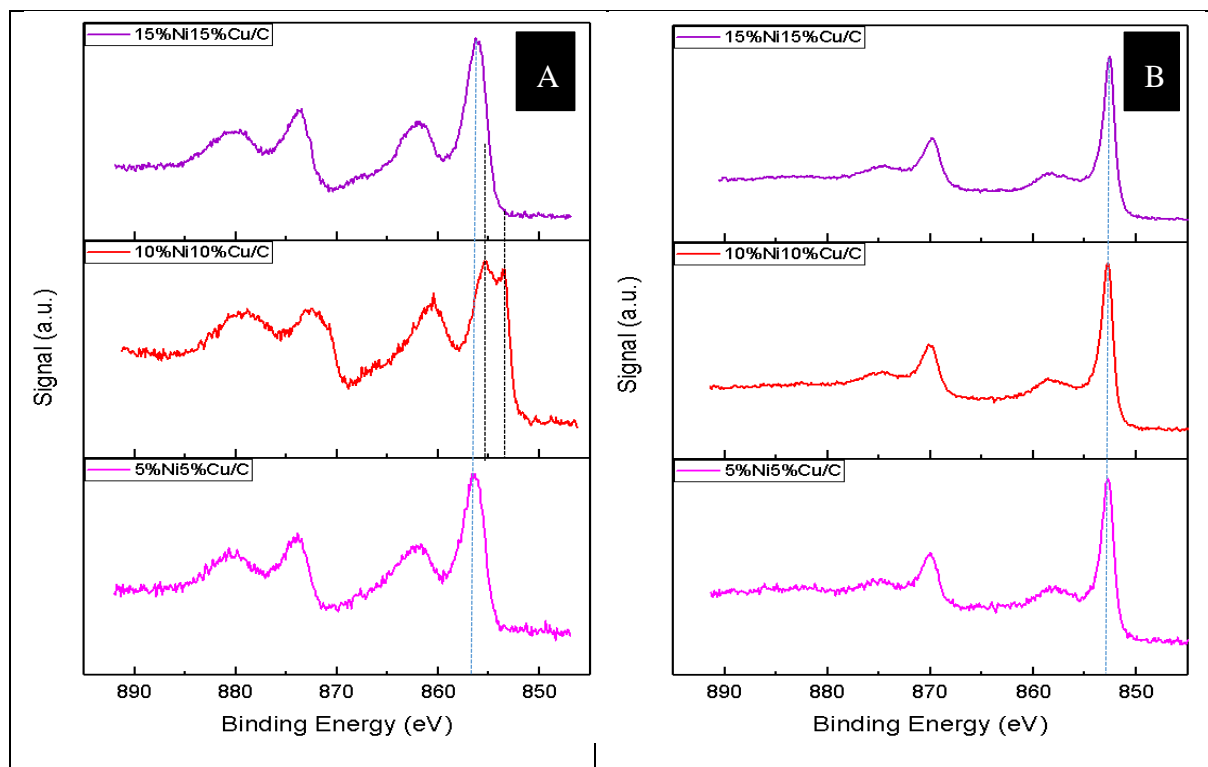


Figure 30: Cu Auger kinetic energy effect of the bimetallic and the Cu monometallic catalyst



**Figure 31 : Ni 2p XPS spectra of the bimetallic catalysts before (A) and after (B) activation**

The amounts of Ni and Cu present on the surface of the bimetallic Ni-Cu/C catalysts were also determined after different treatments. For instance, the surface composition of the 10%Ni10%Cu/C catalyst was determined for fresh, activated-oxidized, recycled-oxidized samples before and after activation. The same analysis was done for the 5%Ni5%Cu/C and 15%Ni15%Cu/C catalysts before and after their activation. The Ni/Cu ratio on the surface was evaluated. The results obtained are reported in Table 16. They show that in all cases, for the fresh catalysts, nickel content on the surface is higher than that of copper. This indicates that the surface layer of the catalysts is enriched in nickel.

For the 10%Ni10%Cu/C, after the activation the Ni/Cu ratio slightly decreased from 2 to 1.7 (entry i) for the fresh catalyst and from 5.4 to 4.3 (entry ii) for the activated-oxidized catalyst and finally from 4.3 to 2.3 (entry iii) for the recycled-oxidized catalyst. This suggests that there is a migration of some Cu particles from the bulk to the surface of the catalyst during the H<sub>2</sub> treatment, because of the increase of Cu and Ni species on the surface layer. However, the surface of the catalyst remains still enriched in nickel.

For the 5%Ni5%Cu/C catalyst, before and after activation, the nickel species on the surface remained constant at 2.1%, while the Cu increased from 0.8 to 1.2%. Therefore, the

Ni/Cu ratio is decreased from 2.6 to 1.7 (entry iv). That could be due to a migration of some Cu particles from the bulk to the surface of the catalyst. In contrast, after activation of the 15%Ni15%Cu/C catalyst, Cu and Ni amounts increase simultaneously on the surface. That means, there is migration of both species (Cu and Ni) from the bulk to the surface of the catalyst. However, the Ni/Cu ratio decreases from 3.3 to 1.6 (entry v), indicating that there is more copper migration than Ni. Nevertheless, the surface layer of the catalyst remains enriched in nickel. Comparing these results to those obtained by ICP analysis (see III.1 section), the bulk of the catalysts studied are enriched in copper, excepted the 10%Ni10%Cu/C catalyst, which is enriched in nickel.

**Table 16: Compositions in Ni and Cu present at the surface of the bimetallic Ni-Cu/C catalysts**

Catalyst	State	Ni 2p (%)	Cu 2p (%)	Ni/Cu ratio	Entry
10%Ni10%Cu/C	fresh	5.2	2.7	2.0	(i)
	activated	7.4	4.4	1.7	
	activated-oxidized	1.9	0.4	5.4	(ii)
	activated-ox-activated	2.7	0.6	4.3	
	recycled-oxidized	1.0	0.2	4.3	(iii)
	recycled-ox-activated	2.4	1.0	2.3	
5%Ni5%Cu/C	fresh	2.1	0.8	2.6	(iv)
	activated	2.1	1.2	1.7	
15%Ni15%Cu/C	fresh	5.4	1.6	3.3	(v)
	activated	7.1	4.4	1.6	

**Table 17: Binding energy of Cu2p3/2 and Ni2p3/2 and Auger kinetic energy of CuLMM**

Sample	Fresh catalysts						Activated catalyst		
	Cu 2p3/2 BE (eV)	Ni 2p3/2 BE (eV)		CuLMM Auger KE (eV)			Cu 2p3/2 BE (eV)	Ni 2p3/2 BE (eV)	CuLMM Auger KE (eV)
	CuO or Cu(NO <sub>3</sub> ) <sub>2</sub>	NiO	Ni(OH) <sub>2</sub>	CuO	Cu(OH) <sub>2</sub>	Cu(NO <sub>3</sub> ) <sub>2</sub>	Cu <sup>0</sup>	Ni <sup>0</sup>	Cu <sup>0</sup>
10%Cu	934.1	-	-	-	916.3		932.8	-	918.5
5%Ni5%Cu/C	935.5	-	856.4	-	-	915.3	932.7	852.8	918.4
10%Ni10%Cu/C	934.1	853.5	855.6	917.6	-	-	932.7	852.8	918.5
15%Ni15%Cu/C	935.4	-	856.4	-	-	915.5	932.7	852.7	918.5

### III. Bulk properties

#### III.1. ICP-OES analysis

In order to determine quantitatively the amounts of metal present in the synthesized catalysts, the ICP-OES technique was used. The results obtained are presented in Table 18. The theoretical and actual loadings are generally close but some differences are observed for a few samples. This could be due to two reasons. First, the difficulty to mineralize carbon-based samples prior to ICP analysis. Some metal particles may be inaccessible for the acids during the digestion process. It is also possible that some metals are lost during the preparation. Indeed, it is possible that all the metal precursors were not adsorbed on the support during the reduction by hydrazine. Some metal could hence stay in the solution and then be eliminated when filtrating or/and be deposited on the walls of the reactor.

Table 18: ICP analysis of the metal contained in the catalysts

Catalysts	Theoretical metal loading (in wt.%)		Measured metal loading (in wt.%)		Ni/Cu
	Ni	Cu	Ni	Cu	
<b>10%Cu</b>	-	10	-	10.3 ±0.4	-
<b>10%Ni</b>	10	-	7.6 ± 0.2	-	-
<b>5%Ni5%Cu</b>	5	5	5.2±0.2	6±0.2	0.9
<b>10%Ni10%Cu</b>	10	10	10.9±2.2	6.5±1.5	1.7
<b>15%Ni15%Cu</b>	15	15	8.5±0.3	14.5±0.7	0.6

#### III.2. XRF

X-ray fluorescence was used to estimate the elemental composition of the materials. It has to be noted that the oxygen and carbon are not detected by this technique. For this reason, the absolute elemental composition cannot be determined. However, metals ratio can be estimated for the bimetallic catalysts supported on carbon. The results obtained are showed in Table 19. As observed, the Ni/Cu ratio of all of the bimetallic catalysts are inferior to 1, which means that the bulks of the catalysts are rich in copper.

**Table 19: Ni/Cu ratio of bimetallic Ni-Cu/C**

Catalyst	Ni/Cu ratio
5%Ni5%Cu/C	0.85
10%Ni10%Cu/C	0.78
15%Ni15%Cu/C	0.59

A comparison of the Ni/Cu ratio determined by XRF and by ICP shows similar results for the 5%Ni5%Cu/C and 15%Ni15%Cu/C catalysts (Table 20). In contrast, for the 10%Ni10%Cu/C catalyst, the Ni/Cu ratio analyzed by ICP is around 3 times higher than the value obtained by XRF. This difference could be explained by the presence of high concentration of oxides in the sample, which are not measured quantitatively by XRF [13]. Therefore, given that XRF cannot detect all the elements so precisely as ICP-OES does [14], it can be considered that the Ni/Cu ratio in the 10%Ni10%Cu/C sample is 1.7. That indicates that the bulk of this catalyst is rich in nickel. Regarding the XPS results, as previously mentioned, the Ni/Cu ratio shows that all the bimetallic catalysts contain higher Ni content than Cu on the surface, meaning that the surface layer of the catalysts is enriched in nickel.

The Ni/Cu ratio of the 10%Ni10%Cu/C catalyst determined by EDX analysis is 1.5. This suggests that the surface of the catalyst is rich in nickel. These results are in good agreement with those obtained by XPS. Therefore, for the bimetallic 10%Ni10%Cu/C catalyst, the surface and the bulk are both enriched in Ni whereas for the 5%Ni5%Cu/C and 15%Ni15%Cu/C catalysts the surface is rich in Ni and the bulk in Cu.

**Table 20: Comparison of the Ni/Cu ratio of bimetallic Ni-Cu/C catalysts determined by XRF, ICP and XPS**

Catalyst	XRF	ICP	EDX	XPS
5%Ni5%Cu/C	0.9	0.9	-	2.6
10%Ni10%Cu/C	0.8	1.7	1.5	2
15%Ni15%Cu/C	0.6	0.6	-	3.3

Figure 32 shows the energy spectrum obtained for the fresh 10%Ni10%Cu/C catalyst. The XRF spectrum shows the presence of Ni and Cu, which are the main elements in the catalyst. In addition, the XRF spectrum showed also the presence of some traces of Fe, Ca, Ti and P originating from the support (activated carbon) as shown on Figure 33. The peak of Zr originates from the detector and that of Rh is from the X-ray tube.

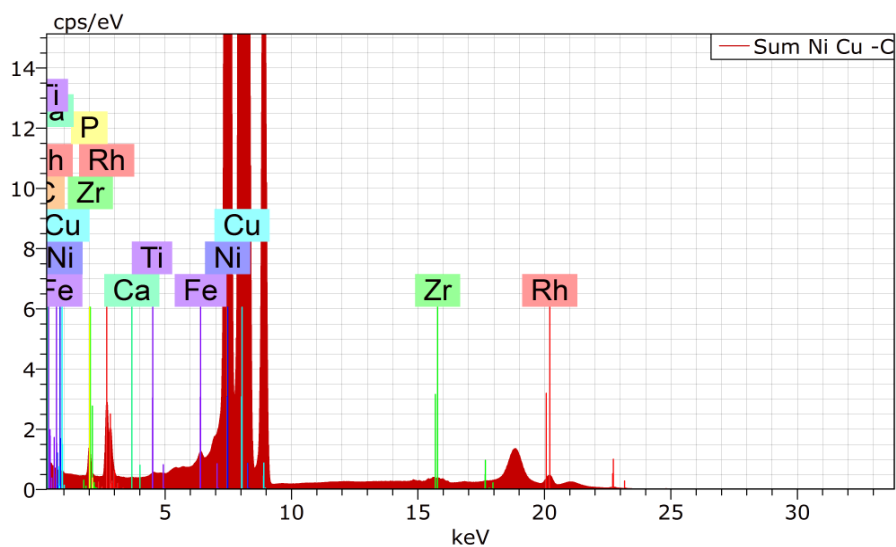


Figure 32: X-ray fluorescence spectrum of 10%Ni10%Cu/C

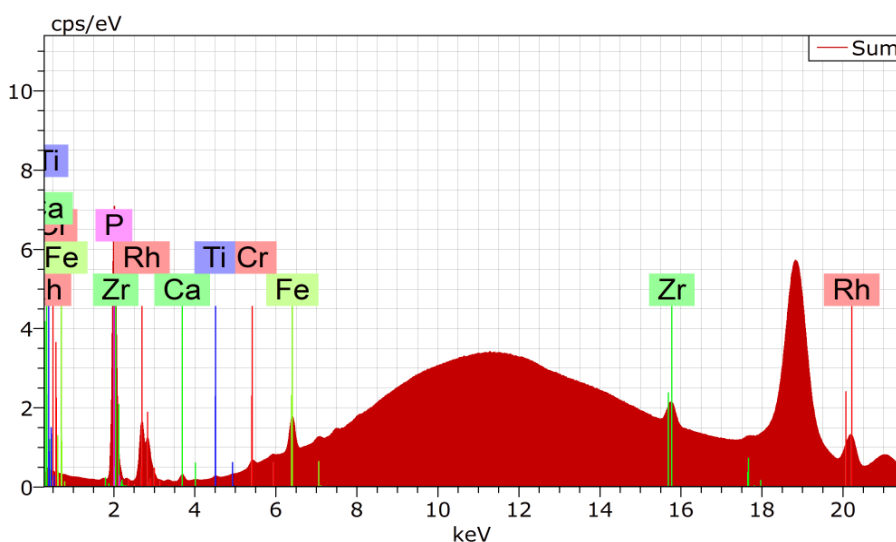
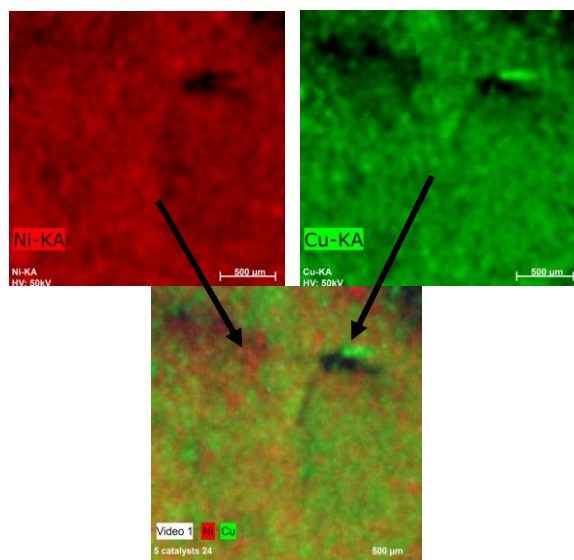


Figure 33: X-ray fluorescence spectrum of bare carbon support

The X mapping obtained for the fresh 10%Ni10%Cu/C catalyst permits to estimate the dispersion of the Ni and Cu species on the surface of the carbon support. Figure 34 shows Ni (in red) and Cu (in green) particles on the surface. The X mapping confirmed a homogeneous dispersion of both metals.



**Figure 34: X Mapping of the fresh 10%Ni10%Cu/C catalyst**

### III.3. XRD

The XRD analyses of the samples were carried out to determine the crystalline structure of the nickel and copper species.

#### III.3.1. XRD analysis of the 10%Ni /C catalyst

The crystallinity of the catalyst 10%Ni/C under three different treatments (i.e. fresh, activated and recycled) was studied. The results obtained are shown in Figure 35. The diffractogram of the fresh catalyst showed several peaks of weak intensity. The comparison of this diffractogram with the PDF card 00-054-1419 showed that the fresh sample contains complex form of nickel species, which is known to decomposed into metal powder in contact with air contact in the temperature range 70-200 °C [15]. It has been reported that this complex decomposition is violently exothermic and could lead to explosion if the sample is heated in a bulk form [13].

After being activated under pure hydrogen, the X-ray diffraction patterns showed the presence of pure Ni at  $44.36^\circ$  and  $51.69^\circ$  corresponding to the diffractions planes (111) and (200), respectively (PDF 00-001-1258). In the same way, for the recycled catalyst, the XRD diffraction patterns showed also the presence of pure Ni, but the diffraction angles were slightly shifted to  $44.42^\circ$  and  $52.28^\circ$ . In fact, compared to the activated catalyst, the width at half height of the peaks (BFWHM) of the recycled catalyst decrease slightly, which corresponds to a slight increase of the average crystal size (Table 21). Nevertheless, the modification of the crystallinity of the catalysts activated and recycled is not significant.

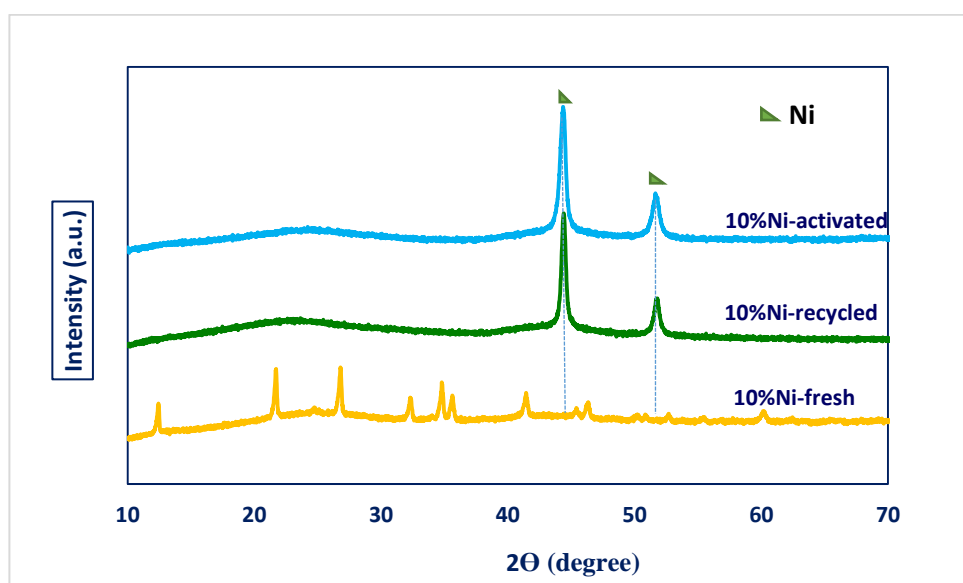


Figure 35: XRD diffractograms of the 10%Ni/C catalyst at different states

### III.3.2. XRD analysis of the 10%Ni10%Cu/C catalyst

The XRD characterization of the 10%Ni10%Cu/C catalyst was also carried out for three different states (fresh, activated and recycled) to determine the different crystalline structures of the metal dispersed on the support. Figure 36 shows the XRD diffractograms obtained. The fresh catalyst revealed the presence of several CuO monoclinic crystallites with various diffractions planes. Thus, the X-Ray diffraction peaks  $32.48^\circ$ ,  $35.5^\circ$ ,  $38.69^\circ$ ,  $38.89^\circ$ ,  $48.66^\circ$ ,  $53.41^\circ$ ,  $58.25^\circ$ ,  $61.46^\circ$ ,  $65.72^\circ$ ,  $67.85^\circ$  and  $68.01^\circ$ , were attributed to the diffractions planes (110), (002/-111), (111), (200), (-202); (020), (202), (-113), (022), (113) and (220), respectively. These results are in good agreement with the standard data from the JCPDS PDF card 04-007-0518. Additionally, the presence of NiO of hexagonal axes structure is confirmed with peaks at  $2\theta$  of  $37.25^\circ$ ,  $43.29^\circ$ ,  $62^\circ$ ,  $85^\circ$  and  $62.91^\circ$  corresponding to the diffractions planes (101), (012), (110) and (104), respectively, according to the standard data from JCPDS PDF card 00-044-1159 [16].

When the catalyst underwent an activation under hydrogen (activated 10%Ni10%Cu), the XRD pattern of the catalyst showed the presence of two components. By superimposing the XRD patterns of pure Ni and Cu on that of the 10%Ni10%Cu/C catalyst, the result showed clearly the presence of a physical mixture of pure Cu with peaks at  $43.30^\circ$  and  $50.43^\circ$  corresponding to the diffractions planes (111) and (200), respectively and pure nickel of cubic structure with peaks at  $44.43^\circ$  and  $51.78^\circ$  corresponding to (111) and (200) planes, respectively. Similar results were observed by Feng *et al.* [17] and Bonet *et al.* [18-19]. Therefore, the 10%Ni10%Cu/C catalyst does not seem to contain any Ni-Cu alloy.

After three catalytic tests, the diffraction patterns of the recycled 10%Ni10%Cu/C catalyst presented the same diffraction peaks at the same diffraction angles  $2\theta$  than the activated catalyst. However, the intensity of the peaks was slightly different (Figure 36). That involves that, the 10%Ni10%Cu/C catalyst was stable after test. Moreover, the XRD pattern showed the presence of two peaks at  $41.67^\circ$  and  $46.54^\circ$  with very weak intensity, which could be assigned to the presence of metal-oxide species, formed when the catalyst was put in contact with ambient air. That is also the reason of the presence of these two peaks on the activated catalyst, with very weak intensity.

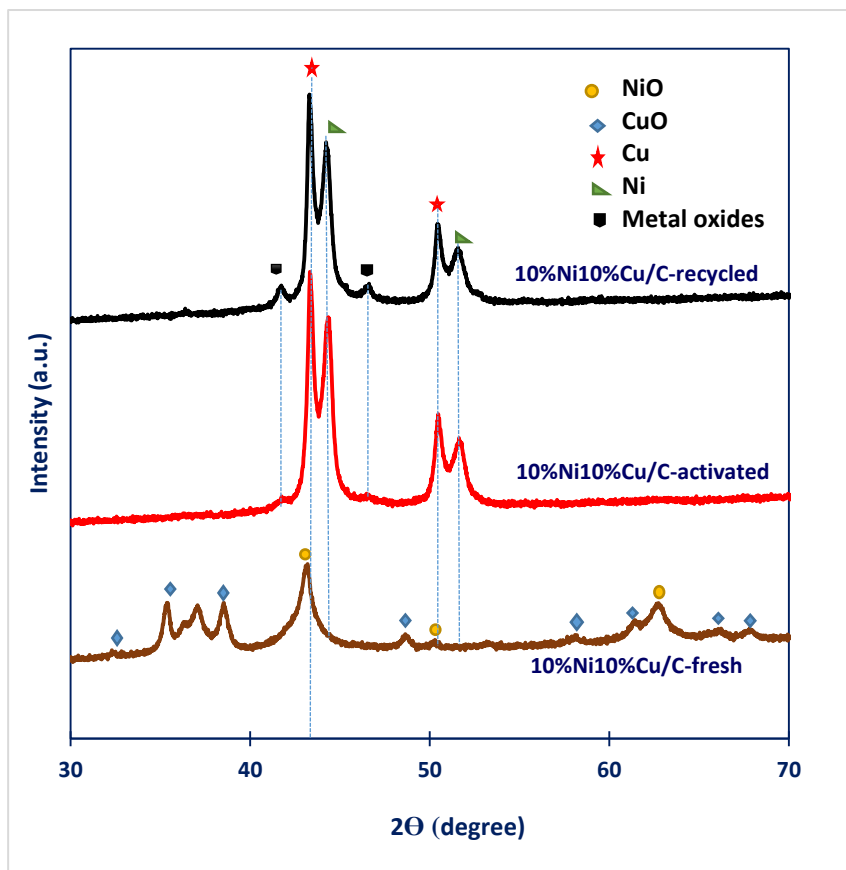


Figure 36: Diffractograms of 10%Ni10%Cu/C at different states

### III.3.3. XRD analysis of the 10%Ni10%Cu/C-calc catalyst

Figure 37 shows the X-ray diffraction spectrum of the 10%Ni10%Cu/C-calc catalysts (prepared by incipient wetness impregnation followed by calcination). As observed, the diffractogram showed the presence of very large peaks without any crystal phase. Normally, NiO and CuO would be expected after calcination under  $N_2$  [20]. The two species are certainly well dispersed on the support and are in amorphous phases, which are not detected by XRD.

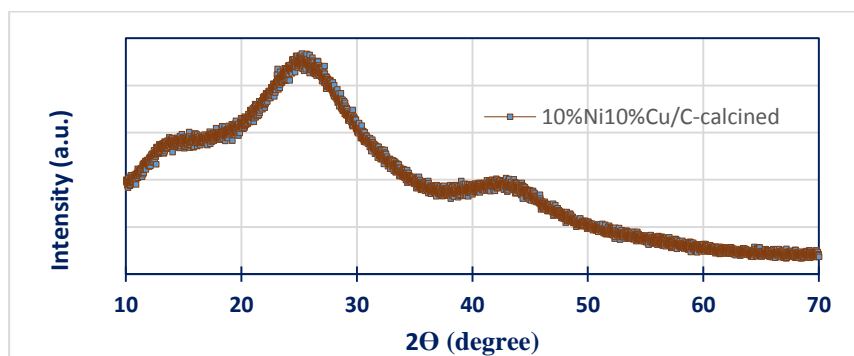


Figure 37: Diffractogram of the 10%Ni10%Cu/C catalyst prepared by impregnation and calcined

### III.3.4. Determination of the crystallite size and of the d-spacings

To estimate the crystal size of the metal particles in activated and recycled 10%Ni10%Cu/C catalysts and determine the distance between two crystallographic planes (d-spacing), Scherrer formula and Bragg's law were used, respectively. These equations were described in Chapter 2.

Given that the XRD pattern showed the presence of both nickel and copper, the peak containing the two components was fitted by Fullprof 2000 software to separate them and to determine their crystal size. The results obtained are presented in Table 21. The size of the metallic crystallite for the activated and the recycled catalysts remains almost the same whatever the diffraction planes considered for the calculation. On the contrary, the crystal size of Ni in the 10%Ni/C catalyst increased slightly after test. Based on Ni (111) plane the crystal size increased from 18.5 to 23.8 nm and based on Ni (200) plane from 15.6 to 19.1 nm. Given that the crystal size of Ni–Cu-based catalyst supported on carbon after the recyclability tests seems to be stable if compared to the monometallic Ni-based catalyst, it can be concluded that, the incorporation of copper increased the stability of the catalyst.

**Table 21: X-ray diffraction data for the different catalysts**

Catalyst	2 $\theta$ (°)	metal	hkl	BFWHM (°)	d-spacing (nm)	D crystal size (nm)
<b>10%Ni10%Cu/C-activated</b>	43.33	Cu	111	0.45	2.09	21.2
	44.34	Ni	111	0.74	2.04	12.9
	50.47	Cu	200	0.56	1.81	17.3
	51.63	Ni	200	0.91	1.77	10.8
<b>10%Ni10%Cu/C-recycled</b>	43.33	Cu	111	0.44	2.09	21.4
	44.23	Ni	111	0.76	2.05	12.5
	50.43	Cu	200	0.52	1.81	18.7
	51.58	Ni	200	0.91	1.77	10.7
<b>10%Ni /C -activated</b>	44.36	Ni	111	0.51	2.04	18.5
	51.69	Ni	200	0.63	1.77	15.6
<b>10%Ni /C- recycled</b>	44.42	Ni	111	0.40	2.04	23.8
	52.28	Ni	200	0.51	1.75	19.1

### III.3.5. XRD analysis of other monometallic and bimetallic catalysts

The XRD analysis was also performed for the monometallic 10%Cu and the bimetallic 5%Ni5%Cu/C and 15%Ni15%Cu/C catalysts. The XRD diffractograms for these catalysts are presented in Figure 38 (A) and Figure 38 (B) for the fresh catalysts and for the activated catalysts ones.

In the case of fresh 10%Cu/C catalyst, the XRD pattern showed two large diffraction peaks at  $43.35^\circ$  and  $50.49^\circ$ , which correspond to the (111) and (200) diffraction planes of the reflection of  $\text{Cu}^0$  of a lattice parameter of  $3.6122 \text{ \AA}$  (PDF 00-003-1005), respectively. When the catalyst was activated, the XRD pattern showed two large diffraction signals at  $43.47^\circ$  and  $50.38^\circ$ , which are characteristic to the (111) and (200) diffraction planes of the reflection of pure  $\text{Cu}^0$  of lattice parameter of  $3.6150 \text{ \AA}$  (PDF 00-002-1225), respectively.

As previously mentioned, XRD pattern of the fresh 10%Ni/C catalyst revealed the presence of complex form of nickel species (PDF 00-054-1419) and the activated catalyst showed the presence of the pure metallic nickel (PDF 00-001-1258). For 10%Ni10%Cu/C, the fresh catalyst showed the presence of a mixture of oxides species (CuO and NiO), while, the activated showed the presence of a mixture of pure Ni and pure Cu.

In the same way, the XRD diffraction of the fresh 5%Ni5%Cu/C catalyst showed the presence of two diffraction peaks at  $44.75$  and  $50.35^\circ$ , which correspond to the presence of  $\text{Ni}_{0.79}\text{Cu}_{0.21}\text{O}$ . However, when the catalyst was activated, the XRD showed a slight offset of the positions of the reflections compared to those of pure copper. Thus, the position is shifted from  $42.28$  to  $42.82^\circ$  and from  $50.68$  to  $50.37$ , corresponding to the synergy between copper and nickel forming an alloy. Hence, the presence of a faced centered cubic phase  $\text{Ni}_{0.79}\text{Cu}_{0.21}$  was detected. Also, two diffraction peaks which, correspond to the presence of  $\text{Ni}_{0.5}\text{Cu}_{0.5}$  were detected at  $43.98$  (111) and  $51.24^\circ$  (200) (PDF 04-001-3172). Thus, the 5%Ni5%Cu/C contains two bimetallic phases with different compositions.

The XRD pattern of fresh 15%Ni15%Cu/C displayed two diffraction peaks at  $43.26$  and  $50.43$ , which correspond to (111) and (200) diffraction planes of copper of lattice parameter of  $3.615 \text{ \AA}$  (PDF 00-004-0836), respectively. After the activation, the presence of faced centered cubic phase alloy  $\text{Ni}_{0.79}\text{Cu}_{0.21}$  and of pure copper are detected according to the standard data from JCPDS PDF cards 04-007-0059 and 00-003-1005, respectively.

In consequence, no peak characteristic of the Cu-Ni face centered cubic (FCC) structure was detected in this 10%Ni10%Cu/C catalyst. Indeed, there is no alloy in this catalyst. However, in 5%Ni5%Cu/C and 15%Ni15%Cu/C the Cu-Ni face centered cubic (FCC) structure is detected. But only 15%Ni15%Cu/C contain a mixture of the pure Cu and  $\text{Ni}_{0.79}\text{Cu}_{0.21}$ . Moreover, 5%Ni5%Cu/C also contains nickel-bonded copper ( $\text{Ni}_{0.5}\text{Cu}_{0.5}$ ,  $\text{Ni}_{0.79}\text{Cu}_{0.21}$ ).

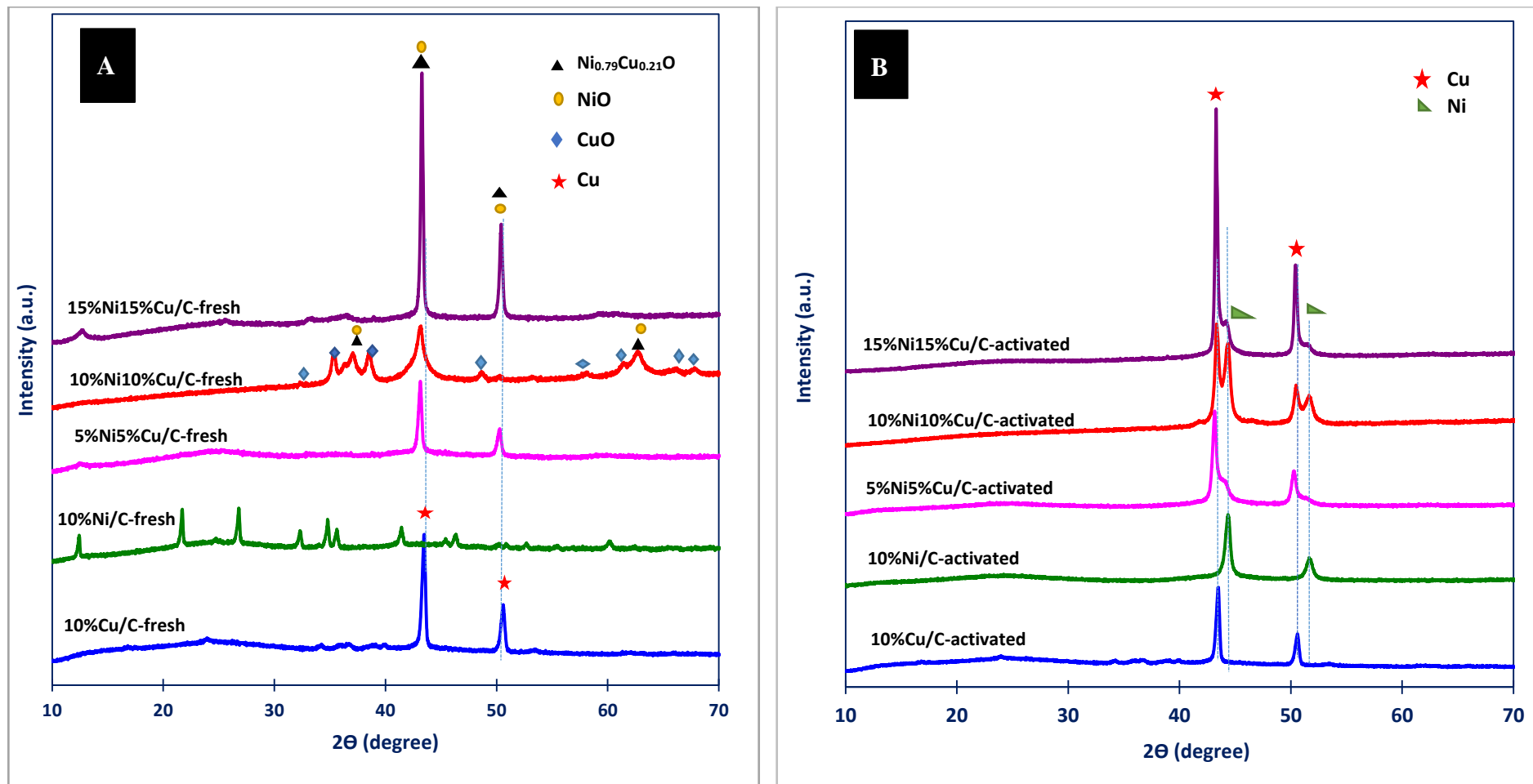


Figure 38: XRD patterns of various fresh (A) and activated (B) catalysts with different metal loadings

### III.4. TPR

To define the most efficient reduction conditions, the monometallic and bimetallic catalysts prepared by deposition-precipitation (DP) using aqueous hydrazine were investigated by H<sub>2</sub>-TPR technique. The TPR profiles of the catalysts are shown in Figure 39 (A) and Figure 39 (B).

At first, the reducibility of the species present in the monometallic 10%Ni/C and 10%Cu/C catalysts were identified. The monometallic nickel-based catalyst showed three main peaks corresponding to three different Ni species. The first peak at 320.1 °C could be attributed to the reduction of Ni<sup>2+</sup> to Ni, while, the second shoulder peak at around 363 °C could be assigned to the reduction of poorly interacting NiO, which is easily reducible [21]. The third peak correspond to the reduction of bulk NiO, which occurs at high temperature (549.6 °C). For the monometallic copper- base catalyst, two main peaks were observed at 319 °C and 449.2 °C. The former could be attributed to the reduction of Cu<sup>2+</sup> to Cu<sup>0</sup> and the later to the reduction of bulk CuO to metallic Cu [22].

TPR analysis of bimetallic systems was also performed in order to determine the role of the second metal (Cu) on the reduction of the Ni species and to identify different species present in the catalyst as a function of their reduction temperature. To this aim, the reduction behavior of the 10%Ni10%Cu/C catalysts prepared by DP using hydrazine as reducing agent was compared with the catalyst prepared by classical wet impregnation method followed by calcination at 450 °C for 3 h under inert atmosphere (denoted as 10%Ni10%Cu-calc). The TPR profiles of all of the catalysts are presented in Figure 39 (A) and (B). As could be observed, three reduction peaks can be distinguished in the TPR profile of the bimetallic 5%Ni5%Cu catalyst. The first one at 316.7 °C could be attributed to the reduction of Cu<sup>2+</sup> to Cu, while, the second peak at 322 °C could be assigned to the bulk CuO reduction to metallic Cu. Finally, the third peak at 362.3 °C could be ascribed to the reduction of bulk CuO–NiO to bimetallic Cu–Ni [22-23].

Regarding the bimetallic 10%Ni10%Cu catalyst prepared by DP, the reducibility of the species present in the catalyst showed three major peaks. The first peak was observed at 238.2 °C and could be assigned to the reduction of the well-dispersed CuO particles to Cu metal. The second broad peak centered around 308.7 °C is very large and combined the reduction of two species, namely the reduction of Cu<sup>2+</sup> species to Cu<sup>0</sup> and this of Ni<sup>2+</sup> species to Ni<sup>0</sup>. The third

observed large peak at 488.7 °C could be ascribed to the reduction of NiO to Ni. In comparison to the 10%Ni10%Cu-calc catalyst, the TPR profiles showed that the reduction of species present in the catalyst occurred in two stages with peak maxima at 389.1 °C and 630 °C, that could be ascribed to the reduction of the NiO-CuO to a Ni-Cu alloy and to the reduction of species more strongly interacting with the support, respectively [21].

The TPR profile of the bimetallic 10%Ni10%Cu/C-calc catalyst prepared by classical wet impregnation showed only two peaks with low hydrogen consumption compared to the bimetallic 10%Ni10%Cu/C catalyst prepared by DP. The possible reason of this difference of TPR profiles is that 10%Ni10%Cu/C-calc contains less oxidized species compare to 10%Ni10%Cu/C prepared by DP. Furthermore, 10%Ni10%Cu/C-calc contains surely a Ni-Cu bimetallic alloy, whereas, 10%Ni10%Cu/C prepared by DP does not. In view of the above, it could be confirmed that the catalysts preparation method influences not only the formation of the species in solution, but also the particle size and their interactions with the support. Finally, the different species present in the catalyst obviously influence the catalytic performances. The effect of the catalyst preparation on the performances will be discussed in detail in Chapter 5.

At higher Ni-Cu loadings (15%Ni15%Cu catalyst), three major peaks were also observed. The shoulder peak at 273.8 °C was attributed of the reduction of highly dispersed CuO species or of the reduction of very big CuO particles to Cu metal. The strong peak at 313.0°C could indicate the reduction of Cu<sup>2+</sup> to Cu<sup>0</sup> and finally, the larger peak observed at 348.2 °C, could be assigned to the reduction of CuO–NiO to a Cu–Ni alloy [22-23]. In contrary to the bimetallic 10%Ni10%Cu/C catalyst, the peak of reduction of Cu<sup>2+</sup> to Cu<sup>0</sup> of the catalyst 15%Ni15%Cu/C is not large. That confirmed that the peak of 10%Ni10%Cu/C centered at 308°C contains the reduction peak of Cu to Cu<sup>0</sup> which could be overlapped with Ni to Ni<sup>0</sup> peak.

By comparing the bimetallic systems with the monometallic 10%Ni/C catalyst prepared under the same conditions, it can be seen that the addition of copper in the bimetallic catalyst shifts the temperature of reduction of the species in presence towards lower temperatures. Thus, it can be said that the addition of copper facilitates the reduction of the nickel catalyst. However, for the bimetallic catalysts, it was observed that species present in the catalysts depend on the Ni-Cu loading. Thus, the 10%Ni10%Cu/C catalyst showed a peak of reduction of NiO to Ni, while, this characteristic peak was not found for the 5%Ni5%Cu/C and 15%Ni15%Cu/C catalysts. In contrast, the 5%Ni5%Cu and 15%Ni15%Cu catalysts showed a

peak of reduction of NiO-CuO to a Cu-Ni alloy, whereas, this species are not detected in the 10%Ni10%Cu/C sample.

Other differences were observed for the 5%Ni5%Cu/C catalyst. Indeed, no presence of the CuO species highly dispersed on the catalyst was observed, but, only the bulk CuO and NiO-CuO species were present. In contrary to 10%Ni10%Cu/C catalyst, the bimetallic 5%Ni5%Cu/C catalyst contains a bimetallic Ni-Cu alloy. Similarly, the 15%Ni15%Cu contains a Ni-Cu alloy as well. In addition, this catalyst showed the peak of CuO species well-dispersed just as the 10%Ni10%Cu/C catalyst. However, compared to the 10%Ni10%Cu/C, this CuO peak is shifted to higher temperatures as the Ni-Cu loading increases. Therefore, it could be concluded that the temperature of reducibility of species depends on the metals content.

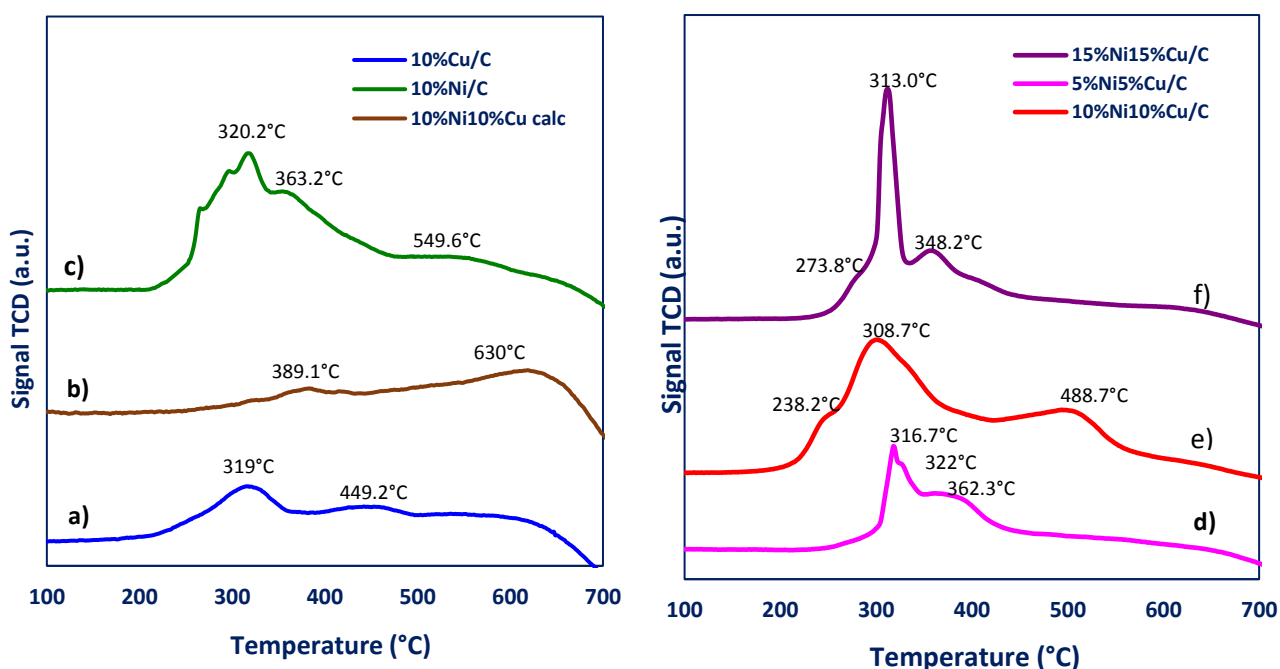


Figure 39 (A): TPR profiles of 10%Cu/C, 10%Ni/C and 10%Ni10%Cu/C-calc catalysts

Figure 39 (B): TPR profiles of 5%Ni5%Cu/C, 10%Cu10%Ni/C and 15%Ni15%Cu/C catalysts

Figure 39: TPR profiles of monometallic Ni and Cu and bimetallic Ni-Cu catalysts

## Conclusion

Several characterization methods were used to determine the composition, the textural, structural and morphological properties of two monometallic (10%Ni/C and 10%Cu/C) and four bimetallic (5%Ni5%Cu/C; 10%Ni10%Cu/C, 15%Ni15%Cu/C and 10%Ni10%Cu/C-calc) catalysts. All the catalysts were synthesized by the same method (DP), excepted the 10%Ni10%Cu/C-calc catalyst which was prepared by a classical wet impregnation method before being calcined under N<sub>2</sub>. The main findings of this study can be summarized as follows.

The monometallic 10%Cu/C catalyst revealed a higher specific surface area if compared to the monometallic 10%Ni/C sample. Generally, at equal metal loading, the bimetallic Ni-Cu catalysts showed lower surface area compared to the monometallic catalysts. Average metal particle size determined by Debye-Sheerer equation showed that copper particles are generally bigger than Ni ones in the 10%Ni10%Cu/C catalyst. At the same time, the ICP results revealed that, there is more Ni loaded than Cu. Additionally, for the Ni-Cu catalysts, the specific surface area decreases when the metal content increases.

The TEM images showed a homogeneous distribution of the nickel and copper particles of irregular shape and also some particle agglomerates. Distributions of particle size determined for the 10%Ni10%Cu/C catalyst in three different states (fresh, activated and recycled) revealed that it increased significantly after the reduction and remained almost constant after the recyclability tests. Most of the particles in 10%Ni10%Cu/C catalyst were around 18 nm after the reduction and recyclability tests. The particles crystal size for the activated and recycled catalysts showed that in both cases, the crystal size of Ni is smaller than the crystal size of Cu. No significant change of the crystal size for the activated and recycled catalysts was observed. This could explain the good stability of this catalyst after consecutive tests. EDX analysis showed the presence of some traces of P in the fresh 10%Ni10%Cu/C catalyst. However, XRF analysis revealed that this impurity originated from the carbon support. The XRF of the bare carbon support, showed also the presence of some traces of Ti, Fe and Ca.

XPS analysis of 10%Ni10%Cu/C catalyst at four different states (fresh, activated, activated-oxidized and recycled-oxidized) was carried out. For the fresh catalyst, Cu 2p and Ni 2p XPS spectra confirmed the presence of CuO and NiO and Ni(OH)<sub>2</sub> species. However, when the catalyst was activated, only metallic copper and nickel were detected. Thus, the reduction of the catalysts under hydrogen at 350 °C is sufficient to reduce all metal species present in the catalyst. In contrast, for the activated and recycled catalysts which are oxidized in contact with

air, the XPS analysis showed mixtures of several species on the surface of the catalyst. The Cu 2p and Ni 2p XPS showed the presence of metallic Cu and Ni, CuO, NiO, isolated-like ionic  $\text{Cu}^{2+}$  species and  $\text{Ni}(\text{OH})_2$  in both catalysts. However, the  $\text{Ni}^0/\text{Ni}^{2+}$  ratio was different. In fact, in the catalyst activated-oxidized, the  $\text{Ni}^0/\text{Ni}^{2+}$  ratio is 0.6, while, in the case of the recycled-oxidized catalyst the  $\text{Ni}^0/\text{Ni}^{2+}$  ratio was 1.1. Thus, the activated catalyst was more sensitive to the reoxidation with air as compared to the recycled catalyst where the oxidation proceeded more slowly. Nevertheless, working in a controlled atmosphere is essential to avoid the reoxidation of these catalysts.

XPS analysis of the 10%Cu/C catalyst revealed that the surface of the fresh catalyst is composed of CuO and  $\text{Cu}(\text{OH})_2$ , whereas, the activated catalyst showed only metallic Cu on its surface. XPS analysis of other bimetallic catalysts (5%Ni5%Cu/C and 15%Ni15%Cu/C) revealed that the fresh catalysts are composed of  $\text{Cu}(\text{NO}_3)_2$  and  $\text{Ni}(\text{OH})_2$  species, while after the reduction, all of bimetallic catalysts contained only nickel and copper in the metallic state on the surface. The presence the  $\text{Cu}(\text{NO}_3)_2$  species in the 5%Ni5%Cu/C and 15%Ni15%Cu/C catalysts could lead to their rapid deactivation.

The XPS analysis revealed that in all bimetallic catalysts the surface was enriched in Ni. After the reduction of the catalyst under pure hydrogen, a migration of small quantity of copper to the surface of the catalysts took place, but, surface remains rich in Ni. In contrast, ICP analysis and XRF showed that the bulk was enriched in Cu. Thus, both bulk and surface presented different compositions.

The XRD diffraction of fresh 10%Ni catalyst showed of the presence of complex form of nickel species, which is easily activated with air at low temperature. In contrast, the activated catalyst showed the presence of metallic nickel. After the recyclability test, the average crystal size did not change significantly. For the 10%Cu/C catalyst, XRD analysis revealed the presence of copper of lattice parameter of 3.6122 Å on the fresh catalyst and pure copper (3.6150 Å) for the activated catalyst.

TPR analysis of the 10%Cu/C sample showed the reduction peaks of  $\text{Cu}^{2+}$  species to  $\text{Cu}^0$  already at low temperature. The CuO strongly interacting with the support was activated only at higher temperature. TPR of 10%Ni/C showed the reduction peak of ions nickel  $\text{Ni}^{2+}$  (NiO and NiO bulk). TPR of the bimetallic 10%Ni10%Cu/C catalyst showed the presence of CuO and NiO. These observations are in good agreement with XRD, which states that there is the presence of CuO and NiO in fresh catalyst.

## References

- [1] A.-G. Boudjahem, M. Pietrowski, S. Monteverdi, M. Mercy, M.M. Bettahar, *Journal of Materials Science*. 41 (2006) 2025-2030.
- [2] M. Oschatz, T.W. van Deelen, J.L. Weber, W.S. Lamme, G. Wang, B. Goderis, O. Verkinderen, A.I. Dugulan, K.P. de Jong, *Catalysis Science & Technology*. 6 (2016) 8464-8473.
- [3] <http://xpssimplified.com/elements/copper.php>, accessed, September 15, 2017.
- [4] I. Onal, D. Düzenli, A. Seubsai, M. Kahn, E. Seker, S. Senkan, *Topics in Catalysis*. 53 (2010) 92-99.
- [5] <http://xpssimplified.com/elements/nickel.php>, accessed, September 15, 2017.
- [6] K. Kishi, M. Sasanuma, *Journal of Electron Spectroscopy and Related Phenomena*. 48 (1989) 421-434.
- [7] K.S. Kim, N. Winograd, *Surface Science*. 43 (1974) 625-643.
- [8] P. Forzatti, L. Lietti, *Catalysis Today*. 52 (1999) 165-181.
- [9] <https://srdata.nist.gov/xps/>, accessed, September 5, 2017.
- [10] E. Cano, C.L. Torres, J.M. Bastidas, *Materials and Corrosion*. 52 (2001) 667-676.
- [11] [https://srdata.nist.gov/xps/EngElmSrchQuery.aspx?EType=A&CSOpt=Retri\\_ex\\_dat&Elm=Cu](https://srdata.nist.gov/xps/EngElmSrchQuery.aspx?EType=A&CSOpt=Retri_ex_dat&Elm=Cu), accessed, September 8, 2017.
- [12] J.W. Geus, A.J. van Dillen, *Handbook of Heterogeneous Catalysis*, Wiley-VCH Verlag GmbH & Co. KGaA, 2008.
- [13] B.A.R. Vrebo, G.T.J. Kuipéres, *X-Ray Spectrometry*. 20 (1991) 5-7.
- [14] J.Q. McComb, C. Rogers, F.X. Han, P.B. Tchounwou, *Water, air, and soil pollution*. 225 (2014) 2169.
- [15] K. Tamilselvan, *Metal Hydrazine Cinnamates: Synthesis and Characterization*, Anchor Academic Publishing, 2016.
- [16] X. Zhang, C. Li, Q. Ji, *World Journal of Nano Science and Engineering*. Vol.06No.04 (2016) 12.
- [17] J. Feng, C.-P. Zhang, *Journal of Colloid and Interface Science*. 293 (2006) 414-420.
- [18] F. Bonet, S. Grugeon, L. Dupont, R. Herrera Urbina, C. Guéry, J.M. Tarascon, *Journal of Solid State Chemistry*. 172 (2003) 111-115.
- [19] G.H. Mohamed Saeed, S. Radiman, S.S. Gasaymeh, H.N. Lim, N.M. Huang, *Journal of Nanomaterials*. 2010 (2010) 5.
- [20] V.V. Thyssen, T.A. Maia, E.M. Assaf, *Journal of the Brazilian Chemical Society*. 26 (2015) 22-31.
- [21] V. Nichele, M. Signoreto, F. Pinna, E. Ghedini, M. Compagnoni, I. Rossetti, G. Cruciani, A. Di Michele, *Catalysis Letters*. 145 (2015) 549-558.
- [22] X. Chen, S.A.C. Carabineiro, S.S.T. Bastos, P.B. Tavares, J.J.M. Órfão, M.F.R. Pereira, J.L. Figueiredo, *Journal of Environmental Chemical Engineering*. 1 (2013) 795-804.
- [23] M.M. Ambursa, T.H. Ali, H.V. Lee, P. Sudarsanam, S.K. Bhargava, S.B.A. Hamid, *Fuel*. 180 (2016) 767-776.

## Chapter 4

# Reactivity of monometallic catalysts in the decarboxylation of palmitic acid

SUMMARY

<b>INTRODUCTION .....</b>	<b>117</b>
<b>I. DECARBOXYLATION OF PA OVER NOBLE METAL-BASED CATALYSTS.....</b>	<b>118</b>
I.1. BLANK TEST .....	118
I.2. EFFECT OF THE REACTION TEMPERATURE .....	119
I.3. EFFECT OF THE CONCENTRATION OF THE SUBSTRATE .....	120
I.4. EFFECT OF THE REDUCTION OF THE CATALYST WITH H <sub>2</sub> .....	121
I.5. EFFECT OF THE MASS OF CATALYST LOADED IN THE REACTOR .....	122
<b>II. DECARBOXYLATION OF PA OVER NON-NOBLE METAL-BASED CATALYSTS.....</b>	<b>123</b>
II.1. EFFECT OF THE NATURE OF THE METAL .....	124
II.2. NICKEL-BASED CATALYSTS.....	125
II.2.1. Effect of the activation of the catalyst under H <sub>2</sub> .....	125
II.2.2. Effect of the nickel loading .....	126
II.2.3. Influence of the mass of catalyst loaded in the reactor .....	127
II.2.4. Recyclability of the catalyst .....	128
<b>DISCUSSION .....</b>	<b>130</b>
<b>CONCLUSION .....</b>	<b>132</b>
<b>REFERENCES.....</b>	<b>133</b>

### Introduction

Decarboxylation of fatty acids (FA) over carbon-supported metallic catalysts has been extensively investigated in the past decades by Murzin *et al.* [1, 2] and by other researchers [3-5]. Among all catalysts studied, noble metals such as Pd/C and Pt/C showed the highest activities and selectivities to hydrocarbons. Unfortunately, the high cost and the low abundance of the noble metals are major drawbacks for industrial application. Therefore, finding a less expensive catalyst showing similar catalytic performances is a challenge.

For this current work, the noble metal catalysts 5%Pd/C and 5%Pt/C were used as benchmark catalysts. Then, the non-noble monometallic-based catalysts were screened in order to find the best candidate. In addition, the influence of the reaction conditions such as: the temperature, the reaction time, the concentration of palmitic acid (PA), the mass of the catalyst were also studied. Finally, the effect of the preliminary thermal activation of the catalyst under H<sub>2</sub> was also investigated.

## I. Decarboxylation of PA over noble metal-based catalysts

The noble metal catalysts such as 5%Pd/C and 5%Pt/C, known to be highly active and selective to hydrocarbons were used as benchmarks for the catalytic decarboxylation of PA to n-pentadecane (n-PD). The influence of the temperature, the initial concentration of PA, the mass of the catalyst, as well as the effect of the thermal activation of the catalyst on the catalytic performances of the materials were studied.

### I.1. Blank test

PA was first submitted to the reaction conditions (temperature = 320 °C, time = 6 h, PA loading = 0.197 mmol) in the absence of catalyst in order to determine the extent of the decarboxylation, which could occur spontaneously at high temperature. Figure 40 shows the results obtained. As it can be observed, 27% of PA is converted with 28 % selectivity to n-PD. Therefore, the yield of n-PD is only 8%. However, the carbon balance obtained was 81%. These results suggest that other undesired products were formed during the blank test. Analysis of the byproducts obtained showed the presence of saturated products such as 3-methyltetradecane (isomer of n-PD), and few traces of tridecane (C13) and tetradecane (C14) and some unsaturated products (such as 1-pentadecene and its isomers). This result confirmed the observations already reported in the literature. Indeed, according to the results obtained by Murzin and co-workers on the thermal (non-catalytic) decarboxylation of stearic acid, the formation of many byproducts was observed during the blank test [1].

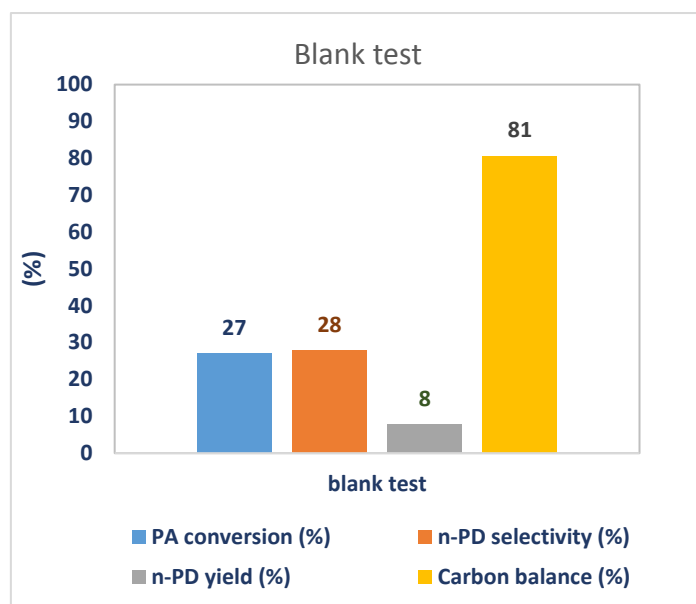


Figure 40: Blank test for the catalytic decarboxylation of PA at  $T = 320^{\circ}\text{C}$  ( $p = 40$  bar,  $t = 6$  h, stirrer speed = 600 rpm; PA loading = 0.197 mmol)

## I.2. Effect of the reaction temperature

The PA decarboxylation over the 5%Pd/C and 5%Pt/C catalysts was studied at three different temperatures: 300, 310, 320 °C. The tests were carried out for 6 h under an initial pressure of 20 bar. The PA loading was of 0.197 mmol in all cases. The results of the catalytic performances are presented in Figure 41 (a) and Figure 41 (b) for 5%Pd/C and 5%Pt/C, respectively. As observed the carbon balances for both catalysts are very low, only around 40%. That is due to the formation of undesired products with relatively high molecular weight, which are known to be difficult to identify by GC [1]. Based on the literature, the main by-product could be a symmetrical ketone [1]. As expected, in both cases, the conversion increased from 79% at 300 °C to 92% at 320 °C. In the same time, the selectivity to n-PD slightly increased. In both cases, 320 °C was the best temperature for the reaction of decarboxylation. In consequence, the optimization of the other reaction conditions was studied at this temperature.

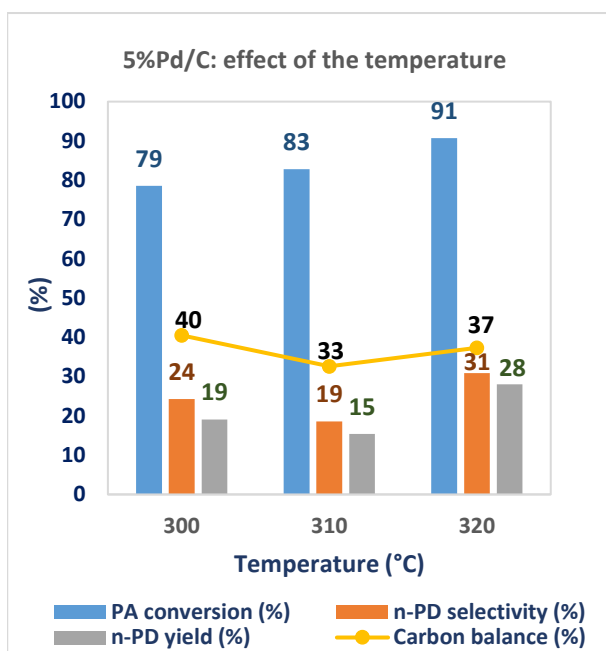


Figure 41 (a)

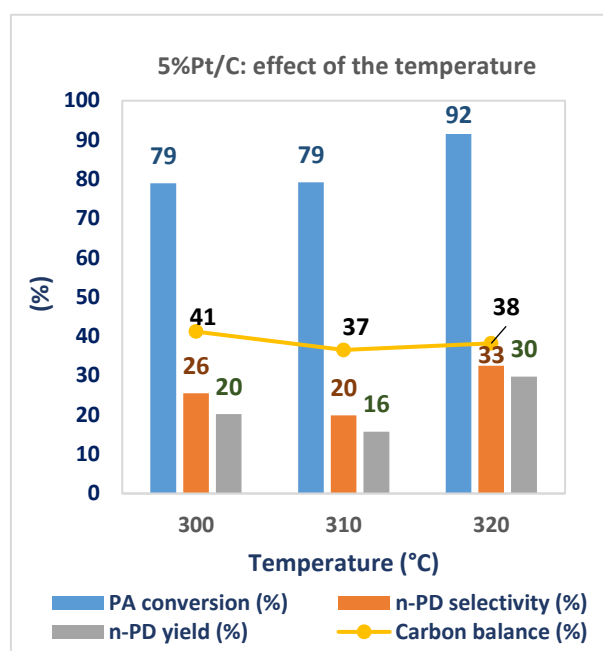
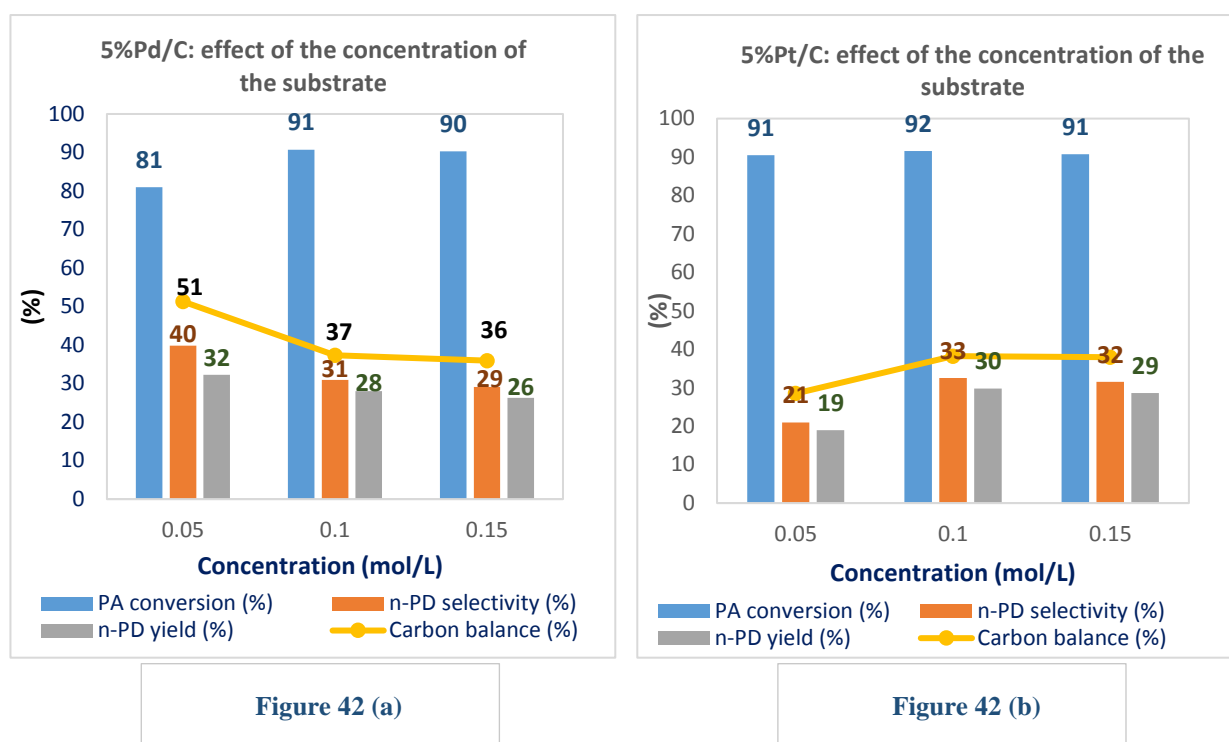


Figure 41 (b)

Figure 41: Effect of the temperature on the catalytic performances of noble metal-based catalysts 5%Pd/C and 5%Pt/C for the decarboxylation of PA. Reaction conditions: initial P=20 bar; gas flow: 10% H<sub>2</sub>/N<sub>2</sub>; [PA] =0.1mol/L

### I.3. Effect of the concentration of the substrate

The effect of the substrate concentration on the catalytic performances of the 5%Pd/C and 5%Pt/C catalysts was studied. In both cases, the catalytic performances of the 5%Pd/C catalyst are slightly better for a lower concentration (0.05 mol/L). In contrast, for the 5%Pt/C catalyst, the better results were obtained for the concentration of 0.1 mol/L of. Taking into account that for the 5%Pd/C catalyst the conversion at 0.1 and 0.15 mol/L was almost the same compared to the conversion at 0.05 mol/L and that the objective of this study was to determine the best catalyst, it was necessary to choose only one concentration. Therefore, 0.1 mol/L is chosen as the optimal concentration for the rest of this study.



**Figure 42:** Effect of the concentration of the substrate on the catalytic performances of the noble metal catalyst 5%Pd/C and 5%Pt/C. Reaction conditions: initial pressure:  $p = 20$  bar,  $t = 6$  h, stirrer speed = 600 rpm;  $m_{\text{cat}} = 12.8$  mg, PA loading = 0.197 mmol.

#### I.4. Effect of the reduction of the catalyst with $\text{H}_2$

In order to evaluate the effect of the activation of the commercial catalysts with hydrogen, the solids were firstly tested such as purchased, without any thermal treatment. The results obtained (Figure 43) showed that the conversion and the selectivity for both catalysts are around of 91% and 31% respectively. Then, the catalysts were treated at 350 °C, under hydrogen for 2 h just before the catalytic test.

As expected the catalytic performances of both catalysts were significantly better after the reduction with hydrogen. The PA conversion over 5%Pd/C increased from 91% to 100%, while, the selectivity to n-PD increased from 31 to 51% and therefore, the yield of the reaction increased from 28% to 51% (Figure 43 (a)). But, the carbon balance only slightly increased from 37 to 51%. The low value of the carbon balance indicates that the formation of other unwanted products still occurs. Regarding the 5%Pt/C catalyst (Figure 43 (b)), the conversion decreased slightly from 91% to 81%, whereas the selectivity to n-PD significantly increased

from 33 to 87%. The yield also increased from 30 to 70%. In addition, the carbon balance increased from 38 to 89%. That indicates that n-PD is predominantly formed. Taking into account these results, the thermal activation of the catalysts under hydrogen is required to enhance their catalytic performances. That why, all the noble metal catalysts were activated under hydrogen before the catalytic tests.

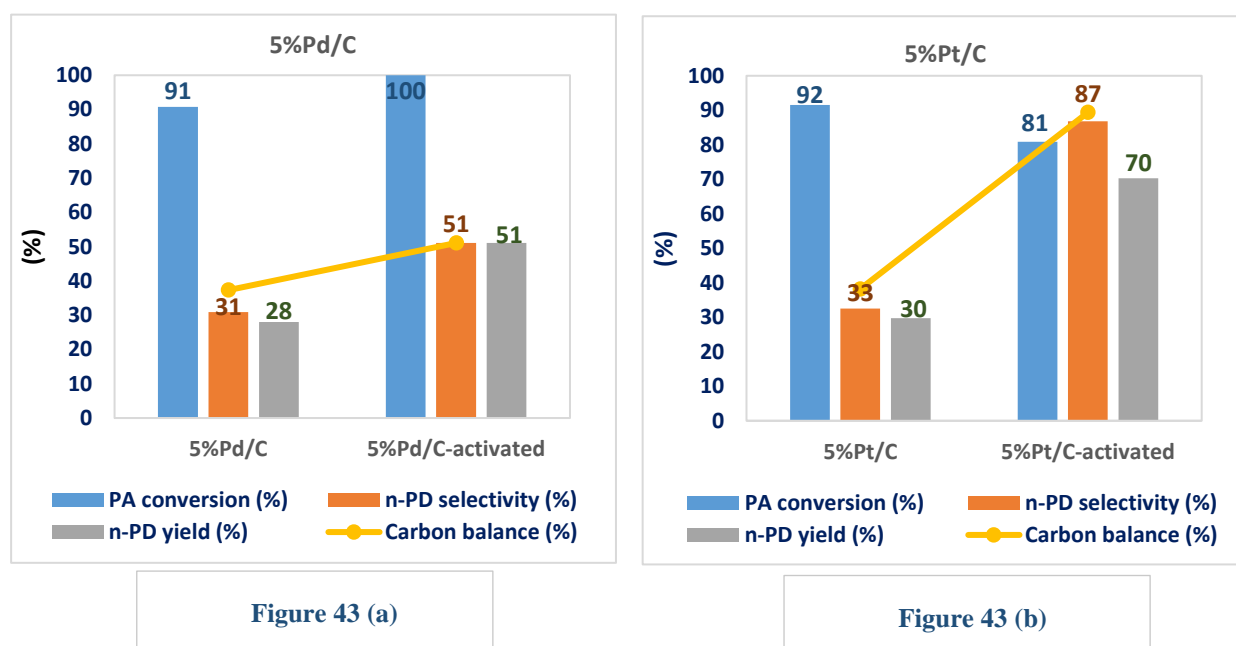


**Figure 43:** Effect of the activation under  $H_2$  on the catalytic performances of the noble metal catalyst 5%Pd/C and 5%Pt/C in the catalytic decarboxylation of PA to n-PD. Reaction condition: initial pressure:  $p = 20$  bar,  $t = 6$  h, stirrer speed = 600 rpm; catalyst amount loading=12.8 mg, PA loading = 0.197 mmol.

### 1.5. Effect of the mass of catalyst loaded in the reactor

The decarboxylation of PA was studied over the 5%Pd/C and 5%Pt/C catalysts, for four different masses of catalyst loadings (12.8, 26, 52, 75 mg). The reactions were performed under the same experimental conditions than previously (temperature = 320 °C, time = 6 h, palmitic acid loading = 0.197 mmol, initial pressure = 20 bar). Figure 44 (a) and Figure 44 (b) illustrate the evolution of the carbon balance as a function of the catalyst loading for 5%Pd/C and for 5%Pt/C respectively. In the case of the 5%Pd/C catalyst, the carbon balance increased when the catalyst loading was increased. This suggests the formation of undesired products for low catalyst loadings. This result could be due to inefficient mass transfer caused by the low mass of the catalyst (12.8 mg). The catalyst loading had no effect on the PA conversion which was total for all the loadings studied. In addition, the selectivity to n-PD increased with the increase of the mass of the catalyst. The yields obtained for these tests were 51, 66, 84 and 91% for

12.8, 26, 52, 75 mg of catalysts respectively. Thus, the best catalytic performances in the case of the 5%Pd/C catalyst were obtained using 75 mg of catalyst.

In contrast, in the case of the 5%Pt/C catalyst, the carbon balance tends to stabilize at around 90%. The conversion of PA, selectivity to n-PD and the yield of the reaction were almost constant (81%, 87% and 70% respectively), when increasing of the amount of the catalyst from 12.8 to 26 mg. However, when the amount of the catalyst increased from 26 to 52 mg, the conversion of PA reached 100%, and the selectivity and yield reached 89%. The increase in the amount of catalyst from 52 to 75 mg increased only slightly (about 2%) the selectivity and the yield of the reaction. Thus, at 75 mg of the catalyst, the selectivity and yield in n-PD were 91%. In both cases, 75 mg of catalyst gave the best catalytic performances in the conditions of reaction studied.

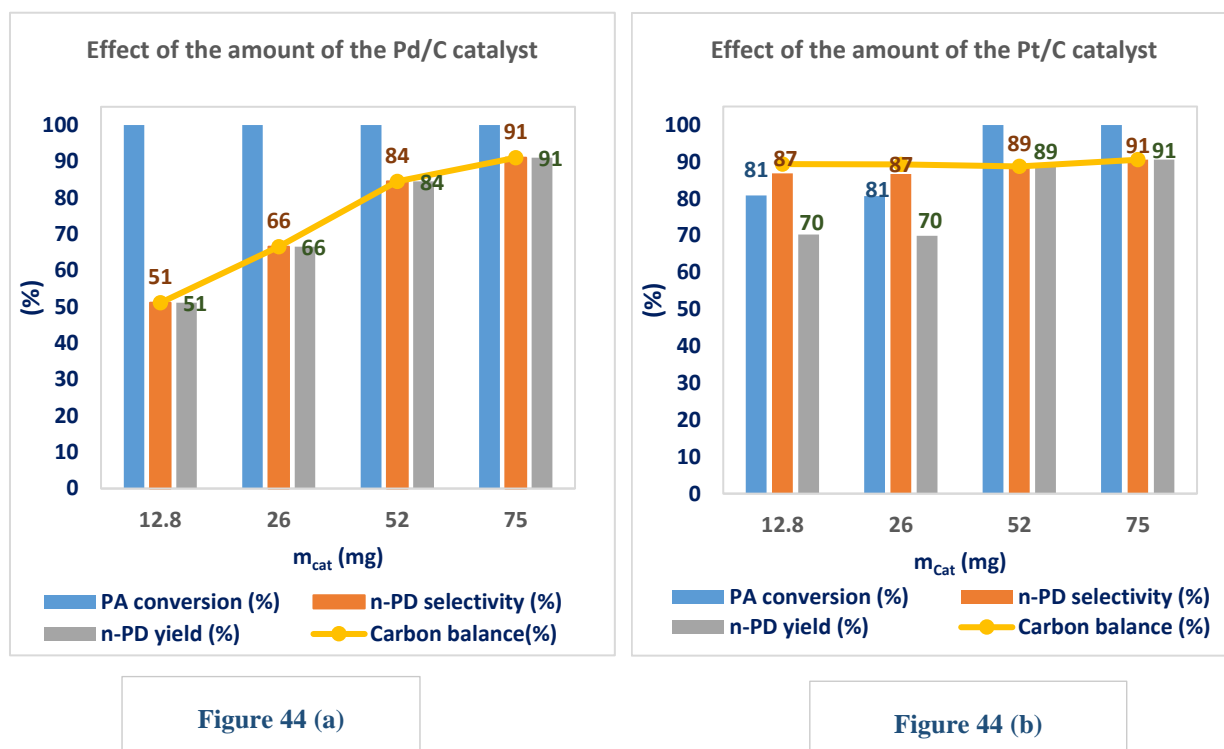


Figure 44: Effect of the mass of catalyst loaded on the performances of 5%Pd/C for the catalytic decarboxylation of PA to n-PD at  $T = 320\text{ }^{\circ}\text{C}$  (initial  $p = 20\text{ bar}$ ,  $t = 6\text{ h}$ , stirrer speed = 600 rpm; PA loading = 0.197 mmol).

## II. Decarboxylation of PA over non-noble metal-based catalysts

The catalytic decarboxylation of PA into n-PD was first evaluated for four different non-noble metal-based catalysts supported on carbon. Among them, platinum is approximately

4,000 times more expensive than nickel and 10,000 times more expensive than iron. Similarly, palladium is 3,000 times more expensive than copper [6]. Silver was also used in this study because it is 50% less expensive and more abundant than palladium.

All reactions were carried out at 320 °C, under 10 vol.% of H<sub>2</sub> in N<sub>2</sub> for 6 h. The initial pressures were 20 bar (final pressures 40 bar in the batch reactor). The mass of catalyst used was 12.8 mg and the PA loading was 0.197 mmol in hexadecane (2 mL).

### II.1. Effect of the nature of the metal

The effect of the type of metal used was studied in standard operating conditions. Prior to the test, the catalysts were activated under hydrogen at 350 °C for 2 h. The results obtained are shown on Figure 45. The 10%Ni/C catalyst gave the best results with 57% of conversion and 20% of selectivity to n-PD. The yield in n-PD was 11%. The 10%Ag/C catalyst reached 33% of PA conversion and 31 % of selectivity to n-PD. The yield in n-PD was 10%. Regarding the 10%Cu/C catalyst, the conversion was only 20%. However, this catalyst showed the best selectivity to n-PD (44%). Finally, the 10%Fe/C catalyst showed a higher conversion than for the Cu-based catalyst (28%), but the selectivity to n-PD was low (26%). Taking into account the results obtained, the 10%Ni/C catalyst was chosen for the following of the study.

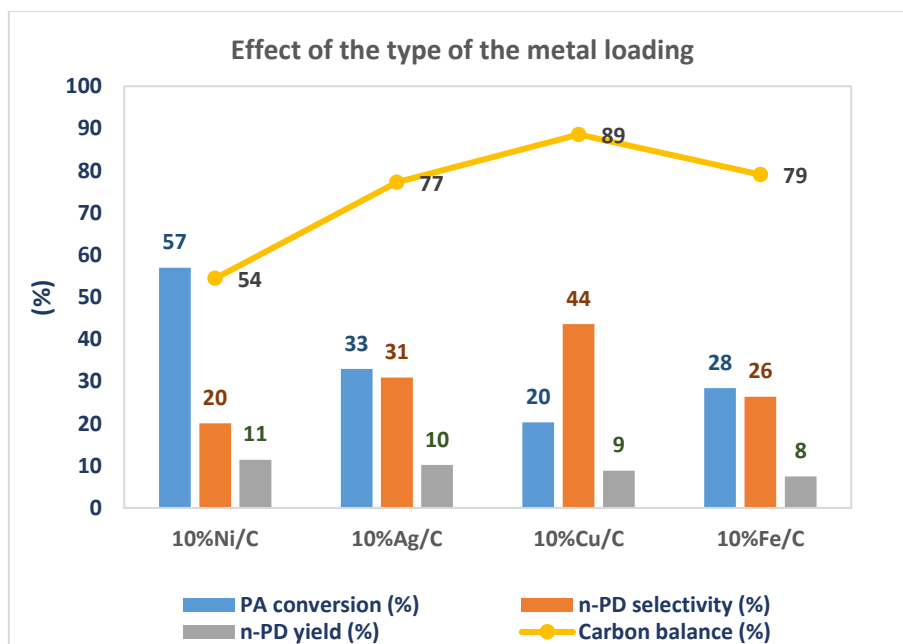


**Figure 45: Effect of nature of the metal on the performances for the decarboxylation of PA to n-PD. Reaction condition: T=320°C, initial pressure = 20 bar, t = 6 h, stirrer speed = 600 rpm; catalyst amount = 12.8 mg, PA loading = 0.197 mmol.**

## II.2. Nickel-based catalysts

Well known for its high potential to catalyze several types of reaction, particularly the hydrogenation reactions, nickel is one of the most widely used elements among the transition metal-based catalysts [7]. Because of its attractive properties, namely its abundance on the surface of the Earth and its relatively low cost, this metal is an essential element for the development of industrial catalysts.

In this section the influence of various parameters, such as the pre-activation of the Ni-based catalysts, the Ni loading, the mass of catalyst loaded in the reactor, on the performances in the decarboxylation of PA to n-PD, as well as the stability of the catalyst will be studied and discussed.

### II.2.1. Effect of the activation of the catalyst under H<sub>2</sub>

As mentioned before, the Ni/C catalyst was reduced chemically by hydrazine during its preparation by a deposition-precipitation method. However, due to its easy reoxidation in contact with air, the catalytic tests were carried out at 320 °C under a 10 vol.% H<sub>2</sub> in N<sub>2</sub> atmosphere. The presence of 10% H<sub>2</sub> in N<sub>2</sub> was used to activate *in situ* the catalyst. Moreover, to check if this *in situ* activation of the catalyst is sufficient, the Ni/C catalyst was also activated at 350 °C under H<sub>2</sub> just before the catalytic test took place (denoted as Ni-activated). The catalytic tests were then performed in the same reaction conditions for both samples. The results obtained (Figure 46) showed that the conversion of PA increases very significantly from 32 to 57% when the catalyst was activated under pure hydrogen before the catalytic test. However, the selectivity to n-PD decreased from 31 to 20%. Similarly, the carbon balance decreased from 78 to 54%, meaning that the reduced 10%Ni/C favored the formation of several undesired products. However, the catalytic performances of the fresh catalyst (tested as prepared) were similar to those obtained for the blank test. Therefore, the presence of 10 vol.% of H<sub>2</sub> in N<sub>2</sub> is not sufficient to reduce *in situ* the Ni/C catalyst in the conditions of reaction. It is preferable to pre-activate the catalysts under hydrogen before reaction. Taking into account this result, in the following all the catalysts were activated under H<sub>2</sub> at 350 °C during 3 h before the catalytic tests.

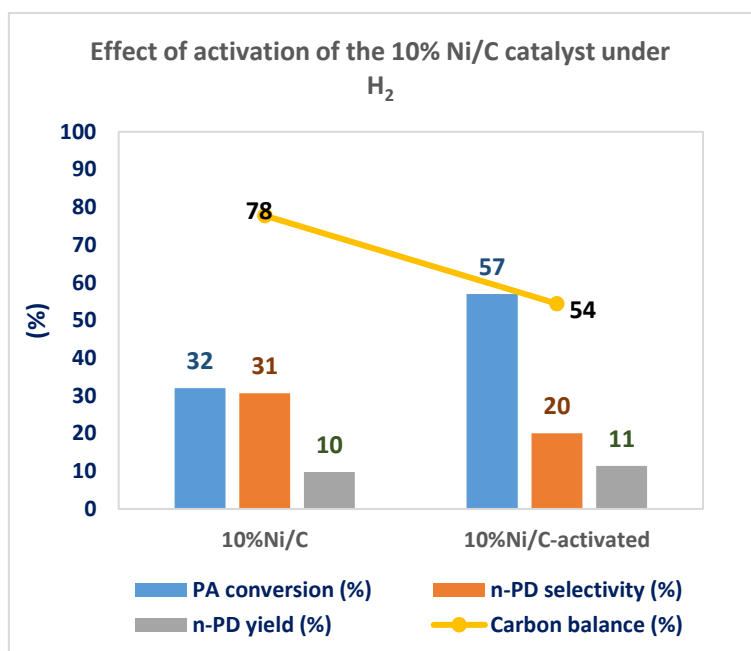


**Figure 46:** Effect of the activation of the 10%Ni/C catalyst under H<sub>2</sub> on the catalytic performances in catalytic decarboxylation of PA to n-PD. Reaction conditions: T =320 °C, initial pressure = 20 bar, t = 6 h, stirrer speed = 600 rpm; PA loading = 0.197 mmol.

### II.2.2. Effect of the nickel loading

In order to evaluate the effect of the nickel loading on the catalytic performances, tests were carried out with a series of three Ni-based catalysts supported on carbon presenting different metal loadings (namely 10, 20 and 30%Ni/C). The reaction parameters were kept constant (320 °C, 20 bar, 6 h and 0.197 mmol of PA). As shown in Figure 47 the PA conversion decreased when the nickel content increased. Thus, the 10%Ni/C catalyst converted 57% of PA, while the 20%Ni/C and the 30%Ni/C catalysts converted 37 and 23% of the PA, respectively. However, the increase of Ni content from 10 to 30% increased the selectivity to n-PD of about 10%. The yield in n-PD remains almost unchanged in all cases around 10%. Regarding the carbon balance, an increase from 54 to 85% with the increase of the nickel loading was observed. This could indicate that, for high metal loading (30%), the formation of by-products is lowered. Although the 10%Ni/C catalyst seemed to favor the formation of undesirable products, it nevertheless remained more active than the 30%Ni/C catalyst. The formation of undesirable products on the 10%Ni/C catalyst could be due to diffusional limitation of the reactants to the outer surface of the metal grains or to an insufficient amount of catalyst [8]. Therefore, a study of the influence of the mass of catalyst loaded in the reactor was done.

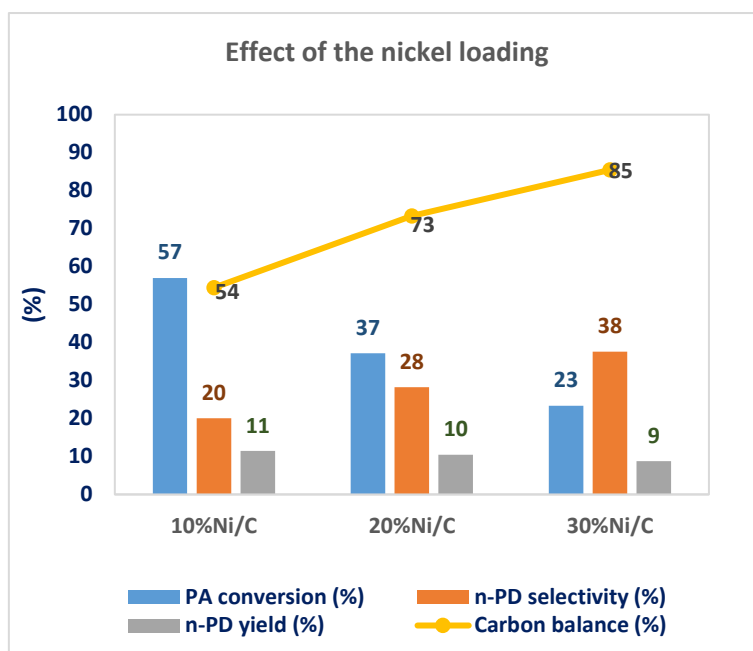
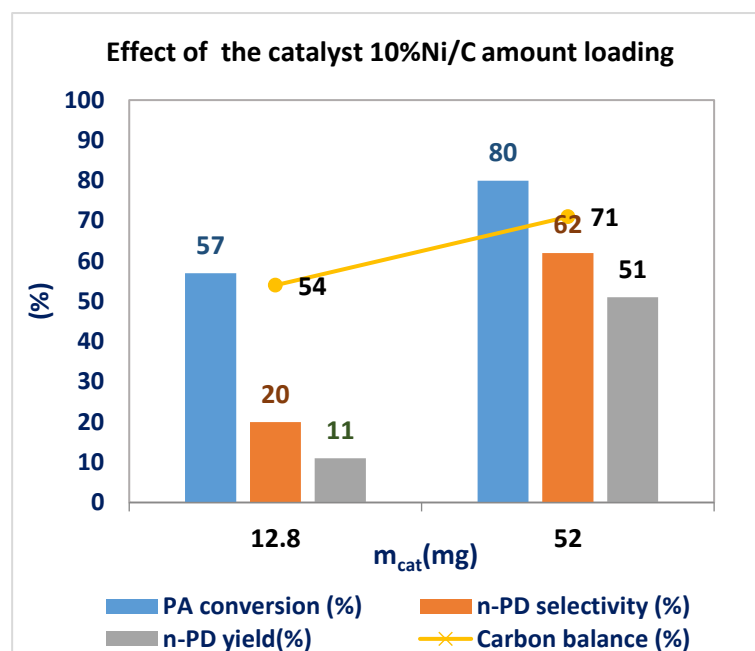


Figure 47: Effect of the Ni loading (10, 20 and 30%Ni/C) on the catalytic performances in PA decarboxylation to n-PD. Reaction conditions:  $T = 320^{\circ}\text{C}$ , initial pressure = 20 bar,  $t = 6$  h, stirrer speed = 600 rpm; catalyst loading=12.8mg; PA loading = 0.197 mmol.

### II.2.3. Influence of the mass of catalyst loaded in the reactor

The influence of the mass of the 10%Ni/C catalyst loaded in the reactor on the performances was studied for 12.8 and 52 mg. The reactions were performed at  $320^{\circ}\text{C}$ , under 10 vol.% of  $\text{H}_2$  in  $\text{N}_2$ . The initial pressure was 20 bar and the reactions were carried out for 6 h. The initial concentration in PA was kept constant at 0.1 mol/L. The results obtained are shown in Figure 48. As observed, the catalytic performances of the 10%Ni/C catalyst increased when the catalyst loading increased from 12.8 to 52 mg. Indeed, the conversion of PA increased from 57 to 80%, the selectivity to n-PD increased from 20 to 62% and the yield and the carbon balance from 11 to 51% and from 54 to 71%, respectively. As reported in the literature, the increase of the catalyst amount increases the initial reaction rate which improves the performances of the catalyst and activated the formation of the desired product [8]. In fact, in the same reaction conditions, the formation of undesired products was found higher for a smaller amount of catalyst. Therefore, in our case the decarboxylation of PA to n-PD is favored for 52 mg of catalyst loading.



**Figure 48:** Effect of the catalyst amount loading on the performances of the catalyst 10%Ni/C for the decarboxylation of PA to n-PD. Reaction conditions: temperature=320°C, initial pressure:  $p = 20$  bar,  $t = 6$  h, stirrer speed = 600 rpm; PA loading = 0.197 mmol in hexadecane.

#### II.2.4. Recyclability of the catalyst

The recyclability of the 10%Ni/C catalyst was studied in the same reaction conditions. Temperature, initial pressure, gas atmosphere, duration of the reaction, catalyst amount and initial reactant concentration were set as follows: 320 °C, 20 bar, 10 vol.%H<sub>2</sub> in N<sub>2</sub>, 6 h, 52 mg and 0.1 mol/L.

A series of three tests was performed consecutively. After the first run (noted 1<sup>st</sup>), the products of reaction were separated from the catalyst using a syringe. To avoid the reoxidation of the catalyst, the spent catalyst was kept at the bottom of the reactor. Then, the same substrate (0.197 mmol of reactant in hexadecane) was immediately introduced to the reactor for a second run. After that, the reactor was closed and the test was performed again in the same conditions as previously. After the second run, the same operation was repeated for the third time. To ensure the repeatability of the results, each test was repeated 3 times. The standard deviation is represented by the error bars in Figure 49.

After 3 consecutive tests, the results obtained (Figure 49) showed a progressive decrease of the catalytic performances of the 10%Ni/C catalyst. The carbon balance remained constant

around 75%. Comparing the first and the third runs, the conversion and selectivity to n-PD decreased from 80 to 62% and from 62% to 59%, respectively. The linear decrease of the conversion showed that the 10%Ni/C catalyst is progressively deactivated. This possible decrease in the activity of the catalyst could be due to coke deposition on the surface of the catalyst [1]. As mentioned in Chapter 1, the side reactions such as aromatization, oligomerization, isomerization reactions or the adsorption of fatty acids and aromatic compounds on the metal sites, favor the poisoning of the catalyst, which decrease its catalytic performances.

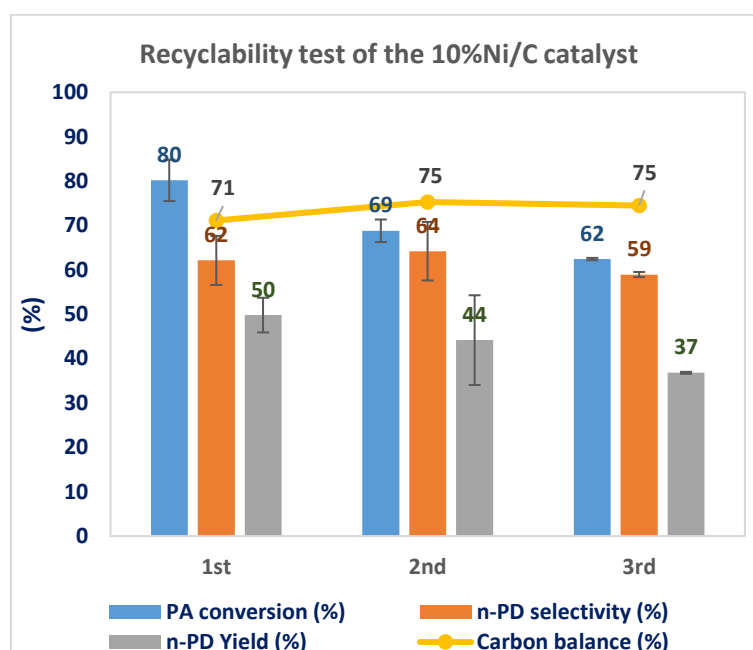


**Figure 49: Recyclability of the catalyst 10%Ni/C for the decarboxylation of PA to n-PD. Reaction conditions: temperature=320°C, initial pressure: p = 20 bar, t = 6 h, stirrer speed = 600 rpm; m<sub>cat</sub>=52 mg, PA loading = 0.197 mmol in hexadecane.**

## Discussion

Catalytic decarboxylation of PA to n-PD was studied on monometallic supported catalysts in this chapter. The goal was to find an inexpensive catalyst showing, if possible, similar performances as the noble metal-based catalysts. At first, the reaction was performed at 320 °C for 6 h in the absence of catalyst with 0.197 mmol of PA loading in hexadecane, in order to see the influence of the thermal activation. The results obtained showed 27% of conversion and 28% of n-PD selectivity. Thus, the yield in n-PD was 8%. Moreover, the carbon balance was 81% indicating the formation of undesired heavy compounds. These results were in accordance with those obtained by Snåre *et al.* [1] and Mark Santillan-Jimenez *et al.* [9].

Based on the literature, 5%Pd/C and 5%Pt/C seemed to be the most promising catalysts for the decarboxylation of fatty acids. Thus, these two catalysts have been used in our study as benchmark catalysts. For that, the decarboxylation reaction of PA to n-PD was optimized as a function of the mass of catalyst loaded, the reaction temperature, the PA concentration and the reduction mode of the catalyst. On one hand, the best catalytic performances were obtained when the reaction was performed at 320 °C under 10 vol.% H<sub>2</sub> in N<sub>2</sub> for 6 h. Indeed, the increase of the temperature showed an increase of both the activity and the selectivity. On the other hand, the optimal concentration in the reactant was found at 0.1 mol/L. These latter results correspond to those obtained in the literature. In fact, it was demonstrated in several studies that the selectivity of the Pd/C catalyst was higher for low concentrations of the substrate (< 0.2 mol/L) at 300 °C) under inert or low quantity of hydrogen atmosphere [2, 5, 10]. Furthermore, it was found that the reduction of the catalyst in pure hydrogen before test improve drastically the catalytic performances. Additionally, increasing the amount of catalyst loaded in the reactor decreased the formation of byproducts, which lead to high activity and selectivity. Thus, with 52 mg of catalyst better results were found. In definitive, the optimal conditions for the decarboxylation of PA to n-PD over the 5%Pd/C and 5%Pt/C catalysts were found at 320 °C, under 10 vol.% H<sub>2</sub> in N<sub>2</sub>, 20 bar of initial pressure and for 6 h. The reactant loading was 0.197 mmol in hexadecane and the mass of catalyst loaded was 52 mg. In these conditions 5%Pd/C and 5%Pt/C showed total conversion and 84% and 89% of n-PD selectivity, respectively. In contrast to the results observed in the literature, the 5%Pt/C catalyst was found more selective than the 5%Pd/C catalyst.

The non-noble monometallic catalysts were also investigated for the decarboxylation of PA to n-PD in order to find the best inexpensive candidate. For that, 10%Ni/C, 10%Ag/C,

10%Fe/C and 10%Cu/C were screened for the decarboxylation reaction. 10%Ni/C showed the highest conversion and the 10%Cu/C showed the highest selectivity to n-PD, whereas, the 10%Ag/C showed low reactivity and 10%Fe/C showed almost no activity. Among the catalysts studied, the most promising one was the nickel-based catalyst. For that reason, this latter was studied for the decarboxylation of PA to n-PD under 10 vol.% H<sub>2</sub> in N<sub>2</sub> flow at 320 °C for 6 h with 12.8 mg of catalyst and 0.197 mmol of PA loading. As observed with noble metals catalysts, the performances were increased when the catalyst was activated prior to the test. Furthermore, given that the noble metal-based samples showed the best performances when 52 mg of catalyst were loaded in the reactor, two different catalysts amount loadings were studied for the 10%Ni/C catalyst. The results obtained showed that when the catalyst amount was increased from 12.8 to 52 mg, the conversion was increased from 57 to 80% and the selectivity from 20 to 62%. Finally, the study of the recyclability of the catalyst over three runs showed the deactivation of the catalyst. This deactivation was attributed to the possible adsorption of byproducts or to coke deposition on the catalyst surface. In fact, the nickel-based catalyst was found to favor decarbonylation reaction in presence of hydrogen, hence producing CO, which is known to be a poison of the catalysts. Furthermore, nickel-based catalysts were also found to exhibit the highest selectivity toward cracking products, leading to the formation of lighter products which deposited on the catalyst and which are hence responsible of its deactivation [1].

## Conclusion

The decarboxylation of PA to n-PD over non-noble monometallic supported catalysts was investigated. After optimization of the reaction conditions the catalytic tests were performed in a batch reactor at 320 °C, under 10 vol.% H<sub>2</sub> in N<sub>2</sub> for 6 h. The initial reaction pressure was 20 bar and the catalyst amount was 52 mg. The catalysts were activated with pure hydrogen at 350 °C during 3 h before each test. The PA loading was 0.197 mmol in hexadecane. Four non-noble monometallic catalysts (namely, 10%Ni/C, 10%Fe/C, 10%Ag/C and 10%Cu/C) prepared by deposition-precipitation method in the presence of aqueous hydrazine were studied. The results obtained showed that 10%Ni/C was the most promising catalyst. Compared to the noble metal catalysts (Pd/C and Pt/C, under the optimal reaction conditions), the 10%Ni/C showed lower activity and selectivity to n-PD. However, considering the cost of the metals, 10%Ni/C could be advantageous for an industrial application. Unfortunately, the study of the recyclability of this catalyst showed a gradual deactivation of the catalyst after 3 consecutive runs. Therefore, the 10%Ni/C catalyst should be improved to be used for the decarboxylation reaction. The incorporation of a second metal could improve the performances of this catalyst and improve its stability. In fact, as it was mentioned before, the addition of a second metal could prevent the coke deposition on the surface of the catalyst [11], which are responsible of the deactivation of the catalyst. For that, the next chapter focuses on the study of the decarboxylation of PA to n-PD over non-noble bimetallic catalysts of Ni-Me type (with Me=Ag, Fe and Cu).

### References

- [1] M. Snåre, I. Kubičková, P. Mäki-Arvela, K. Eränen, D.Y. Murzin, *Industrial & Engineering Chemistry Research*. 45 (2006) 5708-5715.
- [2] P. Mäki-Arvela, M. Snåre, K. Eränen, J. Myllyoja, D.Y. Murzin, *Fuel*. 87 (2008) 3543-3549.
- [3] E. Santillan-Jimenez, M. Crocker, *Journal of Chemical Technology & Biotechnology*. 87 (2012) 1041-1050.
- [4] I. Simakova, O. Simakova, P. Mäki-Arvela, A. Simakov, M. Estrada, D.Y. Murzin, *Applied Catalysis A: General*. 355 (2009) 100-108.
- [5] J.G. Immer, H.H. Lamb, *Energy & Fuels*. 24 (2010) 5291-5299.
- [6] <https://www.ncbi.nlm.nih.gov/books/NBK100035/>, accessed, September 06, 2017.
- [7] S. De, J. Zhang, R. Luque, N. Yan, *Energy & Environmental Science*. 9 (2016) 3314-3347.
- [8] P. Mäki-Arvela, I. Kubickova, M. Snåre, K. Eränen, D.Y. Murzin, *Energy & Fuels*. 21 (2007) 30-41.
- [9] E. Santillan-Jimenez, T. Morgan, J. Lacny, S. Mohapatra, M. Crocker, *Fuel*. 103 (2013) 1010-1017.
- [10] I. Simakova, O. Simakova, P. Mäki-Arvela, D.Y. Murzin, *Catalysis Today*. 150 (2010) 28-31.
- [11] G. Boskovic, M. Baerns, in: M. Baerns (Ed.), *Basic Principles in Applied Catalysis*, Springer Berlin Heidelberg, Berlin, Heidelberg, 2004, pp. 477-503.

## Chapter 5

# Reactivity of bimetallic catalysts in the decarboxylation of palmitic acid

SUMMARY

<b>INTRODUCTION .....</b>	<b>136</b>
<b>I. NI-ME BIMETALLIC CATALYSTS FOR THE DECARBOXYLATION OF PA TO N-PD .....</b>	<b>137</b>
I.1. NI-AG-BASED CATALYSTS .....	137
I.1.1. Effect of Ag addition .....	137
I.1.2. Effect of the Ni-Ag loading.....	138
I.2. NI-FE-BASED CATALYSTS .....	139
I.2.1. Effect of the Fe addition .....	139
I.2.2. Effect of the Ni-Fe loading.....	140
I.3. NI-CU-BASED CATALYSTS .....	141
I.3.1. Effect of the Cu addition.....	141
I.3.2. Effect of the Ni-Cu loading.....	142
I.4. OPTIMIZATION OF THE REACTION CONDITIONS OVER THE 10%Ni10%Cu/C CATALYST.....	143
I.4.1. Effect of the amount of catalyst .....	143
I.4.2. Effect of the reaction temperature .....	145
I.4.3. Effect of the reaction time.....	146
I.4.4. Effect of the reaction atmosphere .....	147
I.4.5. Effect of the solvent .....	148
I.4.6. Manual and robotized preparations of the catalyst .....	149
I.4.7. Effect of the preparation method of the catalyst.....	150
<b>II. RECYCLABILITY TESTS OF THE CATALYSTS .....</b>	<b>151</b>
<b>III. EFFECT OF THE FATTY ACID CARBON CHAIN LENGTH.....</b>	<b>152</b>
<b>DISCUSSION .....</b>	<b>154</b>
<b>CONCLUSION .....</b>	<b>160</b>
<b>REFERENCES.....</b>	<b>161</b>

### Introduction

Nickel-based catalysts supported on activated carbon have shown promising performances in the decarboxylation of PA to n-PD (Chapter 4). Unfortunately, these catalysts also tended to deactivate under reaction conditions and then would require the use of pure costly  $H_2$  to avoid or limit this phenomenon [1]. Indeed, Ni-based formulations are particularly prone to form coke from the CO issued from the decarbonylation reaction. Additionally, Ni-based catalysts are also known to favor cracking reactions then forming short hydrocarbons [2]. Furthermore, Ni-based catalysts require relatively high temperatures or long reaction times to completely convert the fatty acids and reached high selectivity in n-hydrocarbons [3]. For all these reasons, Ni-based catalysts supported on carbon require the addition of a second metal to improve their performances not only in terms of activity and selectivity but also in terms of stability [4].

To this aim, a series of bimetallic Ni-Me catalysts supported on activated carbon were synthesized (with Me=Ag, Fe and Cu) and their catalytic performances in the decarboxylation of PA were studied. In the first part of this Chapter, the influence of the nature of the metal accompanying Ni and of the metals loading is presented and discussed. Then, in the second part, the influence of the reaction conditions on the catalytic performance of the best bimetallic catalyst identified in the first part is presented in detail. The stability of this best catalyst is also investigated. Finally, the best bimetallic system was tested in the optimal set of operating conditions for the decarboxylation of stearic acid (SA) to n-heptadecane.

### I. Ni-Me bimetallic catalysts for the decarboxylation of PA to n-PD

Bimetallic Ni-Me catalysts (with Me=Ag, Fe and Cu) supported on carbon, prepared by a deposition-precipitation method using aqueous hydrazine as reducing agent (see Chapter 2 for detail), were studied for the decarboxylation of PA to n-PD. All the tests described in this section were performed at 320 °C under an atmosphere of 10 vol.% of H<sub>2</sub> in N<sub>2</sub>. The mass of catalyst used was 12.8 mg and the PA loading was 0.197 mmol in 2 mL of hexadecane.

#### I.1. Ni-Ag-based catalysts

##### I.1.1. Effect of Ag addition

The effect of the addition of Ag to Ni-based catalyst on the catalytic performances was investigated. The results are shown in Figure 50. The monometallic 10%Ag/C catalyst led to 33% of conversion and 31% of selectivity to n-PD, which is not significantly different than the values observed in the blank test reported in Chapter 4. The catalytic performances of the monometallic 10%Ni/C were better in terms of activity but worse in terms of selectivity.

The addition of 10% of Ag in the 10%Ni/C catalyst enhanced slightly the catalytic performances. Actually, it can be observed that the conversion of PA increased slightly from 57 to 63% when 10% of Ag was added into the Ni-based catalyst. In the same way, the selectivity to n-PD increased slightly from 20% to 27%. Thus, the yield in n-PD was found slightly improved for the bimetallic catalyst (10, 11 and 17% for 10%Ag/C, 10%Ni/C and 10%Ni10%Ag/C, respectively).

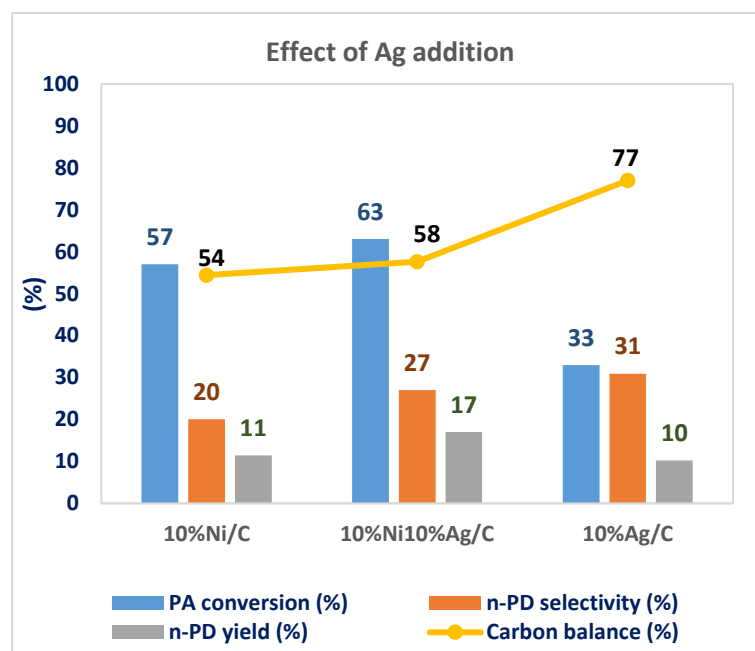


**Figure 50 : Effect of Ag addition on the catalytic performances in the decarboxylation of PA to n-PD.** Reaction conditions: T =320 °C, initial pressure= 20 bar, t = 6 h, stirrer speed = 600 rpm; catalyst loading = 12.8mg; PA loading = 0.197 mmol in hexadecane.

### I.1.2. Effect of the Ni-Ag loading

The amounts of Ni and Ag loaded on the support were varied in the 5-30 wt.% range to evaluate the impact of the loading on the catalytic performances of these bimetallic systems. In practice, four bimetallic catalysts with different Ni-Ag contents were prepared and tested. The total metal loadings used were 5, 10, 20 and 30 wt.% with a constant Ni/Cu weight ratio of 1. The results presented in Figure 51 show a variation of the performances of the catalyst with the Ni-Ag content. The highest conversion (67%) was surprisingly obtained for the lowest metal loading (2.5%Ni2.5%Ag/C), while, the 5%Ni5%Ag/C, 10%Ni10%Ag/C and 15%Ni15%Ag/C catalysts led to 47, 63 and 55% of PA conversion, respectively. However, at the same time the 2.5%Ni2.5%Ag/C catalyst showed a low selectivity to n-PD and a low carbon balance. For the 3 other catalysts the selectivity was always found stable around 26-27%.

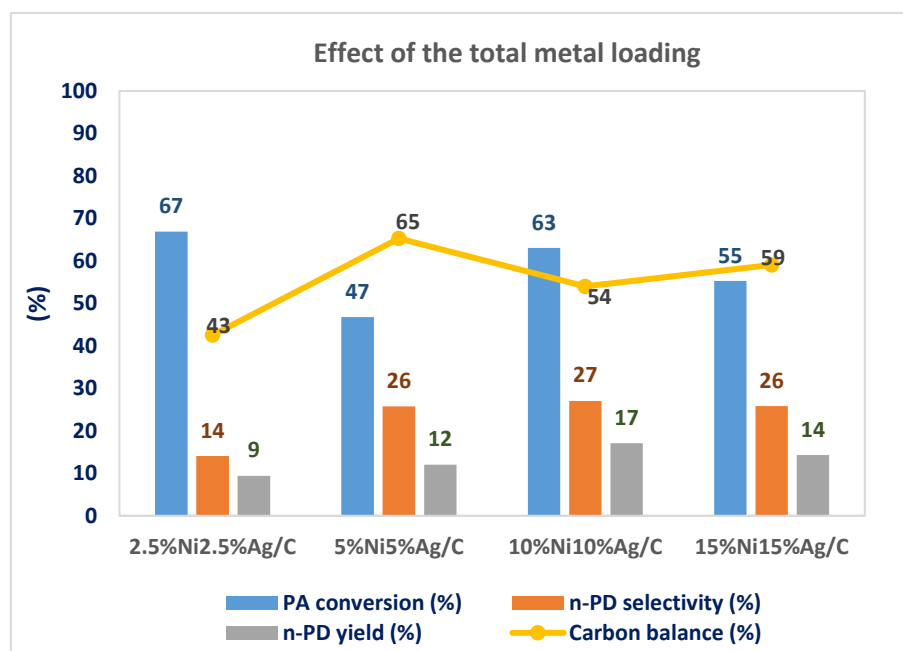
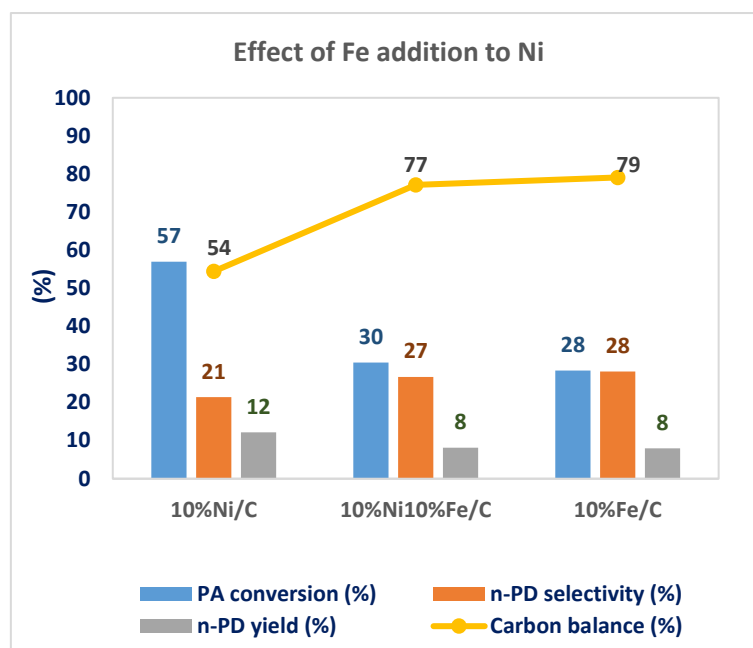


Figure 51: Effect of the total metal loading on the performances of the Ni-Ag/C catalysts in the decarboxylation of PA to n-PD. Reaction conditions: T =320°C, initial pressure= 20 bar, t = 6 h, stirrer speed = 600 rpm; catalyst loading=12.8mg; PA loading = 0.197 mmol in hexadecane.

## I.2. Ni-Fe-based catalysts

### I.2.1. Effect of the Fe addition

The effect of the addition of iron on the performances of nickel-based catalysts was studied. The performances of the 10%Ni10%Fe/C catalyst were compared to those obtained on the 10%Ni/C and 10%Fe/C catalysts (Figure 52). The monometallic 10%Fe/C catalyst showed very low activity in the carboxylation of PA under the conditions studied. In fact, the results obtained with this catalyst are exactly the same as those obtained in a blank test (27%, 28% and 8% of PA conversion, n-PD selectivity and n-PD yield, respectively). Similarly, the addition of Fe to Ni decreased significantly the activity. Indeed, the bimetallic 10%Ni10%Fe/C catalyst showed an activity comparable to those obtained in the blank test. Nevertheless, other bimetallic Ni-Fe/C catalysts with different loadings were studied to check the impact of the metal content on the performances of the bimetallic Ni-Fe/C catalysts.



**Figure 52: Effect of Fe addition on the catalytic performances of the bimetallic 10%Ni-10%Fe/C of decarboxylation of PA to n-PD. Reaction conditions: T =320 °C, initial pressure= 20 bar, t = 6 h, stirrer speed = 600 rpm; catalyst loading=12.8mg; PA loading = 0.197 mmol in hexadecane.**

### I.2.2. Effect of the Ni-Fe loading

As previously done for Ag four different Ni-Fe samples with 5, 10, 20 and 30 wt.% of total metal loading at a constant Ni/Fe weight ratio of 1 were prepared and studied. Conversion of PA and selectivity to n-PD obtained for each sample under reaction conditions are shown in Figure 53. As could be observed, all these catalysts led to catalytic performances which were only slightly better than those observed for the blank test. These catalysts were also less efficient than the 10%Ni10%Ag catalyst previously reported. Iron is therefore not the best promoter for the Ni-based catalysts.

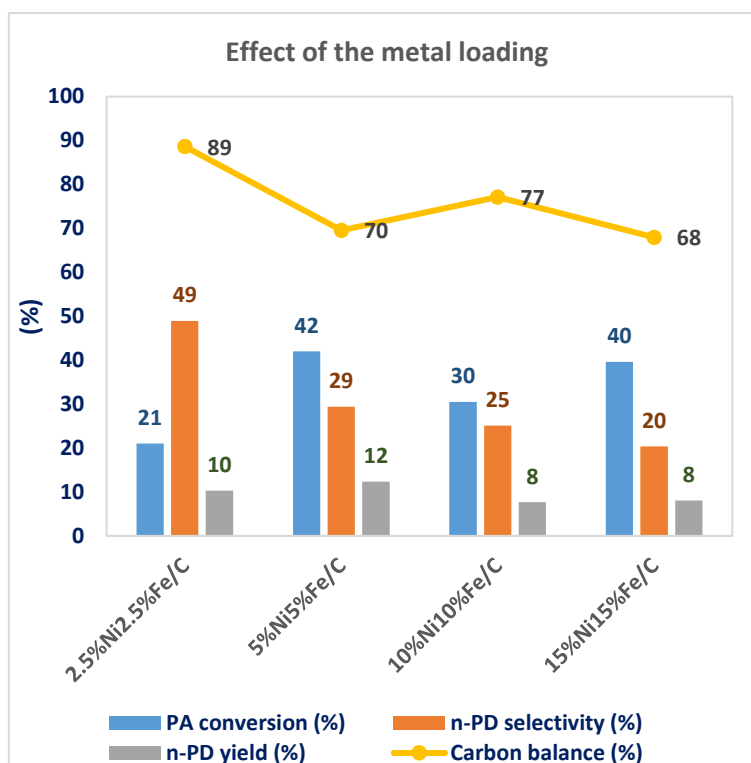
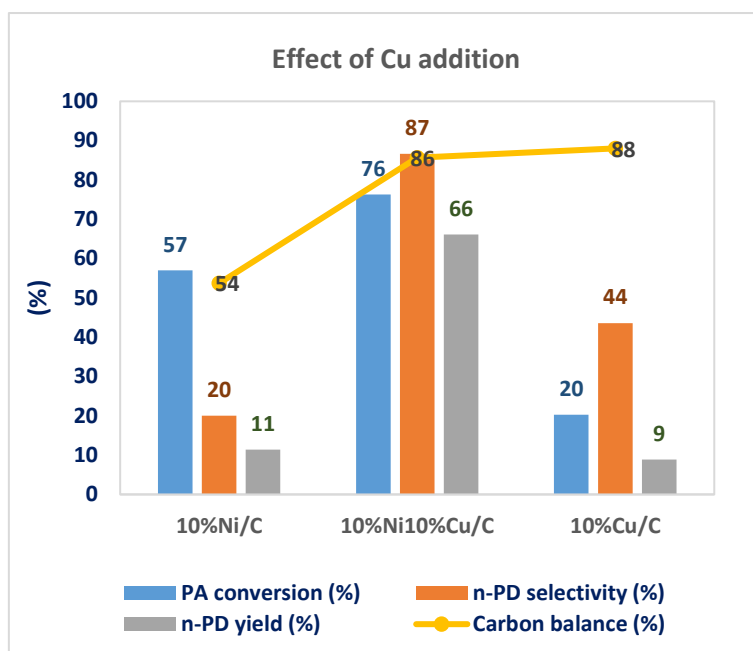


Figure 53: Effect of metal loading on the performances of the bimetallic catalyst of type Ni-Fe/C for the catalytic decarboxylation of PA to n-PD. Reaction conditions:  $T = 320^{\circ}\text{C}$ , initial pressure = 20 bar,  $t = 6$  h, stirrer speed = 600 rpm; catalyst loading = 12.8 mg; PA loading = 0.197 mmol in hexadecane.

### I.3. Ni-Cu-based catalysts

#### I.3.1. Effect of the Cu addition

As it was done previously for Ag and Fe, the effect of Cu addition to the 10%Ni/C catalyst on its catalytic performances was studied. The results are presented in Figure 54. The monometallic 10%Ni/C catalyst showed 57% of conversion of PA but only 20% of selectivity to n-PD and a very low carbon balance of 54%. In contrast, the monometallic 10%Cu/C catalyst showed a low conversion of 20% and 44% of selectivity to n-PD and a much better carbon balance of 88%. The synergy between Ni and Cu increased considerably the conversion of PA to 76% and also increased dramatically the selectivity to n-PD from 20 to 87%. A very good carbon balance of 87% was also obtained. Based on this very promising preliminary result, the bimetallic Ni-Cu/C catalysts were studied in more detail to check the impact of the metal content on their catalytic performances.



**Figure 54:** Effect of Cu addition on the catalytic performances of Ni catalyst for the decarboxylation of PA to n-PD. Reaction conditions: T =320°C, initial pressure= 20 bar, t = 6 h, stirrer speed = 600 rpm; catalyst loading=12.8mg; PA loading=0.197 mmol in hexadecane.

### I.3.2. Effect of the Ni-Cu loading

As done previously for Ag and Fe, the effect of the total metal loading was studied on four different Ni-Cu catalysts at a Ni/Cu weight ratio of 1 (Figure 55). Copper promotion was less apparent for 5 and 10 wt.% of total metal loadings. Only when the total metal loading was bigger than 10%, the beneficial effect of Cu addition appeared. 10%Ni10%Cu/C catalyst showed the best catalytic performances between all the bimetallic Ni-Me catalysts studied. The conversion in PA reached 76%, whereas, the selectivity and the yield to n-PD were 87% and 66% respectively. The carbon balance reached almost 90%, indicating the formation of very low amounts of unidentified products.

The reason of the best performances obtained with the 10%Ni10%Cu/C catalyst could be analyzed as follows. The XPS analysis revealed that the surface of the fresh 10%Ni10%Cu/C catalyst is mainly composed of CuO, Ni(OH)<sub>2</sub> and NiO, while, for the 5%Ni5%Cu/C and 15%Ni15%Cu/C catalysts Cu(NO<sub>3</sub>)<sub>2</sub> was detected on the catalyst surface. The presence of this salt could explain the difference of the results.

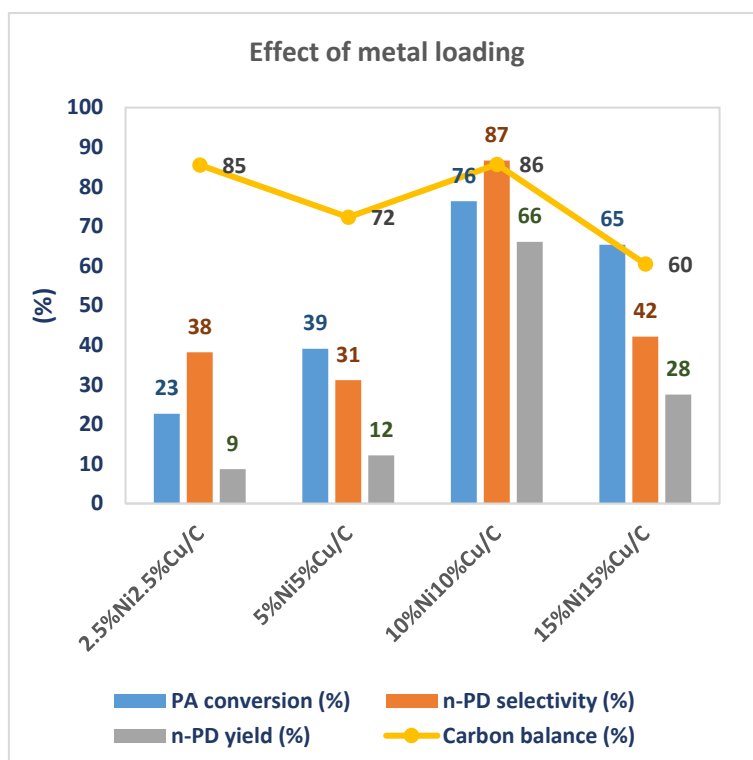


**Figure 55: Effect of the metal loading on the catalytic performances of the bimetallic Ni-Cu catalysts for the decarboxylation of PA to n-PD. Reaction conditions: T =320°C, initial pressure= 20 bar, t = 6 h, stirrer speed = 600 rpm; catalyst loading=12.8 mg; PA loading = 0.197 mmol in hexadecane.**

Among all the bimetallic catalysts tested, the Ni-Cu catalysts are by far the most promising, in particular the 10%Ni10%Cu/C sample. Therefore, in the next part, we will focus exclusively on the 10%Ni10%Cu/C catalyst and the influence of the reaction conditions was studied in order to see if it is possible to still optimize the catalytic performances.

#### I.4. Optimization of the reaction conditions over the 10%Ni10%Cu/C catalyst

##### I.4.1. Effect of the amount of catalyst

The effect of the amount of the 10%Ni10%Cu/C catalyst loaded in the reactor on PA conversion, selectivity and yield to n-PD is shown in Figure 56. As observed the conversion of PA increased from 76 % to 100 % when the amount of catalyst loaded in the reactor was increased from 12.8 to 26 mg. Then, the conversion remained total from 26 to 75 mg. In the same time, the selectivity to n-PD increased from 87 to 95 % when the mass of the catalyst increased from 12.8 to 75 mg. Thus, the best performances of the 10%Ni10%Cu/C catalyst were obtained when the mass of catalyst loaded in the reactor was 75 mg which correspond to

a metal/PA ratio of 1/3. Most importantly, this study showed that the selectivity to n-PD strongly depends on the metal/PA ratio. The results are in good agreement with the studies of Maki-Arvela *et al.* [5] who observed the same effect in the decarboxylation of stearic acid over Pd/C. In fact, it was found that the initial rates increased linearly with the increase of the mass of catalyst loaded in the reactor and that increasing the mass of catalyst loaded in the reactor also improve the selectivity. Indeed, this is due to the improvement of the mass transfer which enhances the rate of reaction and limits the formation of undesired products.

Nevertheless, increasing the amount of catalyst from 52 to 75 mg has almost no effect as the selectivity tends to stabilize around 95%. Consequently, the optimal amount of catalyst was fixed at 52 mg, which led to full conversion of PA and 94% selectivity to n-PD with an excellent 94% carbon balance.

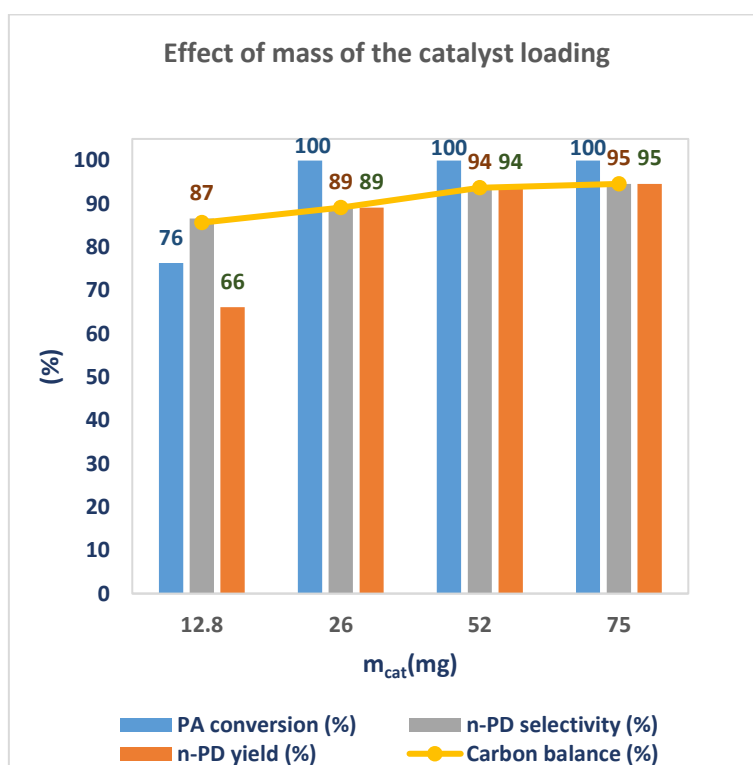


**Figure 56:** Effect of the amount of the catalyst loading on the catalytic performances of the bimetallic 10%Ni10%Cu/C catalyst for the decarboxylation of PA to n-PD. Reaction conditions:  $T = 320^{\circ}\text{C}$ , initial pressure = 20 bar,  $t = 6$  h, stirrer speed = 600 rpm; PA loading = 0.197 mmol in hexadecane.

### I.4.2. Effect of the reaction temperature

The effect of the reaction temperature on the catalytic performances of the bimetallic 10%Ni10%Cu/C catalyst was studied in the 250-320 °C range. All the other reaction conditions were kept the same as above except the mass of catalyst loaded in the reactor which was 52 mg.

The results obtained are presented in Figure 57. As observed, the conversion of PA and the selectivity to n-PD increased from 40% to 100% and from 26 to 84%, respectively, when the temperature of the reaction increased from 250 to 320 °C. Furthermore, when the reaction was carried out at 250 °C, the carbon balance was only 68%. To understand the low performances of the catalysts at 250 °C, the products of reaction were analyzed by GC-MS, and compared to those obtained at 320 °C. The products identification was based on a comparison of the spectra obtained with those of the NIST 2011 MASS Spectral Library. Analysis of the products obtained after the reaction carried out at 250°C showed the presence of some traces of oxygenated compounds such as n-hexadecanol and n-hexadecenol. However, other unidentified heavy compounds were also certainly formed. In the contrary, at 320 °C, the carbon balance was high (95%) and only some traces of hexadecane were detected (< 2 % of selectivity).

The 10%Ni10%Cu/C catalyst favored the reaction of decarboxylation at high temperature. In fact, the increase of temperature enhances the reaction rate reaching 100% of PA conversion at 300 °C. On the other hand, the selectivity to n-pentadecane was 84% and 95% at 300 and 320 °C, respectively. At 250 °C, the reaction rate was low and the conversion was only 40%. Furthermore, the selectivity to n-PD was only 26%. Based on the previous observations, it could be concluded that the decarboxylation reaction was limited by thermodynamic factors at 250 °C. Murzin *et al* [2] showed that at 300 °C, the enthalpy of DCX reaction is 179.1 kJ/mol and that of HDO is -115.0 kJ/mol. Therefore, DCX is endothermic, i.e. favored at high temperature, while HDO is exothermic and favored at low temperature. That is the reason why the decarboxylation of PA is more efficient at high temperature.

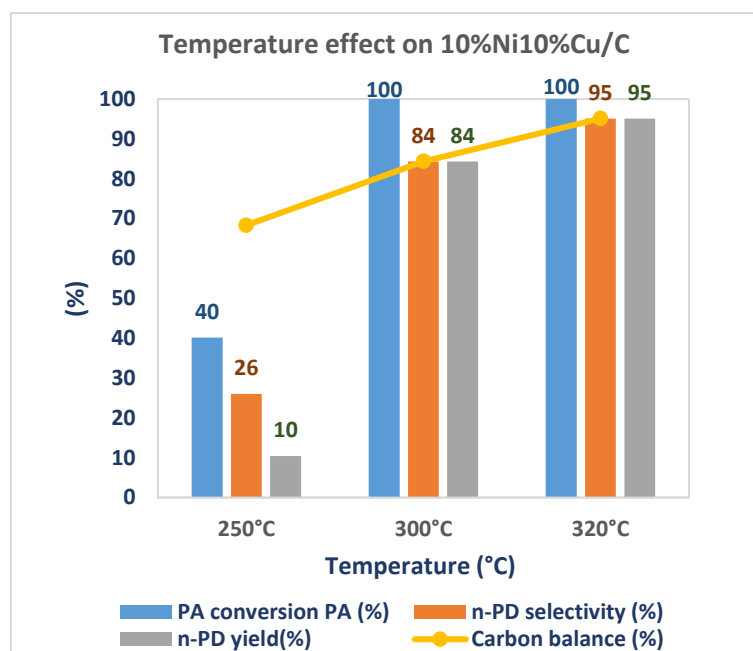


**Figure 57:** Effect of the reaction temperature on the catalytic performances of 10%Ni10%Cu/C for the decarboxylation of PA to n-PD. Reaction conditions: initial pressure= 20 bar,  $t = 6$  h, stirrer speed = 600 rpm; catalyst loading= 52 mg; PA loading = 0.197 mmol in hexadecane.

#### I.4.3. Effect of the reaction time

The effect of the reaction time over 10%Ni10%Cu/C was studied for 1.5, 3, 6 and 12 hours. During each test, the temperature, gas atmosphere, pressure, etc. were kept the same as previously (namely 320 °C, 10 vol.% of H<sub>2</sub> in N<sub>2</sub> and 20 bar of initial pressure). The results obtained are presented in Figure 58. Whatever the reaction time, a total conversion of PA was observed. However, the selectivity to n-PD showed a variation as a function of the reaction time. Indeed, the maximum selectivity to n-PD was observed when the reaction was performed for 6 h. Between 1.5 and 3 h and between 3 h and 6 h, the n-PD selectivity increased from 75 to 91% and from 91 to 95%, respectively. Between 6 and 12h, the selectivity dropped slightly from 95 to 92%. This decrease of selectivity could be due to consecutive reactions such as isomerization, oligomerization that can occur at relatively long reaction times [6]. On the contrary, the increase of the n-PD selectivity in the first hours of reaction could be due to the conversion of intermediate products of relatively high molecular mass (difficult to detect by GC) which are then converted to n-PD with the increase of the reaction time.

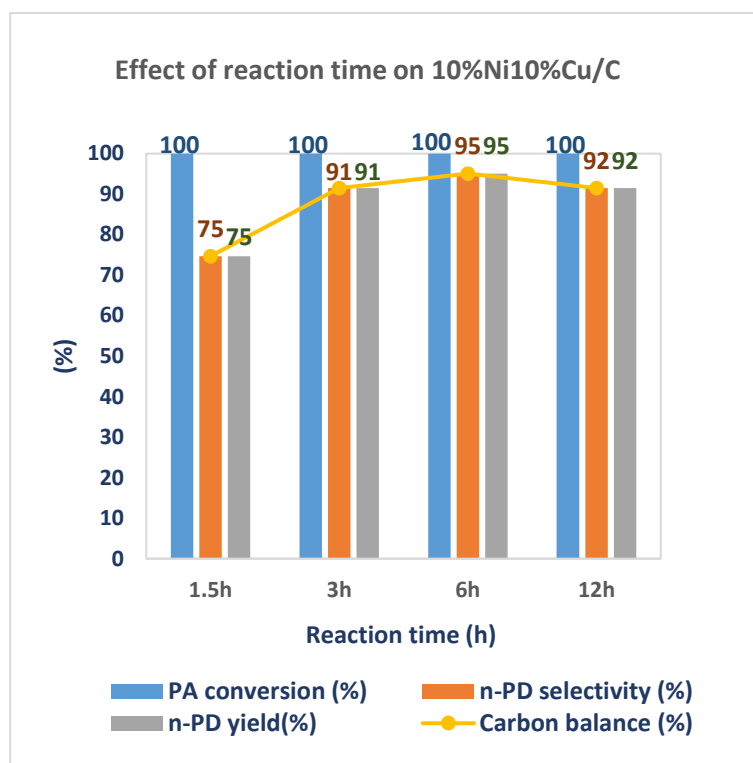


Figure 58: Effect of the reaction time on the catalytic performances of 10%Ni10%Cu/C for the decarboxylation of PA to n-PD. Reaction conditions:  $T = 320^{\circ}\text{C}$  under 10% $\text{H}_2/\text{N}_2$ , initial pressure= 20 bar, stirrer speed = 600 rpm; catalyst loading=52 mg; PA loading = 0.197 mmol in hexadecane.

#### I.4.4. Effect of the reaction atmosphere

The reaction atmosphere is known to affect the deoxygenation pathway of reaction. Hence, the effect of the reaction atmosphere was studied for two different atmospheres (pure  $\text{N}_2$  and 10 vol.% of  $\text{H}_2$  in  $\text{N}_2$ ). To this aim, the reaction was performed at  $320^{\circ}\text{C}$  for 6 h and with an initial pressure of 20 bar in both cases. Experimental results (Figure 59) showed that whatever the reaction atmosphere, the PA conversion remained total. However, the selectivity to n-PD depended strongly of the reaction atmosphere. Indeed, under inert gas, the n-PD selectivity was only 59%, while, 95% was reached under an atmosphere containing a low quantity of  $\text{H}_2$ . The carbon balance obtained under inert gas was also lower (59%) compared to this obtained under 10 vol. %  $\text{H}_2$  in  $\text{N}_2$  (95%). This means that the formation of several byproducts occurred under inert gas. The analysis of the reaction products obtained under each atmosphere was determined by GC-MS. Identification of the products was based on a comparison of the spectrum with those of the NIST 2011 MASS Spectral Library. The results obtained showed that under the  $\text{H}_2$ -containing atmosphere, the main byproduct detected at 320

°C was n-hexadecane. In contrast, under inert atmosphere, the same catalyst showed, 29% of n-pentadecene selectivity and shorter hydrocarbon such as tetradecane and tridecane (<4%).

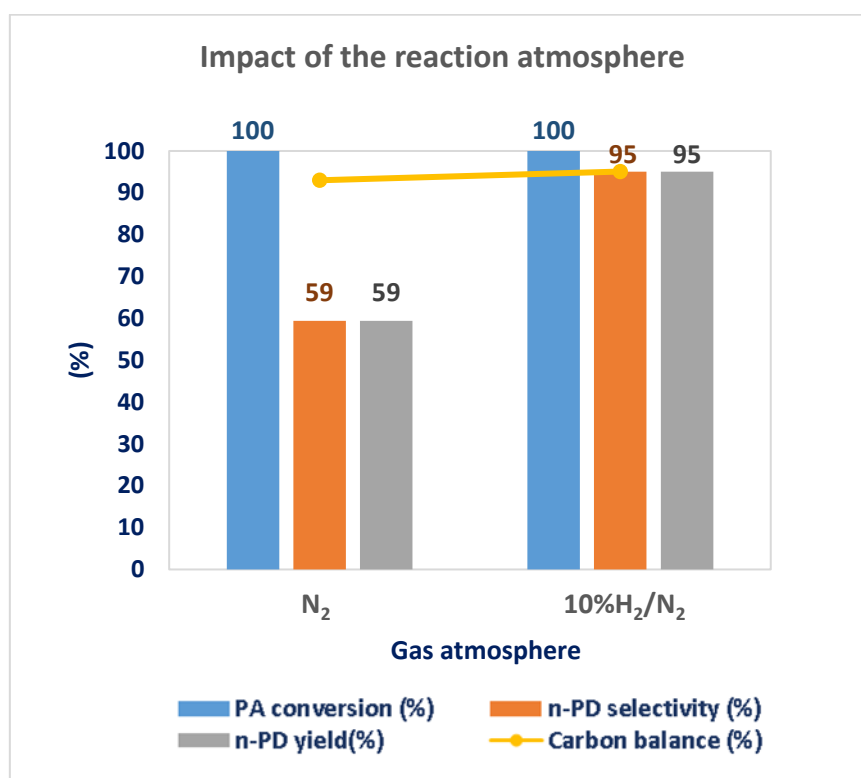
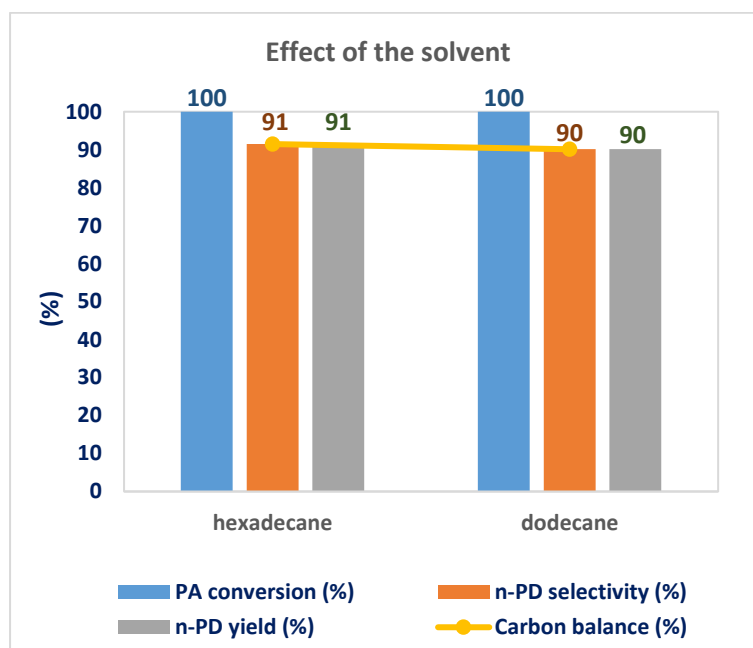


Figure 59 : Effect of reaction atmosphere on the catalytic performances of the 10%Ni10%Cu/C catalyst for the decarboxylation of PA to n-PD. Reaction conditions: T =320 °C, initial pressure= 20 bar, t = 6 h, stirrer speed = 600 rpm; catalyst loading= 52 mg; PA loading = 0.197 mmol in hexadecane.

#### I.4.5. Effect of the solvent

In the literature, many studies of the influence of the solvent on the performances of the catalysts can be found [5] [7]. The solvents used for the DO of fatty acids are of different types. Among them, dodecane was the most widely used for DO reactions of fatty acids and their derivatives [8]. In a process of sustainable chemistry, the solvent should be chosen with particular attention. In the ideal case, no solvent at all should be used. In our case it would be possible to use n-PD as the solvent to facilitate the post-treatment (separation/purification) of the products of reaction. However, even if industrially it would be the best choice in our case the use of n-PD as solvent would hinder the possibility to calculate the catalytic performances.

In this study, dodecane and hexadecane were tested as solvent during the decarboxylation of PA to n-PD to check the effect of the hydrocarbon chain length on the performances. For that, the tests were carried out at 320 °C, under a 10 vol.% N<sub>2</sub> in H<sub>2</sub> atmosphere and 20 bar of initial pressure for 3 h. The results displayed in Figure 60 showed that there is no effect of the solvent on the catalytic performances of the 10%Ni10%Cu catalyst in the reaction conditions tested. Therefore, the decarboxylation of PA to n-PD over the bimetallic 10%Ni10%Cu/C catalyst could probably be carried out directly in n-PD without any other solvent and without any impact on the catalytic performances.



**Figure 60:** Effect of the solvent on the catalytic performances of 10%Ni10%Cu/C for the decarboxylation of PA to n-PD. Reaction conditions: T =320 °C under 10%H<sub>2</sub>/N<sub>2</sub>, initial pressure= 20 bar, t = 3 h, stirrer speed = 600 rpm; catalyst loading=52 mg; PA loading = 0.197 mmol in each solvent.

#### I.4.6. Manual and robotized preparations of the catalyst

The bimetallic 10%Ni10%Cu/C was prepared manually at the bench (noted 10%Ni10%Cu/C-M) and automatically with the CatImpreg® Chemspeed HT robot (noted 10%Ni10%Cu/C-Robot) (see Chapter 2 for details). The comparison of the catalytic performances obtained with these two catalysts is presented in Figure 61. As observed, the catalysts have almost exactly the same catalytic performances. One can conclude that the transposition of the manual preparation protocol to the robot was perfectly successful.

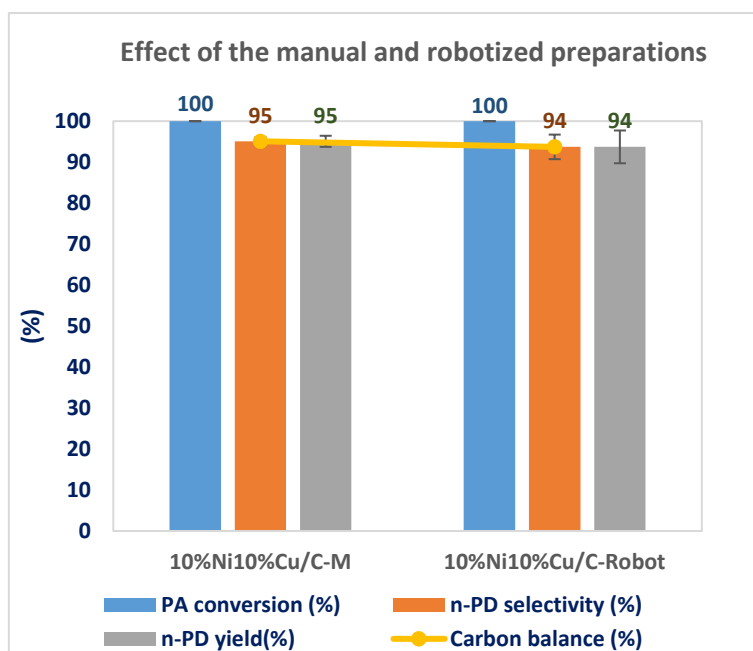


**Figure 61: Effect of the preparation mode on the catalytic performances of 10%Ni10%Cu/C for the decarboxylation of PA to n-PD. Reaction conditions:  $T = 320^{\circ}\text{C}$  under 10% $\text{H}_2/\text{N}_2$ , initial pressure = 20 bar,  $t = 3$  h, stirrer speed = 600 rpm; catalyst loading = 52 mg; PA loading = 0.197 mmol in hexadecane.**

#### I.4.7. Effect of the preparation method of the catalyst

As mentioned in Chapter 2, the bimetallic 10%Ni10%Cu/C was prepared by two different methods: deposition-precipitation (DP) using hydrazine as reducing agent (denoted 10%Ni10%Cu/C) and wet impregnation (WI) followed by a calcination of the sample at  $450^{\circ}\text{C}$ , under inert atmosphere for 3 h (denoted 10%Ni10%Cu/C-calc). In this section, the effect of the preparation method on the catalytic performances of the catalysts was studied, and the results are presented in Figure 62. As observed, the catalytic performances of the catalyst prepared by DP showed much better performances compared to the catalyst prepared by WI. This behavior can be attributed to the huge differences in the physical and structural properties of the two catalysts discussed in Chapter 3. Indeed, XRD analysis revealed the absence of crystalline structure for the 10%Ni10%Cu-calc catalyst, while the 10%Ni10%Cu/C sample is well crystallized. Furthermore, the surface areas, the mean pore sizes and the pore volumes were also completely different for both catalysts. In addition, TPR results revealed that the reducibility of the species present in each catalyst are completely different and that the temperature of reduction of the 10%Ni10%Cu/C catalyst started at much lower temperature ( $238.1^{\circ}\text{C}$ ) in comparison to the 10%Ni10%Cu/C-calc ( $389.1^{\circ}\text{C}$ ) sample.

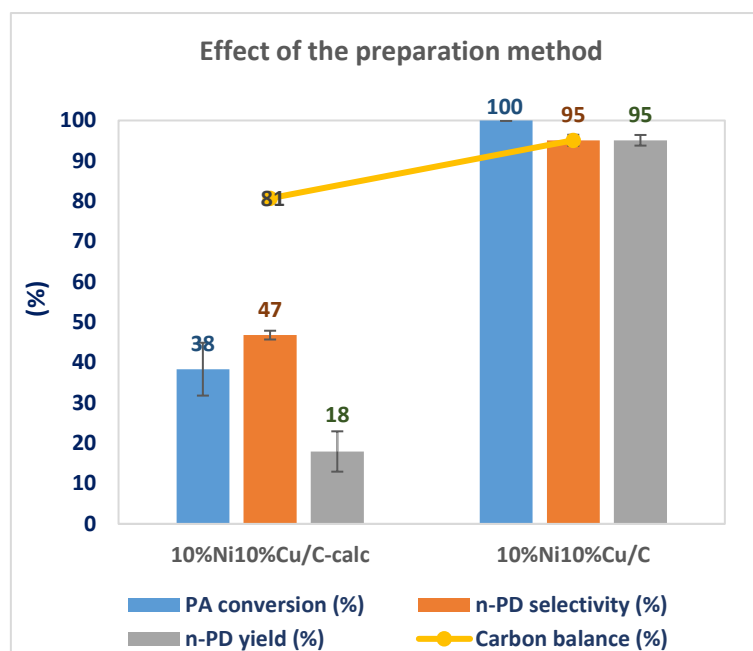


**Figure 62:** Effect of the preparation method on the catalytic performances of 10%Ni10%Cu/C for the decarboxylation of PA to n-PD. Reaction conditions: T =320 °C under 10%H<sub>2</sub>/N<sub>2</sub>, initial pressure= 20 bar, t = 6 h, stirrer speed = 600 rpm; catalyst loading=52 mg; PA loading = 0.197 mmol in hexadecane.

## II. Recyclability tests of the catalysts

The recyclability of the 10%Ni10%Cu/C catalyst was studied at 320 °C under 10 vol.% H<sub>2</sub> in N<sub>2</sub> for 6 h. The amount of catalyst loaded in the reactor was 12.8 mg. In total, three tests were performed. Firstly, the fresh catalyst (1<sup>st</sup> use) was tested and after the reaction, the liquid products were removed (supernatant). The spent catalyst was kept as such at the bottom of the reactor and a new loading of fresh reactant was added rapidly to avoid the re-oxidation of the catalysts by contact with air. The reaction was then carried out again (2<sup>nd</sup> use) in the same conditions as previously. The same operation was applied for the third test with the same catalyst (3<sup>rd</sup> use). The results obtained are presented in Figure 63. It is clear that after three uses of the catalyst without any regeneration between the reactions, the conversion, selectivity and yield remained almost constant. Therefore, the 10%Ni10%Cu/C catalyst could be considered as a very stable catalyst under the reaction conditions used.

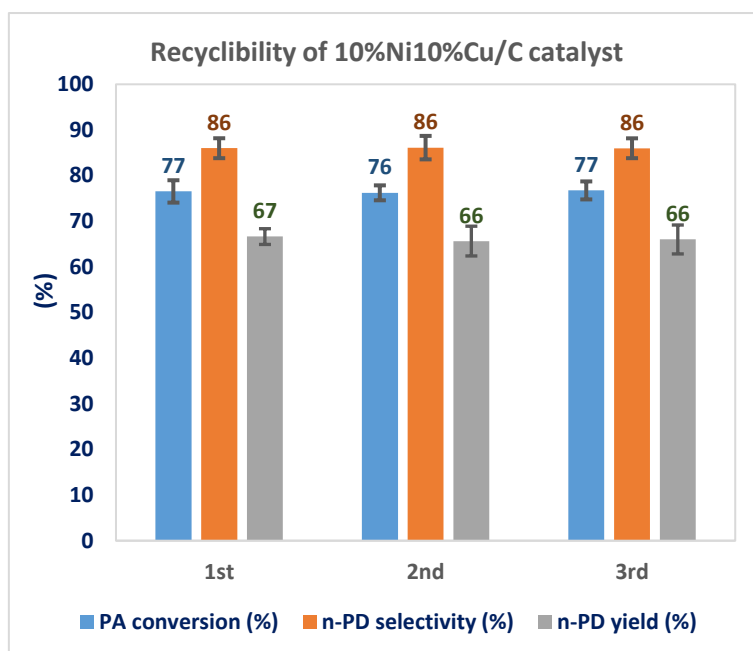


**Figure 63: Recyclability of the catalyst 10%Ni10%Cu/C for the decarboxylation of PA to n-PD. Reaction conditions: T =320 °C under 10%H<sub>2</sub>/N<sub>2</sub>, initial pressure= 20 bar, t = 6 h, stirrer speed = 600 rpm; catalyst loading=12.8mg; PA loading = 0.197 mmol in hexadecane.**

### III. Effect of the fatty acid carbon chain length

In order to start the study of the possible extension of the application of the 10%Ni10%Cu/C catalyst to other fatty acids, stearic acid (C18) was tested in comparison to PA (C16) for the decarboxylation reaction. The tests were carried out at 320 °C under 10 vol.% H<sub>2</sub> in N<sub>2</sub> during 3 h. The reactor initial pressure was 20 bar and the catalyst loading was 52 mg. The PA and SA loading were 0.197 mmol in dodecane. The results are presented in Figure 64. They showed that the catalytic performances for both substrates are almost the same. Both FA conversions were full and roughly 90% of selectivity to n-PD and to n-heptadecane were obtained.

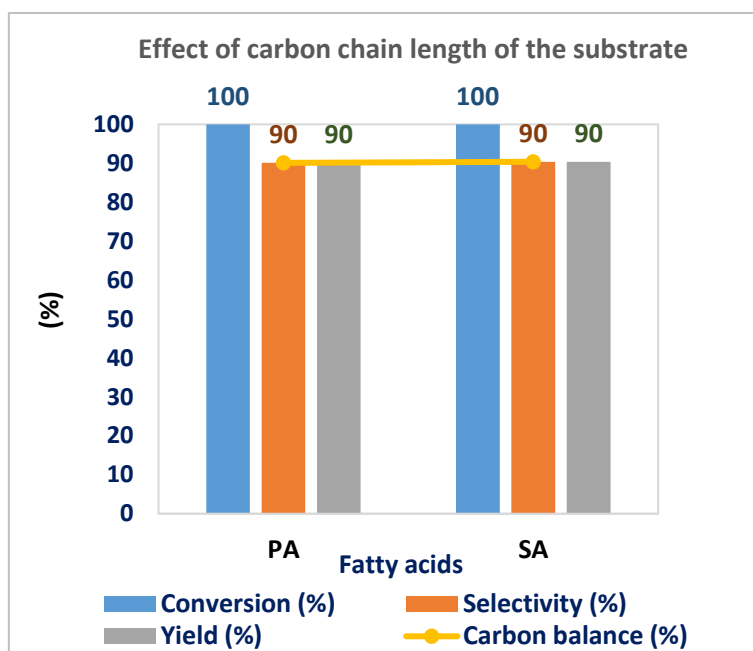


**Figure 64:** Decarboxylation of PA and SA to n-PD and n-C17. Reaction conditions: T =320°C under 10% $H_2/N_2$ , initial pressure= 20 bar, t = 3 h, stirrer speed = 600 rpm; catalyst loading=52 mg; PA and SA loading = 0.197 mmol in dodecane.

## Discussion

Bimetallic Ni-Me (with Me=Ag, Fe and Cu) catalysts supported on activated carbon, prepared by a deposition-precipitation method using aqueous hydrazine as reducing agent, were studied in the decarboxylation of PA to produce n-PD.

The most important finding is that combining nickel with another non-noble metal, such as Ag, Fe or Cu, can play an important role in the improvement of catalyst activity, selectivity and yield. Among the bimetallic catalysts tested, the Ni-Cu/C materials were found the most promising. The studies of four bimetallic Ni-Cu/C (Ni/Cu=1) compositions with different total metal loading (5, 10, 20 and 30%) revealed that the 10%Ni10%Cu/C catalyst is by far the best candidate of the Ni-Cu series for carrying out the decarboxylation of PA to n-PD. The different textural and morphological properties of the Ni-Cu catalysts (Table 22) could explain the differences observed in the catalytic results.

**Table 22: Overview of the fresh Ni-Cu bimetallic catalysts properties**

Catalyst	S <sub>BET</sub> (m <sup>2</sup> /g)	Pore size (Å)	Pore volume (cm <sup>3</sup> /g)	Ni/Cu (XPS)	Ni/Cu (ICP)	Ni/Cu (XRF)	Ni/Cu (EDX)	Species detected by XPS	Phases identified by XRD
5%Ni5%Cu/C	830	64	0.47	2.6	0.9	0.9		Cu(NO <sub>3</sub> ) <sub>2</sub> Ni(OH) <sub>2</sub>	Ni <sub>0.79</sub> Cu <sub>0.21</sub> O
10%Ni10%Cu/C	536	66	0.39	2	1.7	0.8	1.5	CuO, NiO, Ni(OH) <sub>2</sub>	CuO NiO
15%Ni15%Cu/C	645	64	0.39	3.3	0.6	0.6		Cu(NO <sub>3</sub> ) <sub>2</sub> Ni(OH) <sub>2</sub>	Ni <sub>0.79</sub> Cu <sub>0.21</sub> O

First of all, among all the bimetallic Ni-Cu catalysts synthesized, the most active one (10%Ni10%Cu/C) showed the lowest specific surface area and pore volume. Comparing to the 5%Ni5%Cu/C, this decrease of the both textural properties was attributed to the pore filling by the increase of the metal loading. However, compared to the 15%Ni15%Cu/C, the low surface area and pore volume were attributed to the particles size of this catalyst, which are bigger than that of the most active catalyst. Furthermore, TEM images showed the presence of spherical shaped particles of nickel and copper ranging from ~2-6 nm in the most active catalyst, while, several lattice fringes with d-spacings of 6.3, 6.5 and 6.75 Å and big agglomerated particles were detected in the 15%Ni15%Cu/C. These results confirm that the particle size of the most active catalyst is smaller than that of the 15%Ni15%Cu/C sample.

The ICP analyses revealed that there was more copper than nickel in bimetallic 5%Ni5%Cu/C and 15%Ni15%Cu/C catalysts, while for the most active catalyst (10%Ni10%Cu/C), the opposite was observed. Furthermore, ICP results was in good agreement with XRF results for the 5%Ni5%Cu/C and 15%Ni15%Cu/C catalysts. However, for the most active catalyst, the results were opposite. XRD analysis of the most active catalyst showed the presence of NiO and CuO in the bulk of the catalyst. Given that, the XRF analysis technique cannot detect oxygen and carbon, it could be concluded that the XRF results are not precise. Knowing that the ICP analysis of this type of material is more precise than XRF analysis, it could considerer that bulk of the most active catalyst is enriched with nickel.

The interactions between the metal nanoparticles (NPs) inside a bimetallic system is crucial and hence the composition of both the bulk and the surface of the catalysts and the organization of the NPs on its surface has to be considered carefully. Despite their differences in bulk composition, XPS analysis revealed that the surface of all bimetallic catalysts is enriched in Ni. However, the XPS analysis also showed different species on the surface of the catalysts. The XPS spectrum in the Ni 2p and Cu 2p regions of the most active catalyst showed the presence of NiO, Ni(OH)<sub>2</sub> and CuO species on the surface. In contrast, in the case of the 5%Ni5%Cu/C and 15%Ni15%Cu/C catalysts the presence of Cu(NO<sub>3</sub>)<sub>2</sub> and Ni(OH)<sub>2</sub> was observed. In addition, the XRD analysis revealed that, there is the presence of two oxides (NiO, CuO) in the most active catalyst while, the XRD analysis of the 5%Ni5%Cu/C and 15%Ni15Cu/C catalysts revealed also the presence of Ni<sub>0.79</sub>Cu<sub>0.21</sub>O. After the reduction, of the catalysts the presence of metallic Ni and Cu species was observed on the best catalyst, whereas, in the case of the two other Ni-Cu bimetallic systems the presence of a Ni-Cu alloy was revealed. It seems to be detrimental to the catalytic performances. The 5%Ni5%Cu/C sample contained a mixture of two bimetallic alloys: Ni<sub>0.79</sub>Cu<sub>0.21</sub> and Ni<sub>0.5</sub>Cu<sub>0.5</sub>, while a mixture of Ni<sub>0.79</sub>Cu<sub>0.21</sub> alloy with metallic copper was detected on the 15%Ni15%Cu/C catalyst. The H<sub>2</sub>-TPR profile of the bimetallic catalysts also confirmed the presence of different species. The bimetallic 5%Ni5%Cu/C and 15%Ni15%Cu/C catalysts showed that the peaks of reduction originated from NiO-CuO reduction to a Ni-Cu alloy and of Cu<sup>2+</sup> to Cu. In contrast, the most active catalyst only showed the reduction of CuO, NiO and Cu<sup>2+</sup> to Cu and Ni.

The study of the reaction conditions revealed that the most active bimetallic catalyst (10%Ni10%Cu/C) reached a total conversion of PA, when the decarboxylation reaction was carried out at 320 °C, under 10 vol.% of H<sub>2</sub> in N<sub>2</sub> for 6 h. In terms of selectivity, the catalyst reached 95% to n-PD. In contrast, under inert atmosphere, the same catalyst showed total conversion, but the selectivity toward n-PD decreased significantly (only 59%). As expected, the GC-MS analysis of the products obtained for different atmospheres revealed the formation of different byproducts (Table 23).

**Table 23 : Effect of reaction atmosphere on the catalytic performances of 10%Ni10%Cu/C for the decarboxylation of PA to n-PD. Reaction conditions: T =320 °C, initial pressure= 20 bar, t = 6 h, stirrer speed = 600 rpm; catalyst loading=52 mg; PA loading = 0.197 mmol**

Atmosphere	X <sub>PA</sub> <sup>[a]</sup> (%)	S <sub>n-C15</sub> <sup>[b]</sup> (%)	S <sub>1-C15</sub> <sup>[b]</sup> (%)	S <sub>C15</sub> <sup>[b]</sup> (%)	S <sub>C14</sub> <sup>[b]</sup> (%)	S <sub>C16</sub> <sup>[b]</sup> (%)	Carbon balance
10%H <sub>2</sub> /N <sub>2</sub>	100	95	-	95	-	<2	97
N <sub>2</sub>	100	59	29	88	<4	-	93

[a] X<sub>PA</sub>: palmitic acid conversion; [b] selectivity to n-C15: n-pentadecane, 1-C15: 1-pentadecene, C15: total C15, C14 : tetradecane, C16: hexadecane

Under the H<sub>2</sub>-containing atmosphere at 320°C, the main product of the catalytic decarboxylation of PA on the bimetallic 10%Ni10%Cu/C catalyst was n-PD. In addition, ~2% of n-hexadecane was detected as the only other product. This suggests that under 10 vol.% H<sub>2</sub> in N<sub>2</sub>, this catalyst exhibited two main pathways: DCX and HDO. This assumption is confirmed by the similarity in terms of reaction mechanism obtained for the catalytic decarboxylation of another substrate (SA). Indeed, the GC-MS analysis of the products from the decarboxylation of SA revealed the formation of n-heptadecane as the main product and octadecane (<5 % of selectivity) as the only secondary product. These products were formed through the DCX and HDO reaction as it was observed for the decarboxylation of PA. However, under the same atmosphere but, at much lower temperature (250 °C), the decarboxylation of PA showed a significant presence of oxygenated compounds (n-hexadecanol, n-hexadecenol, n-hexadecanal, etc...) beside n-PD. On that basis, we propose the reaction mechanism displayed in Figure 65.

The PA deoxygenation under a 10 vol.% H<sub>2</sub> in N<sub>2</sub> atmosphere could occur via three routes: DCX (1), DCN (2) and HDO (3). The main route (1) is the decarboxylation reaction (DCX), where PA is directly converted to n-PD and CO<sub>2</sub>. The second route (2) is the indirect decarboxylation reaction, via a first decarbonylation reaction to 1-pentadecene (DCN) followed

by an hydrogenation step of the olefin to n-PD. Finally, the third route (3) is the hydrodeoxygenation (HDO) reaction, where PA is converted to hexadecanal which can be further transformed to 1-pentadecene and then n-PD. Alternatively hexadecanal can be converted reversibly to 1-hexadecenol, 1-hexadecanol and finally hexadecane. Thus, the formation of n-PD under a H<sub>2</sub>-containing atmosphere passes through intermediate products (oxygenated compounds).

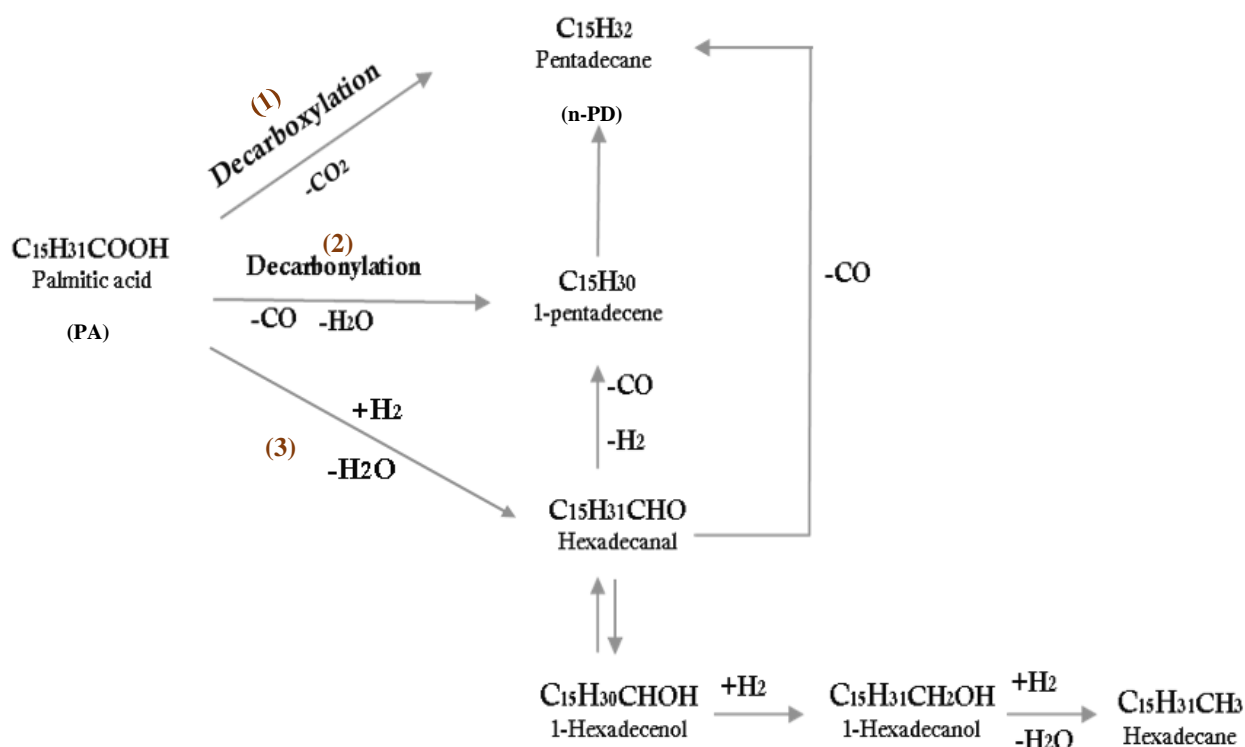
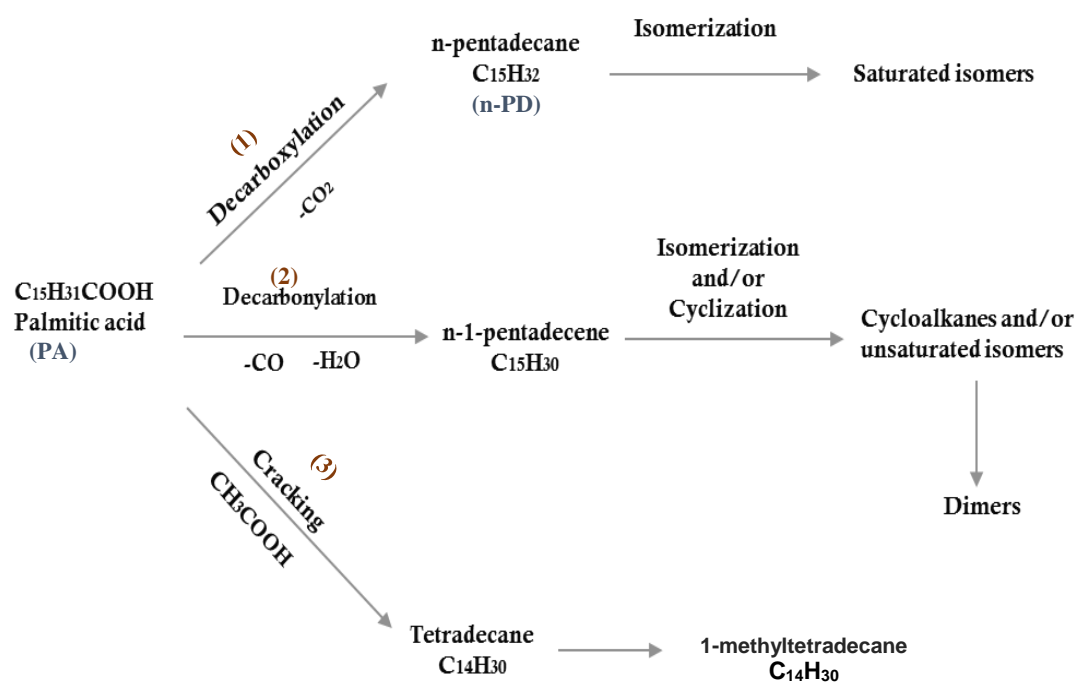


Figure 65: Deoxygenation pathway of PA under H<sub>2</sub>-containing atmosphere over the 10%Ni10%Cu/C catalyst.

Under inert atmosphere the same catalyst showed saturated products such as n-PD (only 59%) and its isomers and few traces of shorter hydrocarbon such as tetradecane (n-C<sub>14</sub>) and its isomer from cracking reaction were detected. Besides that, unsaturated bonds (1-pentadecene (29%) and its isomers) from direct decarbonylation reaction were also observed. The presence of isomers of n-PD and n-pentadecene is probably due to the long residence time. On this basis, we propose the reaction mechanism under N<sub>2</sub> in Figure 66.



**Figure 66: Deoxygenation pathway of palmitic acid under inert ( $N_2$ ) atmosphere over 10%Ni10%Cu/C catalyst**

First of all, the deoxygenation of PA under  $N_2$  was performed via two principle direct reactions: DCX (1) and DCN (2). Direct DCX lead to the formation of n-PD by releasing  $CO_2$  from the fatty acid and DCN lead to the formation of n-pentadecene,  $H_2O$  and  $CO$ . The absence of formation of hydrogen during the reaction prevented the hydrogenation of the olefins. That was why, n-pentadecane and n-pentadecene were observed simultaneously. However, the absence of hydrogen favors also the cracking (3) of the double bond of the olefin formed, which lead to the formation of shorter hydrocarbon. Hence, under inert atmosphere, catalytic decarboxylation reaction of PA with 10%Ni10%Cu/C favors the DCX, DCN and cracking reactions, while under 10% $H_2/N_2$  atmosphere, the DCX and HDO are dominant. Therefore, the decarboxylation of FFA over 10%Ni10%Cu/C is better under 10% $H_2/N_2$  than inert atmosphere.

The bimetallic 10%Ni10%Cu/C catalyst was clearly found more active than the monometallic Ni-based catalyst when the reaction was performed in the same conditions. Indeed, the 10%Ni10%Cu/C catalyst reached 100% of conversion, while, the 10%Ni/C catalyst reached ~80% in the same conditions. The  $H_2$ -TPR revealed that the addition of Cu to Ni/C decreased significantly the temperature of reduction of the Ni species in presence. Therefore,

at the same temperature of reaction, the 10%Ni10%Cu/C catalyst will be easily reduced to a higher extent. Furthermore, compared to the monometallic 10%Ni/C catalyst, the copper addition allows preventing coke deposition. In fact, the recyclability tests revealed that the stability of the 10%Ni10%Cu/C catalyst after 3 runs was higher than that of the monometallic 10%Ni/C catalyst, which gradually deactivated (Chapter 4). The better stability of the 10%Ni10%Cu/C catalyst was attributed to the presence of the copper in the material. Indeed, it was demonstrated that Cu NPs occupied the edge sites where the nickel nucleate the coke formation whereas the terrace nickel site contribute to catalytic activity [9]. Although the activity of the catalyst was maintained after 3 consecutive tests, the nitrogen adsorption showed a significant decrease of the specific surface area and of the pore volume. This could be assigned to two main reasons. The first one is the formation of coke on the catalyst. In this case, the catalyst should be reactivated with hydrogen to remove the coke deposition. The second (most probable) reason could be the blocking of pore by the solvent. Indeed, the hexadecane boiling point at atmospheric pressure is 287 °C and the recycled catalyst was only dried at 100 °C. Therefore, it is highly probable that hexadecane is still in the pore of the catalyst. To confirm this suggestion, it would be important to make several consecutive runs to check if the catalyst is progressively deactivated or if it conserves the activity. Another possibility would be to treat the used catalyst at 350 °C under N<sub>2</sub> to try to remove the solvent.

The catalytic test of the bimetallic 10%Ni10%Cu/C catalyst with SA instead of PA showed a total conversion of SA and a selectivity to n-heptadecane of 90% at 320 °C for 3 h. Almost the same catalytic performances of the catalyst were observed for PA when the reaction was performed in the same conditions. This is due to their close chain length and almost the same acidity of both FA. As it was mentioned in Chapter 1, for different fatty acids having similar chain lengths, the catalytic performances should be similar over the same catalyst and under the same reaction conditions.

### Conclusion

Among all the bimetallic Ni-Me/C systems tested in the decarboxylation of palmitic acid to n-pentadecane the 10%Ni10%Cu/C catalyst was found the best one by far. The best catalytic performances were reached when the reaction was carried out at 320 °C under 10 vol.% of N<sub>2</sub> in H<sub>2</sub> for 6 h. In these conditions, a total conversion of PA and 95% of selectivity toward n-PD were reached with an excellent 95% carbon balance suggesting the formation of very few amounts of by-products. Furthermore, the same excellent performances were obtained using SA instead of PA showing the possibility to extend the range of application of the catalyst to other fatty acids or mixtures of fatty acids. Interestingly the catalyst was found to maintain its catalytic performances after 3 consecutive runs without any regeneration treatments between the cycles. This behavior was attributed to the incorporation of copper on the edge sites where the nickel nucleates the coke formation. Besides, the copper addition was found to decrease the temperature of the reduction of the nickel-based species in presence in the catalysts. Therefore, the conversion started at lower temperature as compared to the monometallic nickel catalyst, resulting in the increase of the catalytic activity of the 10%Ni10%Cu/C catalyst.

## References

- [1] E. Santillan-Jimenez, T. Morgan, J. Lacny, S. Mohapatra, M. Crocker, *Fuel*. 103 (2013) 1010-1017.
- [2] M. Snåre, I. Kubičková, P. Mäki-Arvela, K. Eränen, D.Y. Murzin, *Industrial & Engineering Chemistry Research*. 45 (2006) 5708-5715.
- [3] J. Wu, J. Shi, J. Fu, J.A. Leidl, Z. Hou, X. Lu, *Scientific Reports*. 6 (2016) 27820.
- [4] G. Boskovic, M. Baerns, in: M. Baerns (Ed.), *Basic Principles in Applied Catalysis*, Springer Berlin Heidelberg, Berlin, Heidelberg, 2004, pp. 477-503.
- [5] P. Mäki-Arvela, I. Kubickova, M. Snåre, K. Eränen, D.Y. Murzin, *Energy & Fuels*. 21 (2007) 30-41.
- [6] S. Mohite, U. Armbruster, M. Richter, A. Martin, *Journal of Sustainable Bioenergy Systems*. 4 (2014) 183.
- [7] B.P. Pattanaik, R.D. Misra, *Renewable and Sustainable Energy Reviews*. 73 (2017) 545-557.
- [8] E. Santillan-Jimenez, M. Crocker, *Journal of Chemical Technology & Biotechnology*. 87 (2012) 1041-1050.
- [9] N.M. Galea, D. Knapp, T. Ziegler, *Journal of Catalysis*. 247 (2007) 20-33.

# General conclusion & Perspectives

Based on the literature, the noble metal-based Pd/C catalyst appeared as the best candidate for the decarboxylation reaction, because it presented the highest activity (100% conversion) and also the highest selectivity to hydrocarbon (99% to hydrocarbon). But, the high cost of the noble material and the instability of the catalyst after one cycle run constituted major obstacles to the scale-up and industrial application of the process. That is the reason why non-noble metal-based catalysts have attracted the attention of the researchers in the recent years. In the literature, Ni/C was found as the most promising catalyst for the decarboxylation reactions. Indeed, this catalyst showed total conversion and 80% of selectivity to hydrocarbon when the reaction was carried out at 370 °C. However, given the higher energy consumption and the lower selectivity to hydrocarbon in comparison to the noble metal-based catalyst, the research of new catalytic materials for the decarboxylation of fatty acids showing similar results than those of noble-metals has been continuing to be investigated. Therefore, the aim of this thesis was to develop a new efficient non-noble metal-based catalyst, which would be highly active, selective and stable for the decarboxylation of palmitic acid to n-pentadecane.

Considering that the performances of supported metal catalysts are strongly influenced by the method of preparation as it defines the properties of the active species (size of the metal particles, dispersion, etc.), a series of non-noble monometallic and bimetallic Ni, Fe, Ag and Cu catalysts supported on carbon were prepared by a deposition-precipitation method using hydrazine as reducing agent using the high-throughput equipment of the REALCAT platform available at UCCS. The results obtained showed that the monometallic Fe and Ag-based catalysts were not active for the decarboxylation reaction. However, the nickel-based catalyst converted the fatty acid with high rates and the copper was found very selective to n-hydrocarbon. Based on these results, the synthesis of a library of bimetallic Ni-Cu catalyst was a logical continuation. The bimetallic 10%Ni10%Cu/C catalyst was found very active and it increased drastically the conversion and the selectivity to n-PD as compared to the monometallic 10%Ni/C catalyst. Other bimetallic Ni-Cu catalysts were also investigated to evaluate the effect of the variation of the total metal content on the performances. The bimetallic 2.5%Ni2.5%Cu/C, 5%Ni5%Cu/C and 15%Ni15%Cu/C catalysts were tested in the same conditions as the 10%Ni10%Cu/C catalyst and their catalytic performances were compared. The results obtained showed that the 10%Ni10%Cu/C catalyst is the most promising catalyst for the decarboxylation PA to n-PD as compared to other bimetallic Ni-Cu catalysts. The difference in the activity of these catalysts is based on the difference in their physicochemical properties. In fact, the XPS analyses revealed that the bimetallic 5%Ni5%Cu/C and 15%Ni15%Cu/C

catalysts contain unreduced  $\text{Cu}(\text{NO}_3)_2$  species on their surface. This species is known to be detrimental to the catalyst and leads to its rapid deactivation. In contrast, the more active 10%Ni10%Cu/C catalyst does not contain this species. That could be one of the main reason of the best catalytic performances of the catalyst. Furthermore, the XRD analysis showed that the most active catalyst comprises a physical mixture of Ni and Cu in separated phases. On the contrary, the bimetallic 5%Ni5%Cu/C and 15%Ni15%Cu/C catalysts show the presence of Ni-Cu alloys. In addition, TEM images of the more active catalyst show the presence of dispersed Cu and Ni particles, while the 15%Ni15%Cu/C catalyst shows the presence of agglomerates corresponding to NiCuO. The  $\text{H}_2$ -TPR analysis also shows the presence of different species in each catalyst which could explain the difference of catalytic performances observed.

The catalytic performances are of course also influenced by the conditions of reaction. In this work, we studied the effect of temperature (in the range 250-320°C), of reaction time (in the range 1.5-12 h), of the reaction atmosphere ( $\text{N}_2$ , 10 vol.%  $\text{H}_2$  in  $\text{N}_2$ ), of the amount of catalyst loaded in the reactor (in the 12.8-75 mg range), of the concentration of the reactant (0.05, 0.1 and 0.15 mL/g) and of the solvent used (dodecane or hexadecane) on the catalytic performances of the bimetallic 10%Ni10%Cu/C catalyst.

At first, the study of the variation of the reaction temperature in the 250-320 °C range resulted in an increase of both the conversion of PA and selectivity to n-PD. The best performances were reached at 320 °C. Then, the study of the reaction time showed a total conversion, whatever the reaction time in the 1.5-12h range, in the operating conditions used. In contrast, a variation in the selectivity to n-PD was observed as a function of the reaction time. The maximum selectivity (95%) was observed for a reaction time of 6 h. Between 1.5 and 3 h an increase in the selectivity was observed, and then a decrease for a long reaction time (12 h). This increase was attributed to the formation of reaction intermediates, which were then transformed to the desired product. On the other hand, the decrease in the selectivity after 12 h of reaction is due to n-PD isomerization reactions, which occurred for long reaction times.

The 10%Ni10%Cu/C catalyst showed total conversion, whatever the reaction atmosphere. However, the catalyst exhibited low catalytic performances towards the DCX reaction under an inert atmosphere ( $\text{N}_2$ ). In fact, under inert atmosphere, the reaction DCN occurred preferably resulting in the increase of cracking reactions due to the absence of hydrogen to saturate the double bond of the olefin formed. In contrast, under 10% $\text{N}_2/\text{H}_2$ , the catalyst favored the DCX reaction and 95% of n-PD selectivity was reached. Therefore, the best

results were obtained when the reaction was carried out at 320 °C, under 10 vol.% of H<sub>2</sub> in N<sub>2</sub>, for 6 h, for 0.1 mol/L of substrate in hexadecane and using 52 mg of the catalyst. A short study of the effect of the solvent used (dodecane or hexadecane) showed that, there is no impact on the catalytic performances. Thereby, the use of the desired hydrocarbon (the product of the decarboxylation reaction) as solvent could be a huge industrial advantage to avoid complex downstream separation operations after reaction.

Recyclability tests of the 10%Ni10%Cu/C catalyst were also performed to check its stability under reaction conditions. It was found that after three runs, the catalyst keeps the integrality of its catalytic performances without the need of any regenerative treatments between the runs. On the contrary, the 10%Ni catalyst showed a constant decrease of catalytic activity after 3 runs due to progressive deactivation. Therefore, the addition of copper to the nickel-based catalyst permitted to keep the performances of the bimetallic 10%Ni10%Cu/C catalyst constant. The XRD analysis of the catalyst before (catalyst reduced) and after the recyclability test (catalyst recycled) showed the same diffractions peaks. However, after the recyclability test, the specific surface area and the pore volume of the catalyst decreased drastically, while, the pore size distribution increase significantly. The reason of this was attributed to the filling of the pores of the catalyst by the reaction solvent.

For the continuation of the project, it would be important to carry out additional consecutive tests of catalyst recyclability. If the catalyst deactivates completely after a certain number of consecutive tests, it would be important to find a method to regenerate it under hydrogen. Indeed, hydrogen is known to regenerate this type of catalyst by coke cracking. Furthermore, the decarboxylation reaction should be studied in high-pressure semi-continuous reactors with CO and CO<sub>2</sub> detectors in order to obtain a more accurate mass balance. Finally, the design of a continuous process would be very interesting from an industrial point of view.

On the other hand, a kinetic study of the reaction would be interesting to develop a model where the kinetic constants ( $k_i$ ) and activation energies ( $E_a$ ) would be well defined. This is an important tool to further design a reactor.

In order to extent the application of the 10%Ni10% Cu/C catalyst to other substrates, it would be interesting to test the activity of this catalyst, on unsaturated fatty acids and also on PFAD (Palm Fatty Acid Distillate). Indeed, the PFAD is a residue from palm oil refining process consisting >85% of FFA [1]. The use of PDFA is a good way to utilize natural resources and upgrading the crude palm oil use. However, the application of this catalyst for

decarboxylation of PFAD, could be more difficult taking account of the impurities present in this mixture.

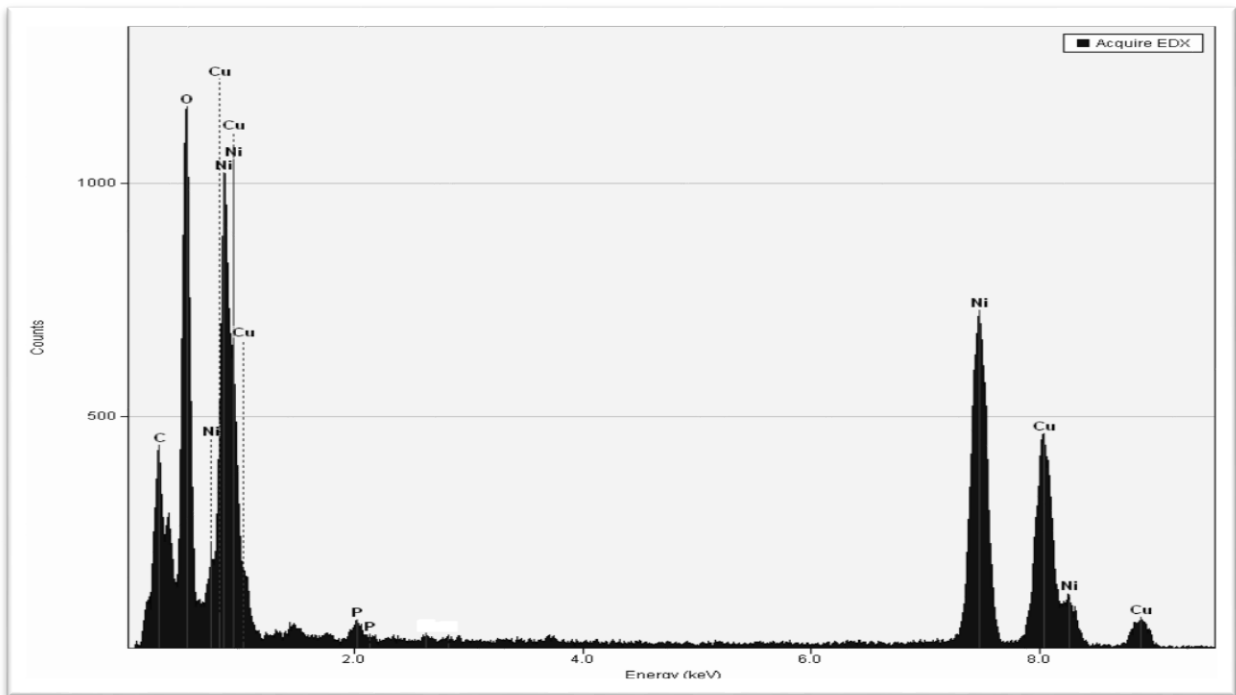
### Reference

- [1] I.M. Lokman, U. Rashid, Z. Zainal, R. Yunus, Y.H. Taufiq-Yap, *Journal of Oleo Science*. 63 (2014) 849-855.

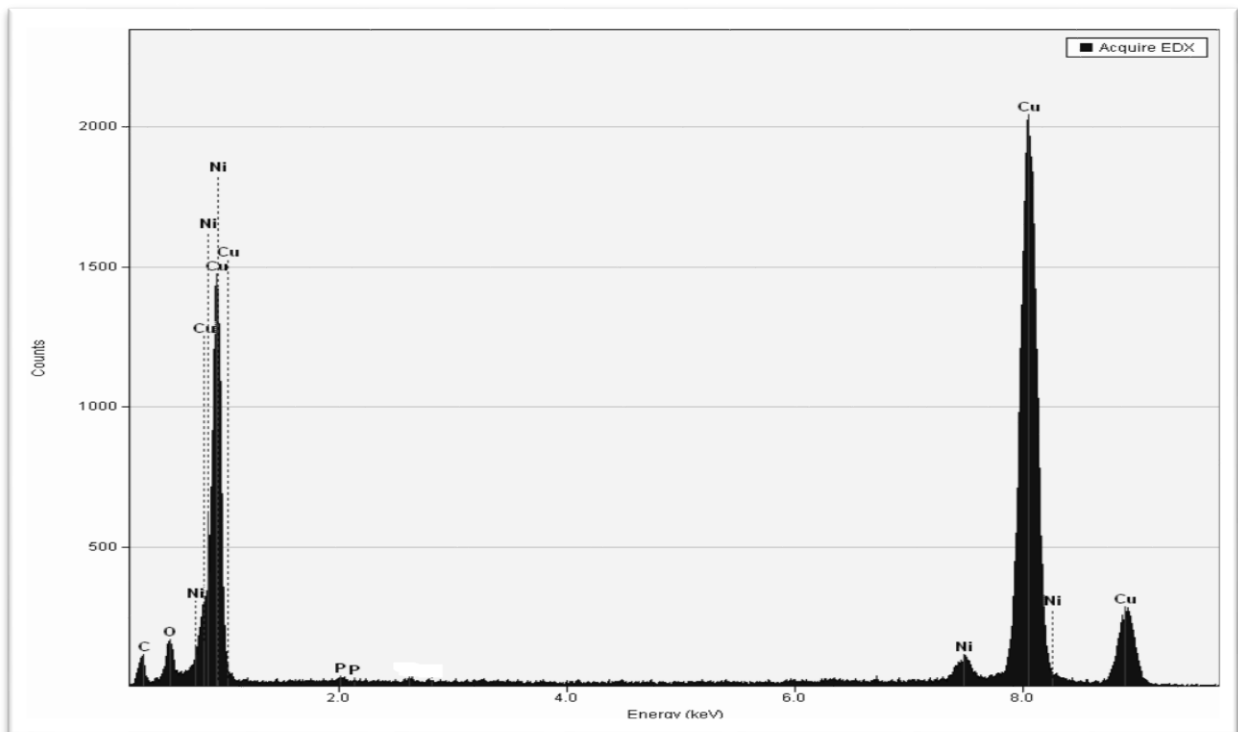
---

# Annexes

Annex 1: EDX analysis of the fresh 15%Ni15%Cu/C catalyst (Zone 1)



Annex 2: EDX analysis of the fresh 15%Ni15%Cu/C catalyst (Zone 2)



**Titre : Décarboxylation catalytique de l'acide palmitique en n-pentadécane**

Les catalyseurs à base de métaux nobles, en particulier ceux à base de palladium supportés sur charbon, sont connus pour catalyser les réactions de décarboxylation d'acides gras et de leurs dérivés avec un très bon rendement. Malheureusement, la forte désactivation sous conditions de réaction de ces derniers et leurs coûts élevés sont autant de freins à leur usage industriel. De ce fait, des catalyseurs à base de nickel supportés sur charbon ont été étudiés. Ils présentent des performances catalytiques moins bonnes que les métaux nobles mais néanmoins prometteuses pour catalyser ladite réaction. Ainsi, la recherche de catalyseurs peu onéreux et présentant des performances catalytiques du même ordre, voire meilleures, tout en étant plus stables que ceux basés sur les métaux nobles, continue d'être d'intérêt. C'est dans cette optique que la réaction de décarboxylation de l'acide palmitique en n-pentadécane a été étudiée en réacteur discontinu en présence de catalyseurs bimétalliques de type Ni-Me (où Me=Fe, Cu ou Ag) supportés sur charbon actif. Ces catalyseurs ont été préparés à l'aide d'un robot haut débit disponible sur la plateforme REALCAT de l'UCCS par déposition-précipitation en utilisant l'hydrazine comme agent réducteur afin de mieux maîtriser la taille des nanoparticules métalliques, leur distribution et leur degré de réduction. Ces derniers ont été caractérisés par ICP, adsorption d'azote, XPS, XRD et TEM afin d'obtenir des informations relatives à leurs compositions, leurs propriétés texturales, surfaciques et morphologiques. Dans cette étude, l'optimisation du procédé catalytique a également été étudiée pour divers paramètres de réaction pour les catalyseurs les plus prometteurs. D'une part, l'impact de l'ajout d'un second métal sur les performances des catalyseurs à base de nickel a été étudié, et, d'autre part, l'effet de la température, de la durée de réaction, des concentrations initiales en réactifs, de l'atmosphère réactionnelle et de la masse de catalyseur utilisée ont été investiguées. Dans ce contexte, le catalyseur bimétallique 10%Ni10%Cu/C convertit complètement l'acide palmitique avec une sélectivité de 95 % en n-pentadécane à 320 °C sous une atmosphère contenant 10% en volume de H<sub>2</sub> dans N<sub>2</sub> et pour une pression initiale de 20 bar. La réaction s'est déroulée pendant 6 h. En outre, dans les mêmes conditions de réaction, ce catalyseur a présenté une excellente stabilité après trois tests de recyclage consécutifs. Par ailleurs, l'utilisation de ce catalyseur pour décarboxyler un autre acide gras plus lourd (l'acide stéarique) s'est avérée possible avec d'excellents résultats. En comparant les performances de ce catalyseur à celles du monométallique 10%Ni/C, il est clair que la présence du cuivre favorise la dispersion des nanoparticules de métal sur le support, empêche la désactivation du catalyseur et améliore le rendement de la réaction. Ainsi, les catalyseurs NiCu/C constituent une alternative très intéressante aux catalyseurs à base de métaux nobles pour conduire la réaction de décarboxylation des acides gras en alcanes linéaires.

Mots clés : décarboxylation, acide palmitique, n-pentadécane, catalyseurs bimétalliques nickel-cuivre

**Title: Catalytic decarboxylation of palmitic acid to n-pentadecane**

The noble metal-based catalysts, in particular those containing palladium supported on charcoal, are known to efficiently catalyze the catalytic decarboxylation of fatty acids and their derivatives with very good yields. Unfortunately, the rapid deactivation and the high cost of these catalysts prevent their industrial application. Consequently, nickel-based supported catalysts have been studied as they have shown promising catalytic performances for the decarboxylation reactions. Thus, the search for catalysts which are inexpensive and have similar or even better catalytic performances and which are more stable than noble metals-based catalysts have been continuously studied in the recent years. It is in that frame that in this thesis the catalytic decarboxylation of palmitic acid to n-pentadecane was studied in a batch reactor in the presence of bimetallic Ni-Me catalysts (where Me = Fe, Cu or Ag) supported on activated carbon. These catalysts were prepared using a high-throughput robot of the REALCAT platform of UCCS by deposition-precipitation using hydrazine as reducing agent. These catalysts were characterized by ICP, N<sub>2</sub> adsorption, XPS, XRD and TEM in order to obtain information relative to their compositions, textural properties, surfaces and morphologies. In this study, the optimization of the catalytic process was also investigated for various reaction parameters for the most promising sample. The main studied parameters were, on the one hand, the impact of the addition of a second metal on the performance of the nickel-based catalysts and, on the other hand, the effect of temperature, reaction time, initial reactant concentrations, atmosphere and mass of catalyst used. The conclusion of this study is that the 10%Ni10%Cu/C completely converts palmitic acid with a selectivity of 95 % to n-pentadecane in 6 h, at 320 °C under 10 vol.% of H<sub>2</sub> in N<sub>2</sub> at an initial pressure of 20 bar. Furthermore, under the same reaction conditions, this catalyst exhibited excellent recyclability after three consecutive tests. Moreover, the use of this catalyst to decarboxylate stearic acid has proved to be excellent. By comparing the catalytic performance of this catalyst with the monometallic nickel-based catalyst, it was found that the presence of copper favors the dispersion of the metal on the support, prevents deactivation of the catalyst and improves the yield of reaction. Therefore, NiCu/C catalysts are very promising alternatives to noble metal-based catalysts to decarboxylate fatty acids to linear alkanes.

Key word: decarboxylation, palmitic acid, n-pentadecane, bimetallic catalysts, nickel-copper